

# DEMONSTRATION OF INTRACELLULAR GLYCOGEN, PEROXIDASES AND VIRUSES BY LIGHT AND ELECTRON MICROSCOPY.

FRIEDRICH A C TIEDT

Thesis submitted in fulfilment of the requirements for the  
**Masters Diploma in Medical Technology**  
in the School of Life Sciences at the Cape Technikon.

Department of Anatomical Pathology,  
Tygerberg Hospital.

External Supervisor: Professor D J Rossouw  
Internal Supervisor: Mr E J Truter

I declare that this thesis is my own work. It is being submitted for the Masters Diploma in Medical Technology, to the Cape Technikon, Cape Town. It has not been submitted before for any diploma or examination at any other technikon or tertiary institution. The work was carried out in the Diagnostic Electron Microscope Laboratory, Department of Anatomical Pathology, Tygerberg Hospital.

The opinions and conclusions drawn are not necessarily those of the Cape Technikon.



Friedrich A C Tiedt



Date

## ACKNOWLEDGEMENTS

I extend my sincere gratitude to the following people:

The late Professor D J Rossouw for allowing me to complete this study in the Department of Anatomical Pathology, Tygerberg Hospital;

my colleagues in the electron microscope laboratory for their co-operation throughout the duration of my research;

my friend Marilyn McIntosh, for her assistance with literature searches, information retrieval and encouragement during this time; and

Mr E J Truter, my Technikon supervisor, for his support and valuable advice.

## SUMMARY

The objective of the present study was primarily to determine whether modifications to the existing osmium tetroxide/potassium ferrocyanide method could be used as a general ultrastructural glycogen stain and whether this glycogen, when so contrasted, differed in appearance in different tumours, such as Ewing's sarcoma, Leiomyosarcoma, Rhabdomyosarcoma and Hepatocellular carcinoma. Normal skeletal muscle and liver were used to obtain a standard for the appearance of glycogen, and then, with diagnostic criteria in mind, the four glycogen-rich tumours, mentioned above were examined to determine the appearance, distribution and amount of glycogen present in them.

Modifications to the osmium tetroxide/potassium ferrocyanide (OPF) method consisted of raising the concentration of the ferrocyanide, and using no en bloc or thin section staining by any uranyl salt solutions, because solutions of uranyl salts leaches glycogen from tissue. This procedure resulted in extremely electron-dense intracellular glycogen being retained, which aided diagnosis of the these tumours. At high magnification, (>X30000) there was no morphological difference between the glycogen particles in the various tumours, so these particles as such could not be used as a diagnostic criterion.

Existing methods for the demonstration of myeloperoxidase and platelet peroxidase were modified to obtain more precise localization of the diaminobenzidine (DAB) reaction product. Different anti-coagulants, one of which was heparin and a modified fixation procedure was followed. Different



concentrations of the DAB in the substrate were also utilised. A myeloblastic, a lymphoblastic and a granulocytic leukaemia were compared to determine the localization of peroxidases in each entity. A chloroma (granulocytic sarcoma) was also described and the above method applied to obtain a diagnosis of this tumour.

The modified myelo- and platelet peroxidase methods demonstrated a much sharper delineation of the reaction product, and in some cases a much more electron-dense reaction product, which aided the differentiation of various leukaemias, ie: myeloblastic, lymphoblastic and granulocytic leukaemias.

A light microscopic detection and typing technique for Human Papilloma Virus (HPV) in cervical biopsies was modified so that this virus could be detected and typed ultrastructurally.

A DNA in situ method was modified and adapted to be used at the ultrastructural level. The digoxigenin (DIG) method was used and coupled with an anti-digoxigenin peroxidase (anti<DIG> POD) antibody, and the result of this combination was detected by the modified DAB method for peroxidase. The reaction product was electron-dense and was made even more so by post-fixing the tissue in the modified OPF medium. Reaction product was seen in viruses in the nuclei of koilocytes from cervical biopsies. This ultrastructural marker for HPV was found to be too coarse for fine ultrastructural studies of viral DNA, but has paved the way

for ultrastructural immuno-gold labelling of the areas in the DNA that require examining.

—ooOoo—

## OPSOMMING

Die doel van die huidige studie was eerstens om vas te stel of aanpassings aan die bestaande osmiumtetroksied/kalium ferrosianied (OPF) metode gebruik kon word as 'n algemene ultrastrukturele glikogeen kleurmetode. Tweedens wou vasgestel word of die glikogeen so gekontrasteer, 'n ander voorkoms toon in verskillende tumore, soos byvoorbeeld, Ewing sarkoom, Leiomiosarkoom, Rhabdomiosarkoom en Hepato-sellulêre karsinoom. Normale lewer-en gestreepte spierweefsel is gebruik om die voorkoms, verspreiding en hoeveelheid van glikogeen te bepaal. Met diagnostiese kriteria in gedagte is vier glikogeenryke tumore op dieselfde manier behandel.

Modifikasies aan die OPF metode het uit verhoging van die konsentrasie van die ferrosianied bestaan. En bloc kleuring van die weefsel sowel as kleuring van dun snitte met uraansout oplossings is ook nie uitgevoer nie. Hierdie prosedure het teweeggebring dat elektrondigte intrasellulêre glikogeen behoue gebly het, wat dan ook die diagnose van die tumore gestaaf het. Daar was ongelukkig geen verskil by hoë vergroting in die voorkoms van die gekontrasteerde glikogeenpartikel in die onderskeie tumore nie, en dus kon hierdie eienskap nie gebruik word as 'n diagnostiese hulpmiddel nie.

Bestaande tegnieke vir beide miëlo- sowel as plaatjie peroksidase is aangepas om 'n beter lokalisasie van diaminobezidien (DAB) reaksie produk te bewerkstellig.

Ander antistolmiddels soos heparien is gebruik in plaas van sitraat en die fikseringsmetode is ook aangepas. Veranderings in die substraat is ook gedoen om 'n donkerder elektrondigte reaksie produk te verkry. 'n Miëloblastiese, 'n lymfoblastiese en 'n granulositiese leukemie is vergelyk om die lokalisasie van die peroksidase in elke entiteit vas te stel. 'n Chloroom (granulositiese sarkoom) is ook beskryf om te bewys hoe hierdie aangepaste metodes gebruik kan word om 'n diagnose van hierdie tipe tumor te maak.

Hierdie aangepaste tegnieke het 'n skerper deliniasie van die reaksieproduk veroorsaak en in sommige gevalle is 'n meer elektrondigte produk verkry.

'n Ligmikroskopiese opsporings-en tiperingstegniek vir Menslike Papilloomvirus (MPV) in serviksbiopsies is aangepas om op ultrastrukturele vlak hierdie virusse te merk. Hierdie DNA in situ tegniek is aangepas deurdat anti-digoxigenin peroksidase (anti<DIG> POD) teen-liggaam daaraan gekoppel is. Hierdie verbinding is met die aangepaste DAB metode vir peroksidase uitgevoer en boonop is die weefsel daarna post-fikseer met die nuwe OPF mengsel. Die reaksieproduk was uiters elektrondig in die koilosiete wat virusse bevat het. Hierdie ultrastrukturele merker vir MPV is ongelukkig bevind om te grof te wees om klein deeltjies virus DNA te bestudeer, maar het die weg gebaan vir 'n immunogoud tegniek wat in die toekoms ondersoek sal word.

—ooOoo—

# CONTENTS

## CHAPTER I

1.0	INTRODUCTION.....	1
1.1	PROBLEMS ASSOCIATED WITH TUMOUR DIAGNOSIS.....	2
1.2	GLYCOGEN.....	3
1.3	PEROXIDASE.....	4
1.4	HUMAN PAPILLOMA VIRUS.....	5
1.5	OBJECTIVES OF STUDY.....	6
1.6	SUMMARY OF FINDINGS.....	7

## CHAPTER II

2.0	LITERATURE REVIEW.....	8
2.1	CHEMICAL NATURE OF GLYCOGEN.....	9
2.2	OSMIUM TETROXIDE/POTASSIUM FERROCYANIDE METHODS..	11
2.3	CHEMICAL NATURE OF PEROXIDASES.....	14
2.3.1	HISTOCHEMICAL LOCALIZATION.....	15
2.4	PEROXIDASE METHODS.....	17

2.5	CHEMICAL NATURE OF DNA.....	21
2.6	IN SITU HYBRIDIZATION METHODS.....	26

### CHAPTER III

3.0	METHODS.....	33
3.1	COLLECTION OF TISSUE, BLOOD AND BONE MARROW SPECIMENS.....	34
3.2	METHODS FOR THE OSMIUM TETROXIDE/ POTASSIUM-FERROCYANIDE (OPF)PROCEDURE.....	35
3.2.1	ORIGINAL OPF METHODS.....	36
3.2.2	MODIFIED OPF METHOD ACCORDING TO EM LABORATORY, TYGERBERG HOSPITAL.....	39
3.3	METHODS FOR THE DEMONSTRATION OF MYELOPEROXIDASE AND PLATELET PEROXIDASE.....	40
3.3.1	METHODS FOR THE DEMONSTRATION OF MYELOPEROXIDASE.....	42
3.3.2	MODIFIED MYELOPEROXIDASE METHOD ACCORDING TO EM LABORATORY. TYGERBERG HOSPITAL.....	43
3.3.3	PLATELET PEROXIDASE PROCEDURE.....	44
3.4	IN SITU DNA HYBRIDIZATION METHODOLOGY.....	45
3.4.1	PREPARATION OF SLIDES.....	45
3.4.2	DNA in situ HYBRIDIZATION PROCEDURE.....	47

3.4.3	PROCEDURE FOR THE ULTRASTRUCTURAL DNAIN SITU METHOD.....	49
-------	---	----

## CHAPTER IV

4.0	RESULTS.....	52
	KEY TO LEGENDS.....	53
4.1	RESULTS OF OSMIUM/TETROXIDE POTASSIUM FERROCYANIDE METHOD.....	54
4.1.1	DISTRIBUTION OF GLYCOGEN IN NORMAL LIVER..	54
4.1.2	DISTRIBUTION OF GLYCOGEN IN NORMAL MUSCLE.....	63
4.1.3	DISTRIBUTION AND ARRANGEMENT OF GLYCOGENIN EWING'S SARCOMA.....	71
4.1.4	DISTRIBUTION AND ARRANGEMENT OF GLYCOGEN IN LEIOMYOSARCOMA.....	78
4.1.5	DISTRIBUTION AND ARRANGEMENT OF GLYCOGEN IN RHABDOMYOSARCOMA.....	86
4.1.6	DISTRIBUTION AND ARRANGEMENT OF GLYCOGENIN HEPATOCELLULAR CARCINOMA.....	96
4.1.7	COMPARATIVE SUMMARY OF PROCEDURES.....	107
4.1.8	SUMMARY OF RESULTS OF THE OPF METHOD..	108
4.2	RESULTS OF THE MYELOPEROXIDASE AND PLATELET SPECIFIC PEROXIDASE METHODS.....	109
4.2.1	MYELO-PEROXIDASE (MPO) RESULTS.....	111

4.2.2	PLATELET SPECIFIC PEROXIDASE (PPO) RESULTS.....	116
4.2.3	USE OF MPO IN THE DIAGNOSIS OF GRANULOCYTIC SARCOMA.....	128
4.2.4	COMPARATIVE SUMMARY OF PROCEDURES. BLOOD BONE MARROW AND TISSUE.....	136
4.2.5	SUMMARY OF RESULTS FOR THE MPO/PPO METHOD.....	137
4.3	RESULTS OF THE DNA IN SITU HYBRIDIZATION METHOD.....	138

## CHAPTER V

5.0	DISCUSSION.....	149
5.1	THE OSMIUM TETROXIDE/POTASSIUM FERROCYANIDE METHOD AS A GENERAL ULTRASTRUCTURAL GLYCOGEN STAIN.....	150
5.2	THE GLYCOGEN PARTICLE AS AN ULTRASTRUCTURAL DISTINGUISHING FEATURE IN TUMOURS RICH IN GLYCOGEN.....	151
5.3	SIGNIFICANCE OF THE OSMIUM TETROXIDE/POTASSIUM FERROCYANIDE METHOD IN TUMOURS OF THE MESODERM AND ENDODERM.....	152
5.3.1	EWING'S SARCOMA.....	152
5.3.2	LEIOMYOSARCOMA.....	153
5.3.3	RHABDOMYOSARCOMA.....	153



5.3.4	HEPATOCELLULAR CARCINOMA.....	154
5.3.5	THE EFFICACY OF THE OSMIUM TETROXIDE/ POTASSIUM FERROCYANIDE METHOD IN THE DIAGNOSIS OF TUMOURS.....	154
5.4	USEFULNESS OF THE MYELOPEROXIDASE AND PLATELET SPECIFIC PEROXIDASE METHODS AND THE EFFECT OF THE OSMIUM TETROXIDE/POTASSIUM FERROCYANIDE METHOD ON THESE TWO TECHNIQUES.....	155
5.5	TYPING OF HUMAN PAPILLOMA VIRUSES.....	157
5.6	ROLE AND USEFULNESS OF THE OSMIUM TETROXIDE/ POTASSIUM FERROCYANIDE AND MYELOPEROXIDASE PROCEDURES IN THE TYPING OF HUMAN PAPILLOMA VIRUSES.....	159
5.6.	THE MYELOPEROXIDASE METHOD AND DETECTION OF VIRUSES IN TISSUE.....	159
5.6.2	THE OSMIUM TETROXIDE/POTASSIUM FERROCYANIDE METHOD AS AN ENHANCER FOR GLYCOGEN IN HUMAN PAPILLOMA VIRUS TYPING.....	160
5.7	DEVELOPMENT OF FURTHER ELECTRON-HISTOCHEMICAL METHODS IN THE FUTURE.....	160

## CHAPTER VI

6.0	CONCLUSIONS.....	162
6.1	GENERAL CONSIDERATIONS.....	163
6.2	THE OSMIUM TETROXIDE/ POTASSIUM FERROCYANIDE METHOD.....	164

**6.3 THE MYELOPEROXIDASE AND PLATELET PEROXIDASE METHODS.....164**

**6.4 ULTRASTRUCTURAL HYBRIDIZATION OF HUMAN PAPILLOMA VIRUS.....165**

**7.0 APPENDIX.....167**

**8.0 BIBLIOGRAPHY.....180**

—ooOoo—

## LIST OF FIGURES

Figure I	:	Glucosyl molecule.....	9
Figure II	:	Linear amylose chains forming glycogen molecules.....	10
Figure III	:	Branching amylose chains in the glycogen molecule.....	10
Figure IV	:	Diamino-benzidine molecule.....	15
Figure V	:	Quinone imine molecules.....	16
Figure VI	:	DAB polymer.....	16
Figure VII	:	Thymine and cytosine molecules.....	22
Figure VIII	:	Adenine and guanine molecules.....	23
Figure IX	:	Digoxigenin molecule.....	26
Figure X	:	Hybridization of probe and target DNA.....	27

—ooOoo—

## LIST OF PLATES

Plate 1 to 89	:	Results of OPF method.....	54 to 106
Plate 90 to 133	:	Results of MPO PPO method.....	110 to 135
Plate 134 to 156	:	Results of LM and TEM DNA in situ hybridization method.....	139 to 148

—ooOoo—

## LIST OF TABLES

Table I	:	Comparative summary of procedures.....	107
Table II	:	Summary of results of OPF.....	108
Table III	:	Comparative summary of procedures, blood, bone marrow and tissue.....	136
Table IV	:	Summary of results of MPO/PPO.....	137

—ooOoo—

## ABBREVIATIONS

A	:	Adenine
ALL	:	Acute lymphoblastic leukaemia
AML	:	Acute myeloblastic leukaemia
anti<DIG> AP	:	Anti digoxigenin alkaline phosphatase
anti<DIG> POD	:	Anti digoxigenin peroxidase
APES	:	3-amino propyl triethoxy silane
C	:	Cytosine
CIN	:	Cervical intra-epithelial neoplasm
CMV	:	Cyto-megalo virus
DAB	:	Di-amino benzidine
<DIG>	:	Digoxigenin hapten
DISH	:	DNA in-situ hybridization
DNA	:	Deoxy-ribonucleic acid
dUTP	:	Deoxy-uridine tri-phosphopyridine
EDTA	:	Ethylene diamine tetra-acetic acid
EPON	:	A four component epoxy resin
ER	:	Endoplasmic reticulum
G	:	Guanine
GER	:	Rough endoplasmic reticulum
H&E	:	Haematoxylin and eosin
HPV	:	Human papilloma virus
HRP	:	Horseradish peroxidase
HSV	:	Herpes simplex virus
IU	:	International units
LM	:	Light microscope
ml	:	millilitre
μl	:	microlitre

mm	:	millimetre
$\mu\text{m}$	:	micro-metre
MPO	:	Myelo-peroxidase
NBT	:	Nitro-blue tetrazolium
nm	:	nano-metre
OCUB	:	Glutaraldehyde/Osmium tetroxide post-fixation/Uranyl and lead staining
OPF	:	Osmium tetroxide/ potassium ferrocyanide
$\text{OsO}_4$	:	Osmium tetroxide
PAS	:	Periodic acid Schiff stain
PAS + D	:	The above with prior diastase digestion
PBS	:	Phosphate buffered saline
PPO	:	Platelet specific peroxidase
RNA	:	Ribo-nucleic acid
SER	:	Smooth endoplasmic reticulum
SSC	:	Standard salt concentration
T	:	Thymine
TAFG	:	Tannic acid/ formaldehyde/glutaraldehyde
TEM	:	Transmission electron microscope
$T_M$	:	Melting temperature of DNA
TRIS	:	Hydroxyaminomethyl-methane

—ooOoo—

**CHAPTER I**  
**INTRODUCTION**



# 1.0 INTRODUCTION

## 1.1 PROBLEMS ASSOCIATED WITH TUMOUR DIAGNOSIS

Pathological cells and structures are identified by standardized light microscopic staining techniques in the routine diagnostic pathology laboratory. In the electron microscope laboratory however, constellations of ultrastructural characteristics are used for the diagnosis of pathological entities. These characteristics, or lack thereof, sometimes cause differential diagnostic problems to such a degree that special transmission electron microscopic (TEM) techniques have to be developed and standardized, to be able to distinguish between these disease states.

The most recent classification of tumours is based on the histogenesis of the cells and tissues involved and histopathologists are relying, to a large extent, on the morphochemical rather than the purely morphological identification of cells of primary tissue types. Methods had to be found to enhance specific morphochemical characteristics for routine diagnostic use. Experience gained in ultrastructural tumour diagnosis in the electron microscopy laboratory at Tygerberg Hospital, and also an evaluation of similar problems at international institutions, indicated that there were some of these diagnostic aspects, (ie glycogen in tissue) that warranted attention.

The existing histochemical methods developed as early as 1964 had a few shortcomings because the results obtained were not always consistent. The principal aim of this study was to modify the existing osmium tetroxide/potassium ferrocyanide (OPF), myeloperoxidase (MPO) and platelet peroxidase (PPO) methods to obtain more consistent and reproducible results. In addition a method for typing Human Papilloma Virus (HPV) at ultrastructural level, derived from a non-isotopic DNA in situ hybridization method, was developed to yield more information as to the type and localization of the papilloma viruses.

Modifications of two ultrastructural histochemical techniques will be described, as well as an adaptation of a light microscopic DNA in situ hybridization method for the typing of HPV at the ultrastructural level.

## 1.2 GLYCOGEN

Determination of the morphochemical heterogeneity of glycogen in different tumour cells was studied to answer two questions:

- a Was the osmium tetroxide/potassium ferrocyanide (OPF) method, or modifications thereof, suitable for general ultra-structural staining of glycogen?

- b Could tumours rich in glycogen such as Ewing's sarcoma, leiomyosarcoma and rhabdomyosarcoma (tumour cells of mesodermal origin), or hepatocellular carcinoma (tumour cells of endodermal origin), be differentiated, on the basis of the ultrastructural morphological appearance of glycogen particles within the cells of these tumours?

### 1.3 PEROXIDASE

The diagnosis of poorly differentiated myeloid, lymphoid and acute granulocytic leukaemias has always been a problem due to the fact that in many cases these diagnoses could no longer be made on purely morphological grounds. Alternative morphochemical methods had to be developed for these purposes. Light microscopic myeloperoxidase techniques were of some help in a number of cases, however when the cells were poorly differentiated, ultrastructural myeloperoxidase cytochemistry together with other special methods had to be employed to obtain an accurate diagnosis. The ultrastructural myeloperoxidase techniques that had been used, were developed as early as 1966, but results had not been altogether satisfactory due to the fact that there was inconsistency of staining results and poor localization of the reaction product. With some modifications of the existing methods, it was hoped to produce a DAB peroxidase technique that was sensitive and highly reproducible to aid in

the diagnosis of myeloid-, lymphoid-, megakaryocytic-leukaemias and granulocytic sarcomas.

#### 1.4 HUMAN PAPILLOMA VIRUS

With the development of recombinant DNA techniques and sensitive methods for analysing the organization, sequence complexity and intracellular location of specific genes or their transcripts, understanding of molecular virology has increased dramatically. The specificity and sensitivity that can be obtained by nucleic acid hybridization is exploited in these methods. Earlier procedures routinely employed polynucleotide probes of high specific radioactivity coupled to autoradiographic detection methods. There are serious disadvantages associated with the use of radioactively labelled probes, especially for routine application in diagnostic medicine. The short half-life of many radio-isotopes, the high cost, the personnel safety and the problems associated with the disposal of the used isotope, made it desirable to have alternative, but equally sensitive methods for detecting or localizing specific nucleic acid sequences in biological specimens. Such methods were developed and were found to be as sensitive and advantageous to use as the autoradiographic methods, but with fewer of the disadvantages. Soon after the development of hybridization techniques, attempts were made to extend these methods to the ultrastructural level. This involved the hybridization of radioactively labelled nucleic acid probes with cellular and

viral DNA on thin sections of resin embedded tissue. These methods were limited by low hybridization sensitivity, poor spatial resolution and long autoradiographic exposure, and hence were not widely used. A pre-embedding technique employing a modified peroxidase enzyme immunoassay method was adapted to detect strains of HPV for light-, as well as electron microscopy using random primed DNA labelling with digoxigenin-dUTP. Ultrastructural investigation of the location and mobility of specific viral and cellular nucleic acids could provide important information with regard to viral pathogenesis and cellular gene expression.

## **1.5 OBJECTIVES OF STUDY**

The objectives of this study were threefold:-

- a To determine if the OPF complex was a general glycogen stain, and whether the glycogen particle so stained could be used as a diagnostic marker for different tumour cells.
- b To develop a sensitive and reproducible method for the determination of the peroxidase found in granulocytic and megakaryocytic precursors.
- c To modify an existing light microscopic technique for detection of HPV and adapt it for typing these viruses ultrastructurally.

## 1.6 SUMMARY OF FINDINGS

The modified OPF method is considered to be a general ultrastructural glycogen stain, but the different tumours could not be differentiated on the basis of the appearance of the stained glycogen particle alone. Other factors such as density, amount and distribution of the stained glycogen had to be taken into account as well.

Although the MPO and PPO methods were not specific for peroxidase per se, the modified techniques were found to be reliable methods for demonstrating myeloid and megakaryocytic precursors in undifferentiated leukaemias. The MPO method also aided in the diagnosis of granulocytic sarcoma.

The modified OPF and MPO techniques were combined in the DISH method to type HPV at the ultrastructural level. Because the viruses are particulate, the OPF technique had to be employed to distinguish between glycogen and the virus particles. With the results obtained it is evident that further research should be undertaken in this field.

—ooOoo—

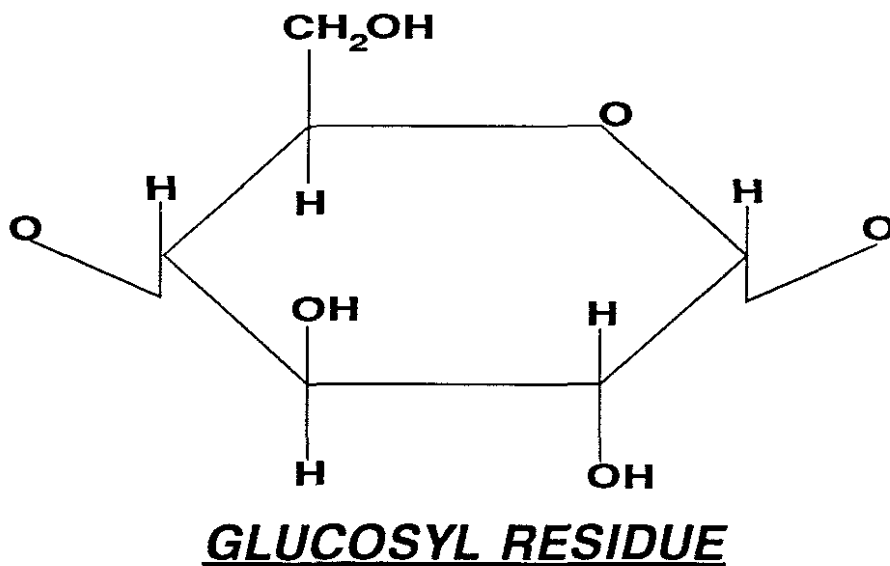
**CHAPTER II**  
**LITERATURE REVIEW**

## 2.0 LITERATURE REVIEW

### 2.1 CHEMICAL NATURE OF GLYCOGEN.\* #&

Glycogen is a polymer containing glucosyl residues joined by ether linkages which are made by loss of water between hydroxyl groups. The linkage always involves the hemiacetal hydroxyl on C-1. Most of the bonds are linked to C-4 of the neighbouring residue, and the kind of polymer known as an amylose chain contains nothing but these 1-4 glucosidic bonds, and is therefore termed a 1-4 glucan.(Fig 1)

**FIG 1.**



Glycogen does not have long amylose chains, due to the presence of many branches. These branches are formed by the additional glucosidic bonds with the hydroxyl group on C-

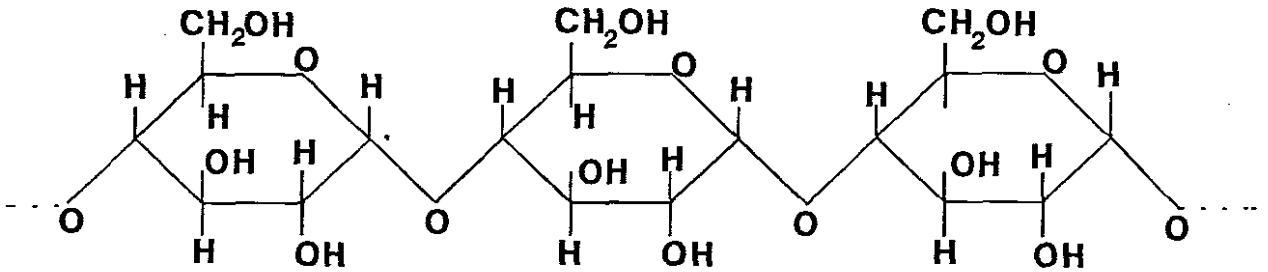
---

\* Histological and histochemical methods. 1st Ed. J A Kiernan  
# Biochemistry: A functional approach R W McGilvery (1970)  
& Principles of biochemistry. Smith et al. (1970)



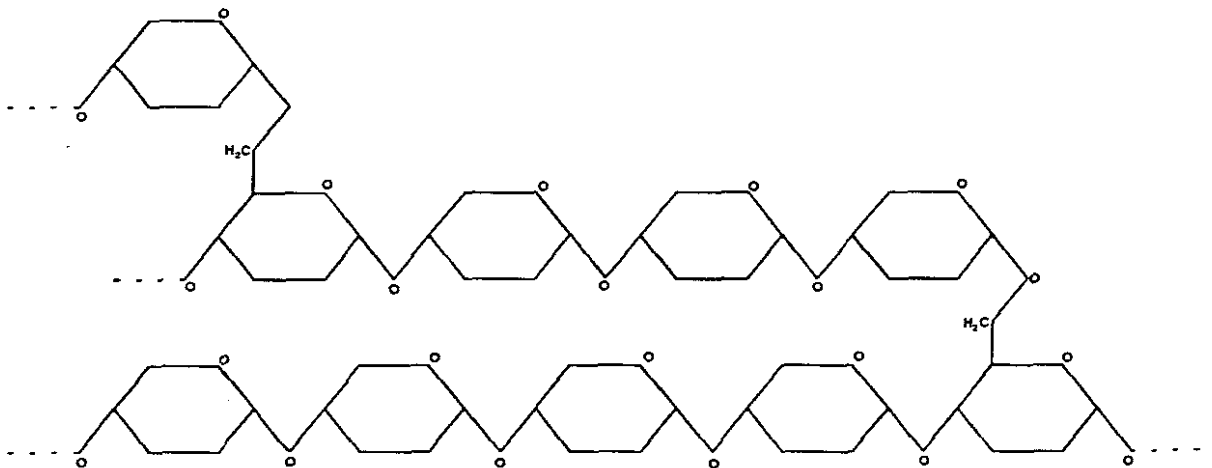
6 (Fig II), and the interior of the molecule which has 1-6 bonds at an average spacing of four 1-4 linked residues (Fig III).

**FIG II**



Glycogen contains linear amylose chains formed by linking carbons 1 and 4 of glucose through oxygen.

**FIG III.**



Branches occur in the amylose chains where carbon 6 of a residue is also linked through oxygen to the C-1 terminal of another chain segment.

Ultrastructurally, glycogen appears as discrete particles in cells, evidently composed of aggregates of molecules with molecular weights ranging around  $10^7$ , of which about two-thirds is water. The particles also contain the enzymes

concerned with the formation and breakdown of glycogen. The amount of glycogen varies widely amongst different tissues. Liver and skeletal muscle tissue contain the largest stores, but the amount depends upon the nature of the diet and the activity of the animal.

## 2.2 OSMIUM TETROXIDE/POTASSIUM FERROCYANIDE METHODS

The earliest known reference to the use of extra contrast enhancing media to enhance ultrastructural glycogen was by Karnovsky in 1967 and 1971, who used ferrocyanides in conjunction with osmium tetroxide. After primary aldehyde fixation, tissue was post-fixed with an osmium tetroxide/potassium ferrocyanide (OPF) mixture. Presumably the osmium was partially reduced, which made the glycocalyx stain extremely dark. With minimal lead staining, the glycogen particles became very electron dense while the nucleoproteins only stained faintly and nuclei had an empty, clear appearance. Ribosomes could only be discerned with difficulty, although with uranyl staining these structures were also observed. Potassium ferrocyanide was used at a concentration of approximately 1,5% however, decreasing this concentration also decreased the contrast of the glycogen particles. The chemical nature and mode of staining of this OPF complex had not been established at that time but it proved helpful in ultrastructural and cytochemical studies.

The same technique was used by de Bruijn in 1973 to selectively contrast glycogen. With a series of blocking and extraction methods this researcher set out to prove that the particles contrasted, were actually glycogen. Not only  $\hat{A}$  and  $\beta$ , but  $\_$  particles, first described by Drochmans (1962), were stained. The chemical nature of the staining had still not been determined at this time, therefore an argument other than those of a chemical nature had to be raised, to support the fact that the stained particles were glycogen. In normal glycogen-containing cells, the contrasted particles were localized in positions similar to those seen in identical cells, stained by conventional lead solutions following  $\text{OsO}_4$  fixation. In the areas occupied by contrasted particles, the application of a lead citrate reaction did not reveal any additional contrasted particles. Particle syntheses, (from glucan 1-phosphate and dextrin by the tissue enzyme phosphorylase), (de Bruijn, 1973) were demonstrated in liver tissue taken from adrenalectomized, starved mice. According to de Bruijn these particles were lacking in the liver tissue incubated in a medium without glucose 1-phosphate. In adrenalectomized starved animals, such particles were not observed in the liver parenchymal cells, whereas in the liver cells of similarly treated animals given glucose or cortisone, numerous contrasted particles were present.

Various workers used Karnovsky's method for contrasting glycogen in tissue and blood buffy blocks for electron microscopy. Amongst these were Dvorak et al (1981), who

used the OPF method for contrasting glycogen in leukemic cells incubated in DAB medium for myeloperoxidase. The improved images provided by this method, as well as their ability to demonstrate glycogen and myeloperoxidase, significantly enhanced their ability to identify cell types and, therefore, to aid in the diagnosis of disease processes.

In their paper published in 1984, Riemersma, Alsbach and de Bruijn tried to explain why the OPF reaction selectively stained glycogen. As has been stated, polysaccharide (glycosaminoglycan) molecules such as glycogen, are characterized by numerous hydroxyl groups. Chelate formation of such hydroxyl groups with potassium osmate is a possible first step in the reaction with glycogen. The resulting compounds would be cyclic osmic acid esters, analogous to the compounds which have been found when unsaturated lipids react with osmium tetroxide. It has, however, remained uncertain whether the contrast-donating osmium/iron complex was formed in a primary reaction step, as proposed by de Bruijn and van Buitenen in 1981, or in one of the later phases of the treatment. Evidence presented by Riemersma et al (1984) lead to the conclusion that ferrocyanide partially regulated the oxidation-reduction potential of the reaction medium in the primary reaction. Adsorption of the ferrocyanide anion to colloidal  $\text{OsO}_4 \cdot n\text{H}_2\text{O}$ , formed later in the reduction of  $\text{Os}^{\text{vi}}$ -intermediates, could account for the observed uptake of iron and the subsequent increase in density.

Generally, none of the investigators thus far, who have contributed to the use of ferrocyanides as extra contrast media for glycogen, have tried to distinguish between disease states using the morphochemical nature of this product.

### 2.3 CHEMICAL NATURE OF PEROXIDASE \*<sup>6</sup> #

The name "peroxidase" embraces several enzymes of plant and animal origin. They are all iron-containing haemoproteins which catalyse the \* reaction in which the nett effect is the removal of two atoms of hydrogen from each molecule of the donor substance.



The substrate is hydrogen peroxide which, when it is bound to the enzyme, oxidises other substances much more rapidly.

In mammals, peroxidase activity is present in the granules of myeloid leukocytes, in some neurons and in secretory cells. A positive histochemical reaction is also given by the haemoglobin of erythrocytes, possibly due to the catalase contained in these cells.

Peroxidase is not inhibited by 70% alcohol, 4% formaldehyde or brief fixation in glutaraldehyde (Burstone 1961).

---

6 Principles of biochemistry. Smith et al. (1970)

\* Histological and histochemical methods. 1st Ed. J A Kiernan

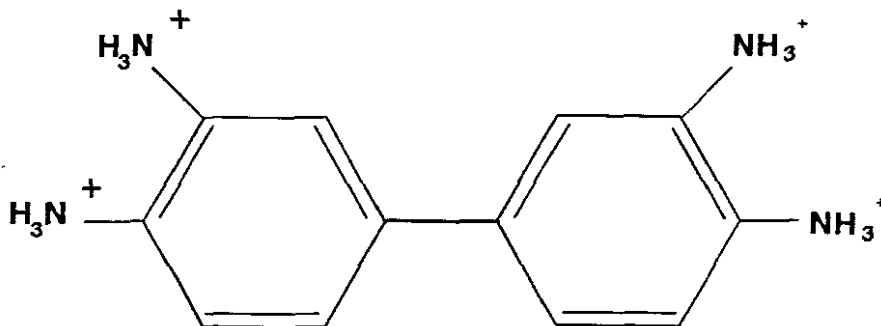
# Biochemistry: A functional approach R W McGilvery (1970)

### 2.3.1 HISTOCHEMICAL LOCALIZATION

Histochemical methods for peroxidase are based on the catalysed reactions of hydrogen peroxide with substances that yield insoluble coloured or electron-dense products upon oxidation.

The donor most widely applicable to the histochemical localization of peroxidases is 3,3'-diaminobenzidine tetrahydrochloride (DAB), (Fig IV), introduced by Graham and Karnovsky in 1966.

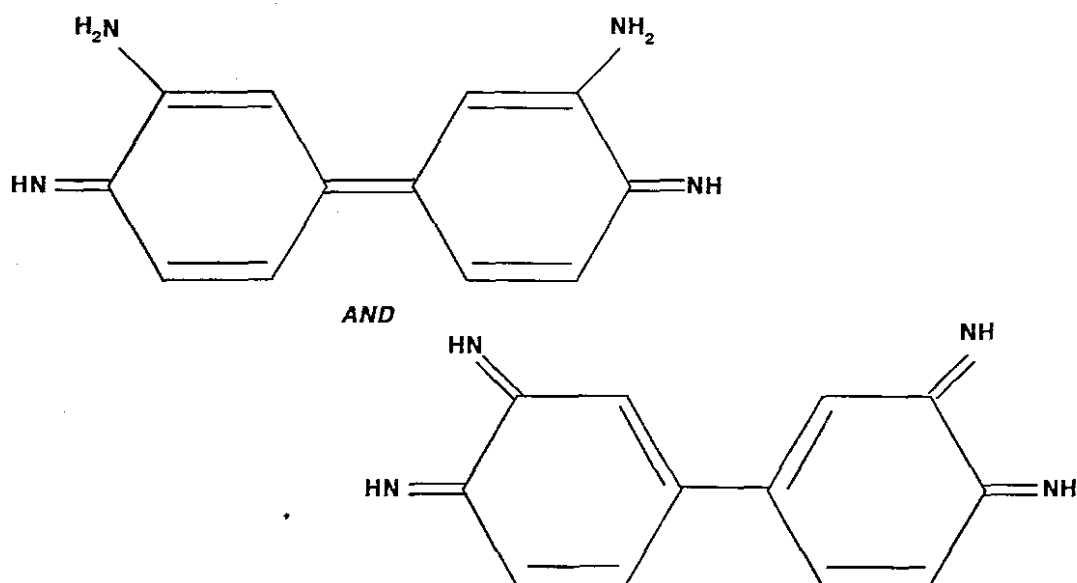
**FIG IV**



**3,3' DIAMINO BENZIDINE**  
**MOLECULE**

The spontaneous oxidation of this amine by hydrogen peroxide is quite slow, but in the presence of peroxidase an insoluble, amorphous, brown electron-dense substance is rapidly precipitated at the site of the enzyme activity. The initial products of oxidation are presumed to be quinone-imines: (See Fig V.)

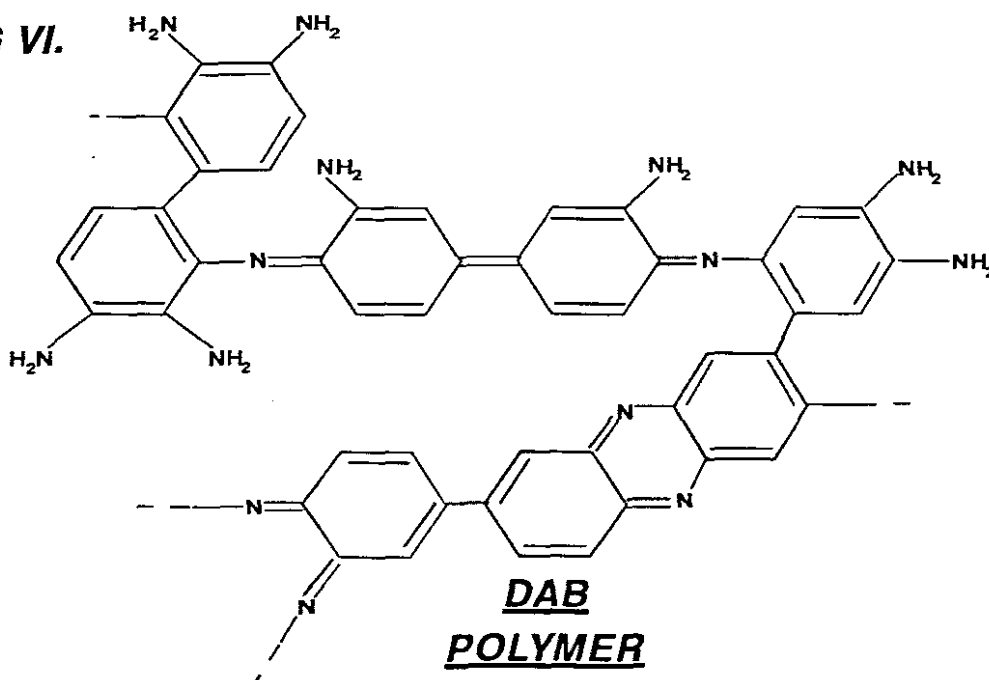
**FIG V.**



**QUINONE IMINES**

These unstable compounds immediately re-react with DAB to yield polymers, which contain the quinonoid and indamine chromophores.

**FIG VI.**



This reaction is an oxidation reaction and may be brought about by hydrogen peroxide and catalysed by peroxidase. The polymers are thought to contain such structures as shown in Fig VI.

The density of this product may be further enhanced by treatment with osmium tetroxide.

## 2.4 PEROXIDASE METHODS

As early as 1967 Karnovsky et al used the DAB peroxidase reaction to successfully detect injected horseradish peroxidase (HRP) in the glomerular capillaries of mice, a technique which was originated by Strauss in 1962. A 2,5% phosphate-buffered glutaraldehyde solution was used for the fixation of the tissue.

Novikoff and Goldfischer (1969) modified the original Karnovsky method so that peroxisomes could be stained with DAB. These experiments were performed at a pH of 9 and high levels of DAB and  $H_2O_2$ , with fixation of the tissue in either buffered glutaraldehyde or formaldehyde, although optimum results were obtained with the former. Their results indicated that the catalase contained in these peroxisomes, was broken down into peroxidase subunits by alkaline hydrolysis, and was consistent with their earlier results that incubation in a highly alkaline medium was required to demonstrate these organelles with DAB.

In their attempt to classify the cells of Hairy Cell leukaemia, Reyes et al (1978) recognized the fact that higher concentrations of glutaraldehyde inactivated the peroxidase found in these cells. The main result of their study was to prove that Hairy Cells yielded a positive reaction in the



presence of DAB and H<sub>2</sub>O<sub>2</sub>, and hence the synthesis of a peroxidase-like activity located in the endoplasmic reticulum of these cells. Reyes and his co-workers (1978) found that although MPO was highly resistant to fixatives, these cells contained a peroxidase activity sensitive to standard glutaraldehyde fixation. With the use of comparative methods, they proved that although a positive reaction for peroxidase was detectable using low concentration glutaraldehyde fixatives, all their samples were strongly positive with no prior fixation. The Hairy Cell peroxidase, as it was known then, was characteristic in that its localization was restricted to the perinuclear cisternae and the endoplasmic reticulum (ER). These criteria also differentiate it from MPO, which, in addition to the ER, always involved the Golgi apparatus and the granules of the granulocytic and monocytic precursors.

Breton-Gorius et al (1978) further modified the above-mentioned technique to detect the peroxidase found in megakaryoblasts during their study of the blast crisis of granulocytic leukaemia, which appeared to be similarly affected by the higher concentrations of glutaraldehyde found in the standard fixatives. These workers applied three different fixatives to blood buffy coats, namely:-

- a 1,25% phosphate buffered glutaraldehyde.
- b Tannic acid paraformaldehyde/glutaraldehyde (TAFG).

- c Fixation in 1,25% phosphate buffered glutaraldehyde, but extended incubation in the DAB medium.

The best results were obtained with the fixation protocol in (b). This peroxidase, which was localized in the perinuclear cisternae and the endoplasmic reticulum of the megakaryoblasts, as well as in similar structures in the platelets, was termed platelet specific peroxidase (PPO). The consensus was that this activity was very sensitive to inhibition by aldehyde fixatives under conditions in which the peroxidase activity was preserved in granulocytic precursors. The true identity of this enzyme, which was present in normal platelets, was unknown, because no biochemical data was available at that time. These workers proved that in spite of the DAB method not being specific for peroxidases, the product that was isolated was not catalase since, when tested with a specific method for this enzyme, the reaction product had an entirely different distribution.

Escrignano et al (1984) studied the peroxidase found in cutaneous mast cells using the same TAFG fixative as Breton-Gorius (1976), and localized this peroxidase which appeared to be similar to PPO in the same structures (ER and perinuclear cisternae). With this method the peroxidase activity could not be localized in the granules of the mast cells which, according to these workers, belies the common origin of mast cells and basophils. However, they do state that different micro-environmental stimuli could modify the phenotypical properties of cells derived from a common precursor. Many arguments do support the haemopoietic origin of the mast cells (Nakahata et al 1982) and even their

common origin with basophil granulocytes (Zucker-Franklin 1980).

Gerrard et al (1976) confirmed that peroxidase was involved in the prostaglandin synthesis by platelets. Similar associations between prostaglandin synthesis and peroxidase had been described in other types of cells, and human mast cells have been shown to generate prostaglandins as well (Cavallo 1976). The fact that peroxidase was localized by similar methods in megakaryoblasts, platelets and mast cells suggested that this was the same substance. (Heynen et al, 1984)

Monahan and Dvorak (1985) used standard fixation techniques and Karnovsky's original peroxidase method to differentiate between acute myeloid and lymphoid leukaemias, where the results of the routine blood smears and clinical opinions were not equivocal. The differential diagnosis between acute myeloblastic (AML) and acute lymphoblastic leukaemia (ALL) is important since the therapeutic strategies differ. The diagnosis of acute leukaemias is a difficult problem for those laboratories that deal with this material on a regular basis, and prognostic implications mandate that all available means be used to differentiate these two leukaemias from each other. In their article on characterising "difficult" leukemias, Hewson et al (1986) concur with these findings. Sampling for ultrastructural studies should be as complete as possible to exclude the possibility of there being more than one cell line present.

Sensitivity of the above-mentioned methods was extremely high provided the proper pre-treatment and subsequent incubation was carefully controlled. De Jong et al (1985) even suggested using different chromogen protocols and they recommended that the use of Dab-imidazole and DAB-Co<sup>2+</sup> or Ni<sup>2+</sup> ions could be advantageous. Strauss (1979 & 1982) encountered similar problems of low sensitivity and suggested similar remedies. Penetration of the substrate into the blood or tissue blocks was the single biggest problem however, and in many cases, where the tissue was extremely dense, the reaction product could not be discerned in thin sections from tissue blocks that were more than a certain thickness. However, careful cutting of these blocks, ensuring that they were thin enough (< 1mm thick), did solve the problem.

A comparative study of various myelo- and lymphoproliferative diseases and the peroxidase content of megakaryoblasts in chronic and acute granulocytic leukaemia has never been undertaken. In this study this aspect will receive some attention.

## 2.5 CHEMICAL NATURE OF DNA. # \$ % \*

Nucleic acids are the macromolecules that carry genetic information and are responsible for transmission of information for the synthesis of proteins. The nucleic acids

---

# Biochemistry: A functional approach R W McGilvery (1970)

\$ Molecular biology of the cell. Alberts et al (1989)

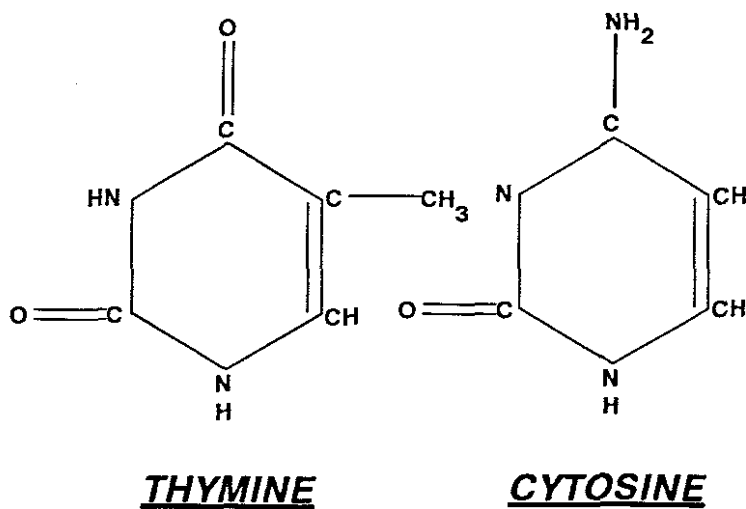
& Principles of biochemistry. Smith et al. (1970)

% Molecular biology of the gene. 4th Ed. Watson et al. (1987)

are of two kinds: those containing ribose and those containing deoxyribose. Both are linear polymers of nucleotides that are formed by phospho-diester linkages between the 5'-phosphate of one nucleotide and the 3'-hydroxyl group of the sugar of the adjacent one, and in the case of DNA, is formed into a double helix.

Nucleotides consist of a pyrimidine or purine base (Fig VII) linked to a sugar, either ribose or deoxyribose, and phosphate esterified to the sugar at carbon 5.

**FIG VII.**

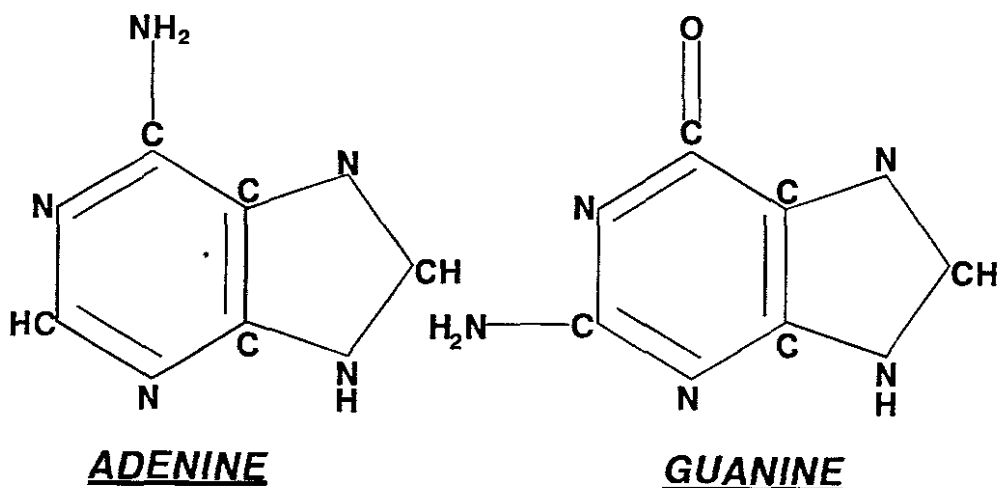


Pyrimidines are derivatives of the heterocyclic compound pyrimidine. The principal pyrimidines found in DNA are thymine and cytosine.

Purines are derivatives of purine which is a six-membered pyrimidine ring fused to a second ring, formed by two additional nitrogen atoms and one carbon atom. Adenine and

guanine (Fig VIII) are the major purines of both types of nucleic acids.

**FIG VIII.**



The deoxyribonucleic acids are polynucleotides in which the phosphate residues of each nucleotide form di-ester linkages between the deoxyribose moieties.

The DNA of each species shows a characteristic composition that is unaffected by age, environmental factors, etc. Samples of DNA from different organs or tissues of the same species are identical in composition in higher organisms.

DNA is a right-handed double helix in which two polynucleotide strands are wound around each other, so that there are ten base pairs for each turn. The double helix, which has a diameter of 2nm, has both major and minor grooves. The two chains are held together in part by

hydrogen bonding, each amino group being joined to a keto group, i.e adenine (A) to thymine (T), guanine (G) to cytosine (C) etc. The two chains are not identical but are complementary in terms of the appropriate base pairing, A to T and C to G, and they are antiparallel. If, for example, one chain is linked 5' to 3' with respect to AG, GT, TC, etc, then the complementary chain is linked 3' to 5' TC, CA, AG, etc.

Denaturation of DNA can be performed by heating a sample of the DNA in a given ionic environment, producing an increase in ultraviolet absorption and decreasing the optical rotation and viscosity, which reflects the disruption of the hydrogen bonds between the two strands in the double helix.

Since the interactions between the bases in the two strands are co-operative in a manner similar to the interactions between the molecules in a crystal, the disruption of the ordered helical structure occurs over a small temperature interval, much like the melting of a crystal. The more uniform the G + C content of the DNA, the narrower the width of the thermal transition. For this reason, the heat denaturation of double stranded DNA is referred to as the "melting" of the DNA, and the temperature at which 50% of the DNA is denatured, is termed the melting temperature or  $T_m$ .

DNA preparations from diverse sources possess different  $T_m$  values, which depend on the absolute amounts of G + C and

A + T. The  $T_m$  is lowered by the addition of urea or by formamide and in 95% formamide, DNA is completely separated into single strands at room temperature, but for all practical purposes such a high concentration would never be used.

Denaturation of DNA is a reversible process. If DNA is completely denatured, the two complementary strands will reassociate (anneal) by a slower process, consisting of two component reactions. The first is of the second order, and involves nucleation of complementary sequences on two strands, followed by a rapid first order zipping reaction.

The principle of this heat denaturation and annealing of the DNA under carefully controlled conditions of ionic concentration and pH, is used as the basis of in situ hybridization. The relevant viral DNA which has been separated into linear fragments by enzymatic action, is marked by random primed incorporation of digoxigenin labelled deoxyuridine triphosphate (dUTP). The dUTP is linked via a spacer arm to the steroid hapten digoxigenin (Fig IX), which is only found in digitalis plants such as *Digitalis purpurea* and *Digitalis lanata*.

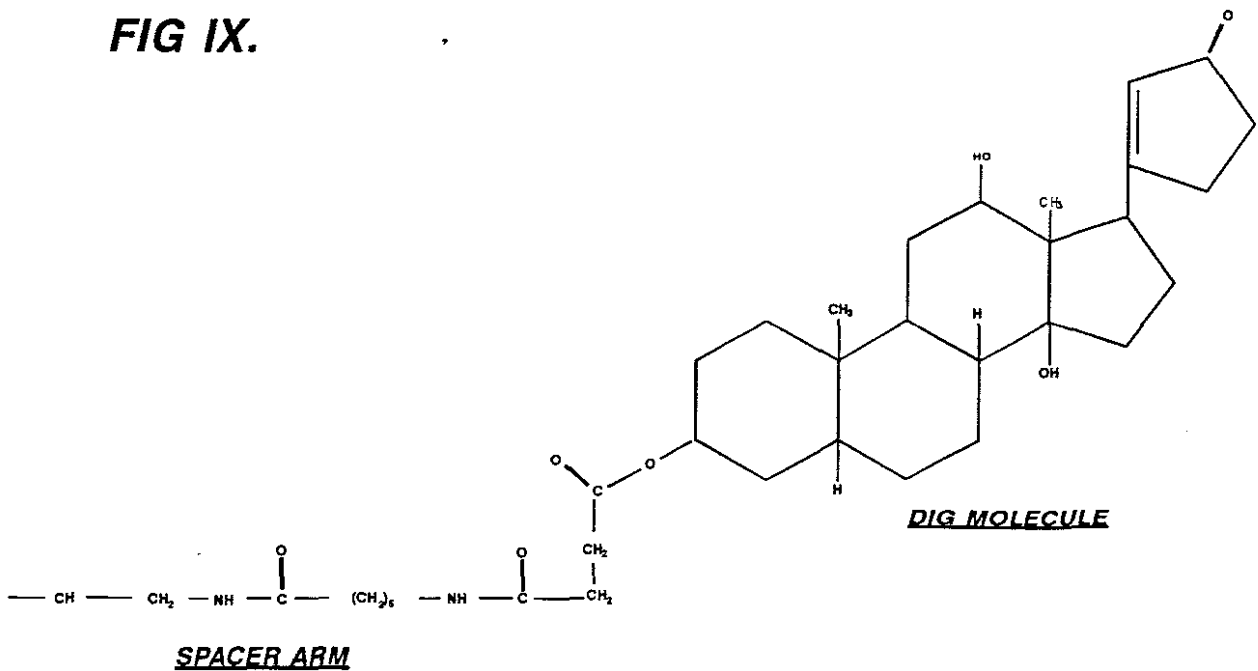
After hybridization to the target DNA, the mis-matched hybrids are eliminated by stringency washes, and detected by enzyme-linked immunoassay using an antibody conjugate (either anti-digoxigenin alkaline phosphatase conjugate anti-



<Dig>AP or anti digoxigenin peroxidase conjugate anti-  
<Dig>POD).

Subsequent enzyme-catalysed colour reactions with the  
appropriate substrate are used in the final process.(See FIG X)

**FIG IX.**



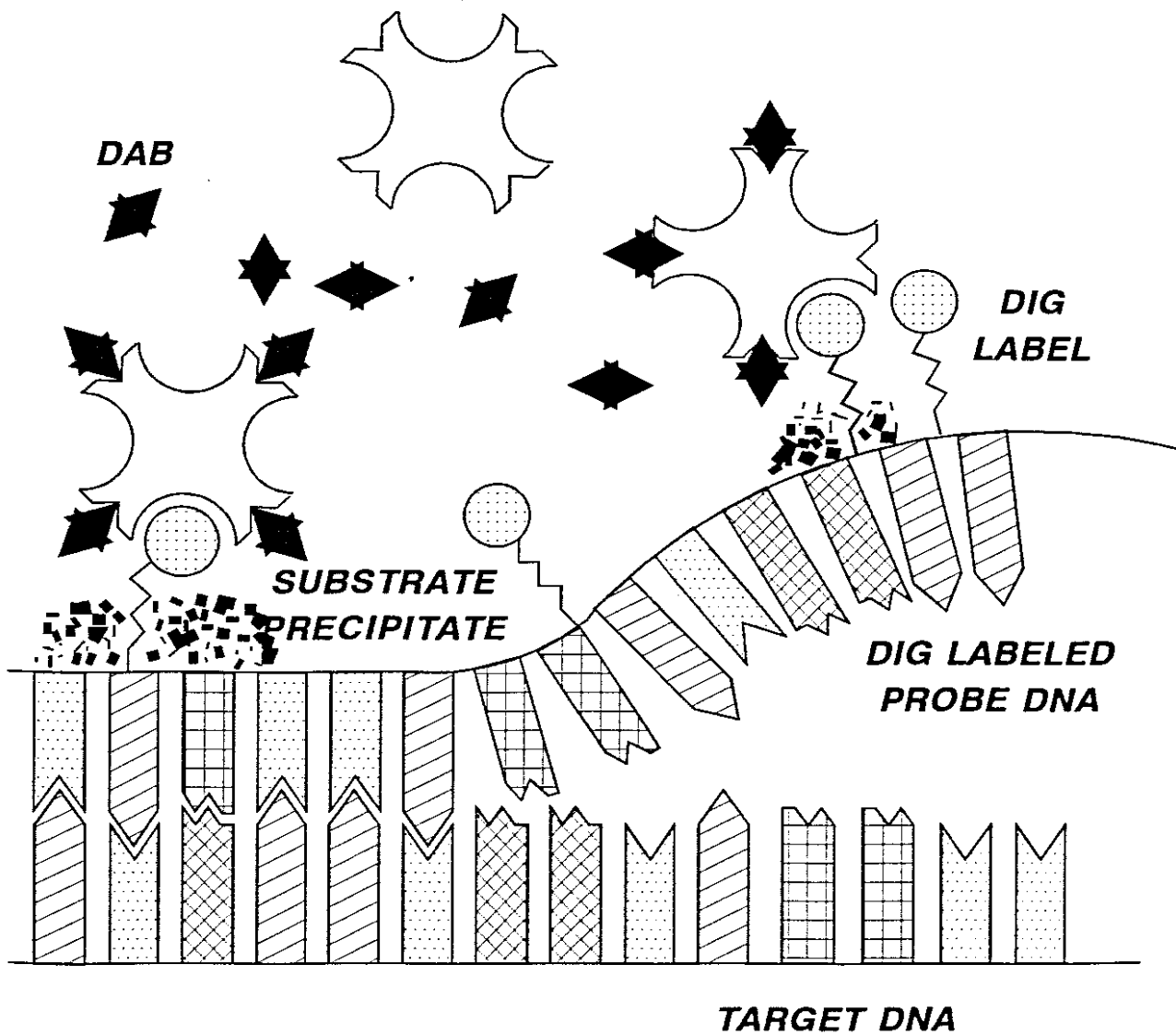
## 2.6 IN SITU HYBRIDIZATION METHODS

As early as 1979 Howley et al described a technique for the  
evaluation of homologous sequences of related DNA with the  
use of different concentrations of formamide, to perform  
annealing at temperatures as low as  $T_m - 50^\circ\text{C}$ . In  
combination with the Southern blotting technique, it was  
possible to map regions of homology and determine the

amount of nucleotide base match for each of the homologous regions.

**FIG X.**

**ANTI <DIG> POD  
CONJUGATE**



Hybridization of probe and target DNA and detection of the final product by enzyme linked immunoassay.

Brigati et al (1983) described a method of in situ cytohybridization for the detection of specific viral genomes in infected cell cultures or paraffin embedded tissue sections. The hybridization mixture contained 50% formamide and 2ug/ml of biotin-labelled probe DNA. This method described

the specific detection of viral genomes in cells, and clearly revealed viral inclusions in routinely fixed paraffin-embedded tissue sections using standard immunohistochemical techniques. The method also distinguished products of viral genome replication from host cell genetic material, and although not as sensitive as the best autoradiographic methods of the time, the procedure did offer several distinct advantages. The probes were easy to prepare and could be safely handled in the laboratory, hybridization reactions could be performed under conditions where significant morphological detail could be obtained and furthermore, retrospective investigations could be carried out on archival material.

Myerson et al (1984) using biotin labelled cytomegalovirus (CMV) probes, and essentially the same procedure as Brigati, studied two immune-compromised cases. Their method differed from the former in that the final labelling was performed with an avidin-biotinylated peroxidase complex. The peroxidase was detected with a modified DAB method. Specificity of the biotinylated CMV probe was tested by hybridizing in situ to lung sections, heavily infected with Herpes Simplex, Varicella Zoster and Adenoviruses. No staining was present in any of the control sections.

As has been stated previously, the formation of nucleic acid hybrids is a reversible process, and an understanding of the parameters which affect their stability enables one to determine the optimal conditions for discriminating between perfect and imperfect hybrids. Wahl et al (1987) defined the melting temperature  $T_m$ , as the temperature at which half the

duplex molecules have dissociated into their constituent single strands. It is affected by the monovalent cation concentration ( $M$  in moles/litre), the base composition expressed as mole fraction of G and C residues, the length in nucleotides of the shortest chain in the duplex ( $L$ ), and the concentration of helix-destabilising agents such as formamide. They derived the following formula, valid from pH 5 to 9, by analysing the influence of the above-mentioned factors on hybrid stability of probes longer than ~50 nucleotides. The melting temperature could then be expressed with the following formula:

$$T_m = 81,5^{\circ}\text{C} + 16,6 \log M + 41 (\text{mole fraction G} + \text{C}) - 500 / L - 0,62 (\% \text{ formamide})$$

They found that it was often convenient to perform the hybridization at low stringency, and washing at increasing stringencies and analysing the results after each wash.

Sato et al (1987) however, used the principle that under stringent conditions ( $T_M -26^{\circ}\text{C}$ ) viral DNA sequences anneal only if 85% of the sequences are identical. They found the presence of HPV DNA in all but one of the cases that they studied.

Lewis et al (1987) used a biotin-streptavidin-polyalkaline phosphatase detection method to visualise in situ hybridizations of cell smears, fresh frozen sections and formalin-fixed paraffin embedded sections with a variety of DNA probes. Amongst the probes that were used were HPV6 (Human papilloma virus type 6), HPV11 and HPV16 and the method yielded results that were comparable to, or better than those using a polyclonal anti-biotin antibody as a primary

reagent. The biotin-streptavidin-polyalkaline phosphatase detection method was rapid, reliable, sensitive and economical to use, and there were no known health hazards associated with the reagents used.

Wolber et al (1989) studied the sub-cellular localization of virally encoded RNA by a pre-embedding in situ hybridization technique, using colloidal gold as an electron-dense marker. Fibroblasts infected with Herpes simplex virus (HSV) were fixed, made more permeable by proteolysis, then hybridized with a biotinylated HSV DNA probe under conditions favouring DNA-RNA hybrid formation. The HSV probe was localized with 5nm streptavidin-gold conjugates, and transmission electron microscopy revealed 5nm gold particles in singlets and clusters in the HSV infected cells. The advantage of this pre-embedding technique was that it avoided the imposition of embedding material between target nucleic acids and biotinylated probes, and furthermore, provided excellent ultrastructural detail.

Yun and Sherwood (1992) drew a comparison between biotinylated and <sup>32</sup>P-labelled probes of type 6b HPV, which showed that the sensitivity of the biotinylated probes was consistent with that of the <sup>32</sup>P-labelled probes.

In-situ hybridization was carried out in the standard manner with a medium containing 50% formamide similar to that of Brigati et al (1983). The pre-embedding EM technique was performed by cutting thick sections of tissue, and incubating them with the biotinylated probe mixture, incubating in anti-

biotin peroxidase conjugate, post-fixing them in OsO<sub>4</sub>, dehydrating in graded alcohols and embedding in resin.

Pre-determined known positive areas were excised from wax blocks, deparaffinized, dehydrated and embedded in LR White resin for the post-embedding technique. Sections were cut and mounted on nickel grids, hybridized and incubated in the colloidal gold solution. The grids were then examined in a transmission electron microscope.

The study demonstrated that biotinylated HPV probes were as sensitive as the <sup>32</sup>P-labelled probes in the detection of target DNA sequences by in-situ hybridization. The findings of this study suggested that the probes could efficiently hybridize non-packaged pre-virion DNA, but that the process was not effective when the mature virion was assembled. Both the DAB method and the colloidal gold method showed reaction product in areas of condensed chromatin, with very little reaction product on the viruses themselves, which could be due to the inability of the proteolytic enzyme to digest the virus protein coat after formalin fixation.

Yun and Sherwood (1992) speculated firstly, that there might be a small number of virus particles in the intra-nucleolar areas which could not be identified as viruses. Secondly, that the viral genome did not fully mature before the infected cells reached the very end of the superficial layer. Thirdly, that viral maturation occurred less frequently than viral DNA replication.

Mulhaupt et al (1992) utilised a post-embedding in situ hybridization technique using non-radioactive materials.

Biopsies were embedded in Lowicryl K4M resin at low temperature, and hybridization was carried out with probes specific for HPV types 6/11, 16 and 18. The hybrids were detected by anti-horseradish-peroxidase antibodies conjugated with 10nm colloidal gold particles.

The gold particles were found in the nucleus as well as some cytoplasmic sites. The gold particles in the cytoplasm, were found on the intermediate filaments, and in the nucleus the localization was episomal, vacuolar and chromosomal.

Mulhaupt et al (1992) emphasized that this method relied on minimal fixation (1% glutaraldehyde/0,1%paraformaldehyde for 30 min), and a low temperature embedding protocol in polar resins.

The result that surprised them was the cytoplasmic localization of the label, which was not observed light microscopically and even on semi-thin sections no labelling was apparent in the cytoplasm. They speculated that due to the fact that viruses had to enter and leave the cytoplasm, viral RNA had to be present in the cytoplasm of infected cells and that their probe labelled this RNA. The fact that the labelling was seen in the intermediate filaments could however have been some vagary of the method and be a non-specific reaction.

—ooOoo—

CHAPTER III  
METHODS



## 3.0 METHODS

### 3.1 COLLECTION OF TISSUE, BLOOD AND BONE MARROW SPECIMENS.

The specimens initially used were pre-collected, 2,5% phosphate buffered glutaraldehyde\* fixed tissue, peripheral blood and bone marrow aspirate specimens for diagnostic purposes. The tissue had been received over a number of years and several specimens were processed immediately for diagnostic purposes, while others were kept in a storage buffer\*\* at pH 7,4 in a refrigerator (4°C) for attention at a later date. Reserve material from processed tissue was also stored similarly.

Blood buffy material was handled similarly to tissue at first, but as the study progressed it became apparent that on receipt of new specimens, be they blood, bone marrow or tissue, alternate methods of fixation had to be employed. Peroxidases, specific to megakaryoblasts, platelets and mast cells were inhibited by higher concentrations of glutaraldehyde found in the standard fixatives. It became evident that a modified fixation protocol had to be developed so that certain specimens could be collected exclusively for a particular method or procedure.

---

\*See appendix no 3.

\*\*See appendix no 8.

In previous years cervical punch biopsies for the diagnosis of condyloma, atypical condyloma and CIN lesions were collected in phosphate buffered formalin#, as well as in phosphate buffered glutaraldehyde, so that both light and electron microscopy could be performed on them. The unused tissue from those specimens that had been kept in storage buffer, was used for part of this study. As with the blood and bone marrow it became apparent that a modified compound fixative would have to be used to obtain optimum results for light and electron microscopic DNA in situ hybridization.

### 3.2 METHODS FOR THE OSMIUM TETROXIDE- POTASSIUM-FERROCYANIDE (OPF)PROCEDURE

Generally all of the tissue used for this part of the project had previously been received in either 2,5% buffered glutaraldehyde\*, or fresh in saline for diagnostic purposes. After fixation (variable from 3-18 hours) the tissue was kept in storage buffer in case further tests were needed. On the day prior to processing, the tissue was trimmed into smaller blocks (approx. 1 cubic mm) and left overnight in fresh storage buffer. Any new tissue that was received was fixed overnight and either processed immediately or stored.

---

#See appendix no 4.

\*See appendix no 3.

Two different methods of glycogen fixation, originally described by Karnovsky (1971) and de Bruijn (1973) were used:

- a Karnovsky's unbuffered OPF medium, consisting of 1,5% potassium ferrocyanide in a 1,5% osmium tetroxide solution.\*
- b A phosphate buffered OPF medium.\*\*

### 3.2.1 ORIGINAL OPF METHODS

Normal liver tissue and striped muscle which are naturally rich in glycogen were used as positive controls. Blocks were cut from stored tumour tissue rich in glycogen and also processed for this part of the experiment. Negative controls were obtained by incubating half of the above-mentioned tissue in diastase@ digestion medium for three hours, changing the reagent hourly. After fixation in the two above-mentioned OPF fixatives for one hour, the blocks were en bloc stained with uranyl acetate# and then dehydrated in graded ethanol solutions (70%, 96%, 96% + 1% uranyl nitrate, 100%). The blocks were then impregnated with equal amounts of Spurr's resin## and 100% ethanol for 90 minutes. Two changes of pure Spurr's resin were used for 60 minutes each at room

---

\*See appendix no 14.

\*\*See appendix no 13.

@See appendix no 53.

#See appendix no 16.

##See appendix no 46.

temperature, then at 60°C for the same length of time. Embedding was performed with fresh Spurr's resin in pre-dried gelatine capsules (Elanco size 0). Polymerization took place overnight at 60-70°C for 16-18 hours in an incubator. The capsules were numbered and trimmed in a Reichert TM 60 block trimmer with a steel cutter. 1 $\mu$ m Survey sections were cut on an LKB Ultratome III with a glass knife, picked up with a toothpick, sharpened to a spade tip, and placed on a drop of water on a glass slide. The slide was placed on a hot plate, regulated to 70°C, until the water had evaporated and the sections adhered to the glass. While still hot, the slides were transferred to sodium methoxide\* to remove the resin. Two 100% ethanol rinses followed, after which the slides were washed in running tap water for 5 minutes. The slides were stained with a heated solution (70°C) of toluidine blue\*\* for 1 minute, washed in tap water, air-dried and mounted in DPX (BDH). The sections were then examined with a light microscope to select a suitable area for viewing with the electron microscope. The most suitable block was trimmed for thin sectioning with a diamond cutter in the block trimmer.

Thin sections (60-90nm thick) were cut on the LKB ultramicrotome with a glass knife, and the ribbons of sections were picked up on 150 or 200 mesh copper grids (Bio-Rad) and stored in a small tissue culture dish (Greiner) on filter paper until dry.

---

\*See appendix no 47.

\*\*See appendix no 49.

When the sections had dried, they were stained upside down on drops of uranyl acetate (Merck) in 50% ethanol\* on strips of dental wax for three minutes, rinsed by the dipping method, first in 50% ethanol, then in two changes of distilled water (30 dips each). The sections were then placed on drops of Reynolds' lead citrate stain\*\* for 5 minutes, rinsed in two changes of distilled water and placed in their respective dishes.

After drying, the sections were viewed in a Hitachi 600/2 transmission electron microscope at 75Kv, and relevant areas photographed. Low magnification (X1500-X2500), as well as intermediate (X7500-X10000) and high magnification (>X30000) electron micrographs were taken.

The film used in the electron microscope was either Ilford EM film, or Agfa Scientia 23D56 and was developed for 4½ minutes in Ilford PQ Universal liquid developer, diluted 1 in 10, fixed in Amfix (Maybaker) (diluted 1+3), and rinsed in running tap water for 10 minutes. After the negatives had dried they were printed in a Simmon Omega enlarger fitted with an Ilford multigrade enlarging head. The negatives were enlarged three times onto Ilford multigrade paper or Agfa multi-contrast paper. These prints were developed for 2 minutes in Ilford Ilfospeed paper developer diluted 1 in 15, fixed in Amfix (diluted 1+7), and rinsed in running tap water for 15 minutes, then hung up to dry. The relevant information such as

---

\*See appendix no 50.

\*\*See appendix no 52.

negative number and final magnification was recorded on the back of the prints.

### 3.2.2 MODIFIED OPF METHOD ACCORDING TO EM LABORATORY, TYGERBERG HOSPITAL

Unsatisfactory results such as low contrast (method a) and tissue damage as well as low contrast (method b), were obtained with the two methods used. Modifications had therefore to be made to either one of the two methods to improve the results. The same tissue, as used in the above experiment was used for the modified method. Tissue blocks similar in size to the above, together with the negative diastase controls were post-fixed in the modified OPF mixture\* for 1 hour at room temperature, rinsed with distilled water and dehydrated in 70%, 96% and 100% ethanol. Increasing the concentration of the potassium ferrocyanide increased the contrast, and it was found that raising the concentration to 2%, gave much more contrast as well as optimum fixation. No en bloc staining was employed with this technique as uranyl salts leach glycogen from tissue. The subsequent treatment of the tissue was similar to the above method up to the grid staining stage. The uranyl acetate thin section stain# was omitted for the reason given above. Photography and subsequent treatment of the negatives and prints was similar to the method described earlier.

---

\*See appendix no 15.

#See appendix no 50.

### **3.3 METHODS FOR THE DEMONSTRATION OF MYELOPEROXIDASE AND PLATELET PEROXIDASE.**

Specimens of peripheral blood and bone marrow previously received, were prepared according to the technique described by Anderson in 1965. The blood (5ml) or bone marrow (>2ml) was centrifuged in a narrow 10mm tube at 3000rpm for 10 minutes. When the yield of marrow was less than 2ml, an Eppendorf tube was used to concentrate the pellet. The plasma was drawn off with a narrow bore Pasteur pipette and 2,5% phosphate buffered glutaraldehyde fixative was carefully pipetted onto the buffy layer of white cells and platelets. After fifteen minutes the now solidified disk of plasma and cells was loosened with a pointed orange stick, and transferred to a small specimen bottle containing the standard buffered glutaraldehyde fixative for further fixation.

The above technique was slightly modified by the electron microscopy laboratory at Tygerberg Hospital at a later stage by replacing the sodium citrate (3,8% soln) with heparin (10-20 IU/ml of blood) as anticoagulant. The reason for using this anticoagulant was that cell size was not affected in the time it took to centrifuge and fix the specimen, moreover a more precise concentration of the enzyme reaction product was obtained in the cells. When the haematological parameters suggested that a rare megakaryoblastic leukaemia was a diagnostic possibility, peripheral blood from the patient was collected with heparin as anticoagulant. The blood was centrifuged to obtain a buffy layer, and this was fixed with

tannic acid formaldehyde/glutaraldehyde\* (Breton-Gorius 1978), because the standard phosphate buffered glutaraldehyde fixative inhibited the platelet specific peroxidase (PPO). The disc of cells was fixed at 4°C for a maximum period of three hours, because prolonged immersion in this fixative had a deleterious effect on the morphology of the cells as well as an inhibitory effect on the PPO. After three hours the specimen was washed in two changes of storage buffer and kept in this buffer until needed.

Any tissue received was fixed in 2,5% phosphate buffered glutaraldehyde and divided in half. One half was kept and fixed overnight while the other half was routine wax processed. A Haematoxylin & Eosin stained section was used to determine the area of interest in the opposing face of the tissue (which had been kept in storage buffer). When fresh tissue was received on a saline swab it was divided so that one half could be fixed in standard phosphate buffered glutaraldehyde fixative, and the other half in tannic acid formaldehyde/glutaraldehyde (TAFG). When blood and bone marrow specimens were collected for the platelet peroxidase procedure (PPO), the same TAFG fixation protocol, as described above, was followed.

---

\*See appendix no 5.



### 3.3.1 METHODS FOR THE DEMONSTRATION OF MYELOPEROXIDASE

Methods for myeloperoxidase were originally developed by Graham and Karnovsky in 1966 and Dvorak in 1972 which consisted of fixing tissue in buffered glutaraldehyde and cutting tissue and blood buffy layers into 1 mm<sup>2</sup> blocks and placing into 0,05M Tris buffer, (pH 7,6)\* for approximately 18 hours at 4°C. Peroxidase in the control blocks from the same buffy layer was blocked for half an hour at room temperature (~22°C) with the blocking reagent.@ All the specimen blocks were transferred to the DAB incubating medium+ for 60 minutes at ~22°C, after which they were rinsed in two changes of Tris buffer and post-fixed in either 1,5% buffered osmium tetroxide++, or alternatively in an OPF fixative# for 60 minutes. En bloc staining was performed with 4% uranyl acetate in 70% ethanol## for 30 minutes. This had the effect of enhancing contrast in the tissue, and also of starting preliminary dehydration. The blocks were subsequently dehydrated in 70%, 96%, 96% + 2% uranyl nitrate and 100% ethanol. Impregnation of the tissue was carried out in a 50:50 mixture of Spurr's resin@@ and 100% ethanol for 90 minutes. Two changes of pure resin followed, the first at room temperature (~22°C) for 60 minutes and the second at 60-70°C for the same length of time. The blocks were then

---

\*See appendix no 19.

@See appendix no 29.

+See appendix no 20.

++See appendix no 12.

#See appendix no 14.

##See appendix no 16.

@@See appendix no 46.

embedded in fresh resin in pre-dried gelatin capsules, and placed in an incubator at 60-70°C for  $\pm$  18 hours to polymerise and harden.

The blocks were trimmed, cut and stained similarly to the method described earlier.

### 3.3.2 MODIFIED MYELOPEROXIDASE METHOD ACCORDING TO EM LABORATORY, TYGERBERG HOSPITAL.

Thin slices (< 1mm) of the buffy layer were cut with a sharp razor blade into blocks approximately 1mm<sup>2</sup> and transferred to Tris buffer at pH 7,6. Blocks had to be thin (0,5mm) so that the reagents could penetrate the full thickness. Control blocks were similarly cut and the endogenous peroxidase blocked with blocking reagent@ at ~22°C for half an hour. For detection of peroxidase, incubation of the tissue took place in the modified DAB medium\* with continuous agitation at ~22°C in the dark. After incubation, the blocks were rinsed twice with Tris buffer and distilled water and post-fixed in either standard osmium fixative, or modified OPF medium\*\* for one hour. No en bloc staining or staining of thin sections with uranyl salts was performed after the OPF fixation. The rest of the processing was executed as set out in section 3.3.1.

---

@See appendix no 29.

\*See appendix no 23.

\*\*See appendix no 15.

### 3.3.3 PLATELET PEROXIDASE PROCEDURE

The platelet peroxidase method of Breton-Gorius (1976), Zucker-Franklin (1964) and the EM laboratory at Tygerberg Hospital (1989) was performed by cutting the tissue blocks thinly as before ( $\mu 0,5\text{mm}$ ) and placed in Tris buffer at pH 7,6 for 18 hours, then transferred to the DAB medium\*. Control blocks incubated in the blocking reagent were also included. A higher concentration of hydrogen peroxide (0,015% instead of 0,010%) was used to make more peroxide molecules available in the medium. Incubation was carried out in the dark with continuous agitation at  $\sim 22^{\circ}\text{C}$  for 60 minutes. Further treatment of the tissue blocks was similar to that in section 3.3.1.

The areas chosen for photography were carefully selected to illustrate the positivity of the myeloperoxidase reaction in the granules, as well as other structures of the cells. Where possible a cell or organelle which would normally react positively with the DAB reagent such as an erythrocyte would be included in the field of view to act as a positive control of the method.

Low power photomicrographs were taken in the range of 2000-3000X magnification to show as many cells as possible. An intermediate magnification, depending on the size of the cell, was then used to show each individual cell and was generally in the 6000-8000X range. To illustrate the DAB

---

\*See appendix no 23

positivity in the various structures, a higher magnification in the X10000-X30000 range was used.

The procedure for developing and printing of micrographs was similar to section 3.2.1.

### **3.4 IN SITU DNA HYBRIDIZATION METHODOLOGY**

The light microscopic methods according to Beckman et al (1985) and Brigati et al (1983) were employed for this study. Tissue was received both in the standard buffered formalin and glutaraldehyde fixatives and consisted of cervical punch biopsies for light and electron microscopy. Electron microscopy of these biopsies was used to confirm and correlate the cytological and histopathological diagnoses of dysplasia, condyloma, atypical condyloma and CIN III lesions.

#### **3.4.1 PREPARATION OF SLIDES**

Glass microscope slides were placed in a solution of non-ionic detergent such as Extran (Merck) for 30 minutes, rinsed in running tap water for 30 minutes, and then rinsed in distilled water. The slides were then taken through 96% ethanol and air dried in a 37°C incubator for 20 minutes, dipped in a solution of APES\* for 5 seconds, rinsed in two changes of 100% acetone and one change of distilled water and dried in a

---

\*See appendix no 24.

37°C incubator for approximately 18 hours. Note that silanes produce sulphuric acid fumes in contact with water vapour in air, therefore this procedure must be carried out in a fume cupboard and the slide racks handled while wearing gloves. Because this solution deteriorates, it should be made up freshly every time. The APES coating has the effect of creating a co-valent bond between the slide and the section picked up on it.

Paraffin wax processed sections, 5µm in thickness, were cut from formalin or glutaraldehyde fixed tissues, and floated out on distilled water in a water-bath at 56°C, picked up on APES coated slides and incubated for ~18 hours in a 60°C incubator. The knife was carefully cleaned with a swab dipped in 70% alcohol and wiped dry with a clean swab between sections so as to exclude contamination between blocks. The sections were de-waxed in xylol, taken through two changes of 100% ethanol, placed in 1% H<sub>2</sub>O<sub>2</sub> in 100% methanol for 30 minutes to destroy endogenous peroxidases, and then hydrated through descending concentrations of ethanol to distilled water. The slides were dipped in PBS<sup>+</sup> and incubated for 10 minutes in 0,02M HCl<sup>\*\*</sup> to facilitate hydrolysis of the hydroxyl bonds between the bases in the DNA molecule. The slides were neutralized for 6 minutes in PBS, after which the cellular membranes were delipidised in Triton X<sup>#</sup> for 1,5 minutes. The sections were again neutralized in PBS for 6 minutes and placed in the proteolytic

---

+See appendix no 25

\*\*See appendix no 26.

#See appendix no 27.

digestion medium## at 37°C for 10 minutes. The proteolytic digestion step is extremely critical as it must facilitate efficient intracellular penetration of the probe, without excessive disruption of cellular morphology or adhesive interactions, which anchor the sections to the glass surface. The reaction was stopped in Glycine/PBS+ for 6 minutes and secondary fixation took place in Para-formaldehyde/PBS++ for 5 minutes. This second fixation was reported to increase the strength of the hybridization signal three to five fold. (Brigati et al 1983)

The slides were washed in distilled water, then dehydrated in graded solutions of ethanol and air dried. The slides could now be stored for a week at 4°C if so desired.

#### 3.4.2 DNA in situ HYBRIDIZATION PROCEDURE.

A drop of hybridization mixture (20-40ul/slide)\* was placed on the sections, and siliconed coverslips carefully lowered onto the drop, as to allow the mixture to spread evenly without formation of air bubbles on the tissue. Six different Human papilloma viral (HPV) genomes were tested for, namely HPV 6, 11, 16, 18, 31 and 33. Positive and negative controls were also included. The slides were placed on a heating block at 95°C for 10 minutes to denature the viral target DNA. At the end of this period, the slides were cooled on a thick sheet plate glass which had been kept in a refrigerator at 4°C, then transferred to glass racks in a stainless steel dish. The bottom of the dishes contained folded paper towel which had been

---

##See appendix no 31.

+See appendix no 32.

++See appendix no 33.

\*See appendix no 37.

soaked with 2XSSC\*\* and formamide, to maintain a humid atmosphere inside the dish. A glass sheet was placed over the dish and the edges sealed with masking tape. The dish was placed in a 37-42°C incubator for 16-24 hours, for renaturation (annealing) to take place.

Following this the dishes were unsealed and the coverslips carefully shaken off or rinsed off with a carefully directed jet of 2xSSC. The slides were replaced in the glass staining racks and post-hybridization stringency washes were performed in the staining dishes, firstly in 2xSSC, then in 0,2xSSC\* for 20 minutes each at ~22°C on a shaker.

Immunological detection of the hybrids was carried out according to the *Boehringer Mannheim manual (1988)* and was performed at room temperature ~22°C. All the steps set out below were done at room temperature on a shaker except for the immunological labelling.

The slides were placed in Tris/HCl buffer solution# for 1 min, then packed onto glass strip racks and the tissue covered with anti <DIG>POD-conjugate\$ (Boehringer Mannheim), diluted 1 in 100 for 30 minutes. 100ul Of the diluted anti-body was used for each slide. The slides were then replaced in the staining racks and washed in Tris/HCl buffer% for 30 minutes.

---

\*\*See appendix no 38

\*See appendix no 39.

#See appendix no 40.

\$See appendix no 45.

%See appendix no 40.

They were placed in buffer solution 3<sup>+</sup> for 2 minutes then repacked onto the glass strip racks, the tissue covered with the DAB reagent and placed in a dark cupboard for the colour to develop. The reaction was visually checked after 30 minutes, then every 15 minutes thereafter. Too long incubation caused unacceptable background staining. When the reaction was considered adequate (this took approximately an hour), the slides were replaced in the staining racks and the process stopped by washing in buffer 4<sup>#</sup> for 5 minutes. The sections were further rinsed in distilled water and lightly counterstained with Mayer's haematoxylin (1minute), rinsed in tap water, dehydrated, cleared and mounted in DPX. The reaction was visually checked with the aid of a light microscope, and the slides showing a positive reaction for the different types of viruses were marked and the numbers recorded. The peroxidase method was preferred to the alkaline phosphatase method, because permanent preparations could be made in that way.

### 3.4.3 PROCEDURE FOR THE ULTRASTRUCTURAL DNA IN SITU METHOD.

Cervical biopsies kept in storage buffer were used for this part of the study. Sections with a suitably high density of koilocytic cells were matched with their corresponding tissue in the buffer. The whole length of the epithelium of the tissue was sliced into slivers, cut approximately 100-200 $\mu$ m in

---

+See appendix no 41.

#See appendix no 42.



thickness, dehydrated in graded ethanol and the endogenous peroxidases quenched by soaking in 1% H<sub>2</sub>O<sub>2</sub> in 100% methanol for 30 minutes.

The tissue was then rehydrated, dipped in PBS and placed in 0,02N HCl for 10 minutes to denature the bonds between the bases in the DNA molecule, neutralized in PBS for 6 minutes and then placed in 0,01% Triton X in PBS for 1,5 minutes to make the lipid membranes more permeable. The tissue was then treated with an 0,20mg/ml Pronase (Sigma type 24) in Tris/EDTA for 10 minutes at 37°C to facilitate efficient intracellular penetration of the probe. The reaction was stopped in 0,2% Glycine in PBS for 6 minutes and post-fixation took place in 4% Paraformaldehyde in PBS. The tissue was further rinsed in PBS/Glycine, dehydrated in graded alcohols, and finally placed in an Eppendorf reaction vial in a drop of 100% Ethanol. The open vial was placed in an incubator at 37°C for a few minutes so that the alcohol could evaporate. 50µl Of the relevant probe was added to the tissue in the vial which was closed and placed in a pre-heated dry block heater at 95°C for 10 minutes so that denaturing of the DNA could take place. Negative controls were incubated without probe DNA added to the hybridization mixture. After this time, the vial was rapidly cooled in crushed ice and placed in an incubator at 37°C for 18-24 hours so that annealing could take place. The tissue was then washed in two stringency washes, first in 2xSSC for 20 minutes at room temperature with agitation and secondly in 0,2xSSC for a further 20 minutes at room temperature with agitation.

The tissue was transferred to a Tris/HCl buffer@ for 5 minutes and then to the anti <DIG>POD labelling reagent\* for 30 minutes. The tissue was then rinsed in Tris/HCl buffer# and placed in DAB medium\$ for 1 hour in a dark box on a rotary agitator. The tissue was again rinsed in buffer## and distilled water. Post-fixation of the blocks proceeded in three ways:

- a Standard buffered osmium tetroxide.
- b Modified OPF mixture.
- c No post-fixation.

En bloc staining with uranyl salt solutions was only performed when the tissue was post-fixed in the standard way. When the OPF mixture was used for post-fixation, no en bloc or thin section staining was performed with any uranyl salts. Further processing of the tissue proceeded routinely, except that just prior to embedding the epithelium was cut into easily manageable blocks and serially embedded in pre-dried gelatin capsules.

Section cutting, staining with uranyl acetate\* and lead citrate\*\*, electron microscopy and photography were performed as described earlier.

---

@See appendix no 40.

\*See appendix no 42.

#See appendix no 18.

\$See appendix no 23.

##See appendix no 18.

\* See appendix no 50

\*\*See appendix no 51.

# CHAPTER IV RESULTS

## KEY TO LEGENDS

BL	:	Basal lamina
C	:	Chromosomes
Col	:	Collagen
ER	:	Endoplasmic reticulum
GER	:	Granular endoplasmic reticulum
Gly	:	Glycogen
Go	:	Golgi apparatus
F	:	Filaments
K	:	Keratin
L	:	Lysosome
Li	:	Lipid
N	:	Nucleus
Nu	:	Nucleolus
M	:	Mitochondrion
Mv	:	Microvilli
P	:	Plasma cells
PC	:	Perinuclear cisternae
PMN	:	Polymorphonuclear leucocyte
PV	:	Pinocytotic vesicle
R	:	Erythrocyte
SER	:	Smooth endoplasmic reticulum
V	:	Viruses
Z	:	Z-bands

—ooOoo—

# 4.0 RESULTS

## 4.1 RESULTS OF OSMIUM-TETROXIDE POTASSIUM FERROCYANIDE METHOD

### 4.1.1 DISTRIBUTION OF GLYCOGEN IN NORMAL LIVER

Normal liver tissue was processed with the original as well as the modified OPF method, to obtain a norm for the appearance of glycogen in this organ. Plate 1 shows the appearance of wax processed normal liver tissue stained with Haematoxylin & Eosin stain.

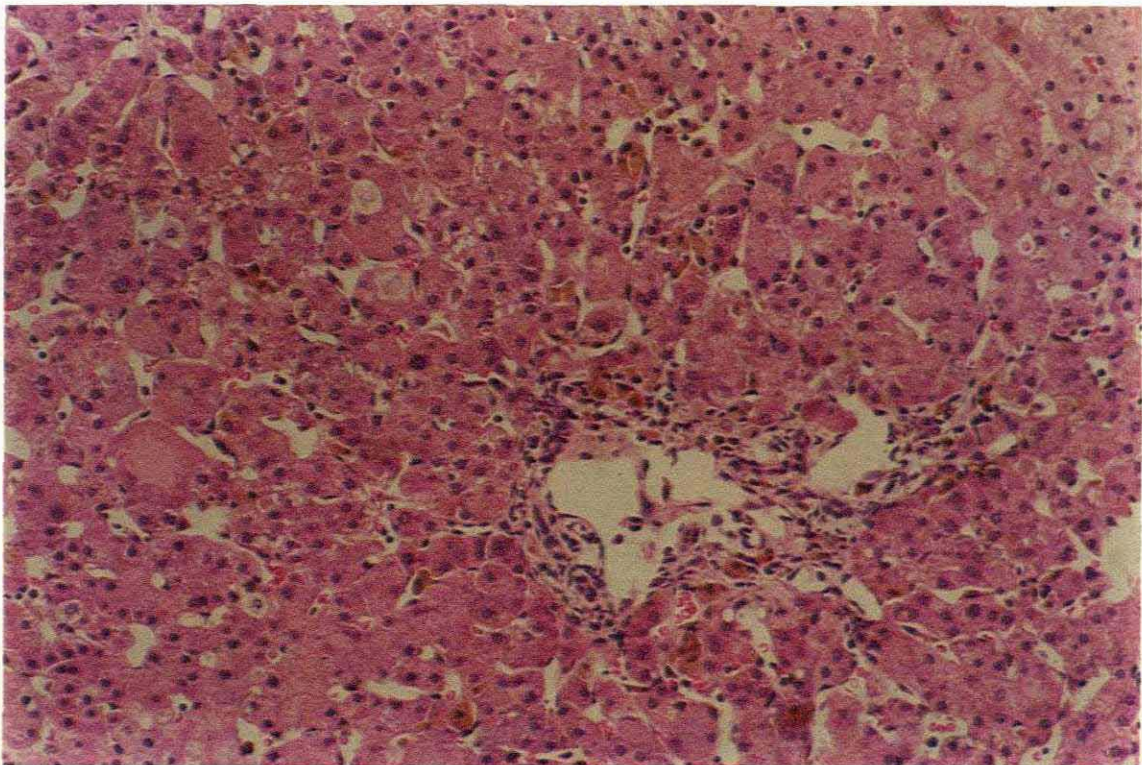


Plate 1

Paraffin wax section of normal liver cells.  
(Haematoxylin & Eosin X225)



With the normal glutaraldehyde fixed, osmium tetroxide post-fixed and uranyl stained processing method (OCUB), most of the glycogen was removed. At light microscopic level the toluidine blue stained resin section revealed that the glycogen had been leached out. Washed out empty looking areas were clearly visible in the cells of the section of normal liver tissue. (Plate 2)

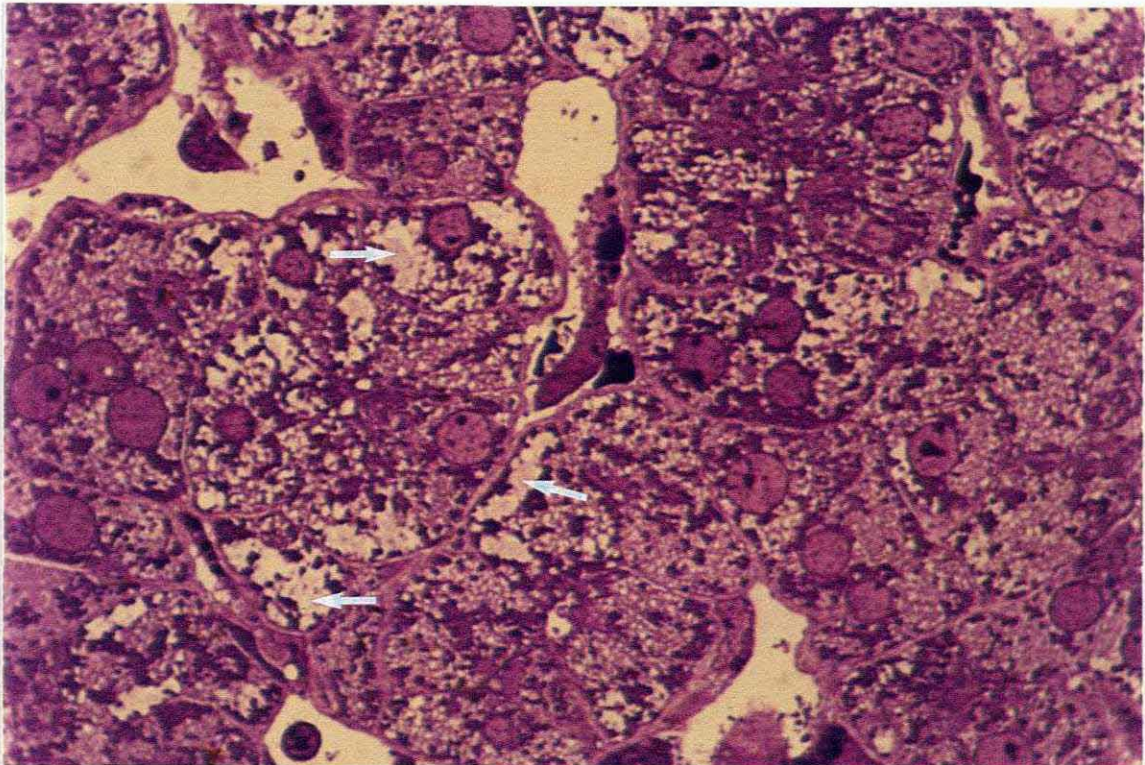


Plate 2

High light microscopic magnification of a section cut from an epoxy resin block of tissue processed with the standard OCUB method. Note the washed out areas (white arrows) clearly visible in the liver cells. (Toluidine blue stain X1125)

With the standard OCUB processing method, the electron microscope showed electron-lucent areas in the cells, and it appeared that in many cells the glycogen had been removed



completely. The results of this processing artefact can be clearly seen in the low power photomicrograph Plate 3.

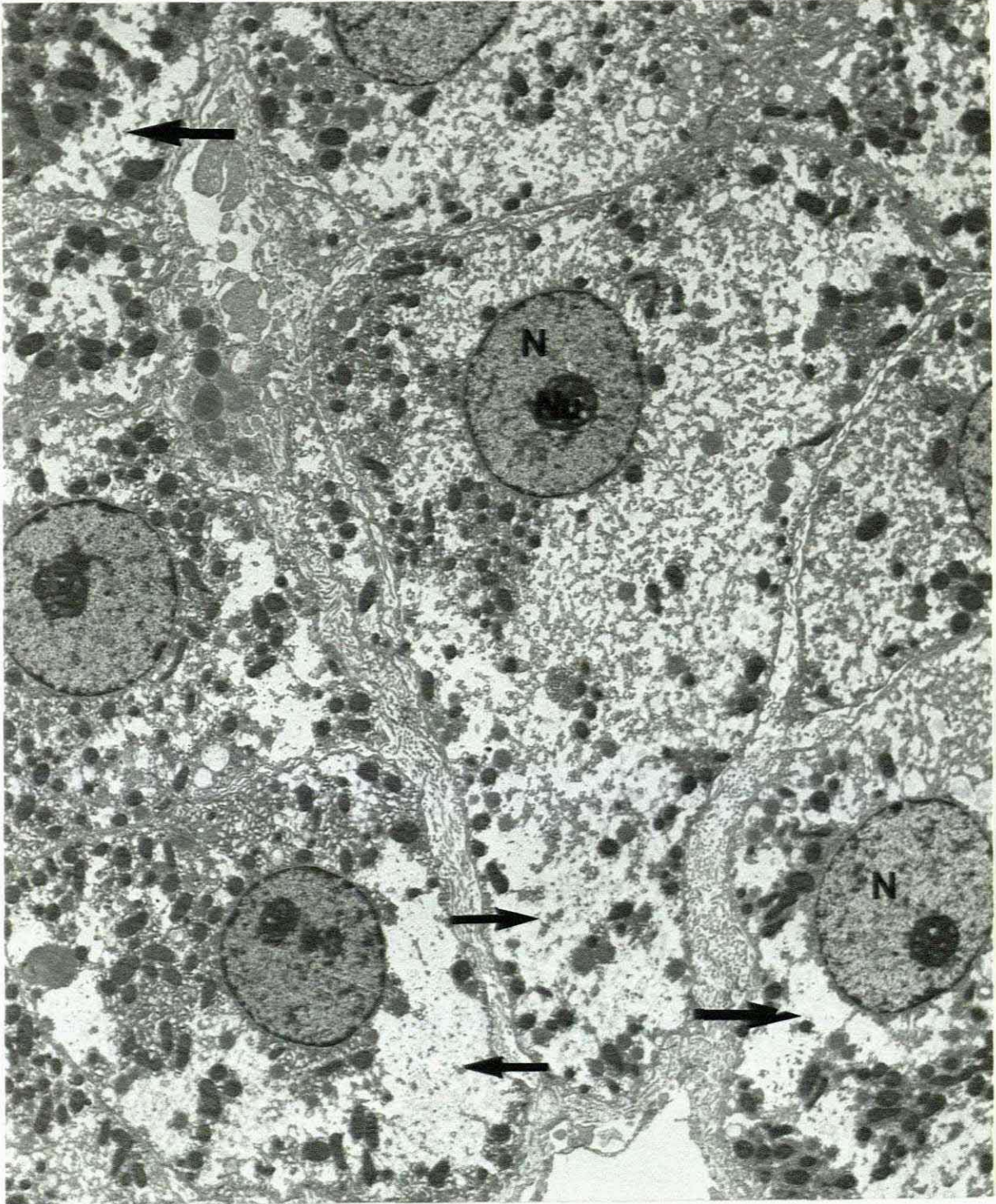


Plate 3 Low magnification of normal liver tissue processed with the standard method for electron microscopy to show the electron-lucent areas (black arrows) in the parenchymal cells where the glycogen has been leached out by the processing. (Resin, lead and uranyl X4500)



These electron-lucent areas are even more marked at higher magnification, as can be seen in plates 4 & 5.

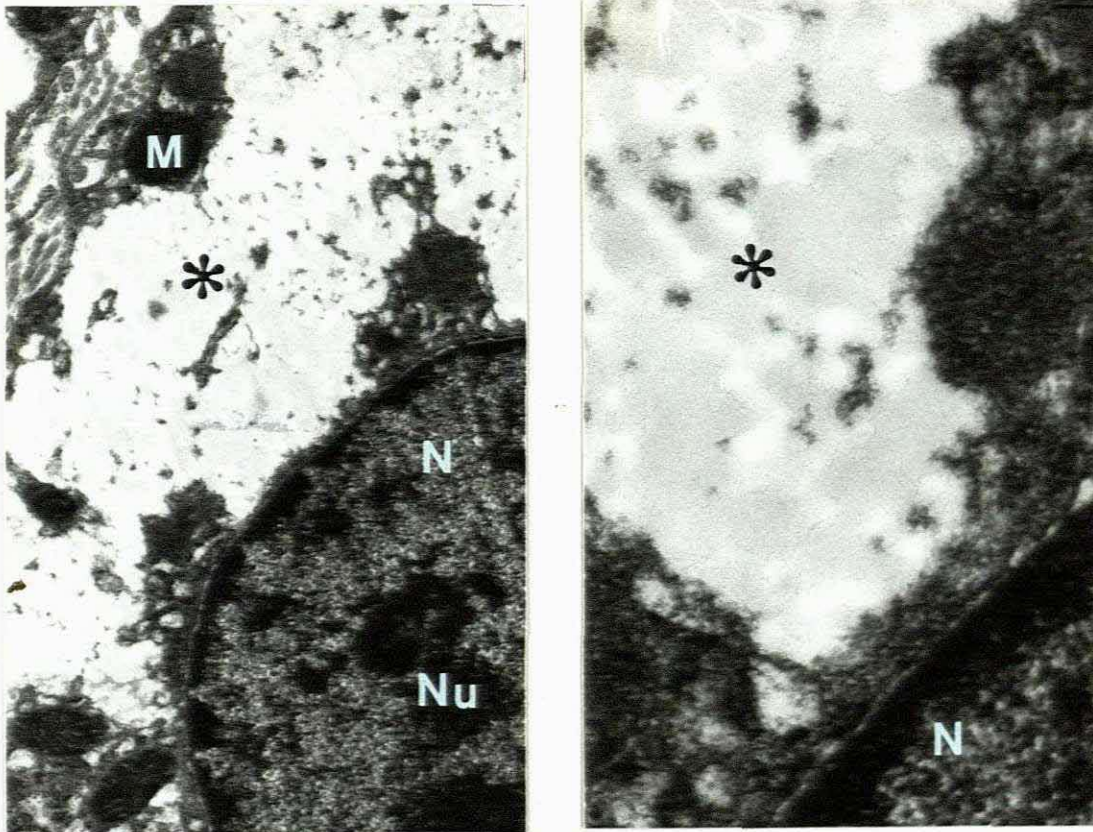


Plate 4 & 5

Higher magnifications of the same tissue showing detail of the electron lucent areas (black \*) in the liver parenchymal cells. (Resin, lead and uranyl X15000 and X60000)

Parallel sections from wax processed blocks of normal liver tissue were stained with the periodic acid Schiff's (PAS) method with and without diastase digestion to prove the presence of glycogen in the tissue. (See plates 6 & 7)

Duplicate blocks of normal liver tissue for electron microscopy were also subjected to diastase digestion (negative control) and processed in parallel together with the undigested blocks with the modified OPF method (Tygerberg Hospital).



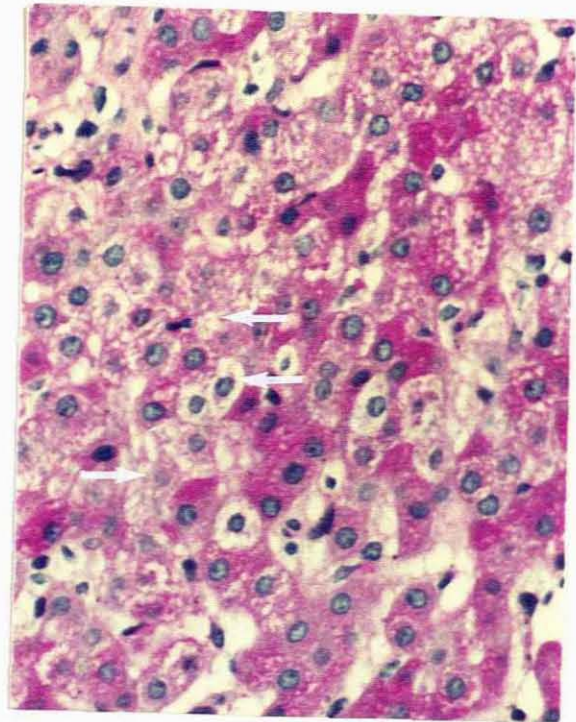
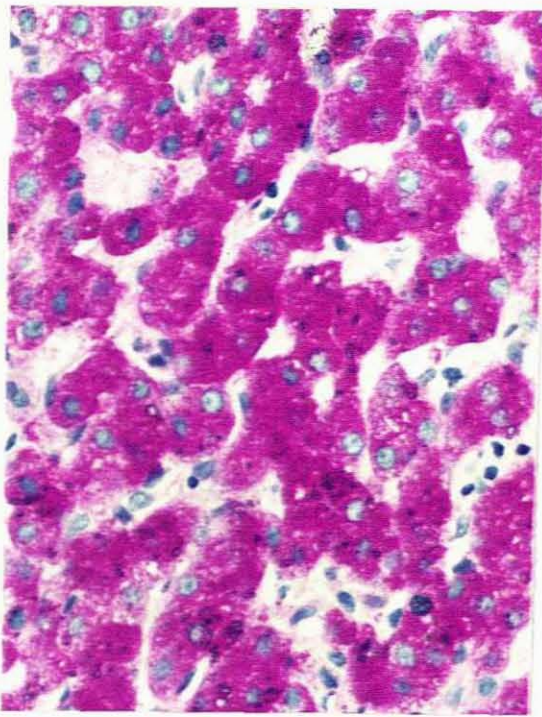


Plate 6 & 7 Paraffin wax processed sections stained with PAS method with and without diastase digestion. Note the removal of the glycogen in Plate 7. (W. arrows)(Wax, PAS + D X450)

A section from the negative control block is shown in plate 8. Although the diastase was applied for three hours the centre of the block still shows some positivity.

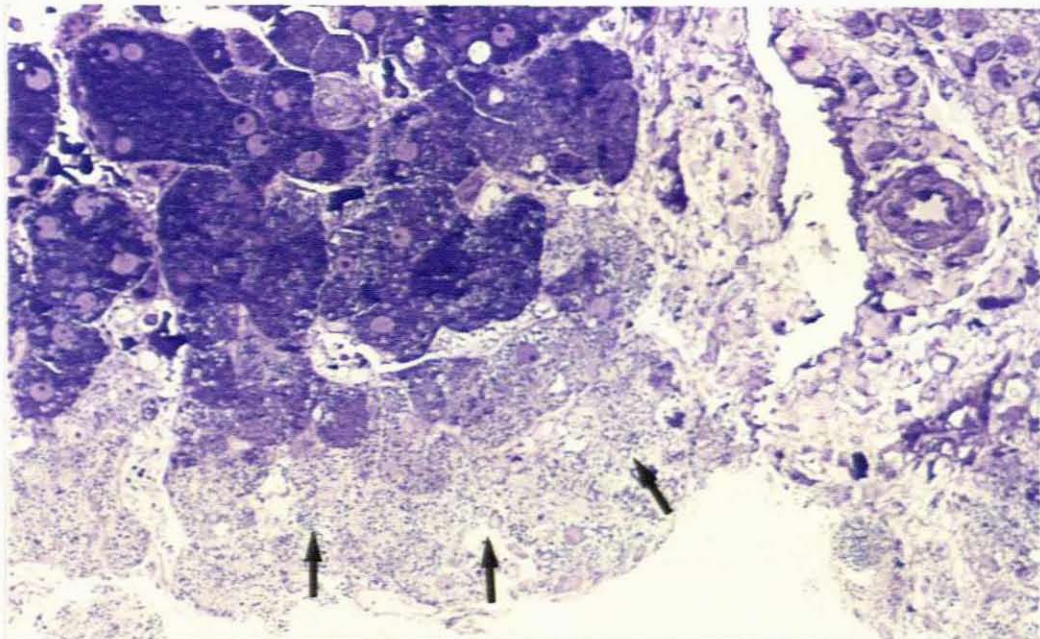


Plate 8 Resin section of liver tissue subjected to diastase digestion and processed with the modified OPF method. Note loss of glycogen. (B. arrows)(No en bloc uranyl staining, Tol. blue X450)



With this modified OPF method glycogen was retained in the tissue not subjected to diastase digestion. (See plate 9 & 10)

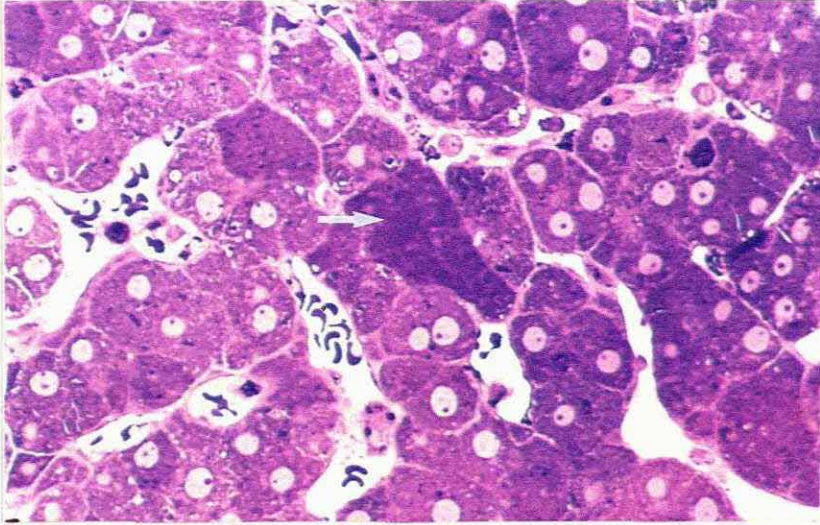


Plate 9 Epoxy resin section of the positive control liver that has been OPF processed to show the retention of glycogen. (No en bloc uranyl staining, Tol. blue X450)

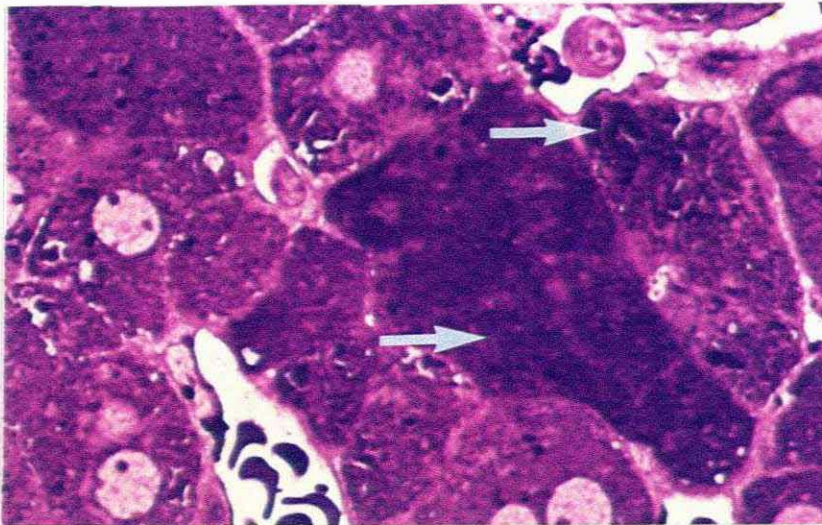
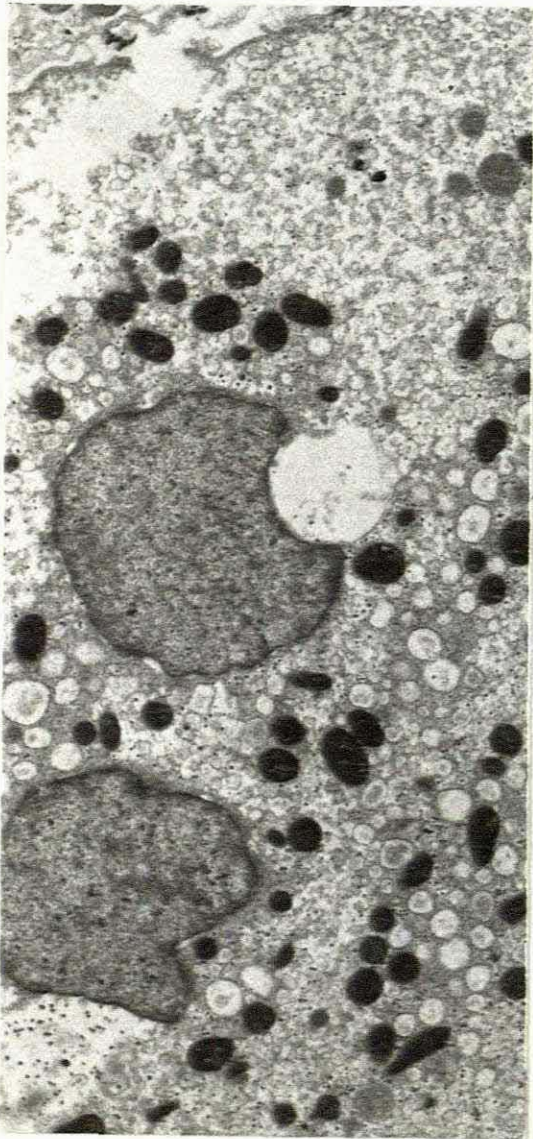


Plate 10 Higher magnification of previous area that clearly shows the dense staining glycogen in the liver cells (white arrows). (Tol. blue X1125)



A low and a high power electron micrograph that the major portion of glycogen has been digested in the control tissue. In plates 11 and 12 isolated moth-eaten looking particles of glycogen are still retained. The diastase digestion of the glycogen also had a deleterious effect on the morphology as can be seen from the damaged mitochondria. (Plate 12)



Plates 11 & 12

Low and high power micrographs of a thin section cut from a resin block to show digestion of glycogen by diastase. Note a few isolated glycogen particles that were retained. (Black arrows)(Resin, lead, no uranyl staining. X7500 & X45000)



The low power electron micrograph of a thin section, cut from tissue that was not subjected to diastase digestion, clearly shows retention of the glycogen. This appears as  $\hat{A}$  particulate glycogen and is extremely electron dense as can be seen in plate 13.

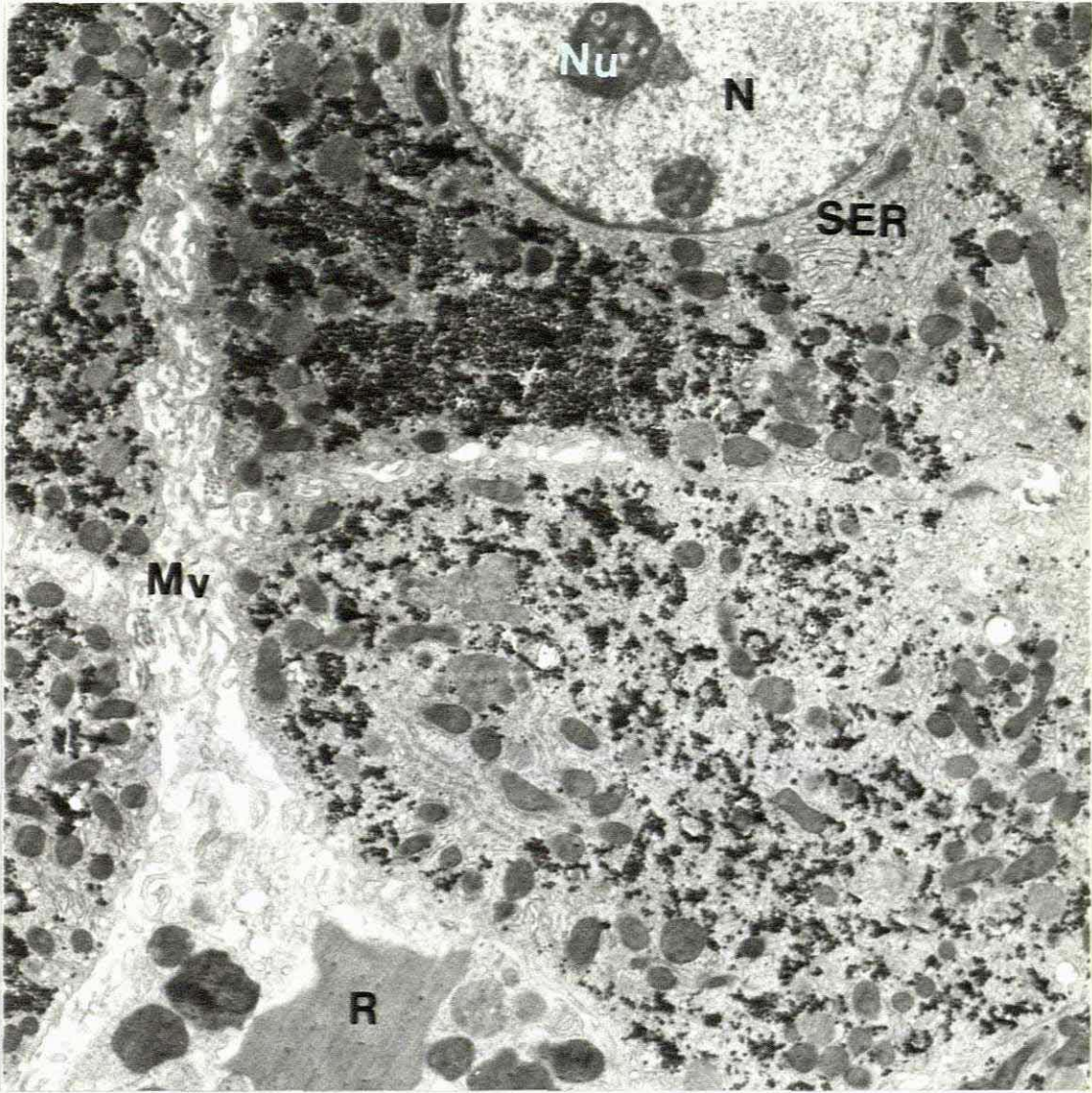


Plate 13 Low magnification micrograph of the tissue shown in plate 9 & 10, which was OPF processed with the modified method to show retention of glycogen (white arrows). (Resin, lead, no uranyl staining. X7500)

A higher magnification of the same resin section as in plate 13, shows the extreme electron density of the glycogen



particles when the tissue has been processed with the OPF method. (See plate 14)

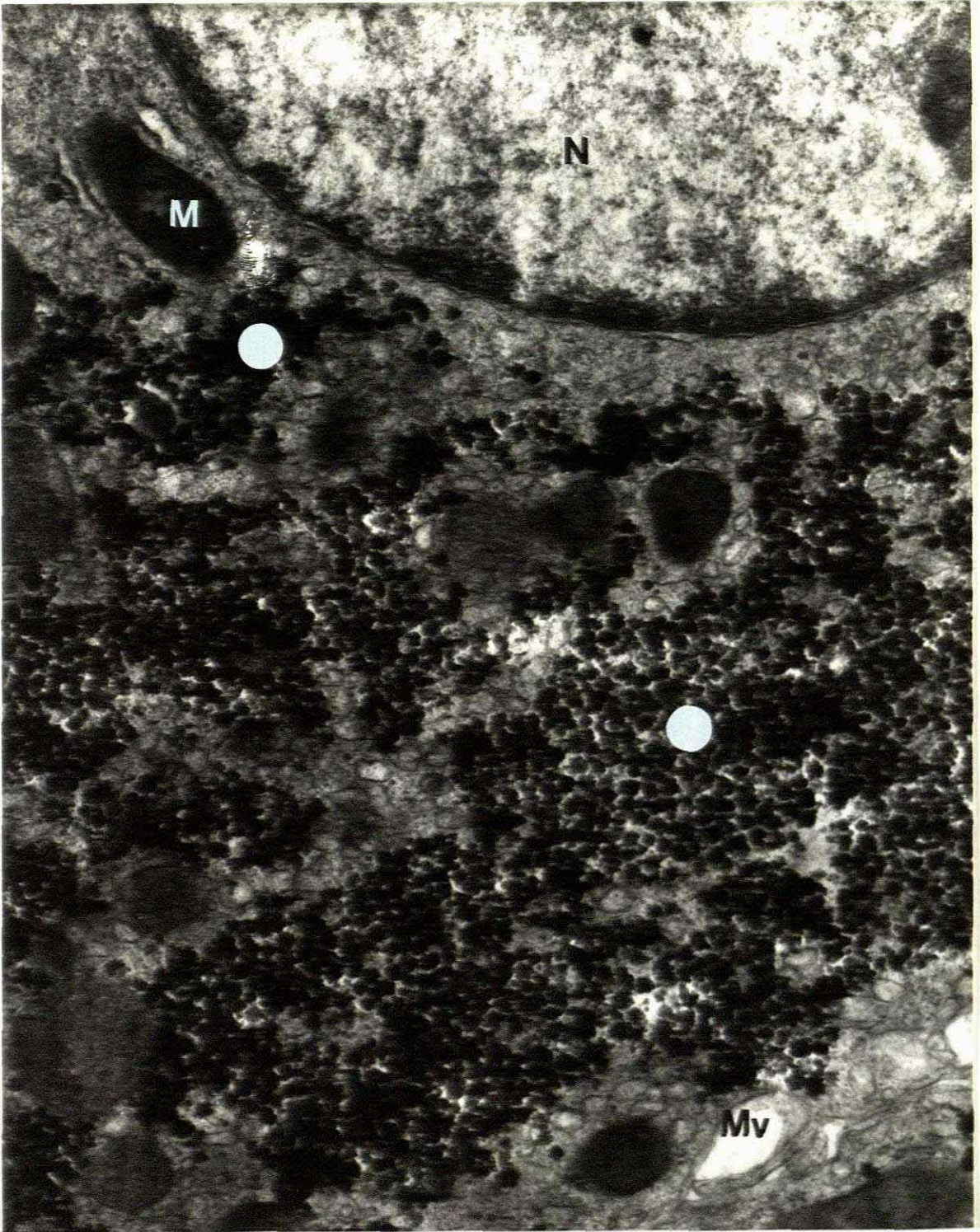


Plate 14

Higher magnification micrograph of the same tissue to show the normal distribution of glycogen in liver parenchymal cells, which in this case appears to be mainly  $\text{\AA}$  particles (white dots). (OPF, resin, lead, no uranyl staining. (X30000)



#### 4.1.2 DISTRIBUTION OF GLYCOGEN IN NORMAL MUSCLE

Taking into consideration that the tumours that were studied, were essentially tumours of mesodermal origin, it was necessary to process normal striated muscle tissue as well.

The first two photographs show the structure of normal skeletal muscle which was processed for routine histology. Haematoxylin and Eosin was the staining technique employed and the structure and staining of the muscle tissue appeared be normal. (Plate 15 & 16)

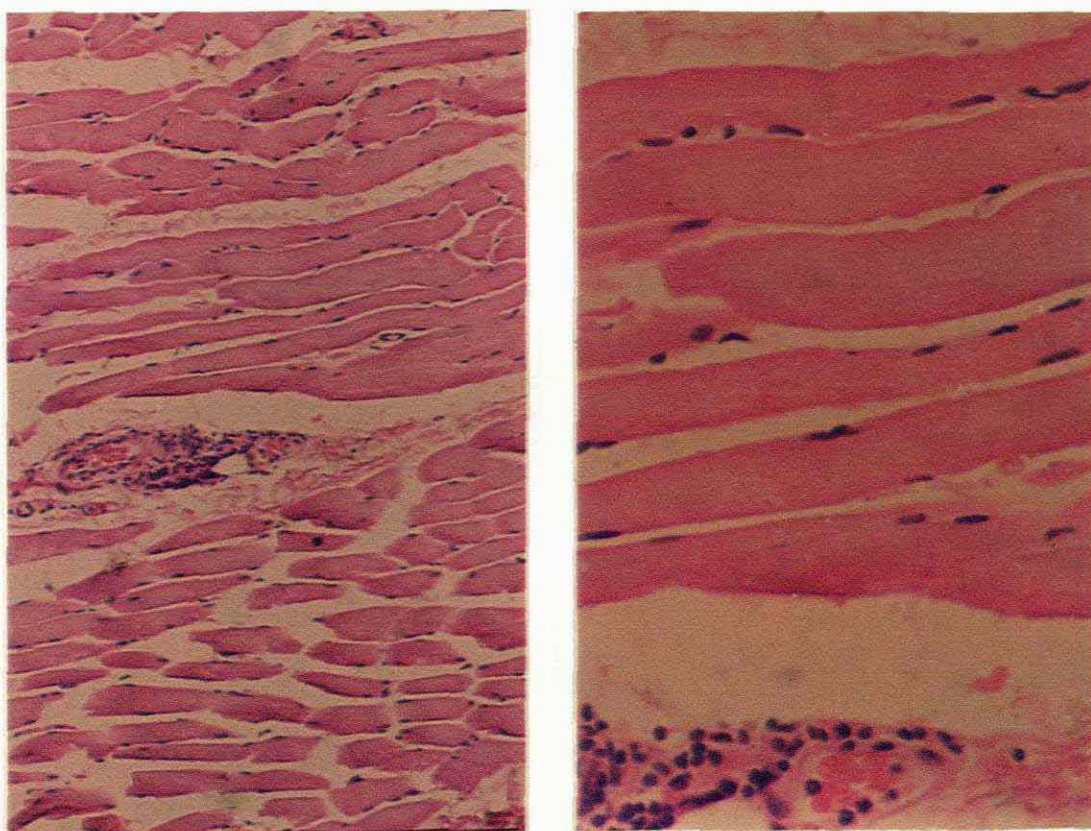


Plate 15 & 16

Paraffin wax section of normal skeletal muscle. (H&E X115 & X450)

With the standard OCUB processing method for electron microscopy, the toluidine blue stained resin sections showed clear areas between the muscle fibres, where the glycogen had been leached out during fixation with standard osmium fixatives and the dehydration, impregnation and embedding that followed. (See plates 17 & 18)

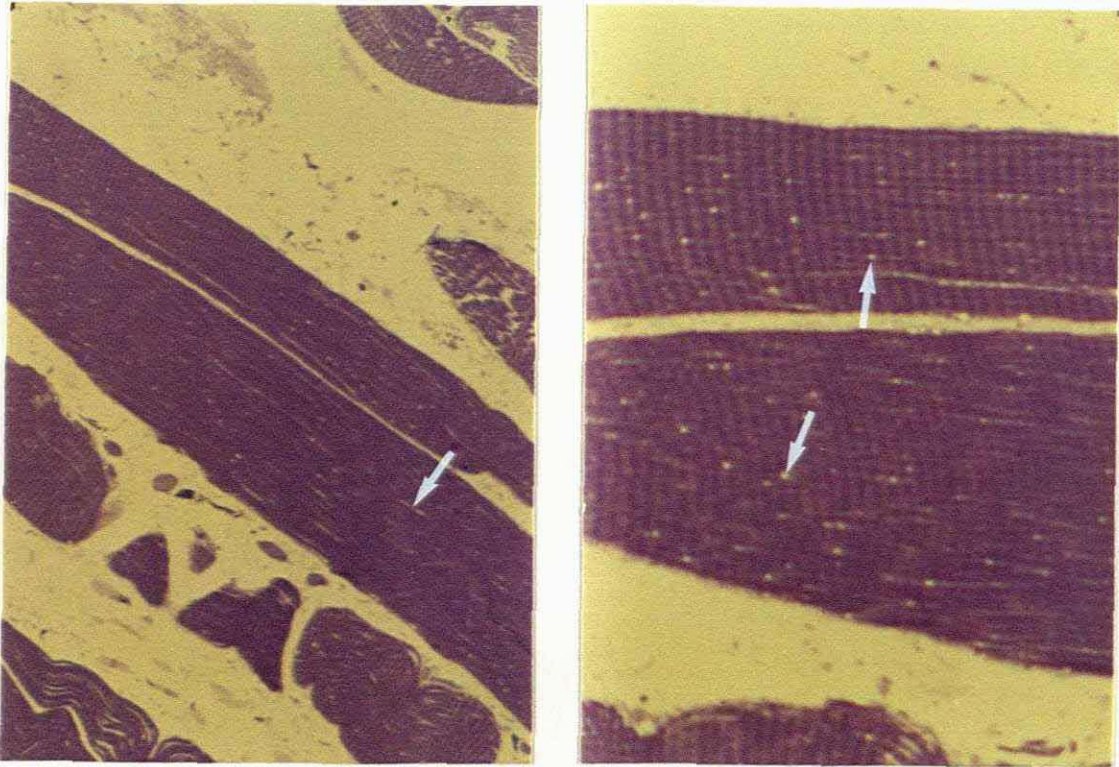


Plate 17 & 18

1  $\mu$ m resin section of normal muscle to show the clear areas where glycogen has been leached by standard EM processing (white arrows). (Tol blue X450 & X1125)

When thin sections were cut and viewed with the electron microscope, large electron-lucent areas were clearly seen, in the low magnification micrographs. (See plates 19 & 20)



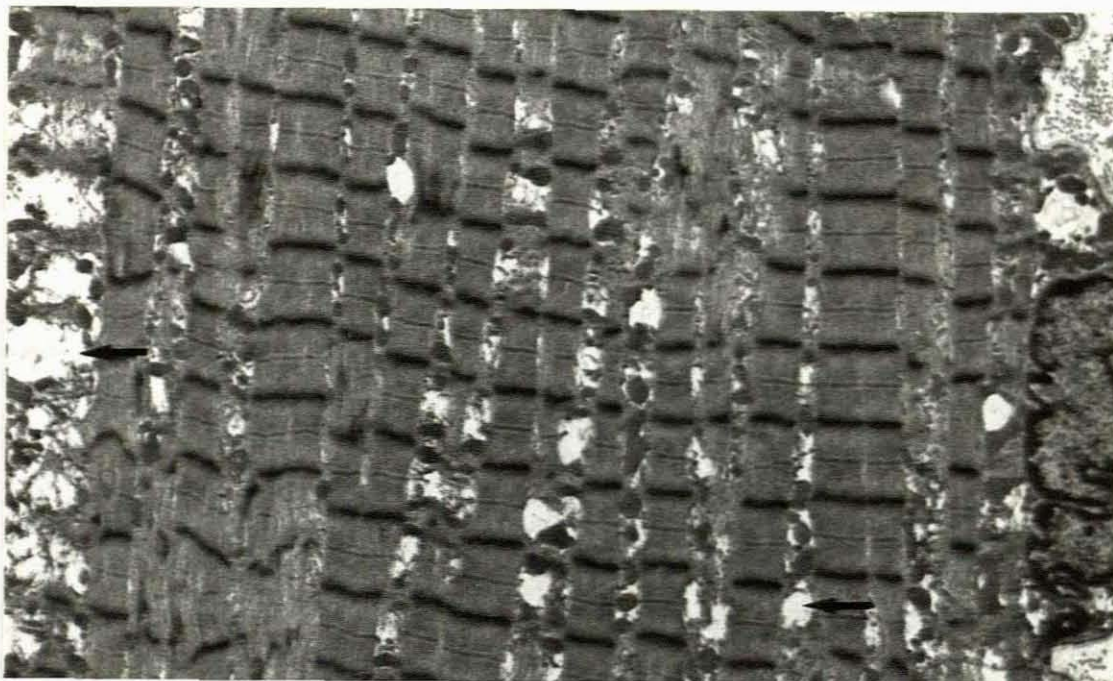


Plate 19

Normal skeletal muscle processed with the standard method for EM showing large electron lucent areas (black arrows) amongst the muscle filaments. (Resin, uranyl and lead X7500)

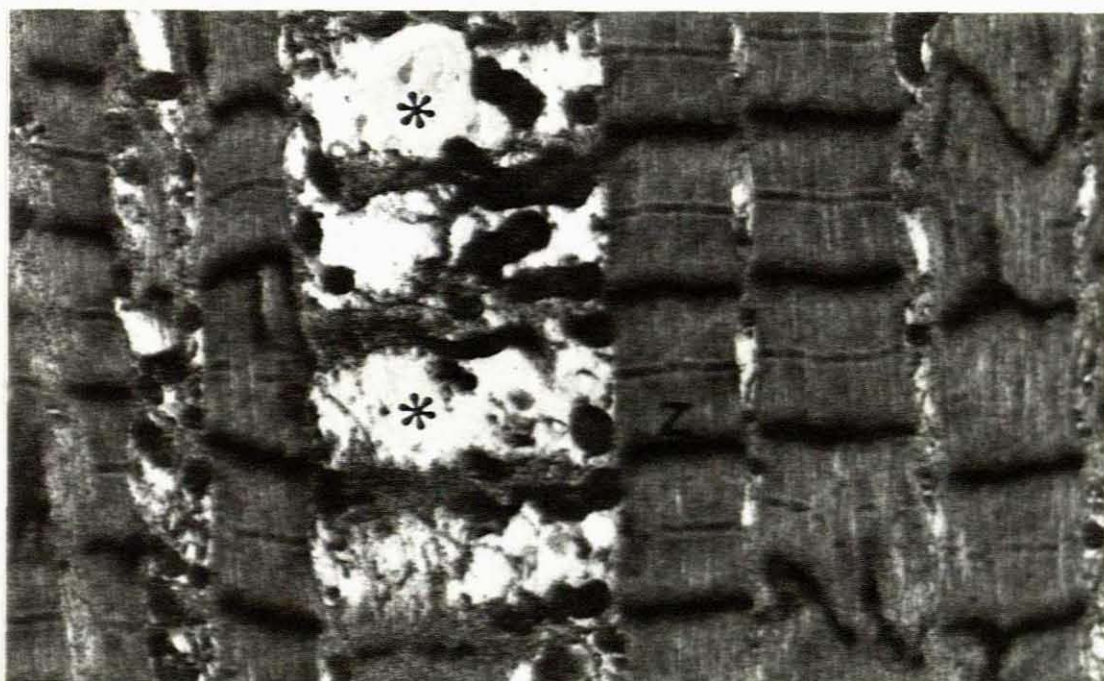


Plate 20

Higher magnification micrograph of the same tissue to show the electron-lucent areas where the glycogen (black \*) has been removed by processing. No  $\beta$  glycogen particles are discernible between the muscle filaments. (Resin, uranyl and lead X15000)



Paraffin wax sections of normal muscle tissue that were stained with the Pas + D method show loss of the glycogen in amongst the muscle fibres. (See plates 21 & 22)

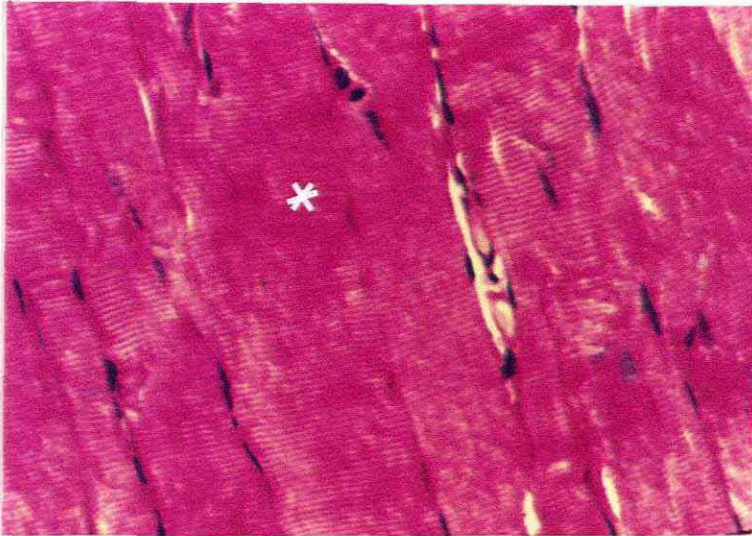


Plate 21 Paraffin wax section of normal muscle stained with the PAS method to show the glycogen in the tissue. (W. \*) (PAS X450)

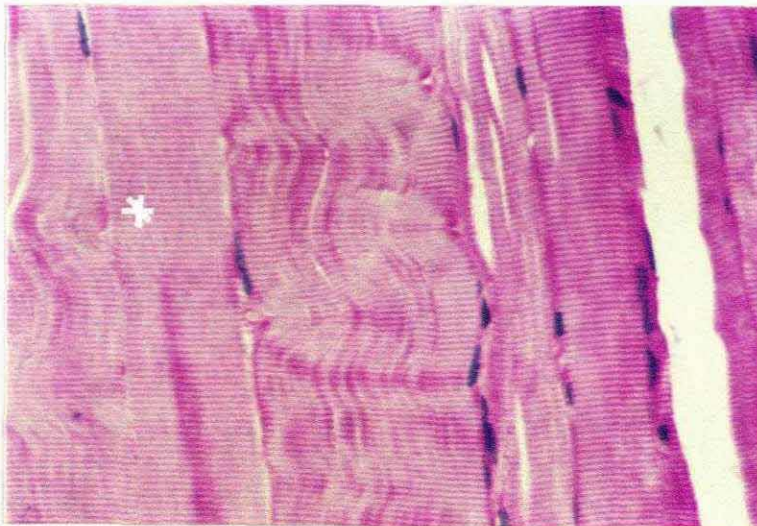


Plate 22 The same muscle tissue stained with the PAS method but with prior diastase digestion to show the loss of glycogen from the tissue. (White \*) (PAS + D X450)

When the muscle tissue was processed with the modified OPF method before and after it had been subjected to diastase digestion however, the toluidine blue stained resin sections clearly demonstrated the glycogen in the positive control (Plates 26 & 27) and none in the negative control. (Plate 23) In the positive control the glycogen was visible as dark blue staining aggregates lying longitudinally between the muscle fibres.



Plate 23 Resin section of normal muscle after diastase digestion, treated with modified OPF to show no aggregates of glycogen in the tissue. (Tol. blue X225)

Thin sections of the above block revealed that all the glycogen had been digested from the muscle tissue by the diastase. No aggregates of highly electron dense particles could be seen amongst the muscle fibres. (See plates 24 & 25)

After staining the tissue with this method it appeared to have a normal density but the nuclei appeared lighter due to the



nucleic acids not being contrasted with this technique, as can be seen in plates 26 & 27.



Plate 24 Electron micrograph of normal muscle tissue subjected to diastase digestion and processed with the modified OPF method to show that no glycogen remains in amongst the muscle fibres. (W. arrows)(Resin, lead, no uranyl. X12000)

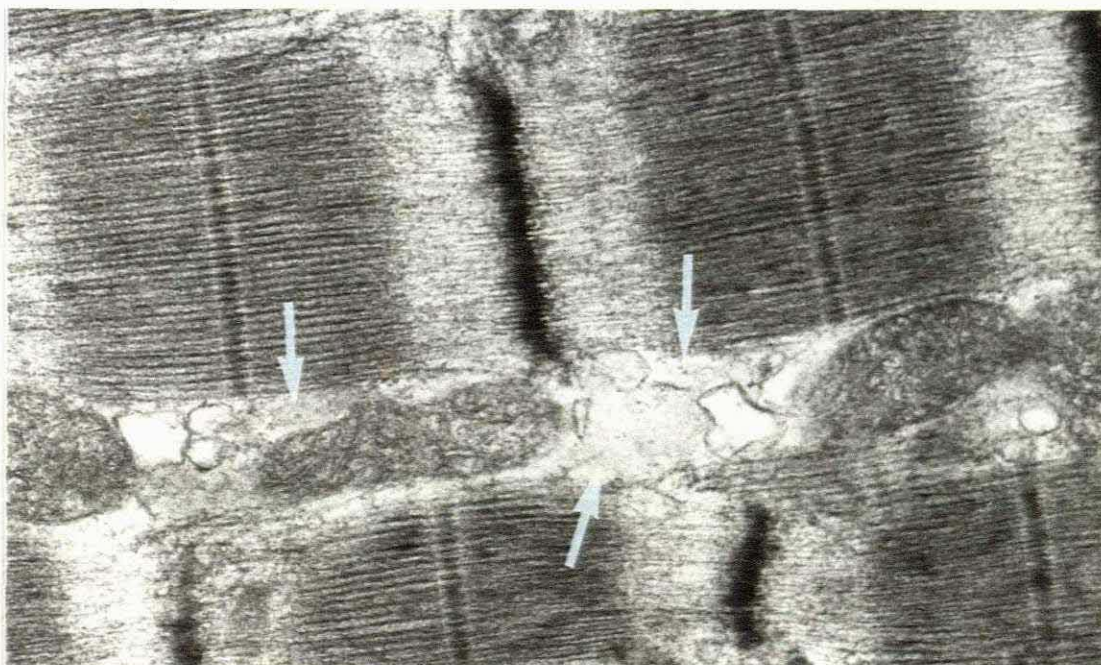


Plate 25 Higher magnification of the same section as in plate 24 to show no glycogen particles in amongst the muscle filaments. (White arrows)(Resin, lead no uranyl X36000)



With the electron microscope, electron-dense particles were seen to lie singly or in aggregates in amongst the muscle filaments of the tissue used as the positive control, and appeared to be mainly  $\beta$  particles. No electron-lucent areas were seen amongst the muscle filaments and the tissue structures and organelles had a crisper appearance. (See plates 28 & 29)

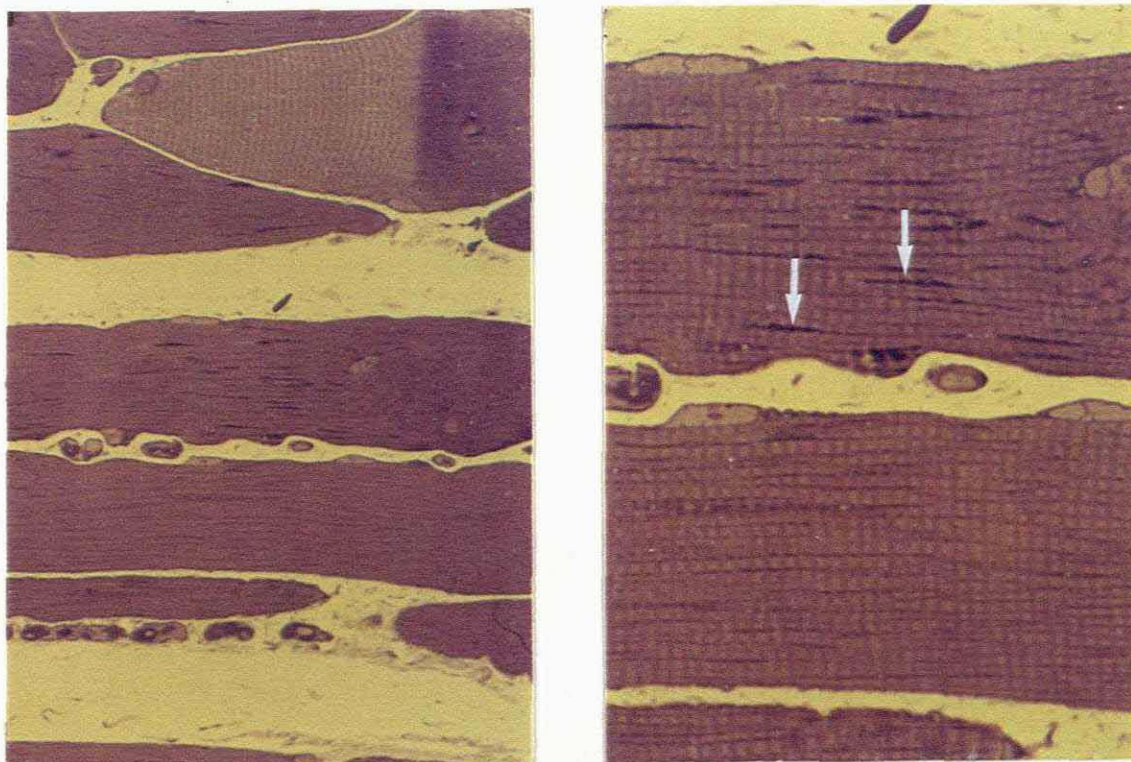


Plate 26 & 27

1 $\mu$ m resin section of normal skeletal muscle processed with the method modified at Tygerberg. In the higher magnification the glycogen can be clearly seen lying longitudinally amongst the muscle fibres (white arrows). (Tol. blue X450 & X1125)

Under carefully controlled conditions this method could possibly be used as a semi-quantitative means of determining the amount of glycogen in tissues with the electron microscope. This is however outside the scope of this thesis and may be tackled at a later stage.



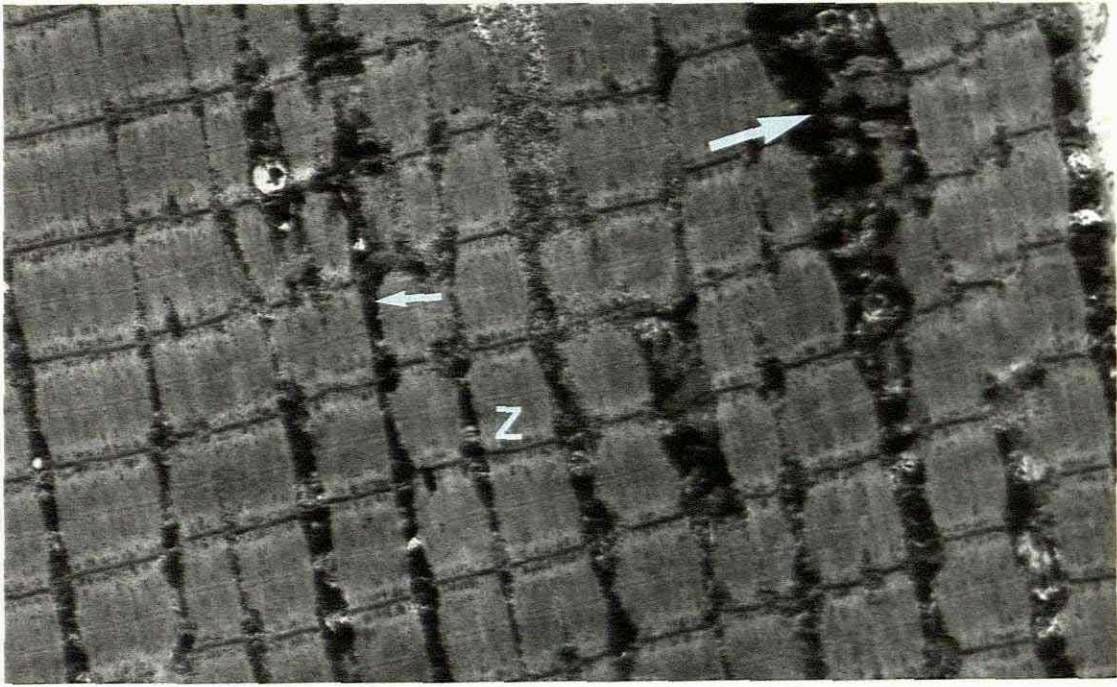


Plate 28

Normal skeletal muscle processed for EM by the OPF method to enhance contrast of the glycogen in the muscle fibres (white arrows). (Resin, lead no uranyl. X7500)



Plate 29

Higher magnification of the same section to show the glycogen particles lying singly between the muscle filaments and in aggregates (white dot) between the fibres. (Resin, lead no uranyl X24000)



4 1.3 DISTRIBUTION AND ARRANGEMENT OF GLYCOGEN IN EWING'S SARCOMA

Haematoxylin & Eosin stained paraffin wax sections of tissue containing Ewing's sarcoma show small primitive round cells with a clear appearing cytoplasm. See plate 30 & 31.

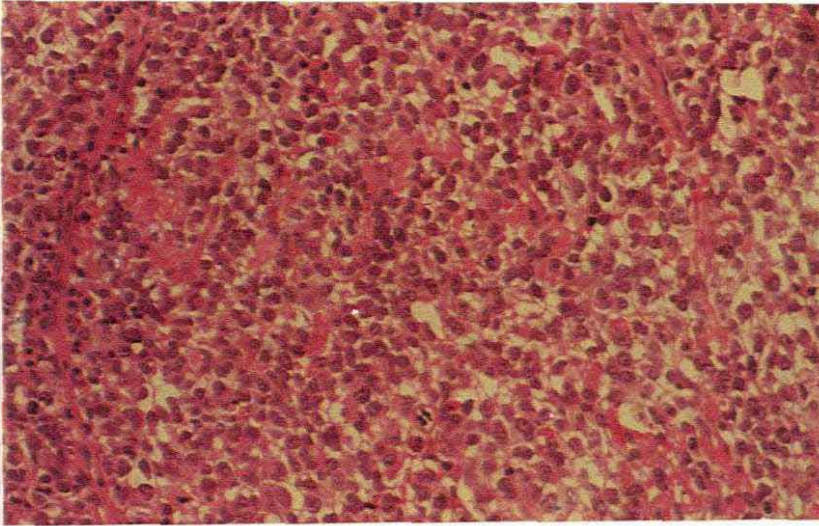


Plate 30

Paraffin wax section of a small cell tumour with primitive looking cells. (H&E X225)

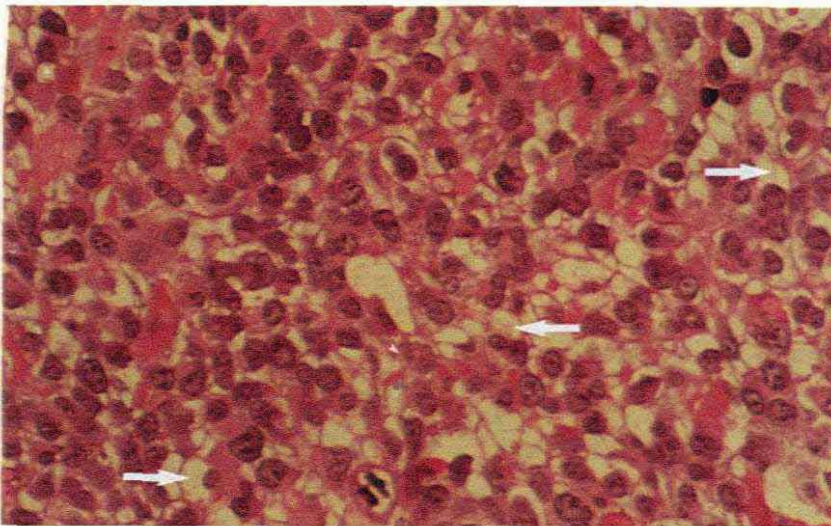


Plate 31

Higher magnification micrograph of the same field to show the empty appearance of most of the cells. (H&E X450)



On the toluidine blue stained resin sections, this effect is even more pronounced. (See plates 32 & 33)

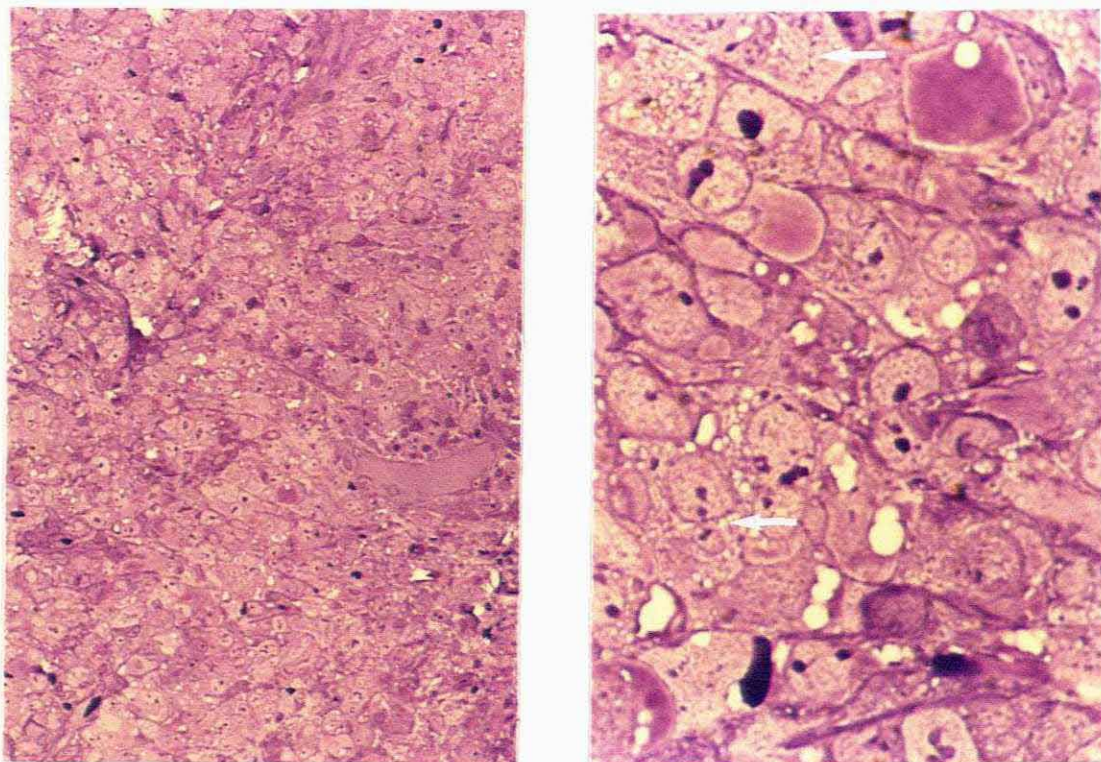


Plate 32 & 33

1 $\mu$ m epoxy resin sections of representative areas from Plate 31. Plate 33 shows several cells that have empty looking areas (white arrows) where the glycogen has been removed by the processing. (Tol blue X450 & X1125)

With the electron microscope, primitive sarcomatous cells with pleomorphic euchromatic nuclei were seen. Large electron-lucent areas were very prominent in the cytoplasm. The cells had clearly defined borders and the nuclei contained misshapen nucleoli. Lysosomes, SER, GER and Golgi were also prominent. See plate 34.

Higher magnification of the section showed the large electron-lucent area in one of the cells clearly. Note part of the



pleomorphic nucleus as well as part of the nucleolus in the left hand corner of plate 35.



Plate 34

At low magnification with the EM, primitive sarcomatous cells are seen. Many of the cells have electron-lucent areas (black \*) in their cytoplasm. (OCUB processing X6000)



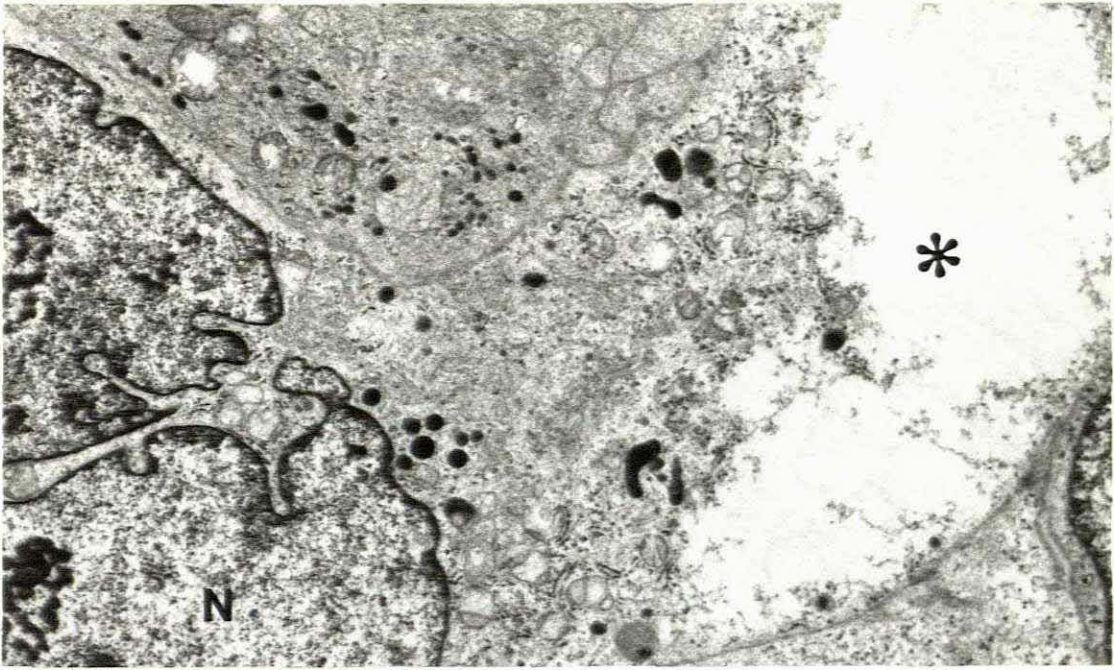


Plate 35

The electron-lucent area in the cell is well demonstrated in this photograph (black \*). Part of the pleomorphic nucleus and strange-looking nucleolus is clearly seen. (OCUB processing X7500)

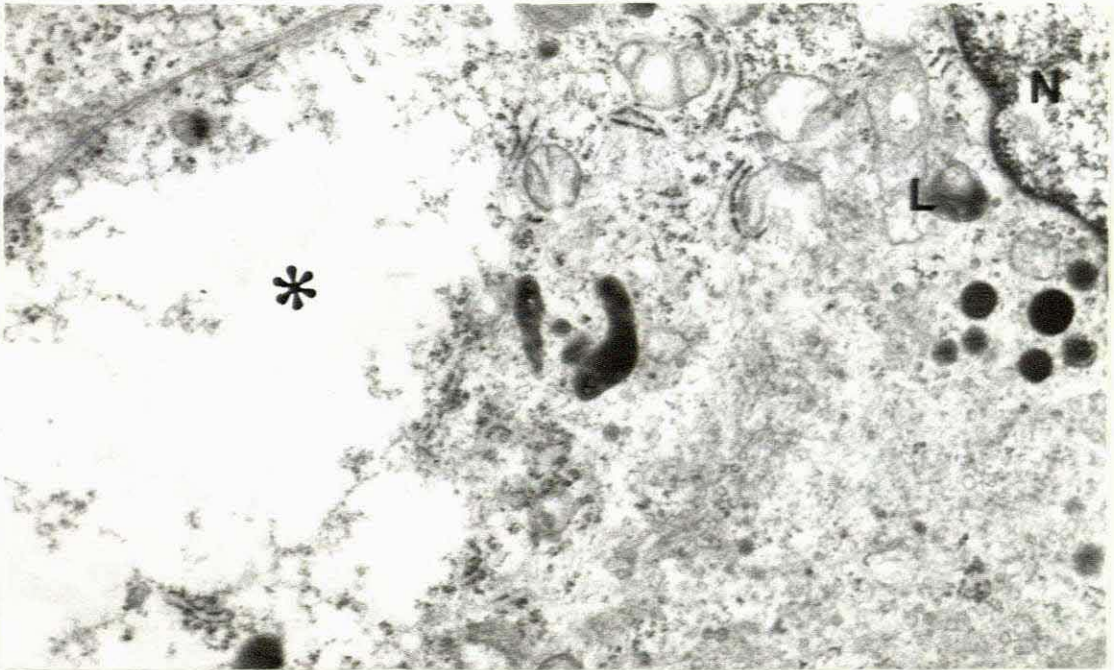


Plate 36

At higher magnification, the clear area can be seen in more detail (black \*). Mitochondria, lysosomes and GER are prominent. (OCUB processing X15000)



The clear area is shown in more detail, and the micro-organelles in the cell cytoplasm are clearly seen in Plate 36.

When the tissue was processed with the modified OPF method, the empty-looking areas seen on the toluidine blue sections of the standard processing contained large aggregates of dark blue staining material. See plate 37 & 38.

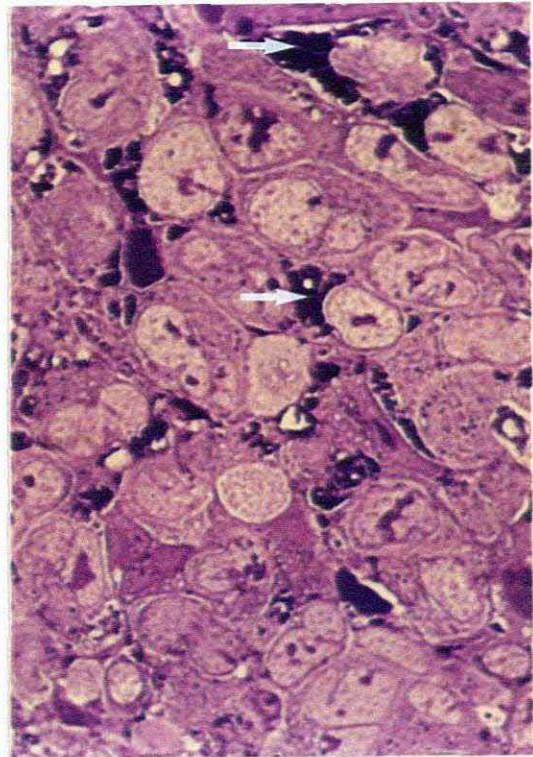
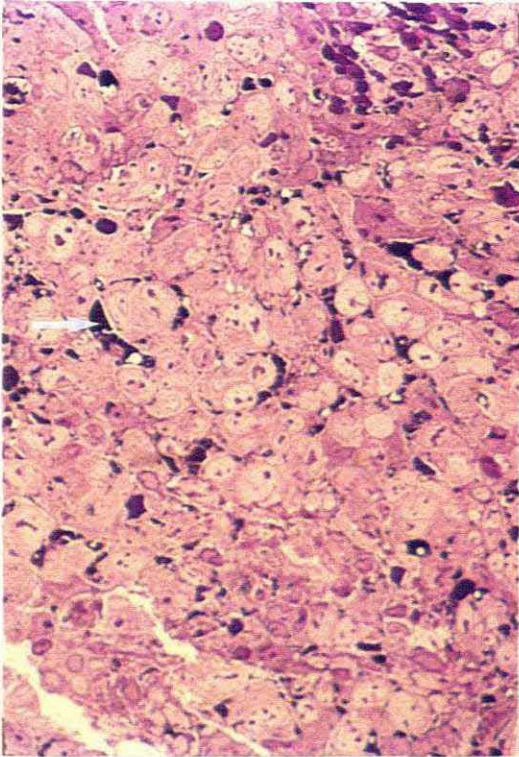


Plate 37 & 38

1 $\mu$ m resin sections of the same issue processed by the OPF method. The glycogen is clearly visible as darkly staining material (white arrows) in the cytoplasm of several of the cells. (Tol. blue, no en bloc uranyl staining X450 & X1125)

When thin sections were cut, and viewed with the electron microscope, the cytoplasm of the cells were seen to contain electron dense particulate matter resembling glycogen. Only



the single  $\beta$  particulate glycogen was seen and no  $\alpha$  glycogen particles could be demonstrated. (See plate 39.)

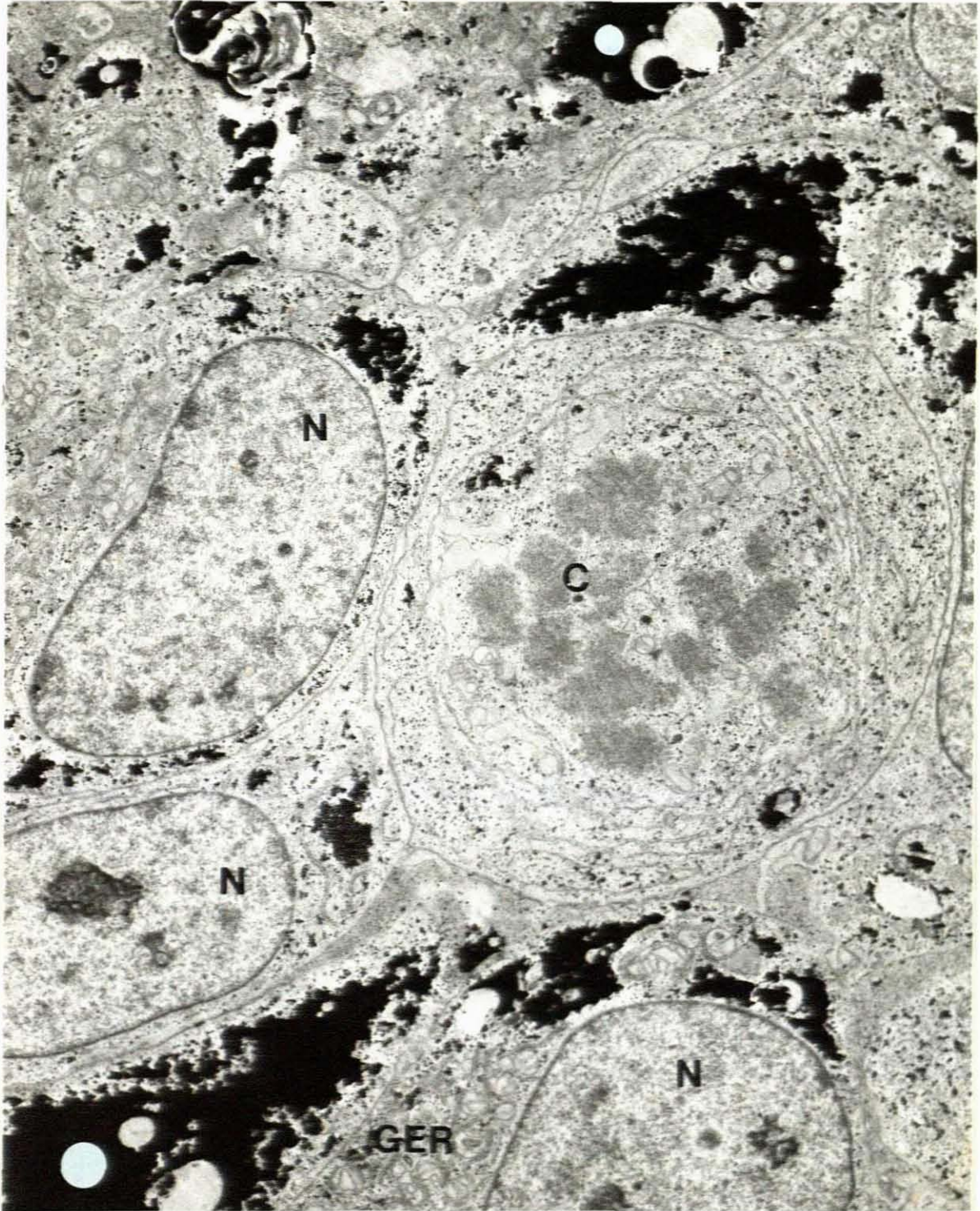


Plate 39

When the same tissue was processed by the OPF method the glycogen was retained as an extremely electron dense finely granular precipitate (white dots) in the cytoplasm of the sarcoma cells. (OPF, no uranyl staining X6000)



At higher magnification the electron-dense aggregates of glycogen were well demonstrated, and even in these aggregates the particulate nature of the material was seen. (Plate 40.) At still higher magnification each individual particle was resolved and appeared to be exclusively single  $\beta$  particulate glycogen. No  $\hat{A}$  particles were seen. See plate 41.

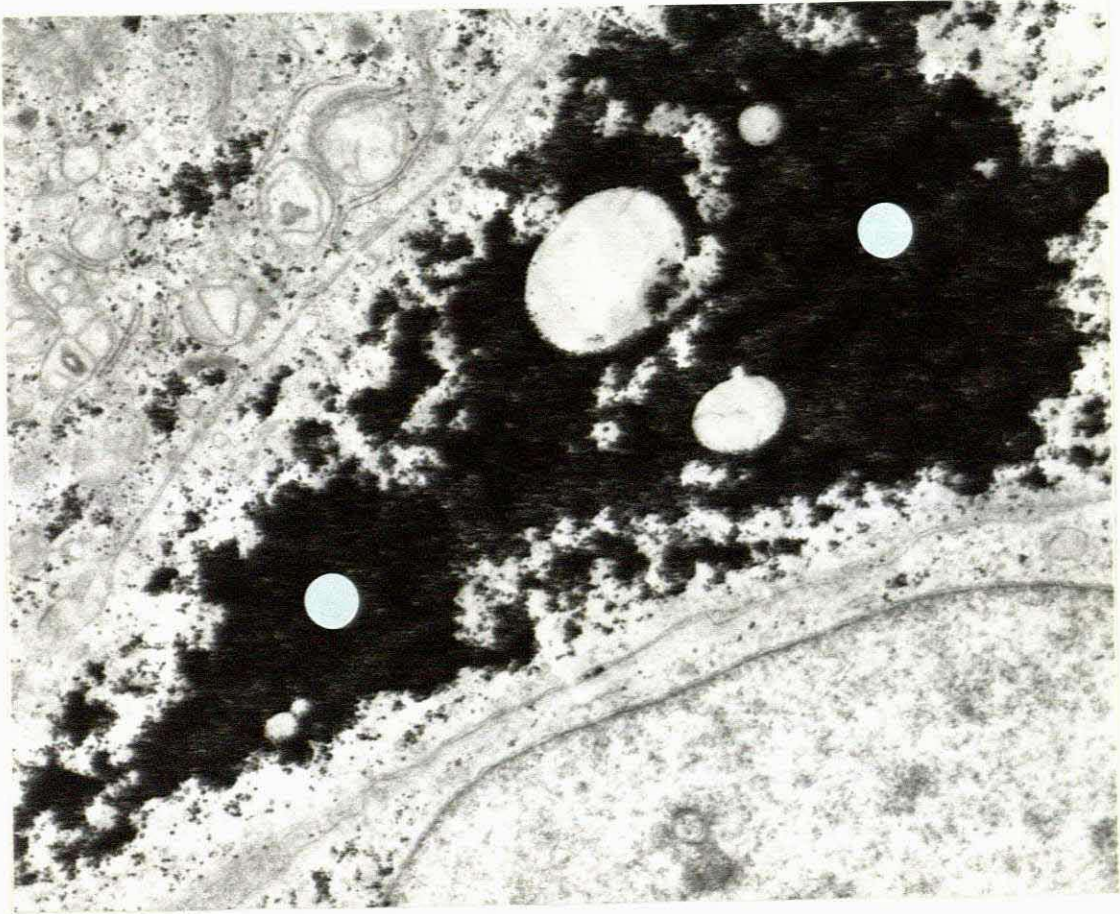


Plate 40

At higher magnification aggregation of extremely electron dense  $\beta$  glycogen granules could be clearly seen (white dots). (OPF, no uranyl staining X12000)



Plate 41

At higher magnification it appears that only  $\beta$  glycogen granules measuring  $\pm 35\text{nm}$  were present (black arrows), as the typical  $\text{\AA}$  glycogen rosettes were not seen. (OPF, no uranyl staining X24000)

#### 4.1.4 DISTRIBUTION AND ARRANGEMENT OF GLYCOGEN IN LEIOMYOSARCOMA

The Haematoxylin and Eosin stained paraffin wax sections of leiomyosarcoma showed spindle shaped cells with pink staining fibrillary cytoplasm. (Plate 42 and 43.)

Cells in the toluidine blue stained resin sections of the tissue processed with the standard method, had a very similar appearance as in plate 44. Only at the higher magnification,



as in plate 45 were clear areas seen in the cytoplasm of these cells.

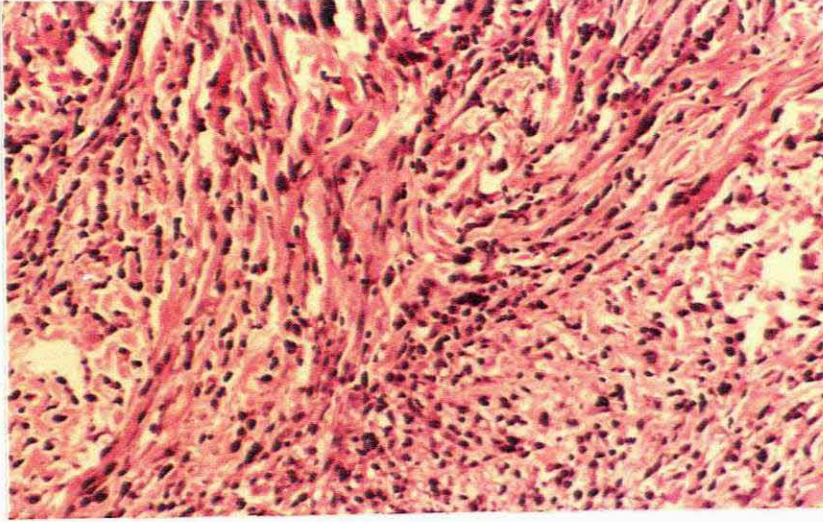


Plate 42

Paraffin wax section of a spindle cell tumour.(Haematoxylin & Eosin X115)

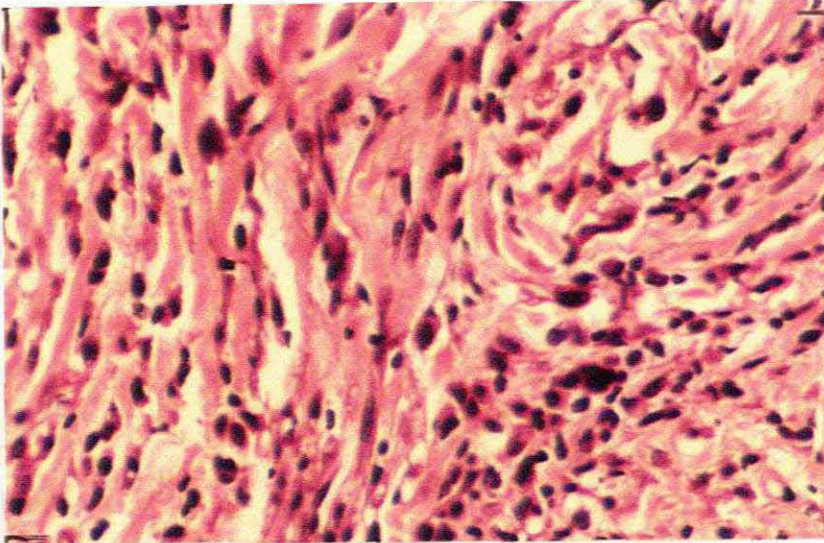


Plate 43

At higher magnification the spindle nature of the cells and the pink cytoplasm is well demonstrated. (Haematoxylin & Eosin X450)



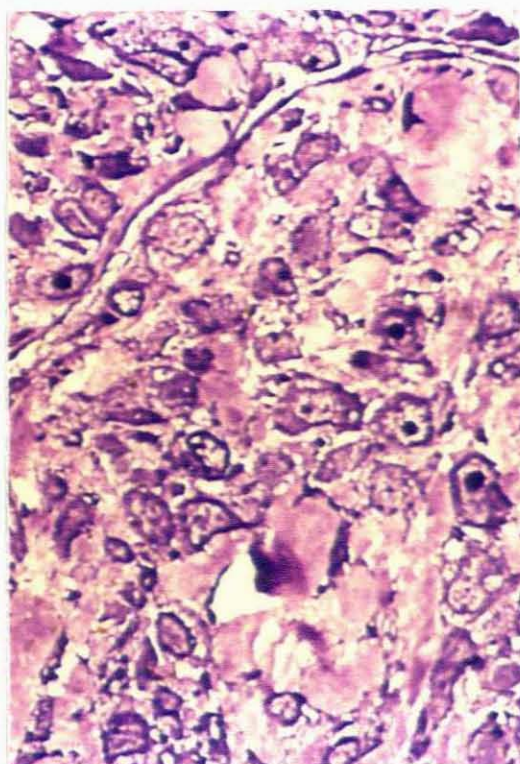
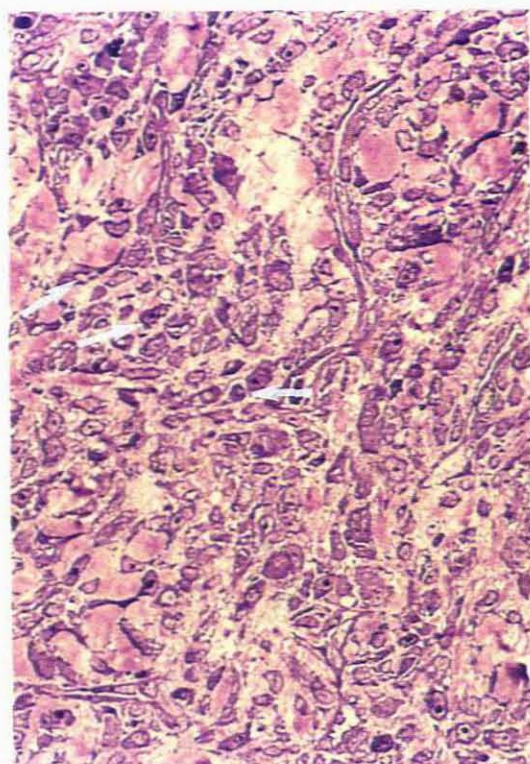


Plate 44 & 45

Resin sections of the same tissue processed for EM demonstrated the spindle nature of the cells (white arrows). (Tol blue, OCUB processing X115 & X1125)

When thin sections of the same tissue were viewed at low magnification (approximately X2000) with the electron microscope, spindle shaped cells were seen that appeared to have filamentous material in their cytoplasm. (See Plate 46.) At high magnification these cells were seen to have junctions between them, that appeared to be hemi-desmosomes. The cells with the above-mentioned features, also contained filaments with dark staining focal densities and all had the characteristics of smooth muscle cells. An electron-dense granular material was also seen with the characteristic appearance of glycogen, but this feature was not prominent. (See plate 47 and 48)





Plate 46

Low magnification electron micrograph of spindle shaped cells that appear to have filamentous material in their cytoplasm (white arrows). (Lead and uranyl X4500)





Plate 47

At higher magnification, filaments with focal densities are just discernible (white arrows). (Lead and uranyl X15000)

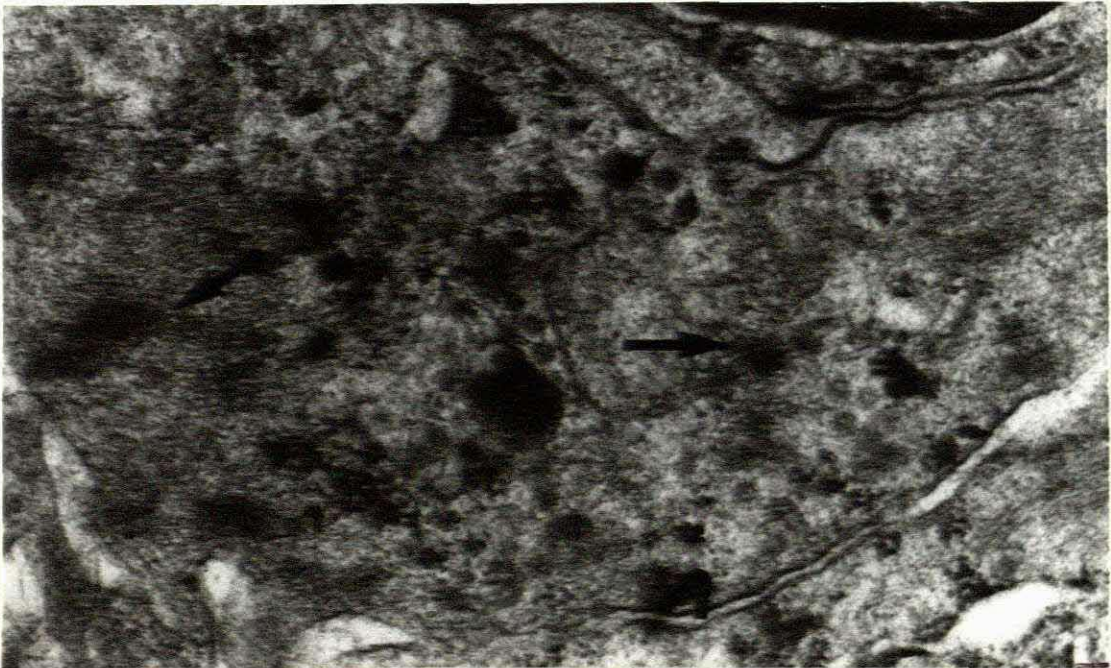


Plate 48

At still higher magnification the filaments and focal densities (black arrows), and desmosomes (curved arrow) can be clearly seen. (Lead and uranyl X45000)



When the tissue was processed with the modified OPF method, very little difference was seen in the toluidine blue stained resin sections of the same tissue. At the higher magnification however, some darker staining material was observed in the cytoplasm of some of the tumour cells. (See Plate 49 and 50.)

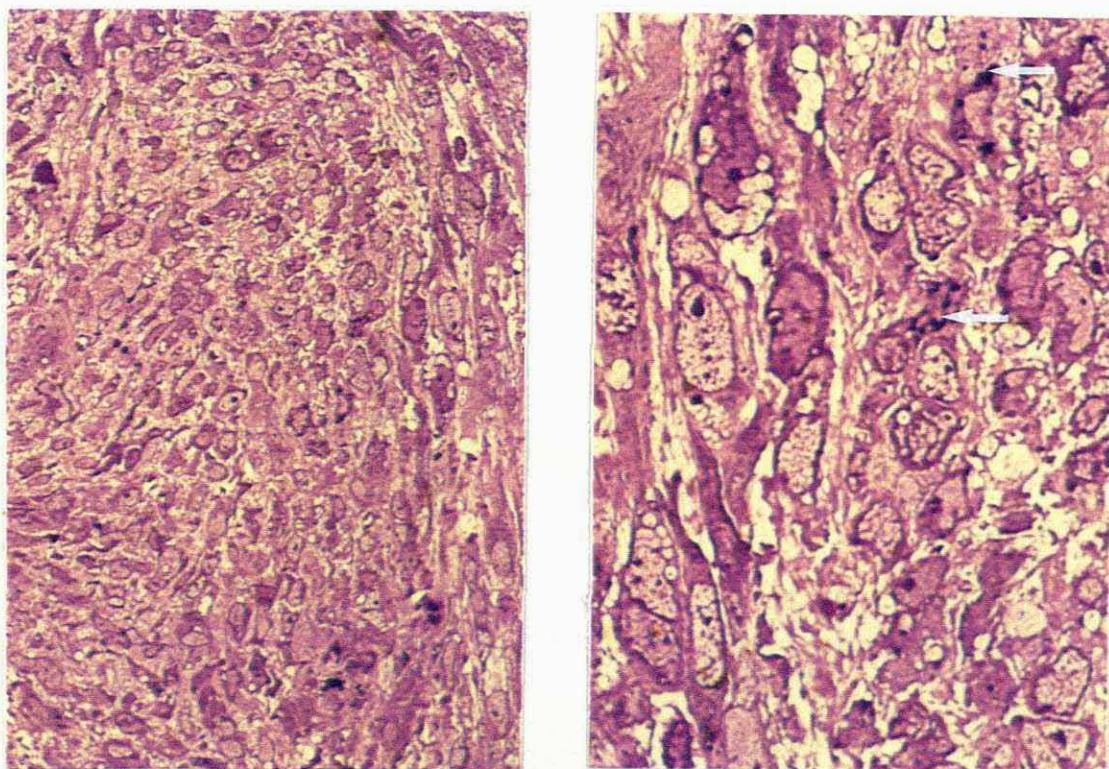


Plate 49 & 50

Resin section of tissue processed by the OPF method. Note the darker staining material in some of the cells in the higher magnification (white arrows). (Tol blue, no en bloc uranyl staining. X225 & X1125)

When thin sections of the OPF processed tissue were viewed with the electron microscope, the spindle shaped cells were seen to contain a fine granular deposit at low magnification. Black granules could also be seen in some electron lucent areas. (See Plate 51.)



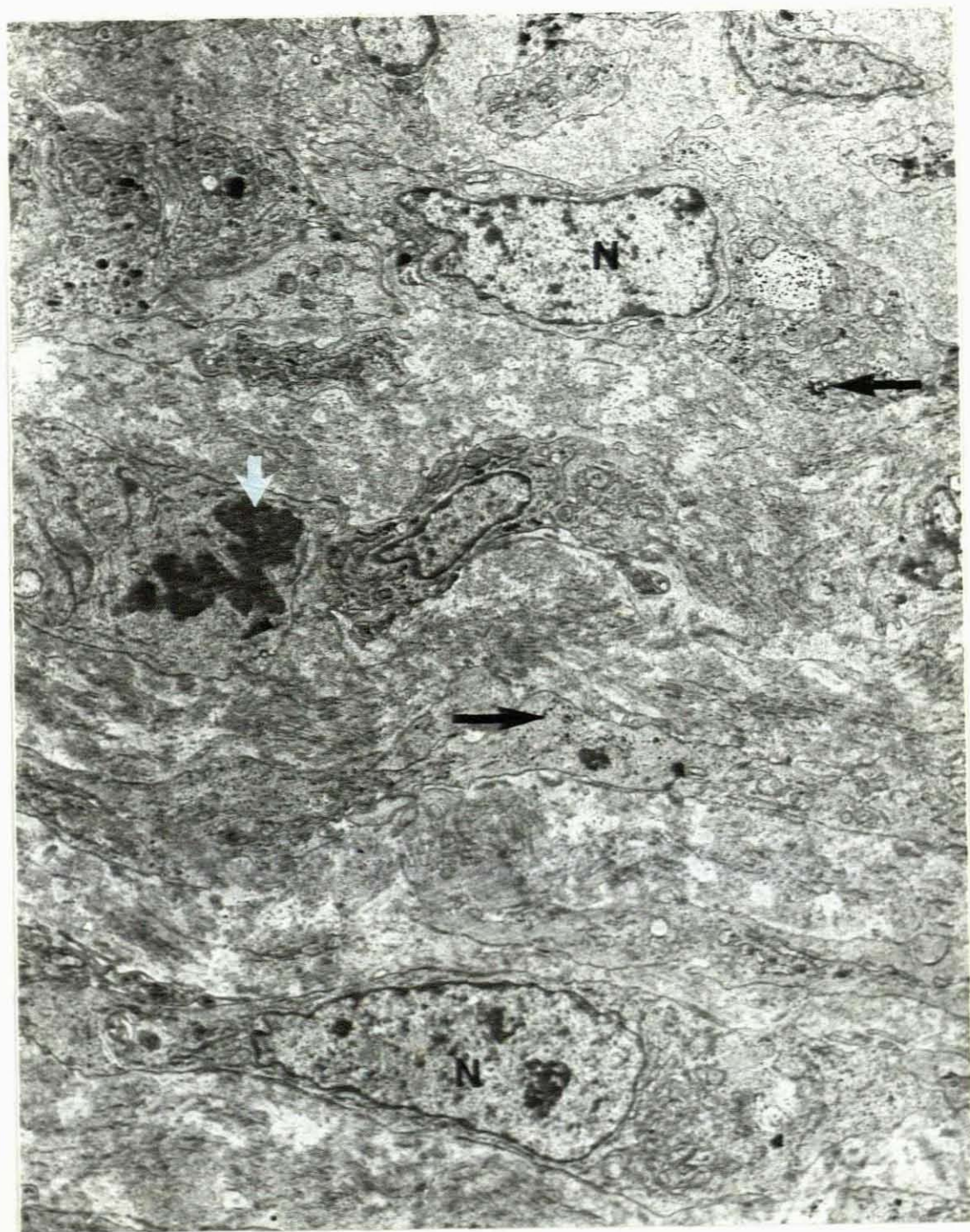


Plate 51

Low magnification of tissue processed for EM by the OPF method. The spindle nature of the cells can be clearly seen. Note the mitotic figure in the left of the micrograph (W. arrow). The dark staining particulate glycogen is just discernible (B. arrows). (Lead only X4500)



At high magnification some cells had basal lamina, pinocytotic vesicles, intermediate filaments and a fine granular extremely electron-dense precipitate. (See plate 52 and 53.)

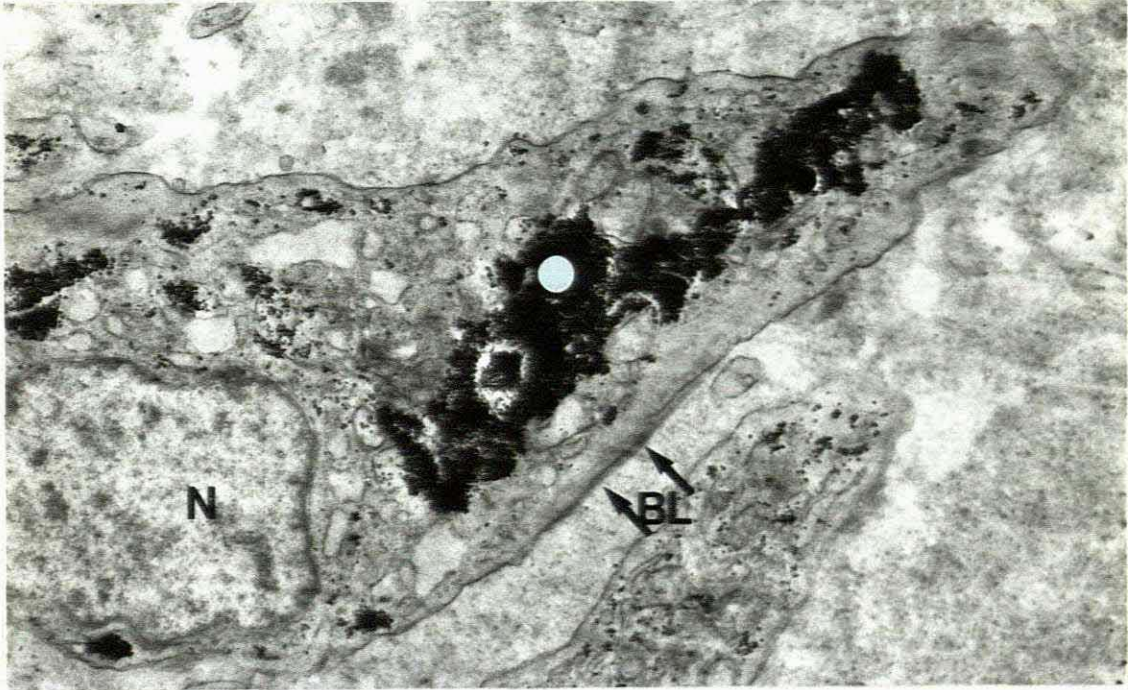


Plate 52 After OPF processing the cells which have external lamina (B. arrows) and intermediate filaments have extremely electron dense aggregations of  $\beta$  glycogen particles in them (white dot). (Lead only X12000)

In plate 53, the typical  $\beta$  particulate glycogen is observed both lying singly and in aggregates. Micro-pinocytosis and an external lamina are clearly visible. Golgi apparatus and smooth endoplasmic reticulum were also seen in the cytoplasm of the cells. A few  $\hat{A}$  glycogen rosettes were also seen.

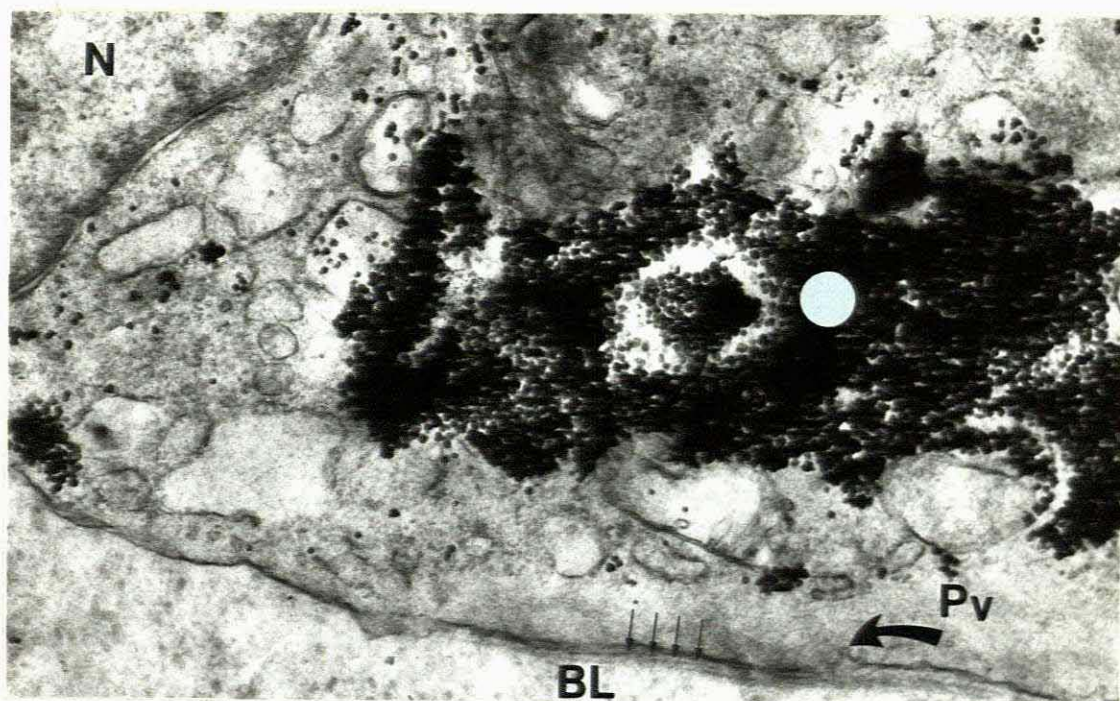


Plate 53

At high magnification the particulate nature of the glycogen particles can be seen (white dot). An external lamina (B. arrows) and micro-pinocytotic vesicles (curved arrow) were also present. (Lead only X30000)

#### 4.1.5 DISTRIBUTION AND ARRANGEMENT OF GLYCOGEN IN RHABDOMYOSARCOMA

Haematoxylin & Eosin stained paraffin wax sections of this tissue, were seen to contain small round cells with an eosinophilic staining material in their cytoplasm. Some of the cells had clear areas in the cytoplasm. (See plate 54 and 55.) In the toluidine blue stained resin sections of the tissue, processed by the standard method, the cells were seen to contain a filamentous material that stained blue. An amorphous material that could have been residual glycogen,



stained metachromatically pink. The filamentous material was seen to have what appeared to be striations in places. (See plate 57.)

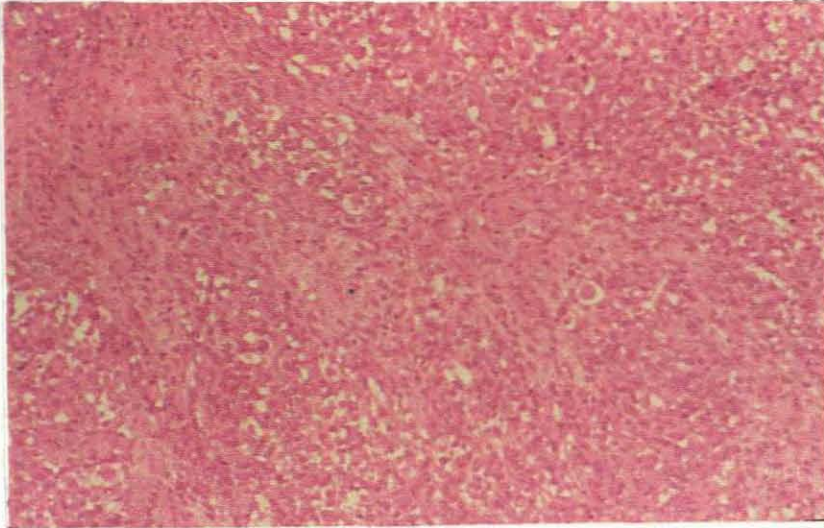


Plate 54

Paraffin wax section of a small round cell tumour of the uterus. The cells have an intensely pink staining cytoplasm. (H&E X115)

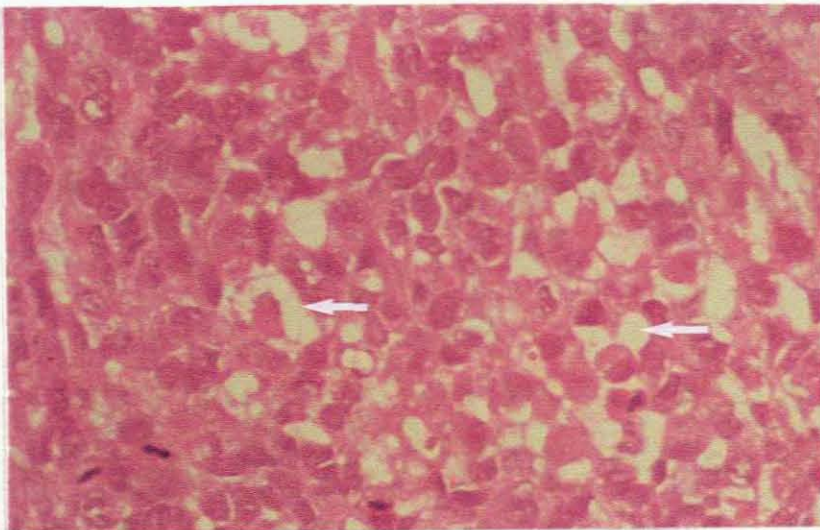


Plate 55

A higher magnification of the same field to show that some of the cells have rarefied areas in their cytoplasm where some material has been partially or completely removed. (H&E X450)



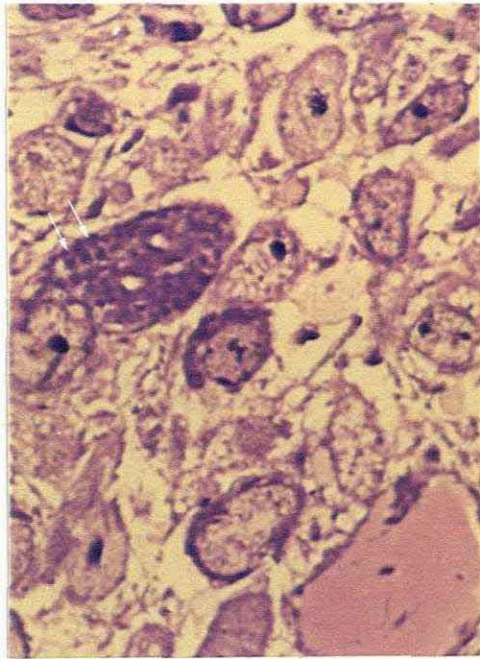
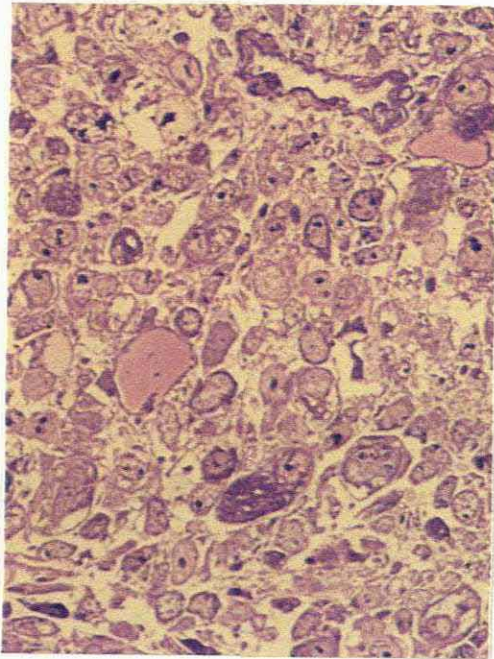


Plate 56 & 57

Low and high power LM photographs of tissue processed in the standard method for EM. Note the washed out appearance of the cytoplasm of some of the cells. A cell containing what appears to be striated muscle fibres is visible in the left of Plate 57 (white arrows). (Resin, Tol blue, X450 & X1125)

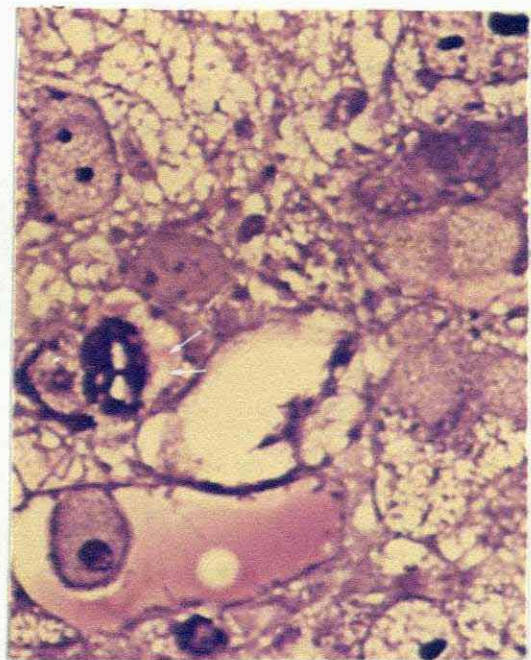
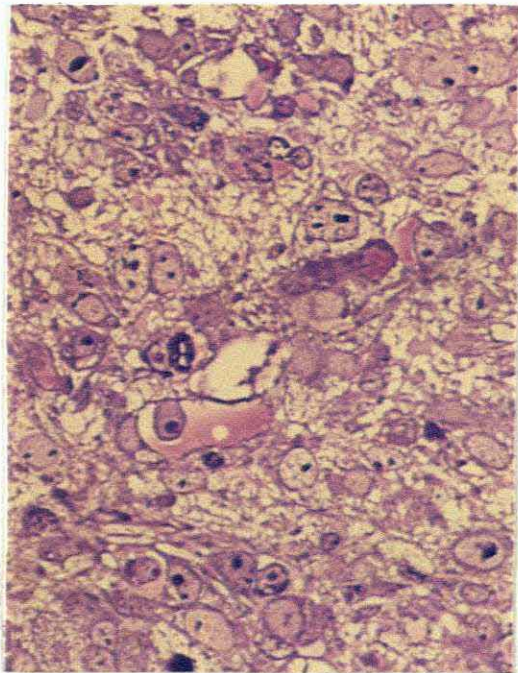


Plate 58 & 59

Low and high magnifications of the same tissue as above to show that there was still residual material left in some of the cells (white arrows). (Resin, Tol blue, X450 & X1125)



When thin sections of the above-mentioned tissue were viewed with the electron microscope, many of the cells that contained the striated muscle fibres were seen to contain large clear electron-lucent areas. (See plate 60.)

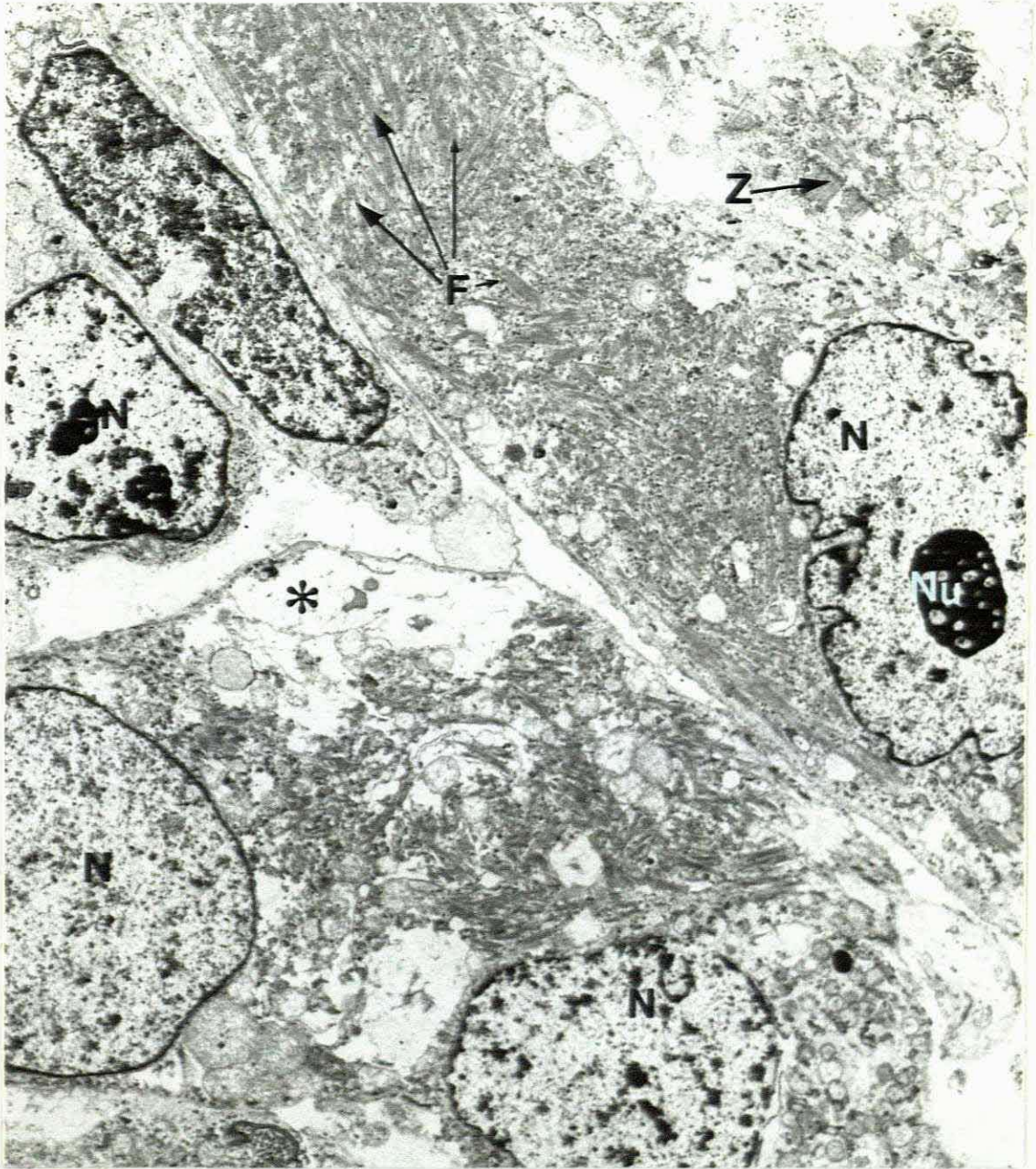


Plate 60

Low magnification of tissue from a Rhabdomyosarcoma processed for EM by the standard method. Cells with bundles of fibres with cross striations resembling striated muscle and cells that have electron-lucent areas where the glycogen has been removed, are demonstrated (black \*). (Lead & uranyl, X4500)



At higher magnification in plate 61, the electron-lucent areas as well as muscle fibres can be seen. Some residual  $\text{\AA}$  glycogen rosettes were seen between bundles of well differentiated muscle filaments (15-18nm) containing cross striations. (See plate 62.)

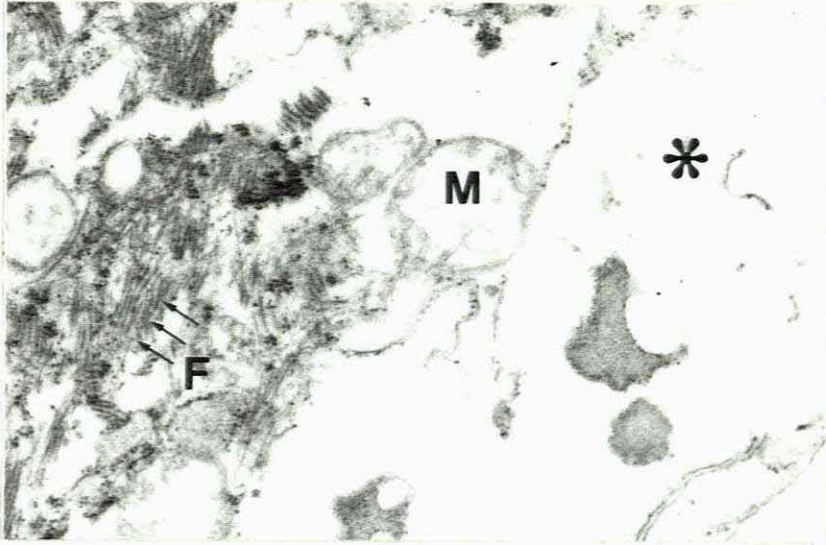


Plate 61

Higher magnification of a cell from the same area to show the electron-lucent area (black \*) and fibres in detail. (Lead & uranyl, X20000)

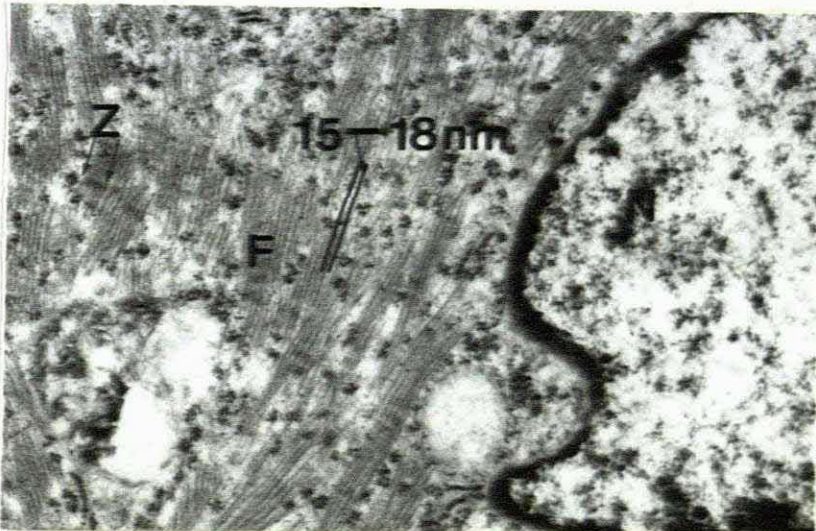


Plate 62

Another cell from the same area that shows well differentiated bundles of filaments (15-18nm) containing cross striations. Note that some glycogen is retained in the section. (Lead & uranyl, X20000)



In the toluidine blue stained section of the same tissue, processed with the modified OPF technique, the cells were seen to contain a very dense black material that corresponded to the clear areas in the tissue processed with the standard method. (See plate 63.) Very dark staining material was seen in the higher magnification of the cell in plate 64. Definite striations were seen in the filamentous material in some of the cells and black precipitate, as well as filaments were seen in other cells in plate 65.

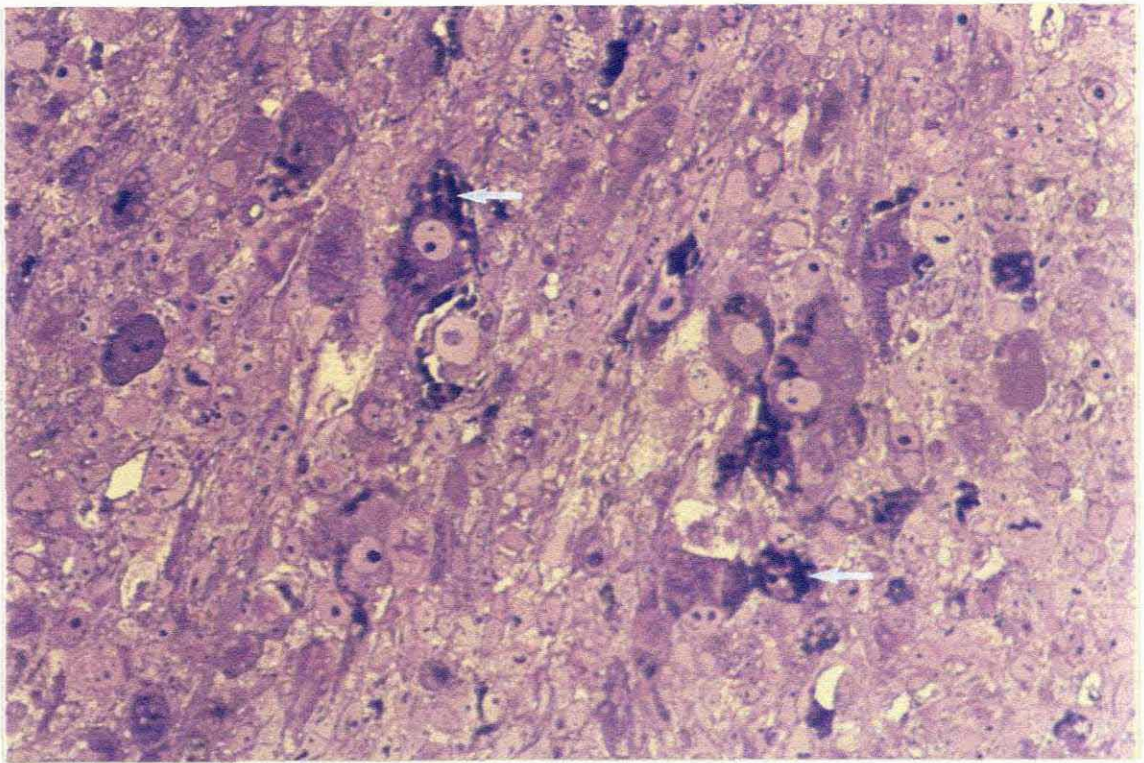


Plate 63 Low magnification micrograph of tissue processed for EM by the OPF method. The glycogen is clearly visible at this low magnification (W. arrows). (Tol blue, X450)



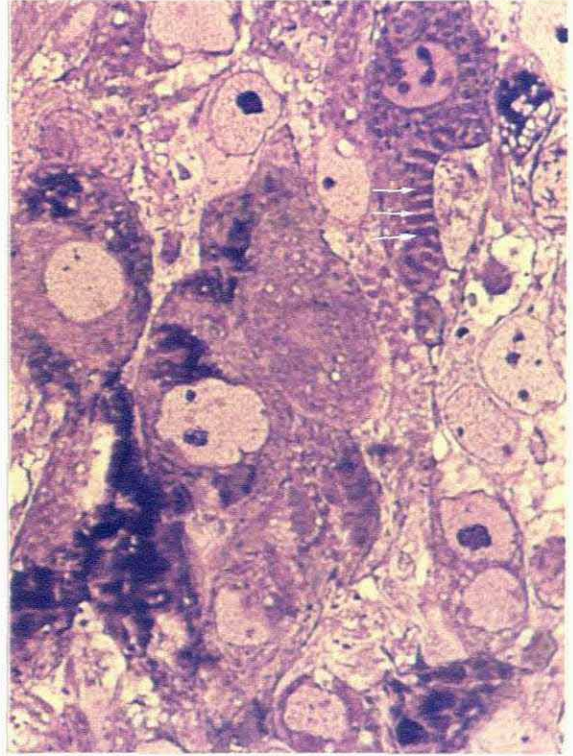
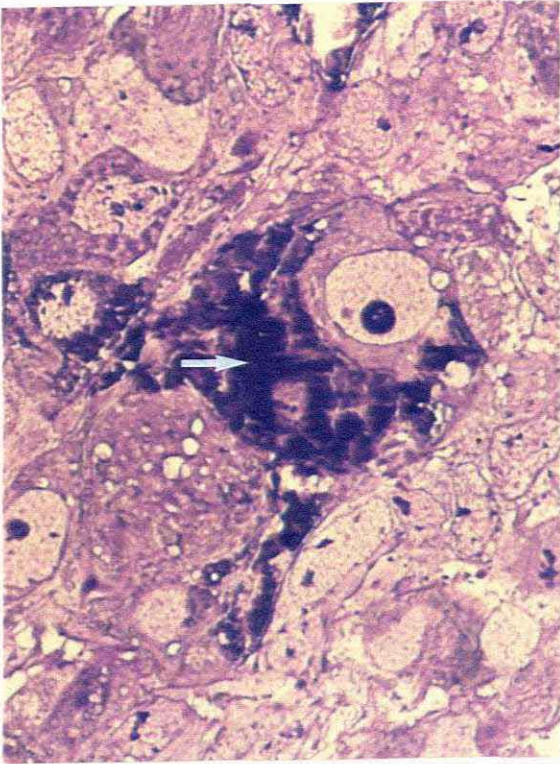


Plate 64 & 65

High magnification micrographs of the same tissue to show the dense black precipitate in some of the cells (W. arrow, plate 64). What appears to be striated muscle fibres are visible in the cell in plate 65 (W. arrows). (Resin, Tol blue, X1125)

When thin sections of the same resin block were viewed with the electron microscope, the cells were seen to contain large masses of densely packed  $\beta$  particulate glycogen lying in and around the striated muscle fibres. The cells had pleomorphic almost-round nuclei that contained unusually shaped nucleoli. (See plate 66.) At high magnification the cells were seen to contain almost exclusively  $\beta$  particulate glycogen, (Plate 67) though what could have been  $\alpha$  glycogen particles could be seen faintly amongst the muscle fibres in plate 68.



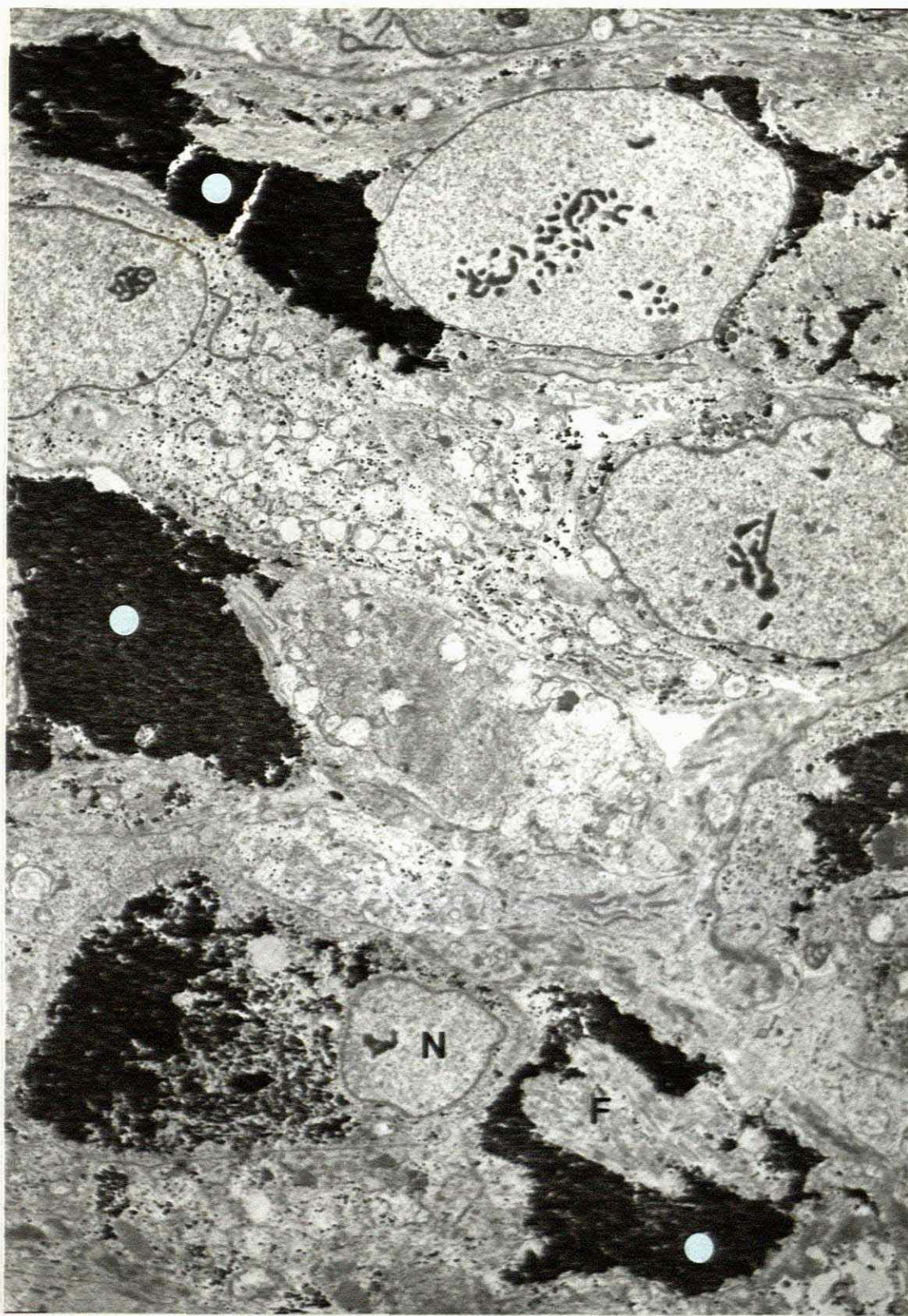


Plate 66

Low magnification micrograph of tissue processed with the OPF method to show large amounts of electron-dense material in the cytoplasm of the cells (white dots). (Lead only X4500)





Plate 67

Intermediate magnification of a cell that contains massive amounts of glycogen (white dot) and bundles of filaments. (Lead only, X6000)

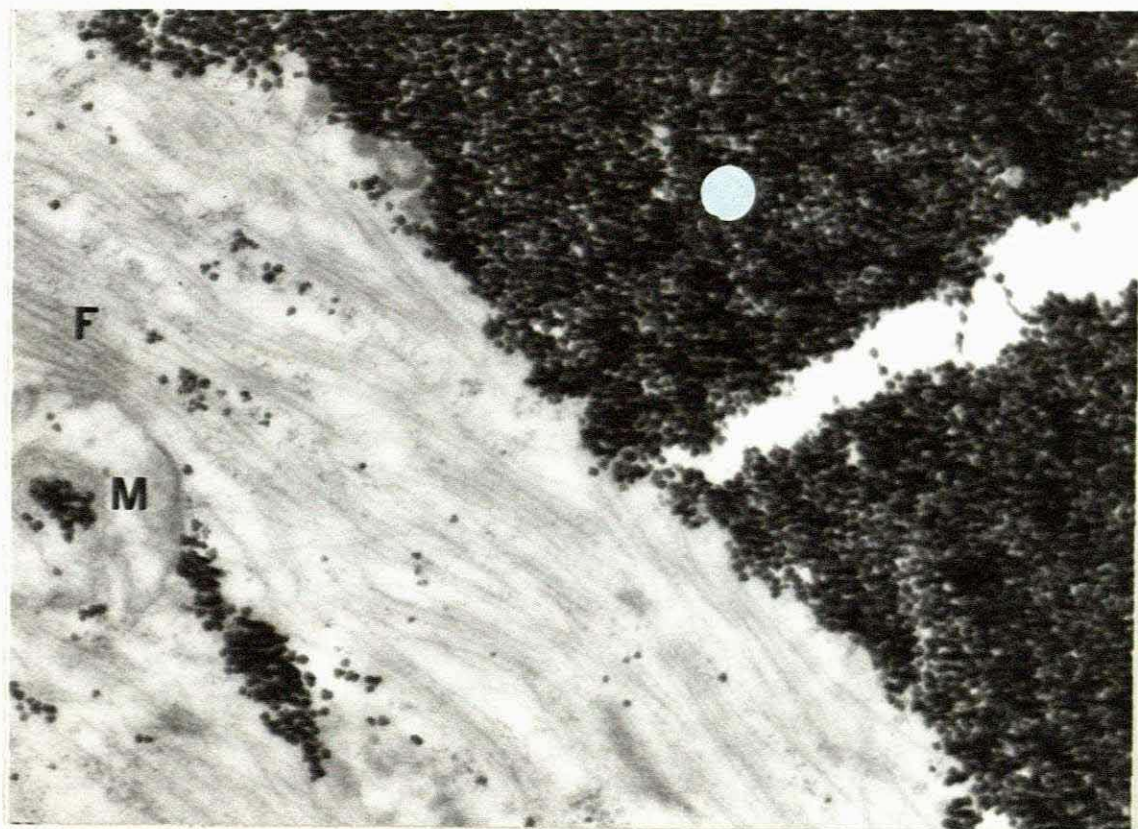


Plate 68

High magnification of the same cell to show the filaments and the glycogen in detail. There appears to be only  $\beta$  glycogen particles present (W. dot). (Lead only, X40000)



Two tumour cells are compared in plate 69 and plate 70, to illustrate the difference between standard and OPF processing. With the standard processing method, a cell is seen containing striated muscle fibres and a large electron-lucent area where the glycogen had been removed, whereas in the tissue that had undergone the OPF processing this electron-lucent area in a similar cell, is filled with highly electron dense particulate glycogen.

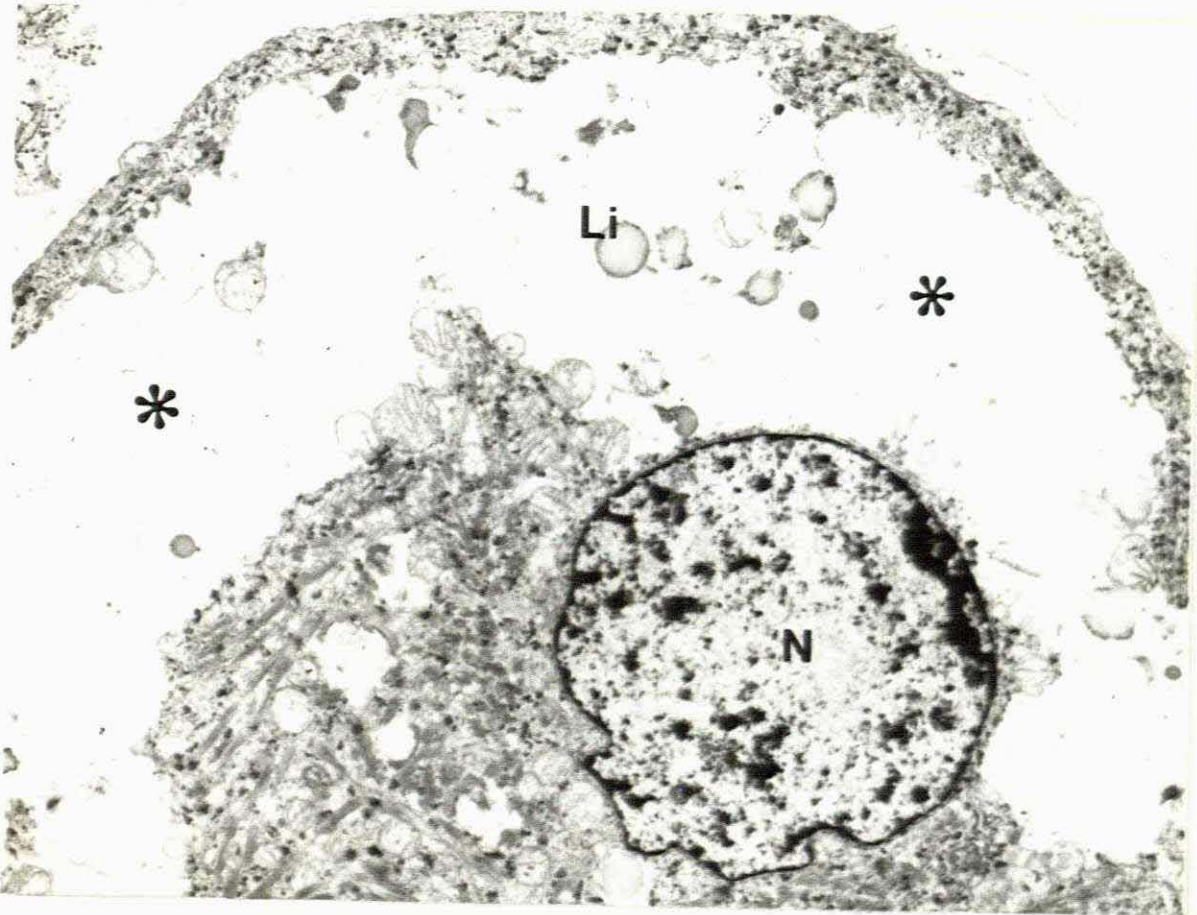


Plate 69

Intermediate magnification of a cell processed by the standard method. Glycogen appears to have been removed almost completely (black \*). (Lead & Uranyl X7000)

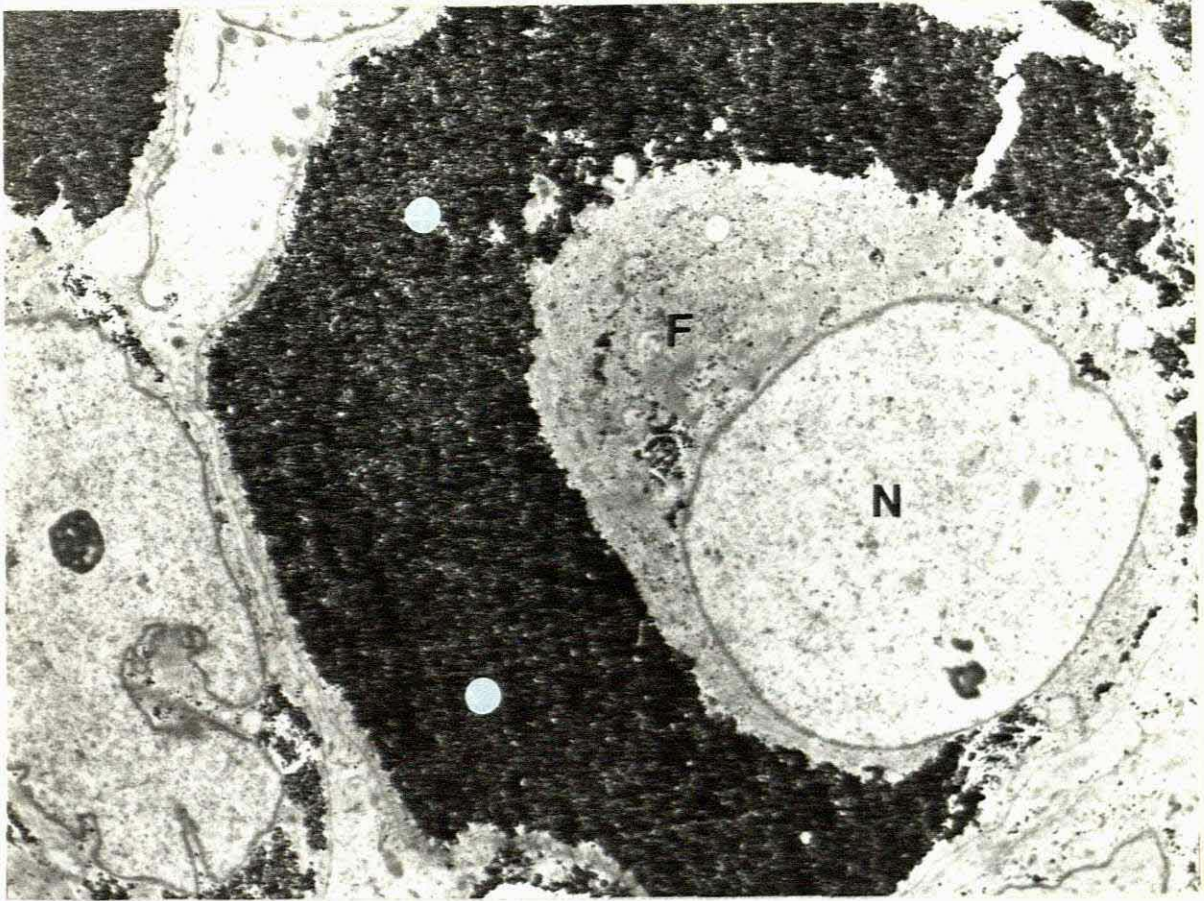


Plate 70

An abundance of very electron-dense material is seen in the cell processed with the OPF method (white dots). (Lead only X6000)

#### 4.1.6 DISTRIBUTION AND ARRANGEMENT OF GLYCOGEN IN HEPATOCELLULAR CARCINOMA

Haematoxylin & Eosin stained paraffin wax sections of this tumour, shows liver parenchyma infiltrated with large pleomorphic cells which may be encapsulated as illustrated in plate 71 but may directly infiltrate the liver as can be seen on the higher magnification in plate 72. Some of the cells have large empty-looking spaces which may be glycogen or lipid.



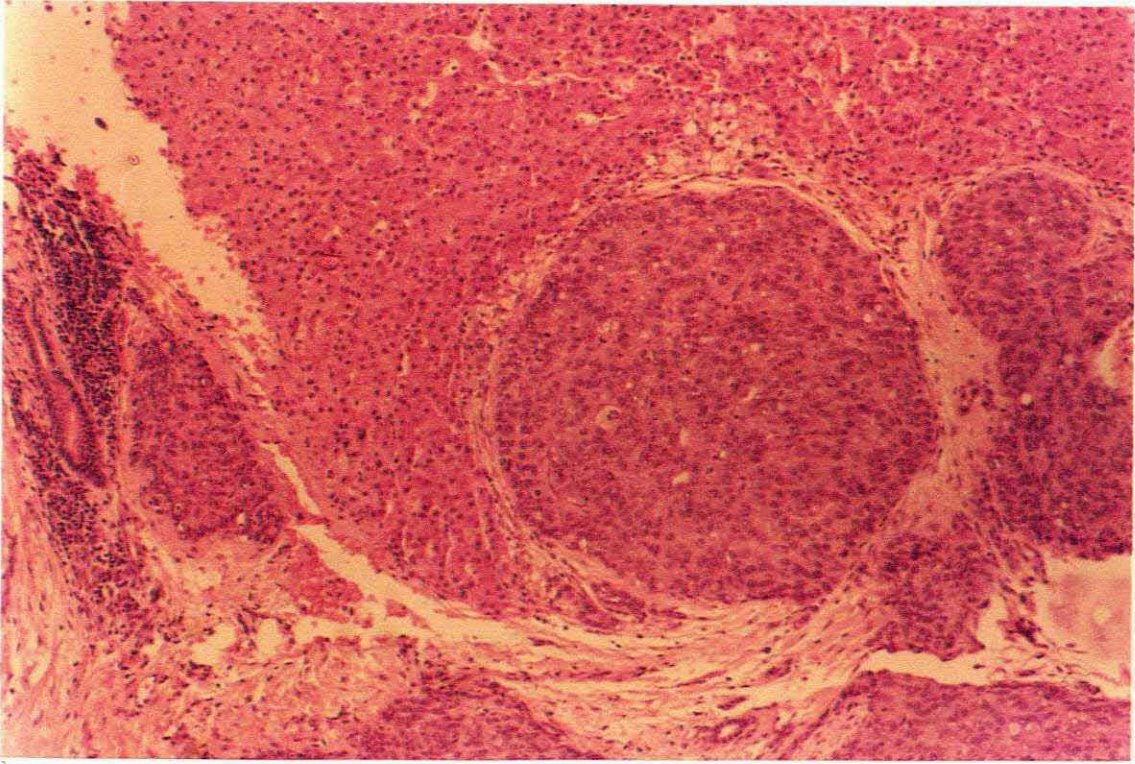


Plate 71

Low power magnification of paraffin wax section of a liver with hepatocellular carcinoma. (H&E X115)

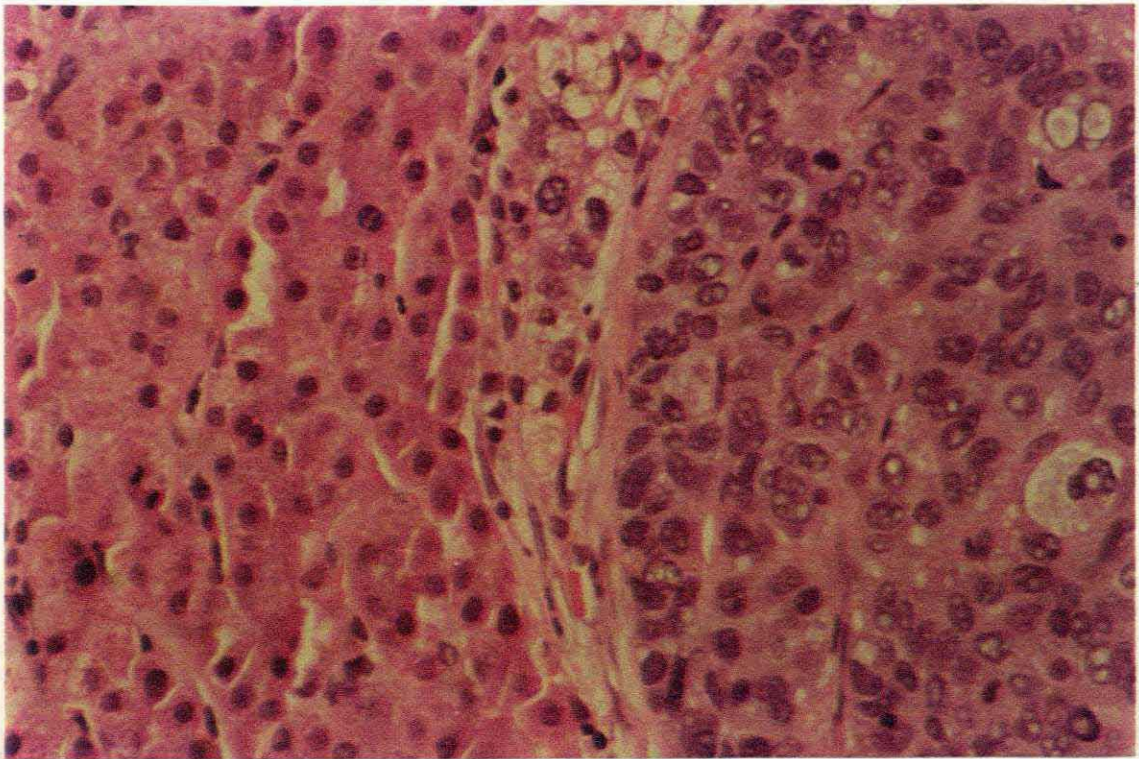


Plate 72

Higher magnification of the same area to show the growth of the tumour cells amongst the normal liver parenchyma. (H&E X450)



Plate 73 shows a resin section of tissue processed by the standard method with tumour cells infiltrating the normal liver cells.

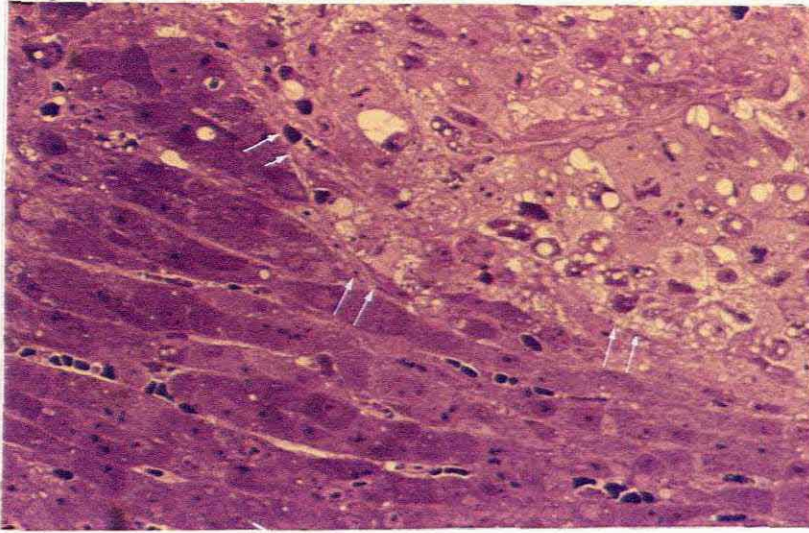


Plate 73

Low magnification of a resin section of an area similar to the one on the H&E to show the infiltration of the carcinoma cells into the normal liver cells (W. arrows). (Tol blue X225)

At higher magnification an area of normal liver is compared to the carcinoma cells. The carcinoma cells appear to have open spaces in the cells which could either correspond to lipid, mucin or glycogen. (See plate 74 & 75.)

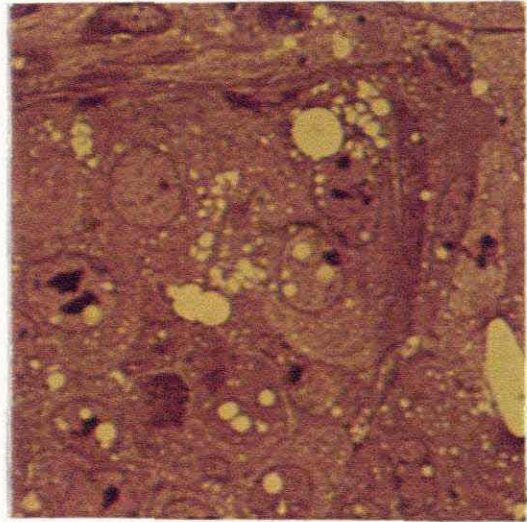
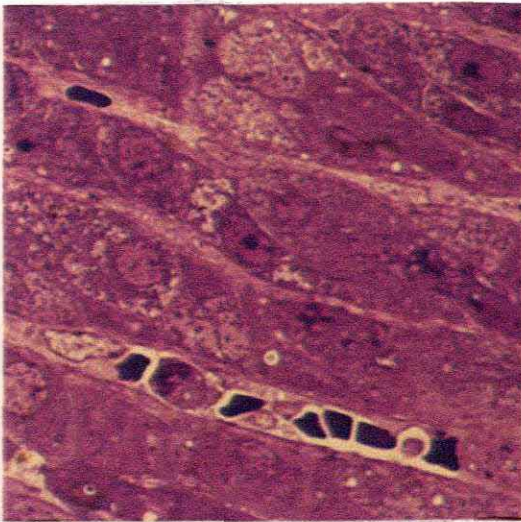


Plate 74 & 75

Higher magnifications of the same resin section to show detail of the normal liver cells and the tumour cells in plate 75. (Tol blue X 1125)



With the electron microscope thin sections of the liver tissue, processed by the standard method, showed large pleomorphic looking cells that contained numerous spaces filled with mucin, lipid and what appeared to be areas where glycogen had been removed. (See plate 76.)

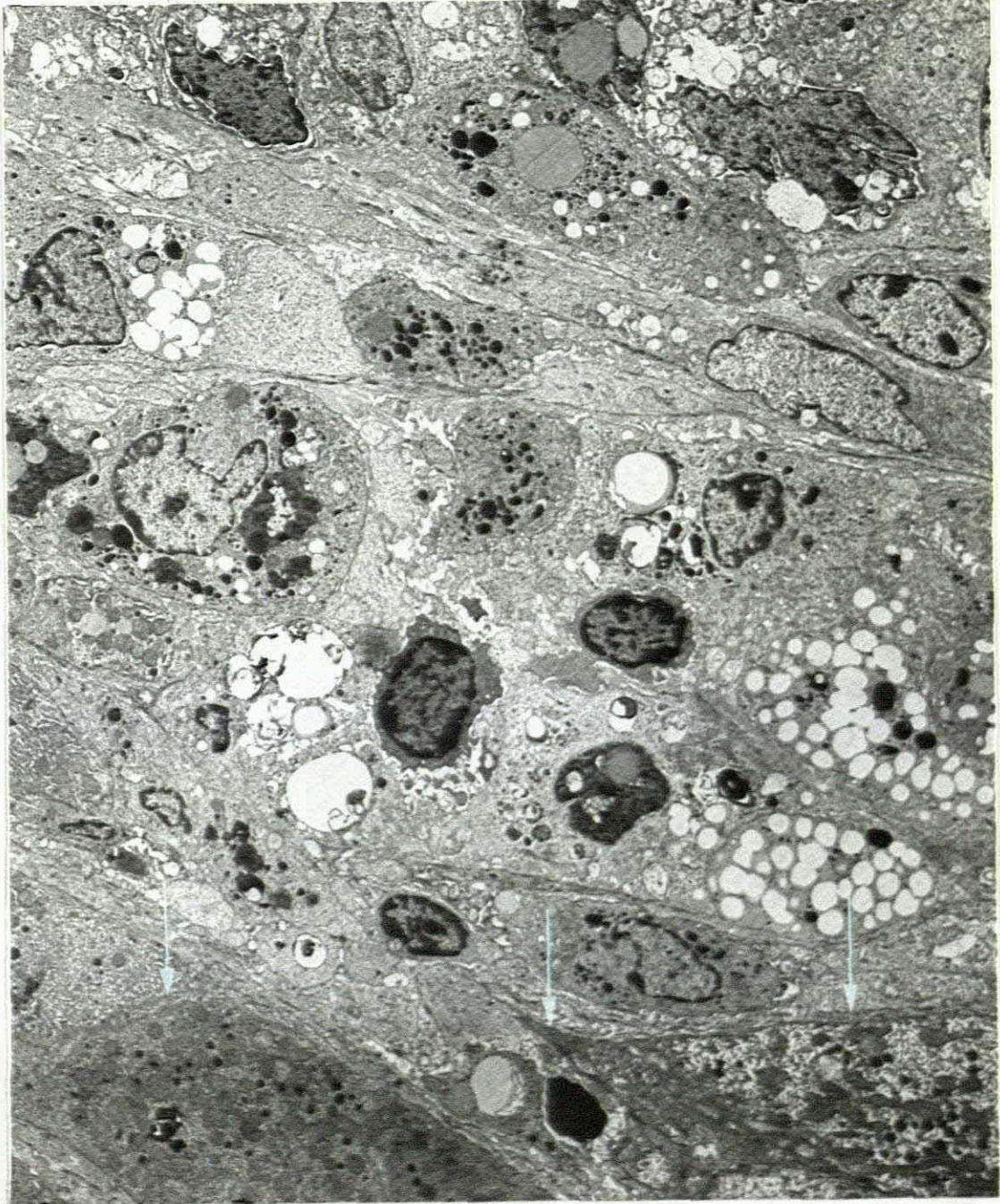


Plate 76

Low magnification of a transitional zone of a hepatocellular carcinoma and normal liver cells in a liver biopsy (W. arrows). (Lead and uranyl, X3000)



Two higher magnifications of normal liver cells and tumour cells from the area shown in plate 76, are shown in plate 77 and 78.

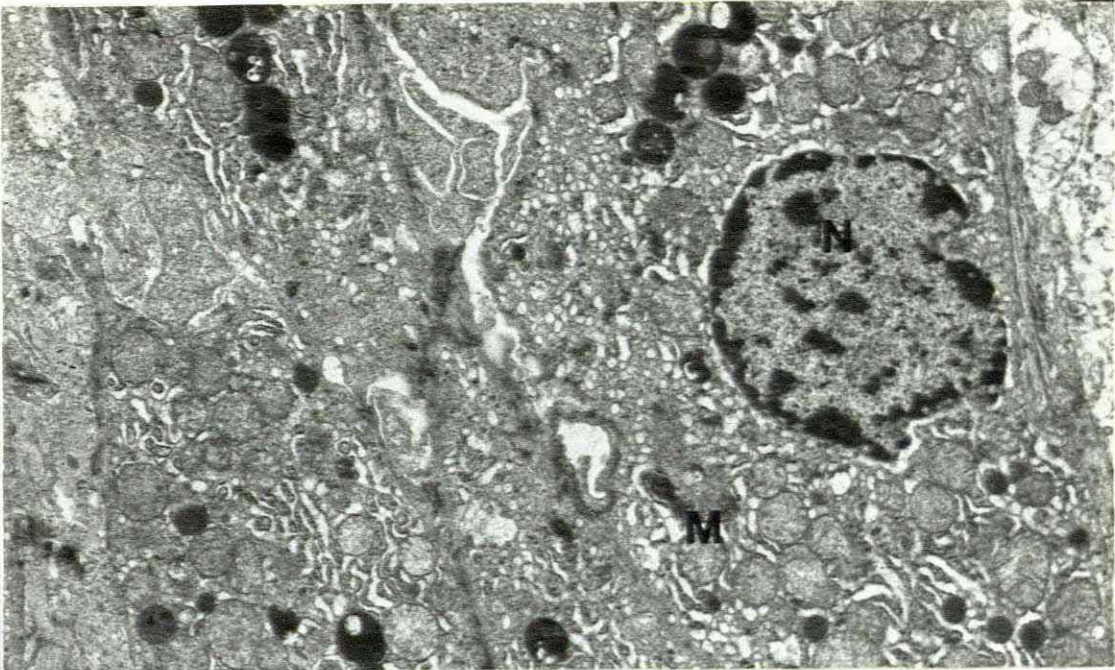


Plate 77

Normal liver cells from the same area as in plate 76. (Lead and uranyl, X7500)

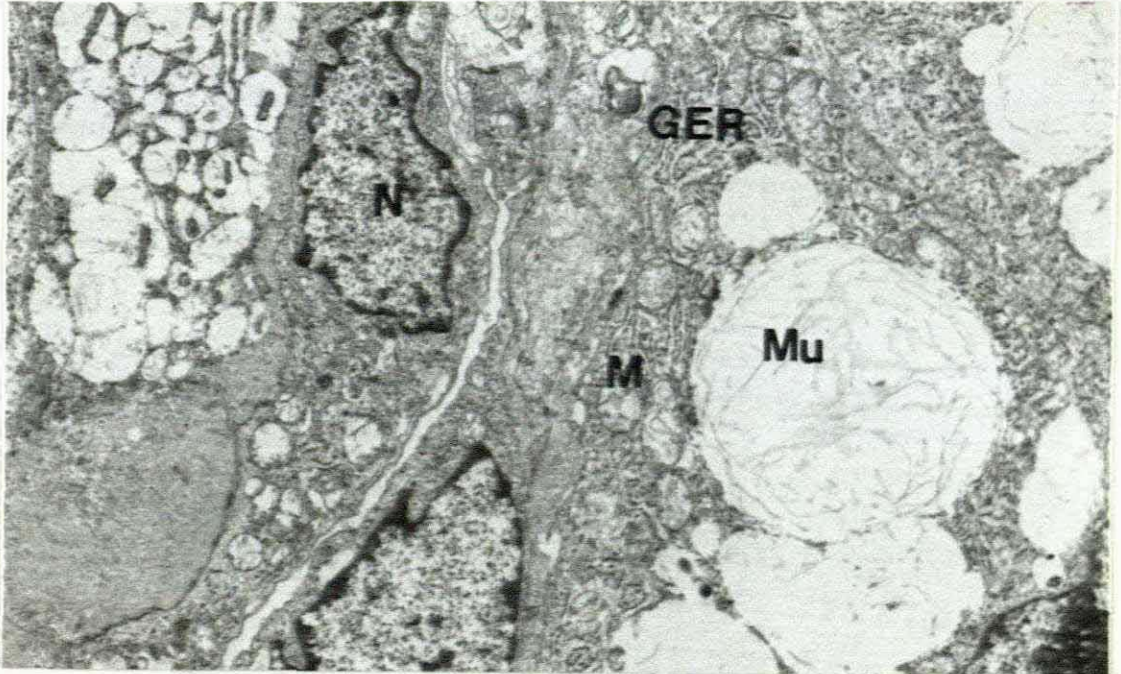


Plate 78

Tumour cells from the previous area. Note the mucin. No glycogen is apparent. (Lead & uranyl X7500)



In plates 79 and 80 a liver parenchymal cell and a carcinoma cell of tissue, processed in the standard way, are compared in the same section.

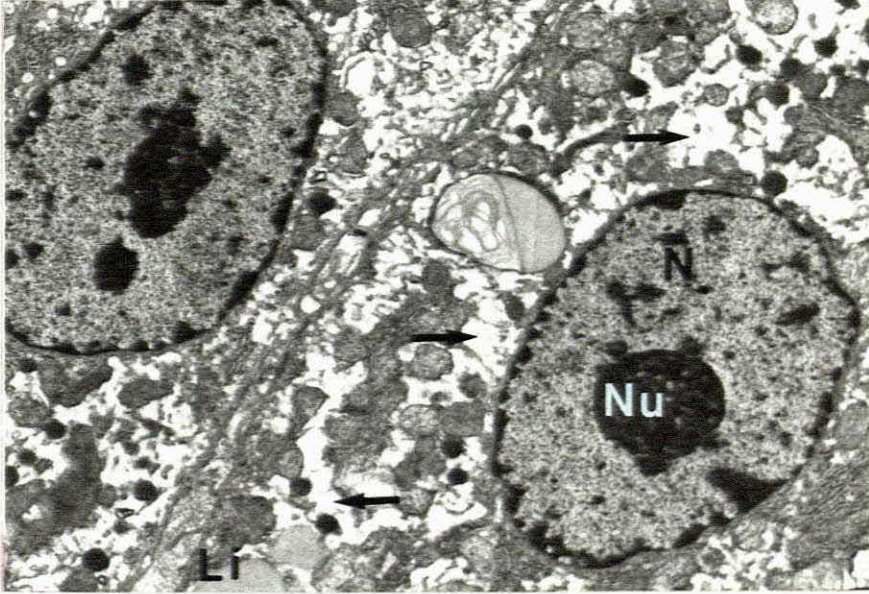


Plate 79

Intermediate magnification of normal looking liver cells from a case of hepato-cellular carcinoma. Note the electron-lucent areas where glycogen has been leached out (B. arrows). (Lead and uranyl X7500)

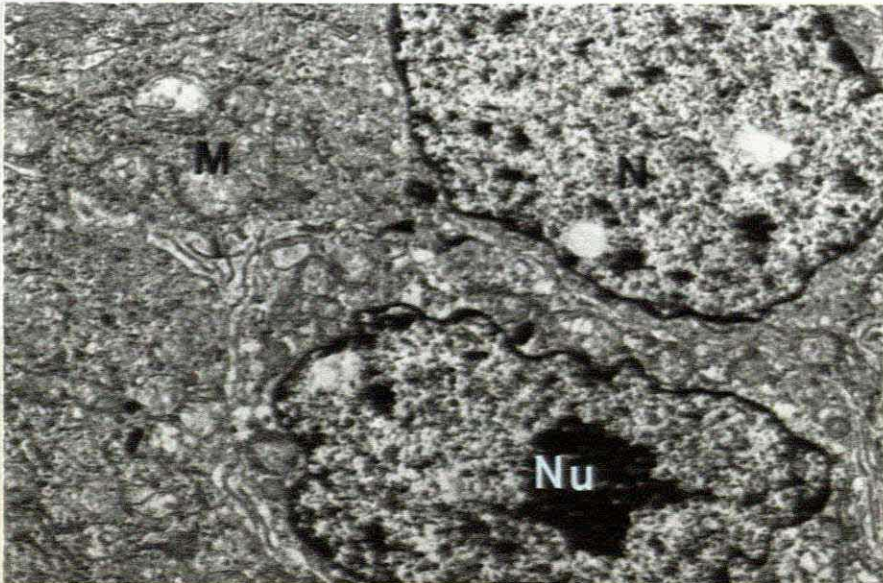


Plate 80

Cells from the tumorous part of the hepato-cellular carcinoma. (Lead and uranyl X7500)



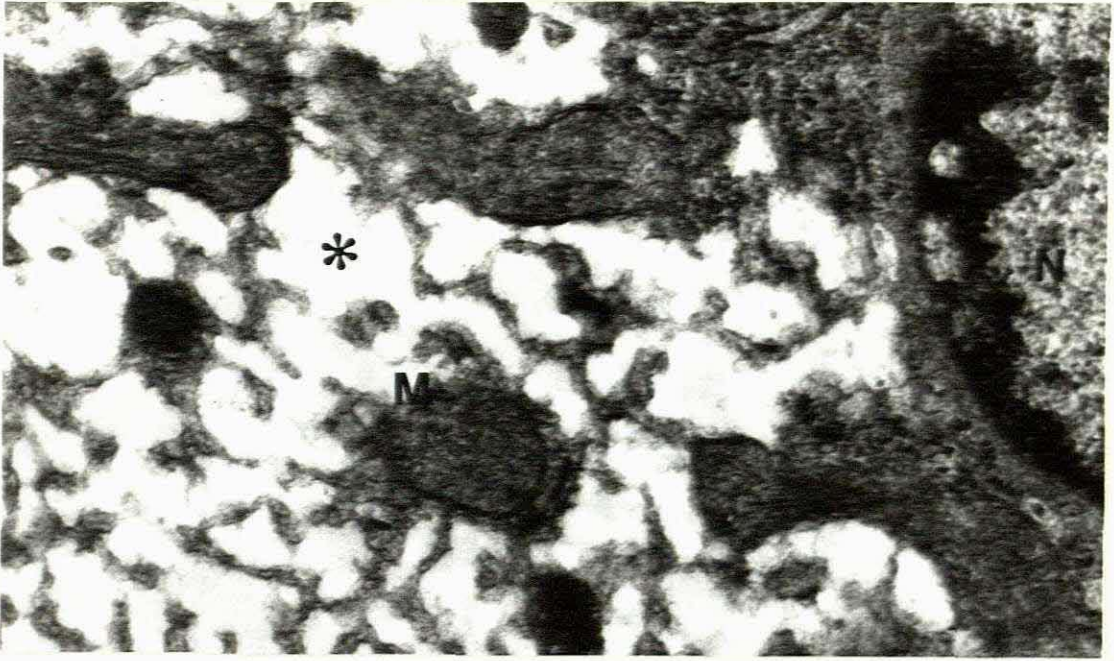


Plate 81

High magnification of a liver cell from the normal area to show that all glycogen appears to have been leached out (black \*). (Lead & uranyl X36000)

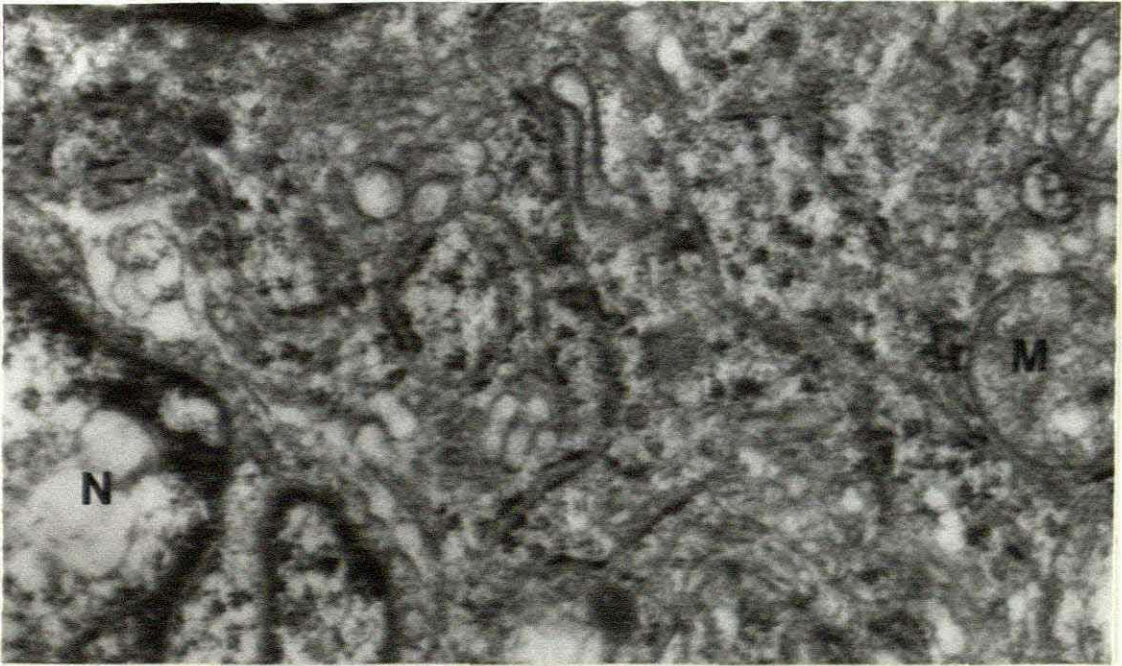


Plate 82

An area from a tumour cell to show that there is scant retention of glycogen with standard processing. (Lead & uranyl X36000)



At high magnification, cells of the tissue processed with the standard method show total loss of the glycogen in the normal liver cells, and only scant retention of some glycogen particles in the tumour cells as can be seen in plate 81 and 82.

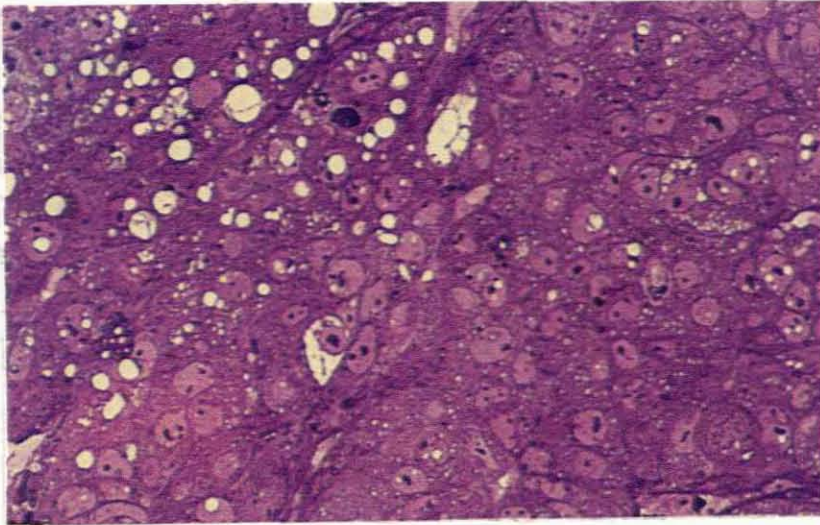


Plate 83

Low magnification of a resin section from a hepatocellular carcinoma, processed with the OPF method. (Tol blue X450)

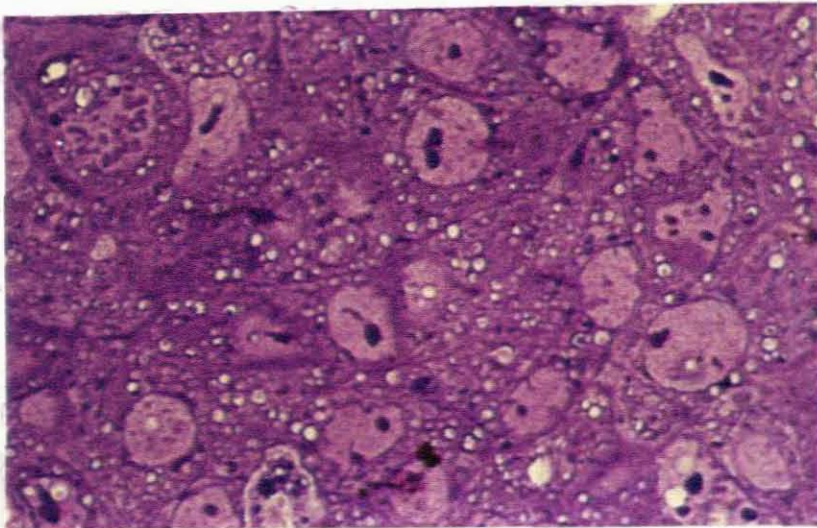


Plate 84

Higher magnification of the above tissue to show that in spite of the OPF processing, glycogen is not prominent. (Lead only X1125)



When liver tissue containing the hepato-cellular carcinoma was processed with the modified OPF method retention of glycogen was not well demonstrated, as can be seen in the micrographs of the resin sections in plates 83 and 84. Low magnification electron micrographs of the tissue, revealed liver parenchymal cells containing normal amounts of glycogen. Large pleomorphic looking cells, containing diffusely scattered glycogen, could be seen infiltrating the liver parenchyma. (See plate 85.)

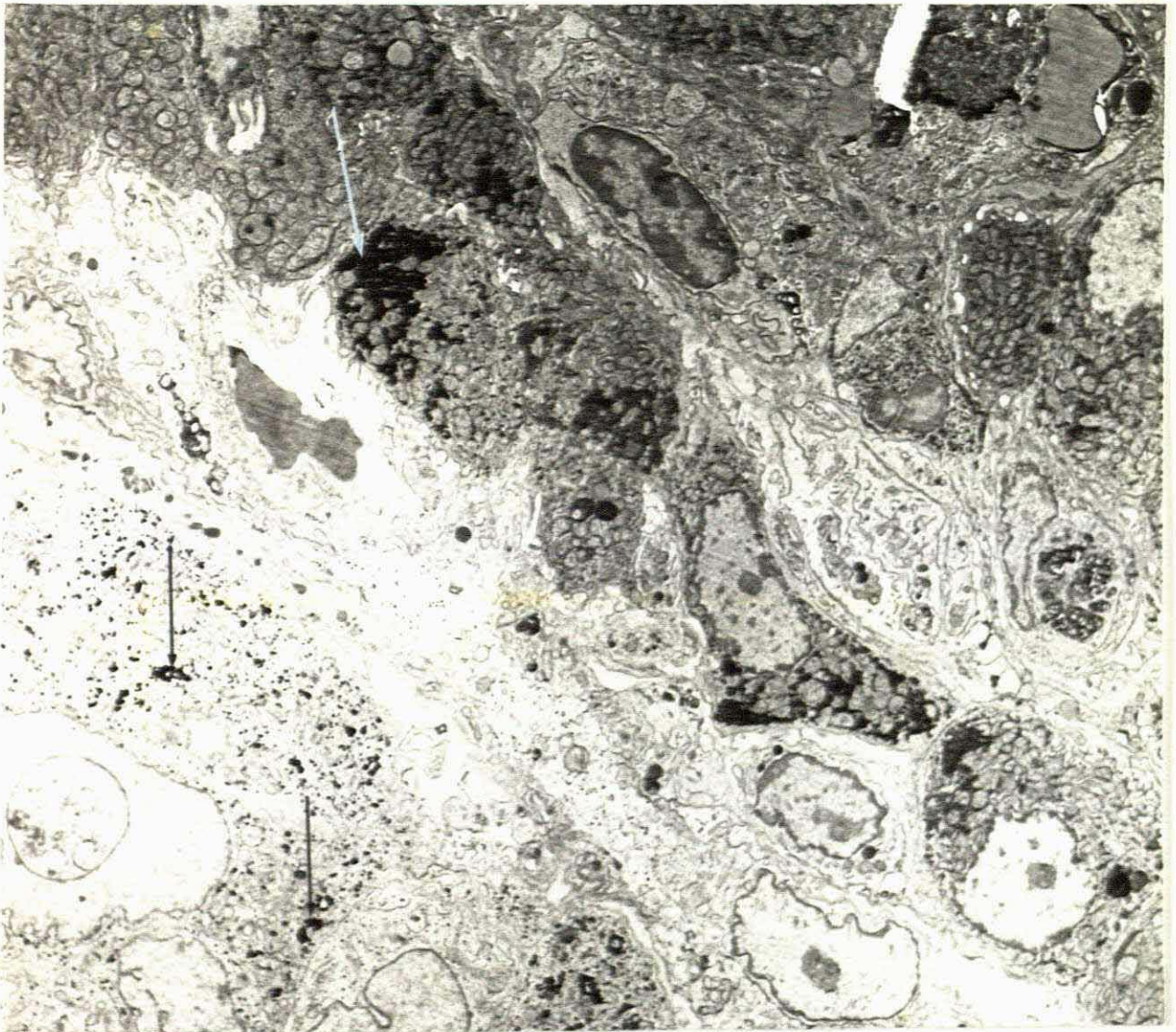


Plate 85

Low power magnification of OPF processed resin embedded tissue to show normal liver cells infiltrated by carcinoma cells. The intracellular glycogen can be seen clearly (B & W. arrows). (Lead only, X3000)



Plate 85 and the higher magnification plate 86 contrasts the difference between distribution of glycogen in liver and tumour cells. Plate 87 demonstrates the diffuse distribution of glycogen in a tumour cell.

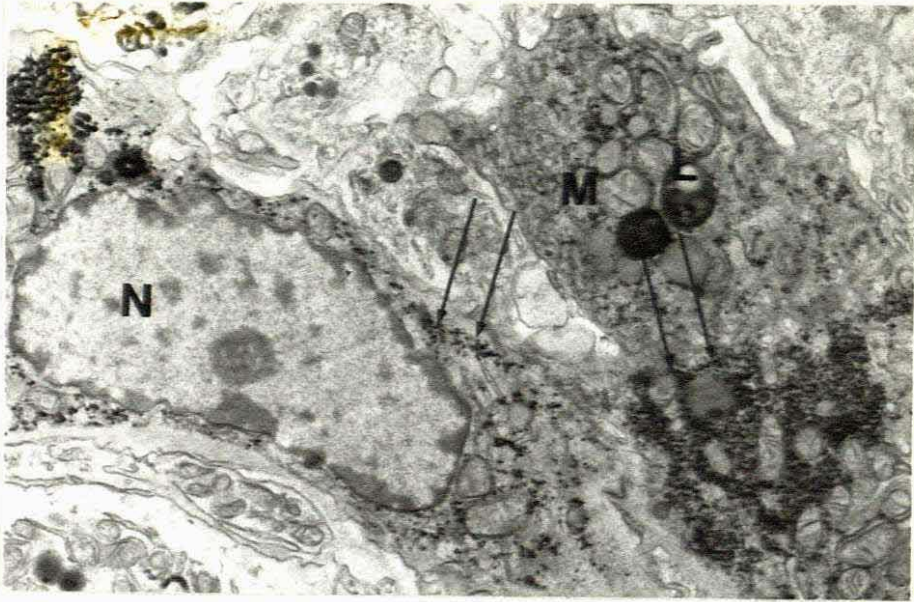


Plate 86

This micrograph shows distribution of glycogen in tumour and liver cells (B. arrows). (Lead only X6000)

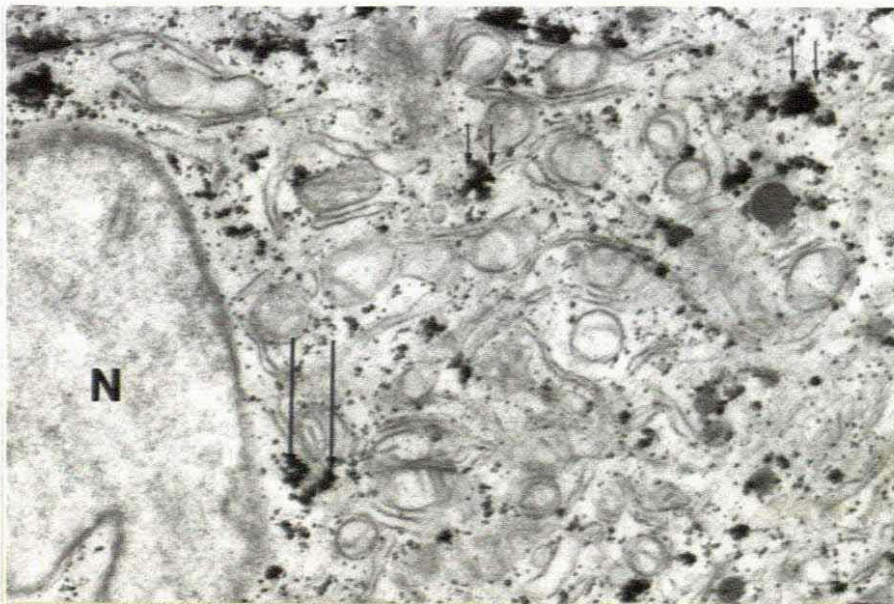


Plate 87

High magnification of a tumour cell to show the diffuse distribution of the glycogen (B. arrows). (Lead only X15000)



At high magnification, it can be seen that the liver cells contain mainly  $\alpha$  glycogen particles in aggregates, whereas the tumour cells contain mainly  $\beta$  glycogen particles distributed diffusely. (See plate 88 and 89.)

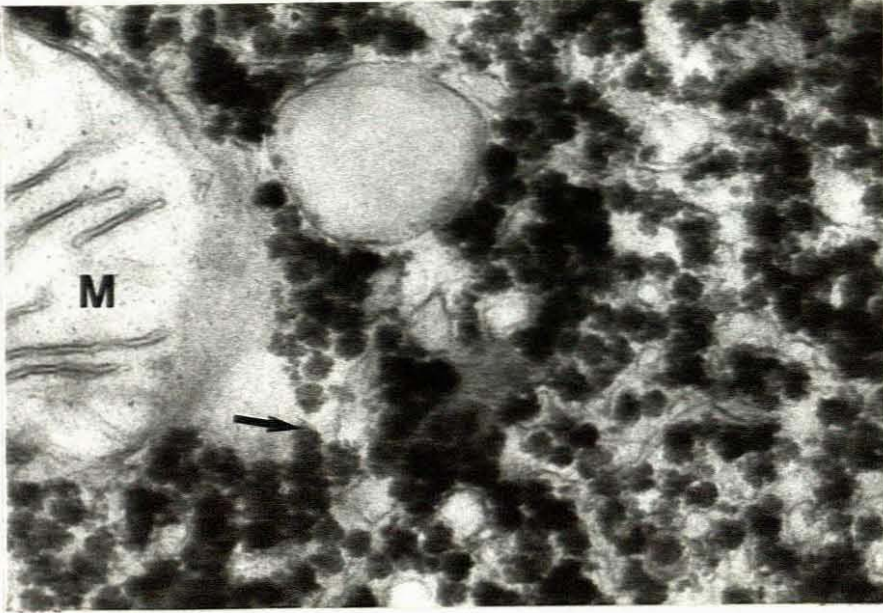


Plate 88

At high magnification the liver cells are shown to contain predominantly  $\alpha$  glycogen particles (B. arrows). (Lead only, X60000)

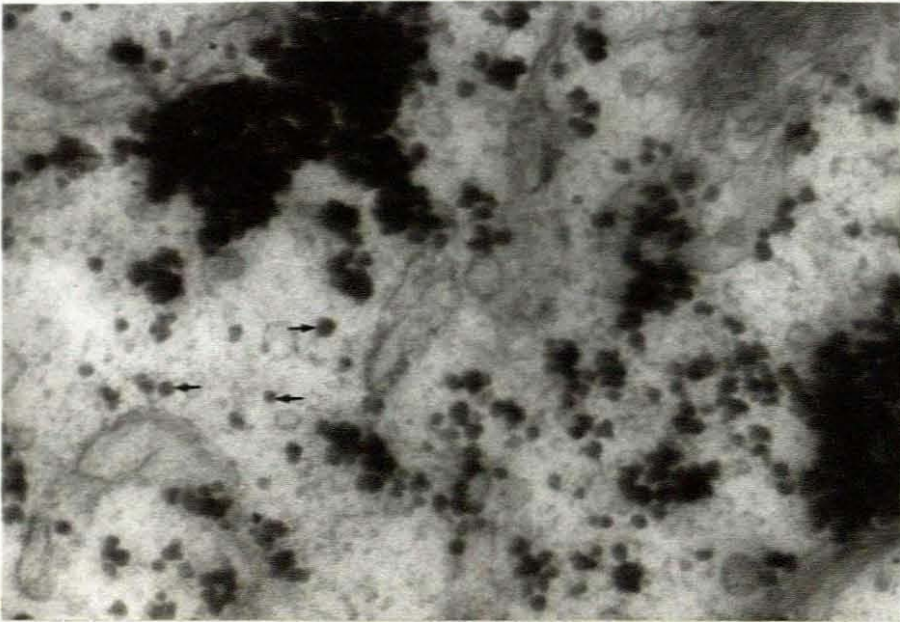


Plate 89

At the same magnification the carcinoma cells are shown to contain  $\beta$  glycogen particles in a more diffusely scattered pattern (B. arrows). (Lead only, X60000)

## 4.1.7

COMPARATIVE SUMMARY OF PROCEDURES

	<u>ROUTINE PROCESSING METHOD (OCUB)</u>	<u>MODIFIED OPF METHOD (TYGERBERG)</u>
FIXATION	2.5% BUFFERED GLUTARALDEHYDE	DITTO
POST-FIXATION	1% BUFFERED OSMIUM TETROXIDE	2% OSMIUM TETROXIDE/POTASSIUM FERROCYANIDE
en bloc STAINING	ALCOHOLIC URANYL ACETATE SOLUTION	NONE
DEHYDRATION	GRADED ETHANOLS	DITTO
IMPREGNATION	50 : 50 RESIN/ALCOHOL	DITTO
EMBEDDING	RESIN	RESIN
POLYMERIZATION	18 HOURS AT 60°C	DITTO
SECTIONING	60-90 nm SECTIONS	DITTO
STAINING	LEAD AND URANYL SALTS	LEAD ONLY
PHOTOGRAPHY	ELECTRON MICROSCOPE	DITTO

4.1.8 SUMMARY OF RESULTS FOR THE OPF METHOD

<u>TISSUE OR TUMOUR</u>	<u>APPEARANCE OF GLYCOGEN</u>	<u>QUANTITY</u>	<u>DISTRIBUTION</u>
LIVER	LARGE DENSE AGGREGATES & SINGLY	++++	DIFFUSE
MUSCLE	LARGE, LOOSE AGGREGATES & SINGLY	+++	DIFFUSE
EWING'S SARCOMA	LARGE & SMALL AGGREGATES & SINGLY	+++	FOCAL
LEIOMYOSARCOMA	LARGE & SMALL AGGREGATES & SINGLY	++	FOCAL
RHABDOMYOSARCOMA	LARGE AGGREGATES	++++	FOCAL
HEPATOCELLULAR Ca	SMALL DENSE AGGREGATES & SINGLY	++	DIFFUSE



## 4.2 RESULTS OF MYELOPEROXIDASE AND PLATELET SPECIFIC PEROXIDASE METHODS

### 4.2.1 MYELO-PEROXIDASE (MPO) RESULTS

An existing ultrastructural enzyme histochemical method was modified and refined, to yield highly selective and reproducible results so as to help in the diagnosis of undifferentiated myelo- and lymphoblastic leukaemias.

Reaction product from the modified method that was used, was only found in the primary lysosomes of the myeloid precursors as well as the mature granulocytes. (See Chapter III for method and Appendix for reagents.) Any granules that were seen in the lymphoid cells, were negative with this method. Not only was the glycogen contrasted when OPF post-fixation was used instead of the standard buffered osmium tetroxide fixative, but the ultrastructural localization of the reaction product was also improved. Electron density of the reaction product in the polymorphonuclear leucocytes (PMN) was also increased. Plates 90 and 91 are light microscopic photographs of a lymphoblastic leukaemia processed with the modified myeloperoxidase method. Note that the erythrocytes show a strongly positive reaction, whereas no positivity was discernible in the leukocytes. By contrast, plates 92 and 93 are of a myeloblastic leukaemia. A positive reaction was shown in the red cells as well as a just visible reaction in the white cells.

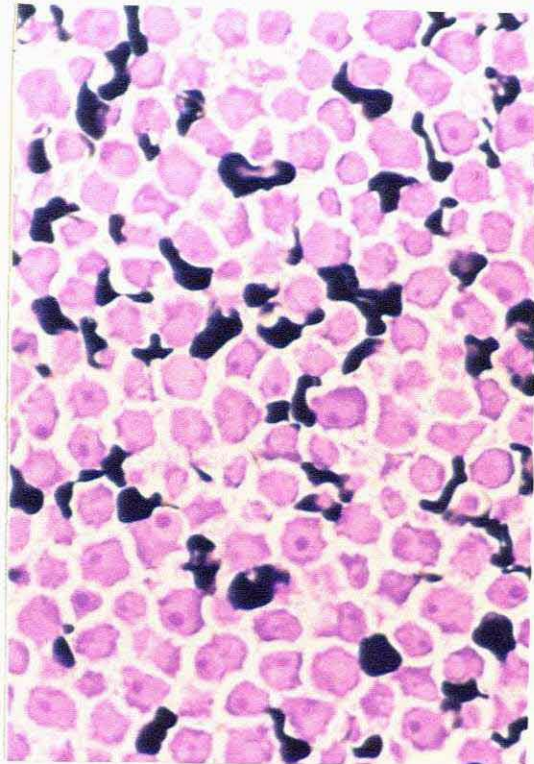
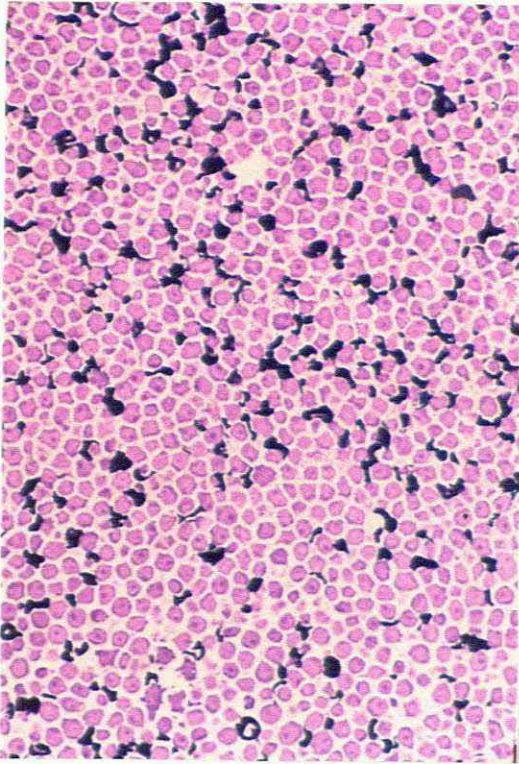


Plate 90 & 91

1 $\mu$ m resin sections of a lymphoid leukemia from blood treated with the myelo-peroxidase method. (Tol blue X450 & X 1125)

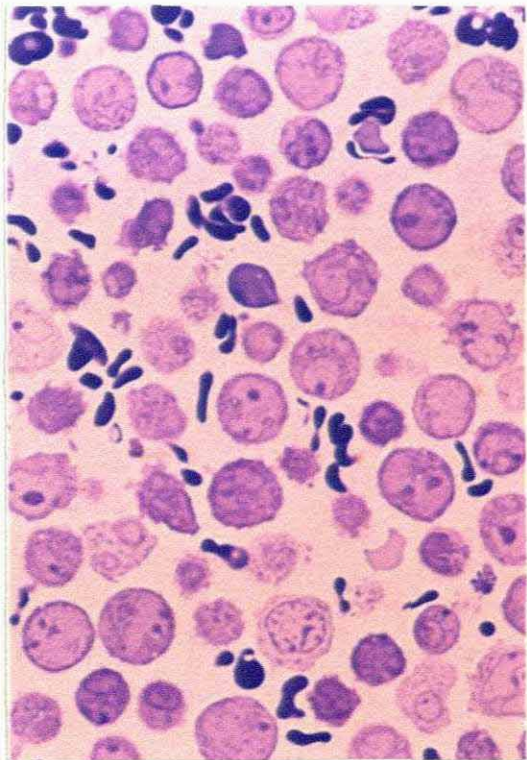
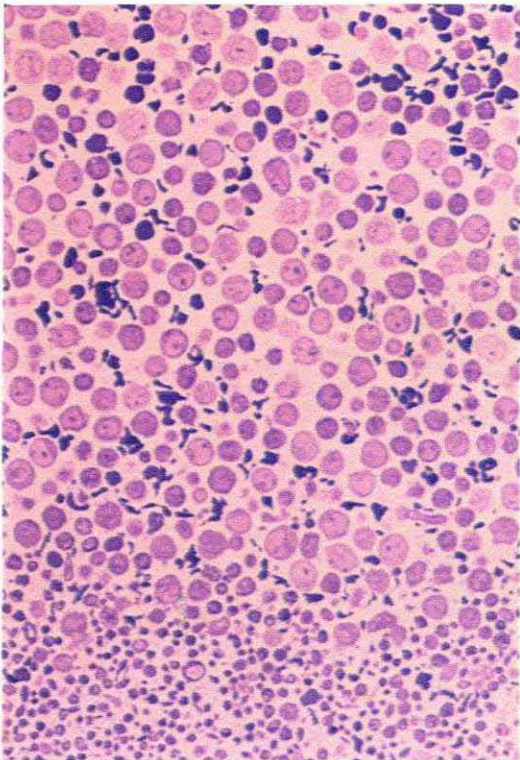


Plate 92 & 93

1 $\mu$ m resin section of a myeloid leukemia from blood treated with the myelo-peroxidase method. (Tol blue X450 & X1125)



Control blocks from the same specimen were subjected to a blocking procedure for peroxidase. The results are shown in plates 94 and 95. No reaction product is discernible in the erythrocytes as well as the granules in the PMN in plate 95.



Plate 94 Low magnification of a control block that was subjected to a peroxidase blocking procedure. No reaction product is visible in the red cells as well as in the granules of the PMN. (Black arrows)(Resin, lead & uranyl X7500)

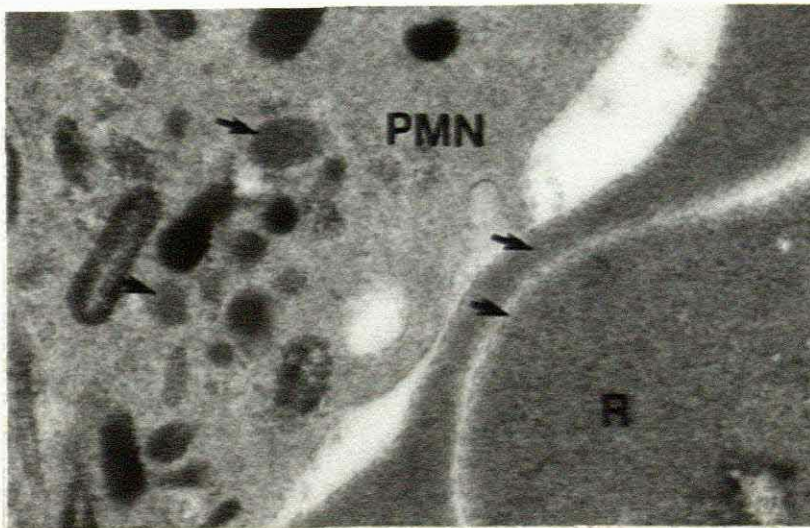


Plate 95 Higher magnification of the previous field to show detail of the red cell and the granules in the PMN. (Black arrows)(Resin, lead & uranyl, X36000)



Plates 96 and 97 are micrographs of a thin section from a lymphoblastic leukaemia processed for myeloperoxidase, but post-fixed with standard osmium tetroxide fixative. There is positive reaction product in the erythrocytes, but none in the leukocytes.

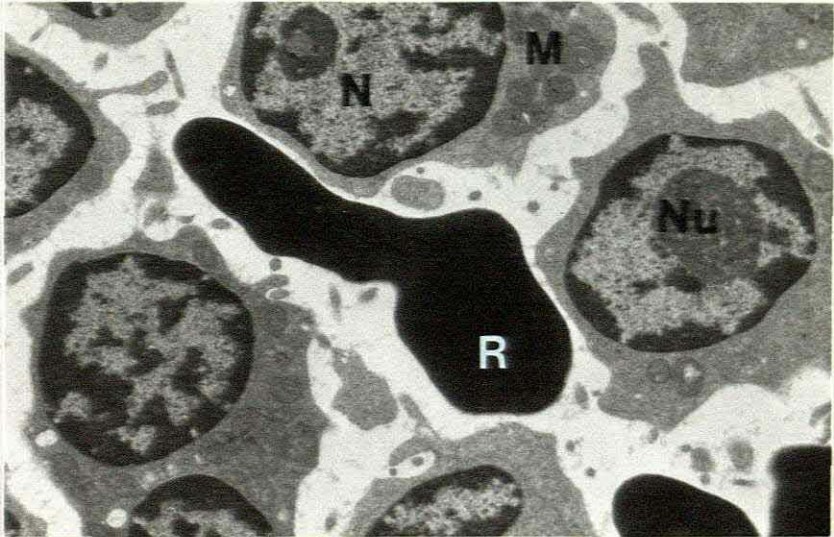


Plate 96

Low magnification of a thin section of tissue processed for myelo-peroxidase to show reaction product in the red cells and none in the white cells. (Lead and uranyl X7500)

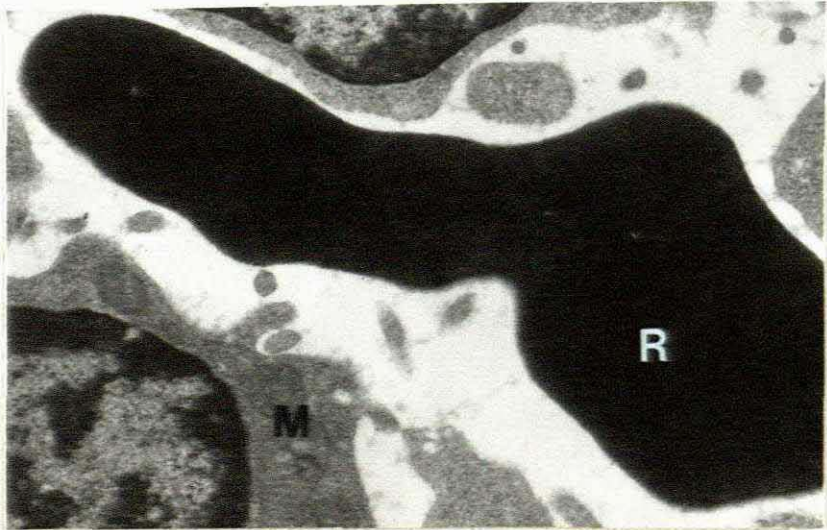


Plate 97

Higher magnification of the previous section to show the positive reaction in the red cell. (Lead and uranyl X 15000)

When the same tissue was processed for myelo-peroxidase, but post-fixed with the modified OPF mixture, glycogen was contrasted and the reaction product was more electron-dense in the red cells. (See plate 98 and 99.)

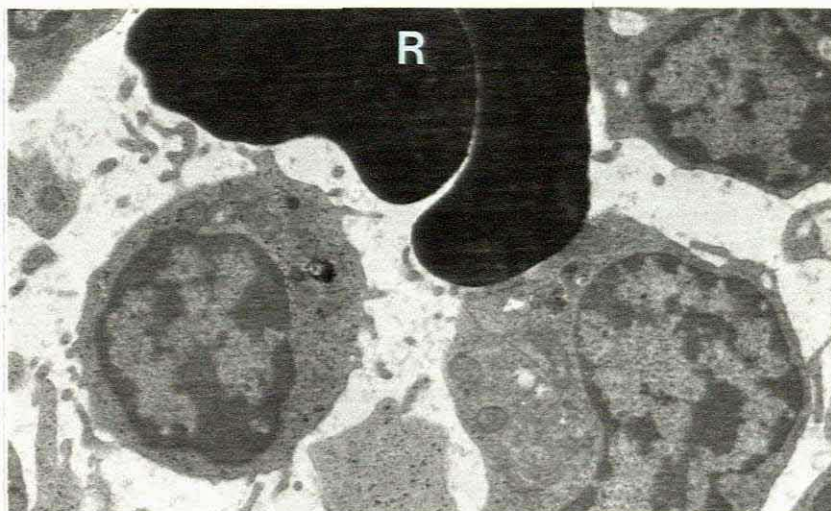


Plate 98

Low magnification micrograph of a thin section of the blood processed with myelo-peroxidase method, but post-fixed with the OPF method. (Lead, no uranyl X7500)



Plate 99

High magnification of plate 98 to show the glycogen in the cells (thin arrows) and a lymphocytic granule which is DAB negative (thick arrow) while the red cell (R) is positive for MPO. (Lead, no uranyl X45000)



A case of myeloblastic leukaemia was also processed for myelo-peroxidase and post fixed with standard osmium fixative. The results are shown in plate 100 and 101.

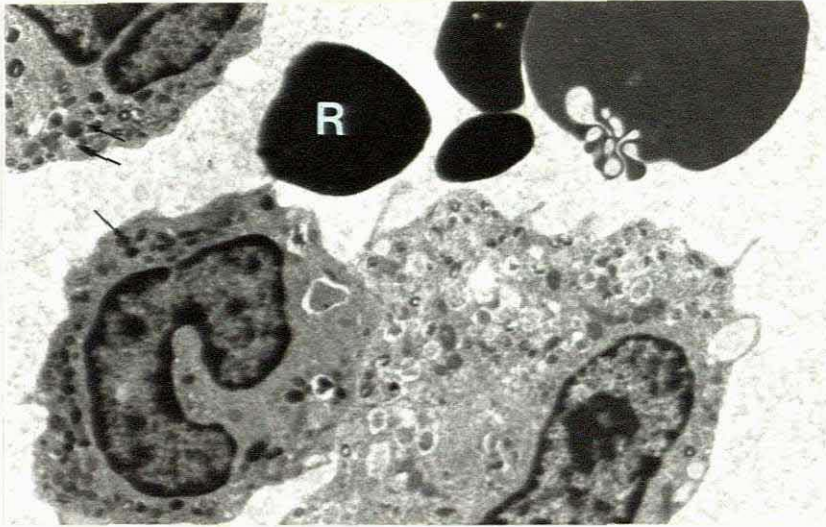


Plate 100

Peripheral blood from a case of Myeloid leukaemia that has been processed for myelo-peroxidase. Note the DAB positive granules in the granulocytic precursors (arrows). The red cells are also positive. (Lead and uranyl X6000)

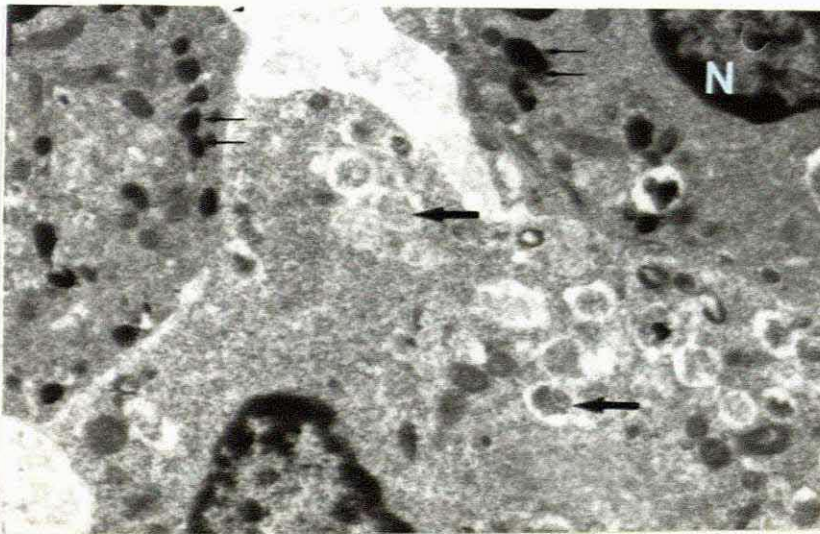


Plate 101

The granules in the white cells (thin arrows) are DAB positive as are the red cells. Note that the granules in the basophil are negative (thick arrows) with respect to this reagent. (Lead and uranyl X12000)



A comparison was made with the same tissue when modified OPF fixative was used for post-fixation. (See plates 102 to 104.)

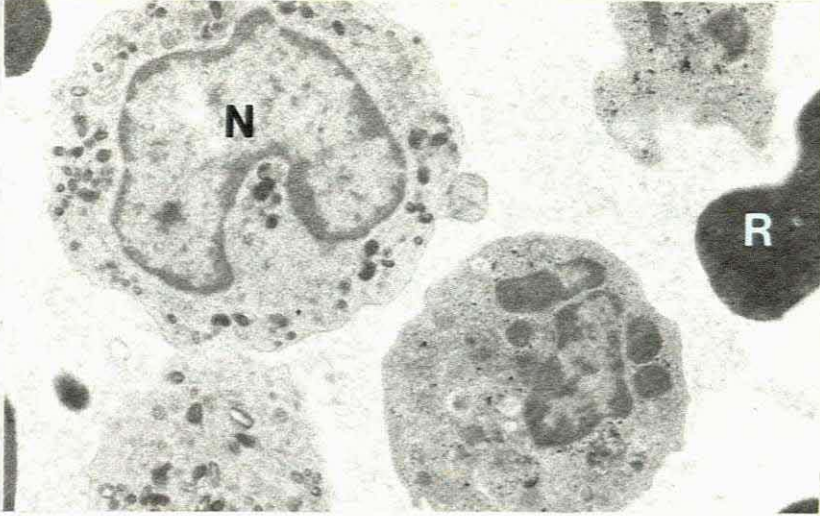


Plate 102

The same specimen on which the myeloperoxidase technique was applied but post-fixed with OPF. (Lead, no uranyl X6000)

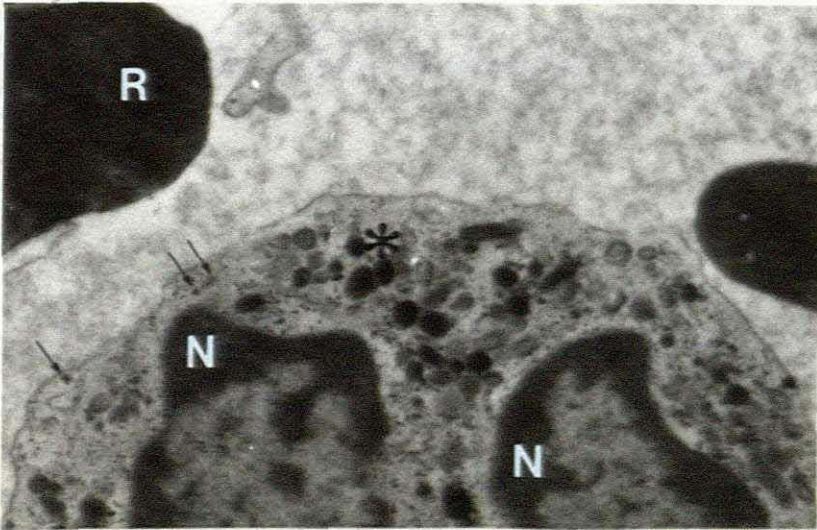


Plate 103

A higher magnification of the same area to show detail of the positive DAB reaction in the granules of the granulocytic precursors (asterisk). Note the glycogen granules (arrows). (OPF post-fixation, lead, no uranyl X12000)

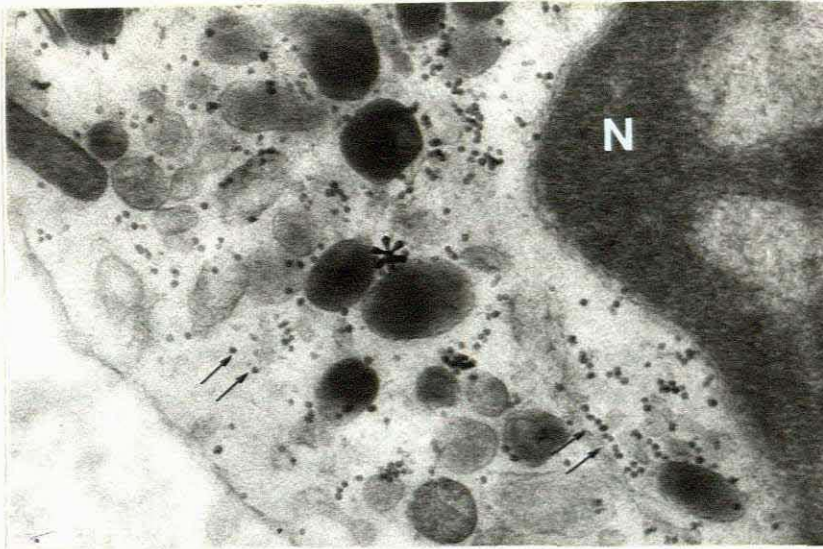


Plate 104

Glycogen is well contrasted (arrows) and there is a positive DAB reaction in the granules of the white cell (black \*). (OPF post-fixation, lead, no uranyl, X36000)

#### 4.2.2 PLATELET SPECIFIC PEROXIDASE (PPO) RESULTS

A similar modification of the method employed by Breton-Gorius et al (1978) was used for the diagnosis of Acute granulocytic leukaemia. (See Chapter III for method and Appendix for DAB reagent.)

An extremely strong reaction product was observed, not only in the granules of the white cell and megakaryocytic precursors, but also in the peri-nuclear cisternae and endoplasmic reticulum of the megakaryocytic precursors. This reaction was inhibited by normal glutaraldehyde fixation under conditions in which the peroxidase activity is preserved in granulocytic precursors. Localization in the endoplasmic reticulum was similar to that found in the normal megakaryocytic series (Breton-Gorius et al, 1976).



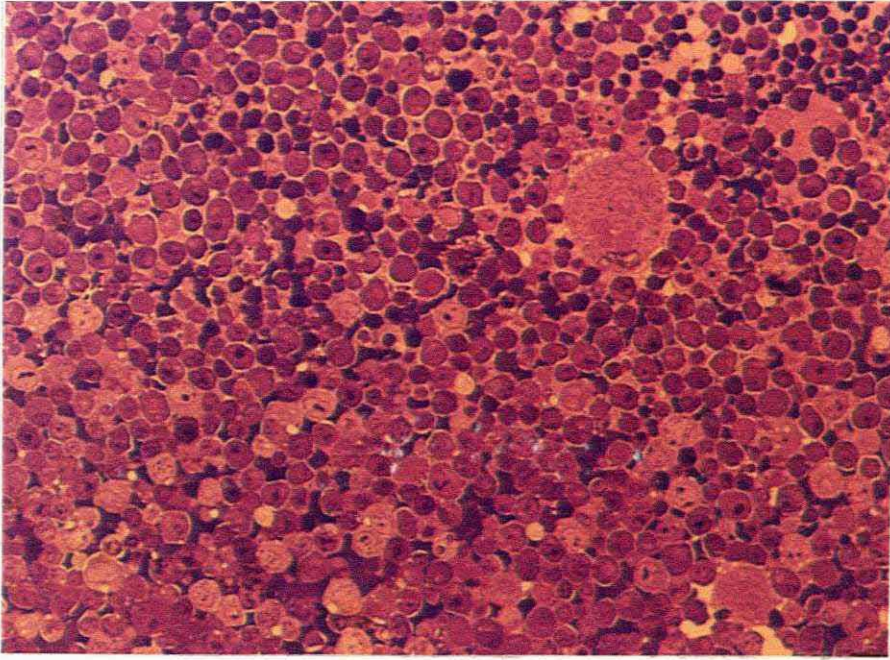


Plate 105

1 $\mu$  resin section of bone marrow with suspected Granulocytic leukaemia. Observe the bland appearance of the cells at this magnification. (OCUB processing, Tol blue X450)

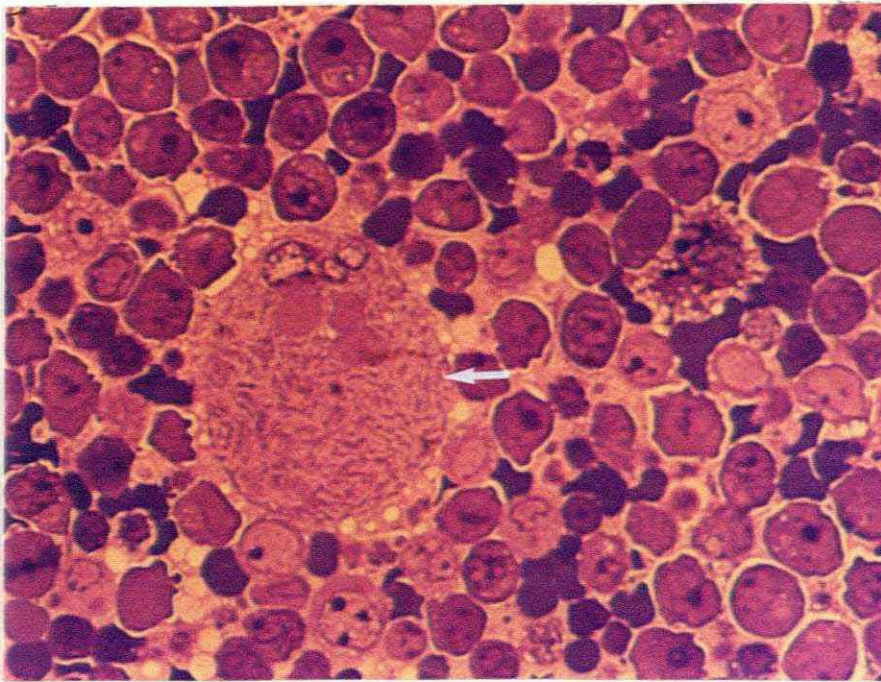


Plate 106

Higher magnification of the preceding area. Note the megakaryocyte (W. arrow) on the left of the picture. (Tol blue X1125)



When thin sections of the above tissue were viewed with the electron microscope, large bland looking cells interspersed with plasma cells and other precursors of the white cell series were seen. (See plate 107.)

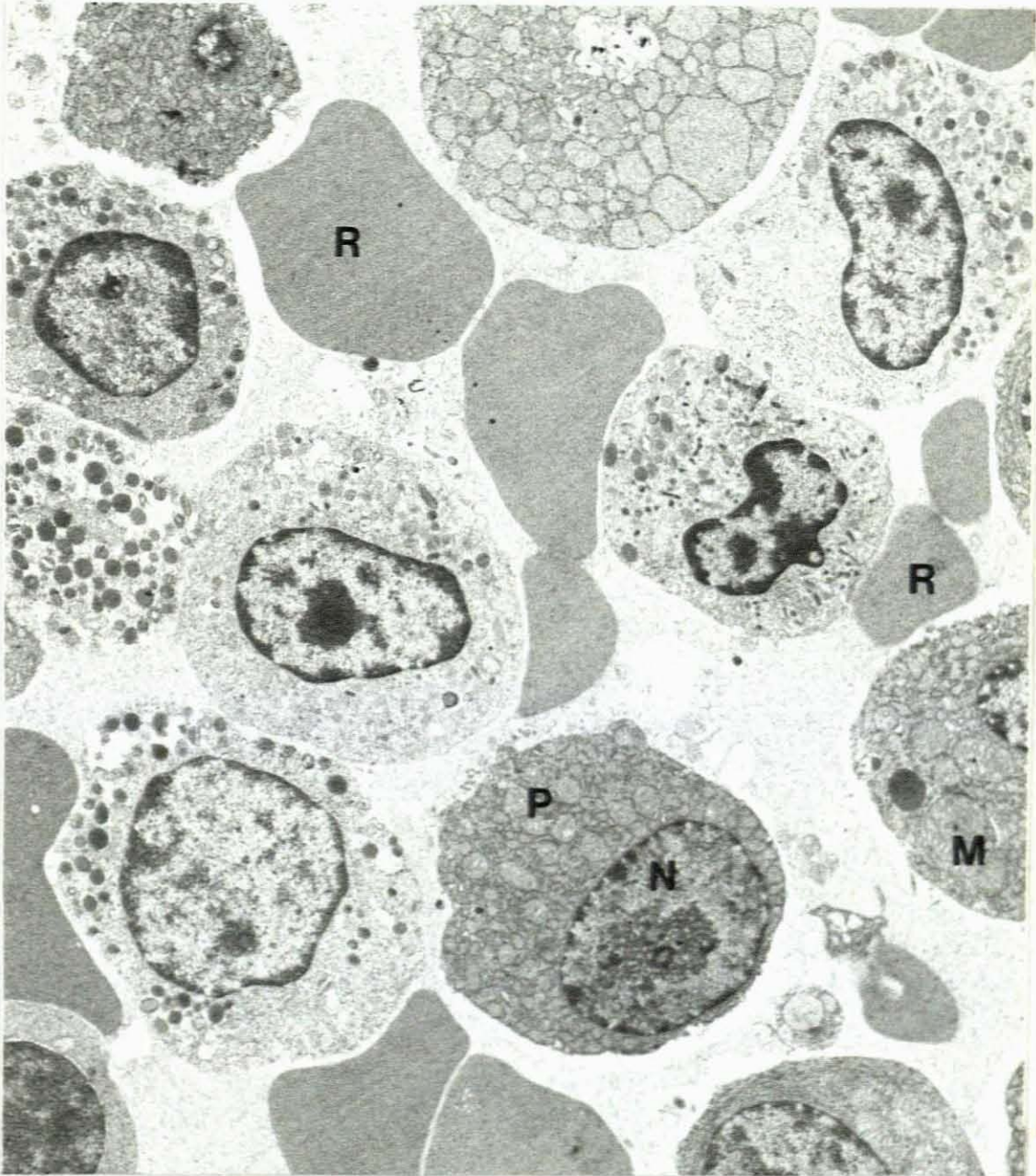


Plate 107 Low magnification of a thin resin section of bone marrow from a case of suspected granulocytic leukaemia. There are a few plasma cells interspersed with white cell precursors, as well as a few bland-looking cells which may be leukaemic megakaryocytes. (OCUB processing X6000)



Large mature looking megakaryocytes were seen in the sections. (See plate 108.)



Plate 108

Low magnification micrograph of a megakaryocyte from the same section. (Lead and uranyl X4500)



At an intermediate magnification detail of the nucleus and the specific granules was clearly seen. See plate 109 and 110.

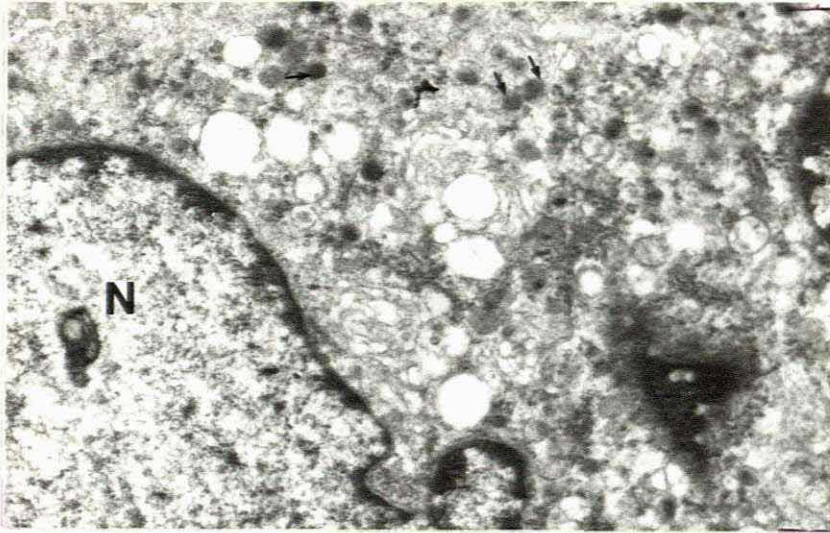


Plate 109

Intermediate magnification of megakaryocyte to show nucleus and granules. (Lead and uranyl X12000)

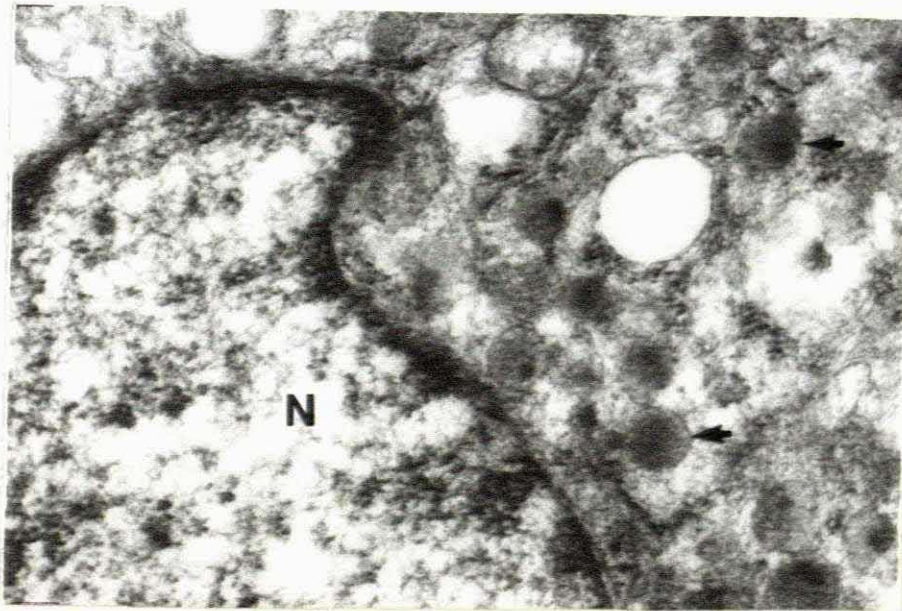


Plate 110

High magnification micrograph of the same area to show detail of nucleus and granules. (Lead and uranyl X36000)



When bone marrow from a case of granulocytic leukaemia was fixed and processed according to the method of Breton-Gorius, platelet-specific peroxidase was not inhibited by the tannic acid/para-formaldehyde/glutaraldehyde fixative employed. It was noted that as megakaryocytes matured the peroxidase disappeared from the specific granules and was only found in the perinuclear cisternae of the cells. Plate 111 shows bone marrow processed for platelet peroxidase.

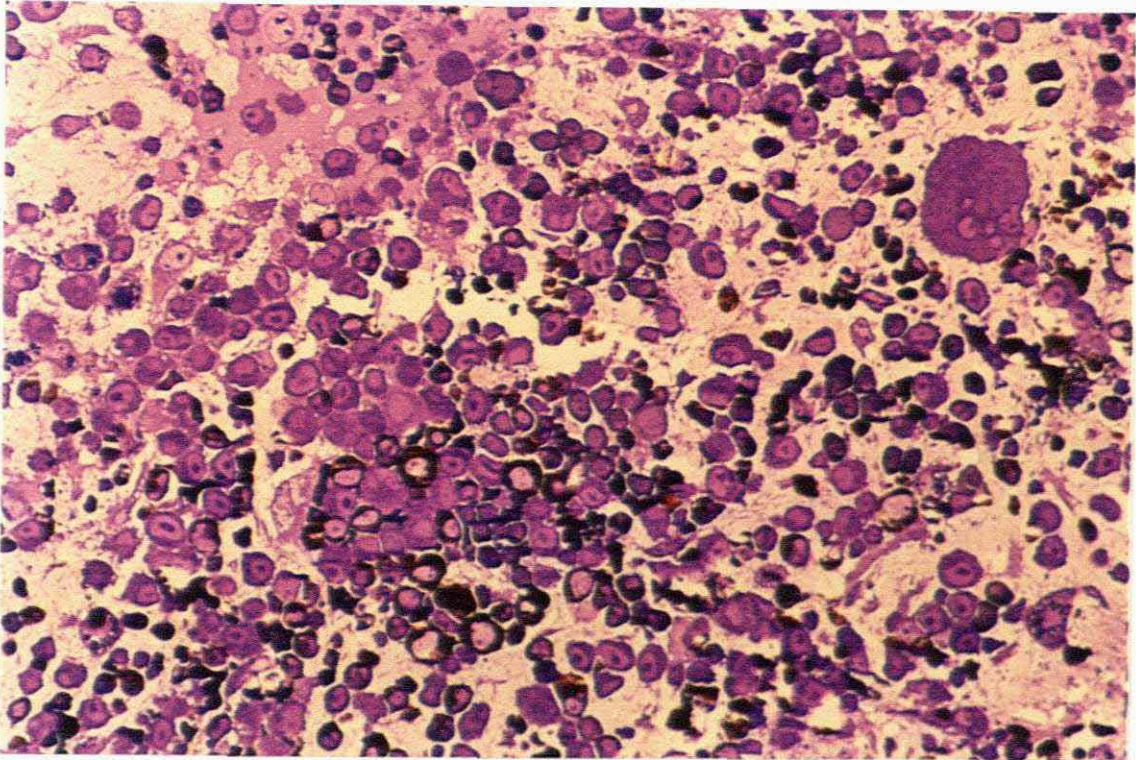


Plate 111

1µm resin section of bone marrow with suspected granulocytic leukaemia. The PPO technique was employed here. Note the high degree of DAB positivity in some of the cells (thin arrows). There is a megakaryocyte in the upper right of the picture (thick arrow). (Tol blue X450)

The following two photographs show the megakaryocyte at higher magnification, and some of its precursors that have an



extremely dense reaction product in the cytoplasm. (See plate 112 and 113.)

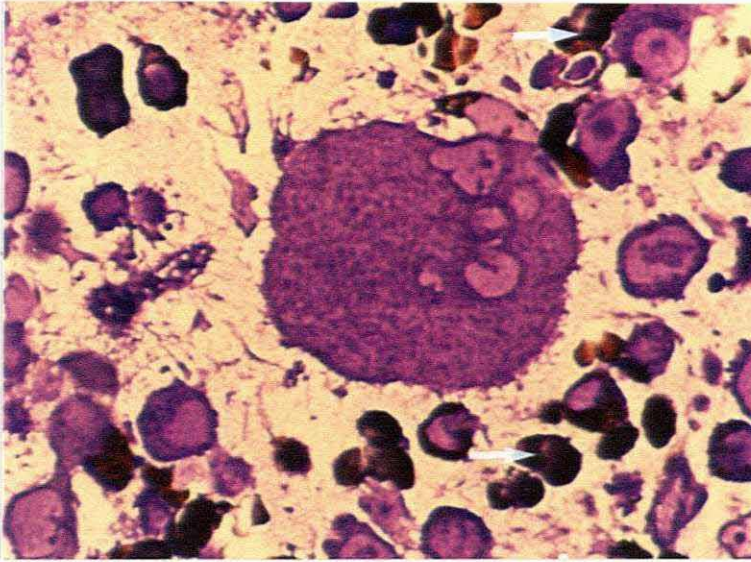


Plate 112

A higher magnification of the same field. No reaction product is visible in the megakaryocyte at this level although the surrounding cells have reaction product (W. arrows). (Tol blue X1125)

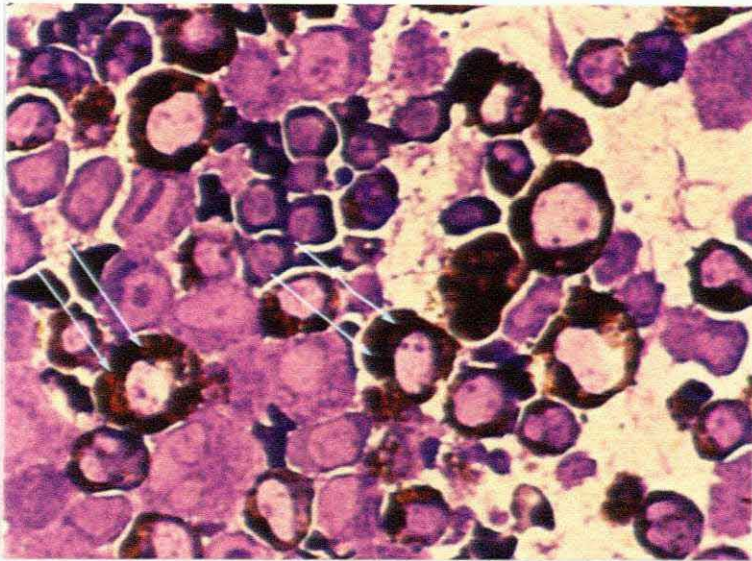


Plate 113

The cells which have the high nuclear/cytoplasmic ratio have large amounts of reaction product in their cytoplasm (W. arrows). (Tol blue X1125)

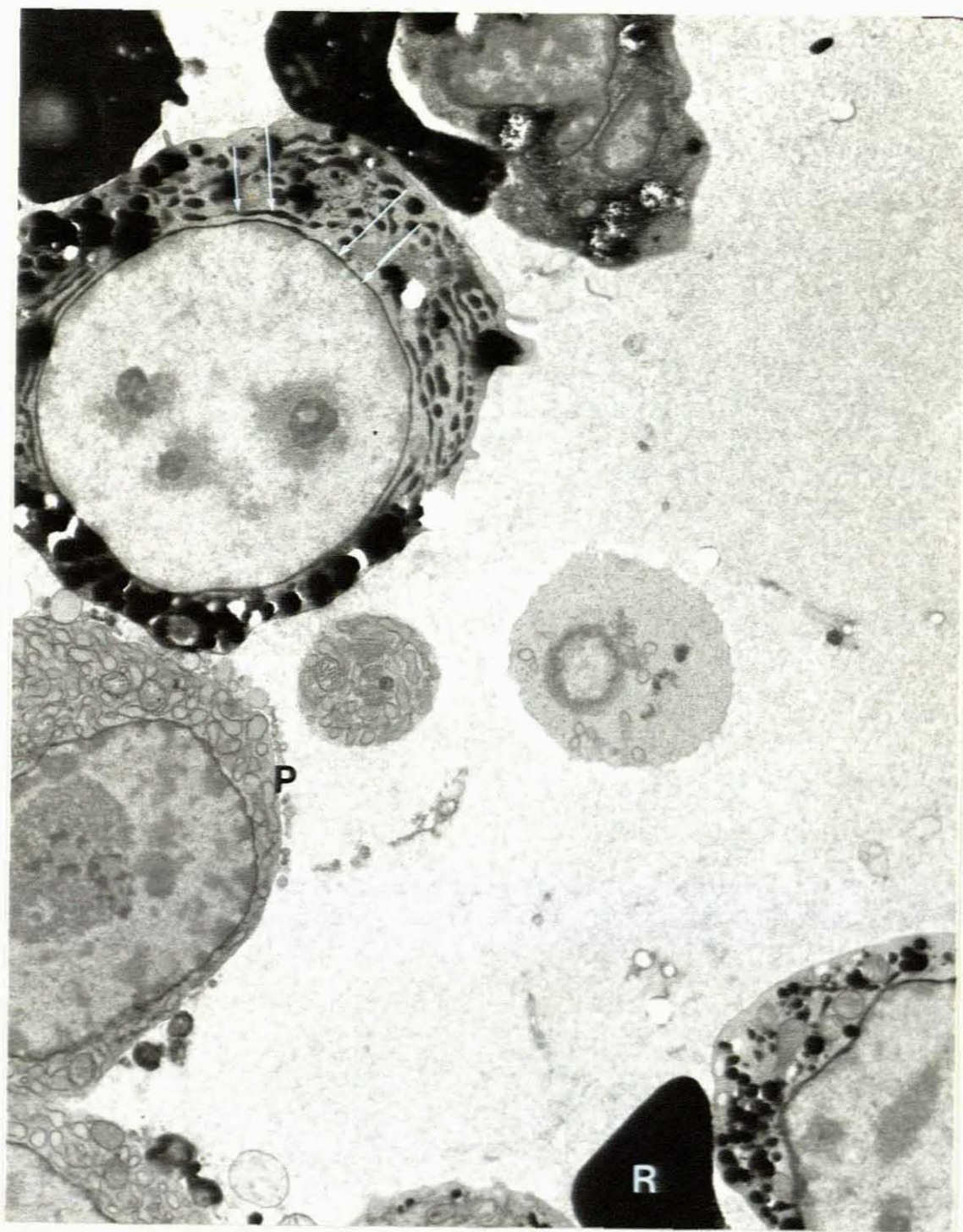


Plate 114

Low magnification of a representative area of the bone marrow for PPO. Note the high nuclear/cytoplasmic ratio of the blast cells. An extremely dense reaction product is not only found in the granules due to the presence of MPO, but also in the crypts of the endoplasmic reticulum as well as in the perinuclear cisternae of the cells (W. arrows). (PPO and OPF method, lead, no uranyl X7500)



When thin sections of the bone marrow processed for platelet peroxidase were viewed with the electron microscope, blast cells with a high nuclear/cytoplasmic ratio were seen. An extremely electron dense reaction product was found, not only in the specific granules, but also in the crypts of the endoplasmic reticulum and the peri-nuclear cisternae of the blast cells. (See plate 114.)

Plate 115 and 116 shows the reaction product in the granules, endoplasmic reticulum and peri-nuclear cisternae clearly at a higher magnification.

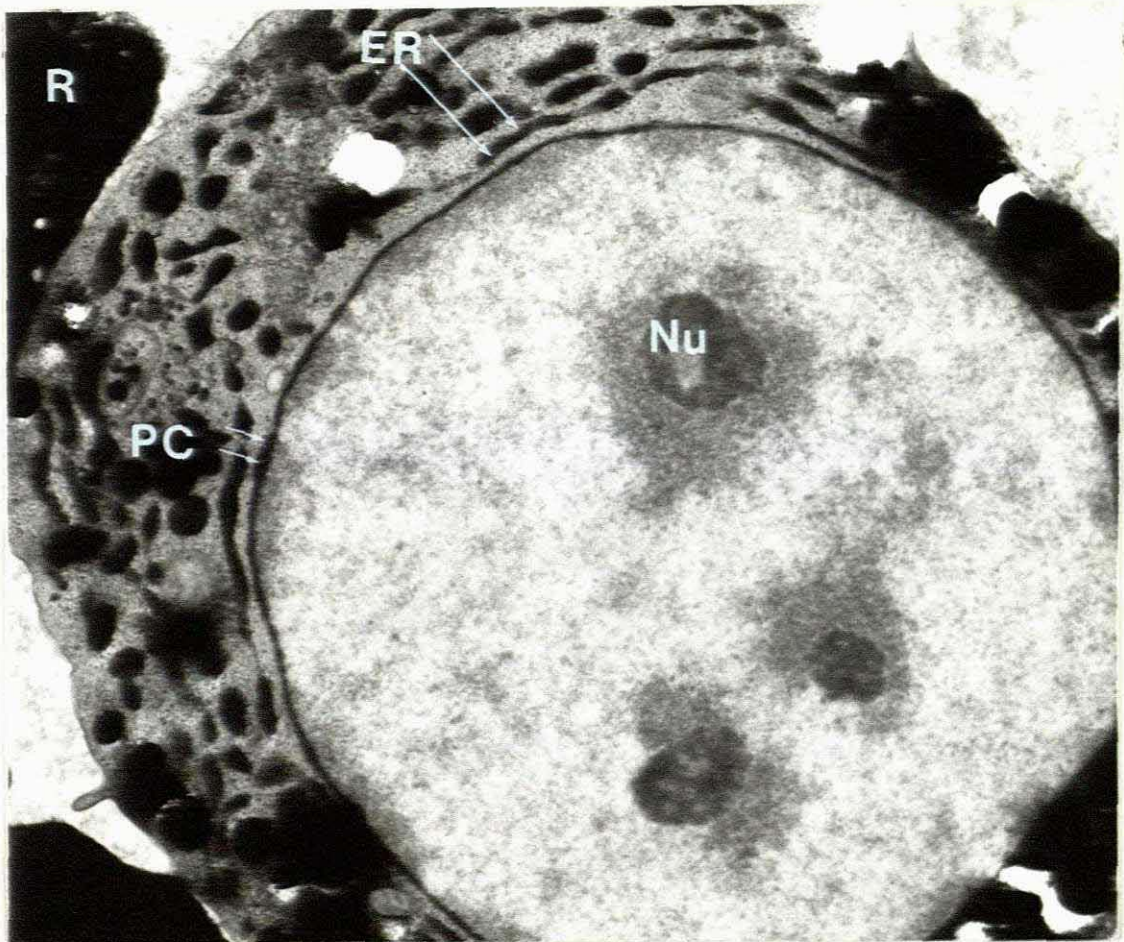


Plate 115

Higher magnification of a cell which exhibits PPO reaction product in the endoplasmic reticulum (arrows) and the perinuclear cisternae (arrows). (Lead, no uranyl X15000)



Plate 116

The cell in the photograph exhibits PPO reaction product in the endoplasmic reticulum and the perinuclear cisternae (arrows). Note the extremely strong reaction in the granules and the red cells. (Lead, no uranyl X15000)

At high magnification, the reaction product was seen to be extremely electron dense in the granules and in the red cells. In the endoplasmic reticulum and the perinuclear cisternae the reaction appeared less dense. (See plate 117.) No reaction was seen in a plasma cell that was in the same field. (See plate 118.)

Mature megakaryocytes that were in the same section, exhibited no reaction product in the granules, but a definite product in the peri-nuclear cisternae. No endoplasmic reticulum was seen in the megakaryocyte which was probably on the point of setting free the mature platelets,



therefore no comment could be made as regards this organelle. (See plate 119 and 120.)

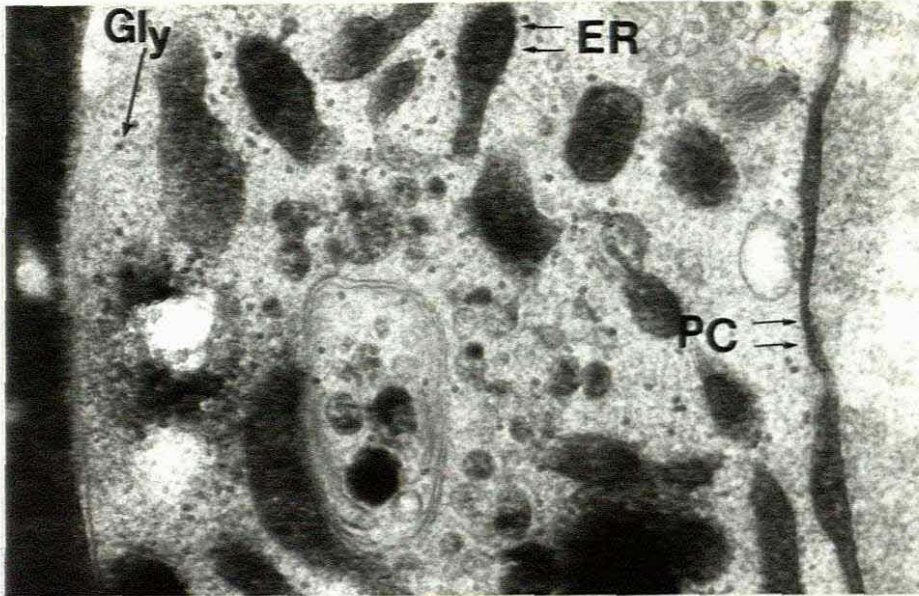


Plate 117

Detail of the reaction product in the ER and the perinuclear cisternae (thin arrows). Some glycogen granules can be seen in the cytoplasm in the cell. (Lead, no uranyl X45000)

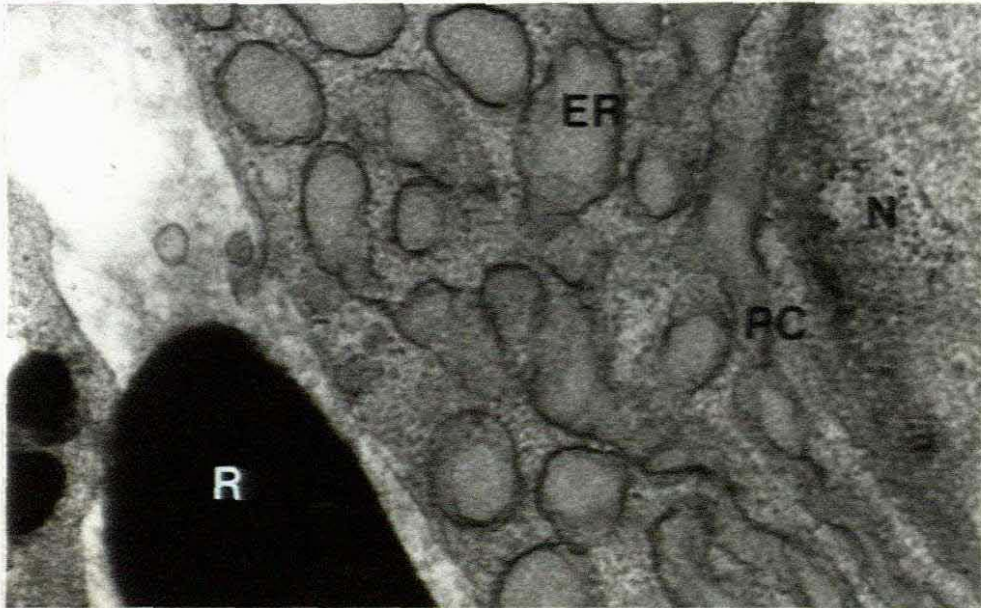


Plate 118

The plasma cell is devoid of reaction product in the ER as well as the peri-nuclear cisternae. (Lead, no uranyl X45000)



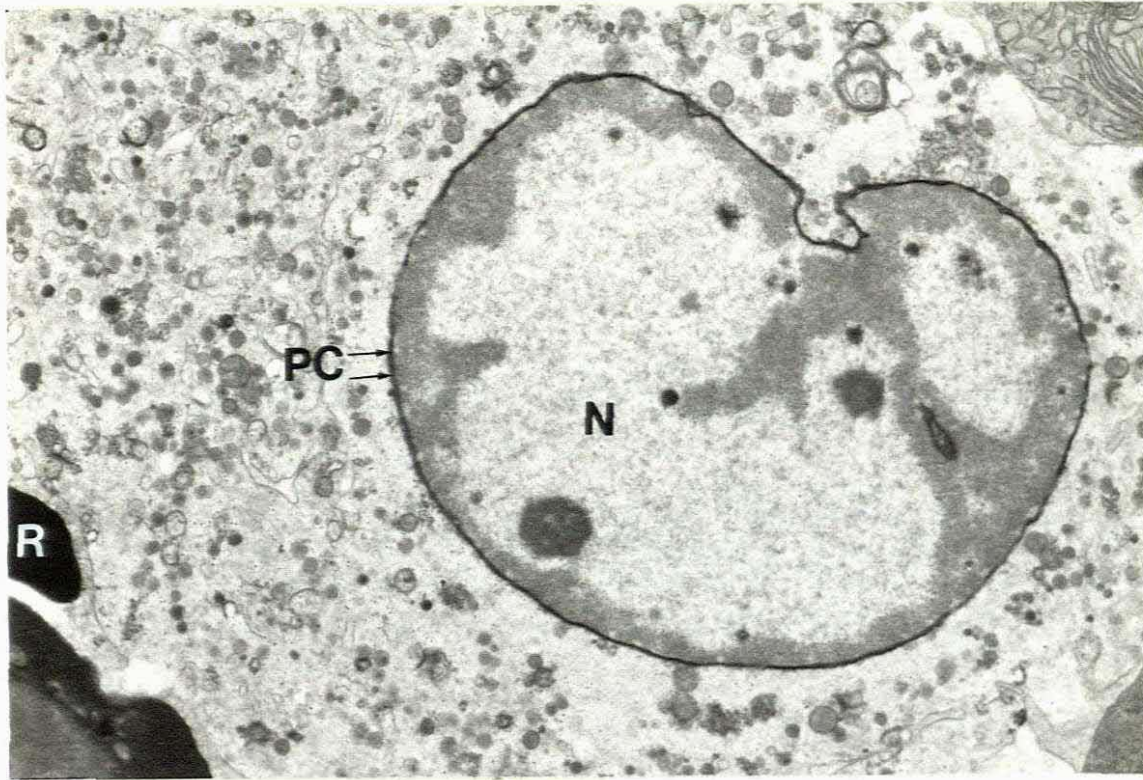


Plate 119

Low power magnification of a megakaryocyte to demonstrate that the granules show no reaction product, but that the perinuclear cisternae has quite substantial positive material in it. (Lead, no uranyl X7500)

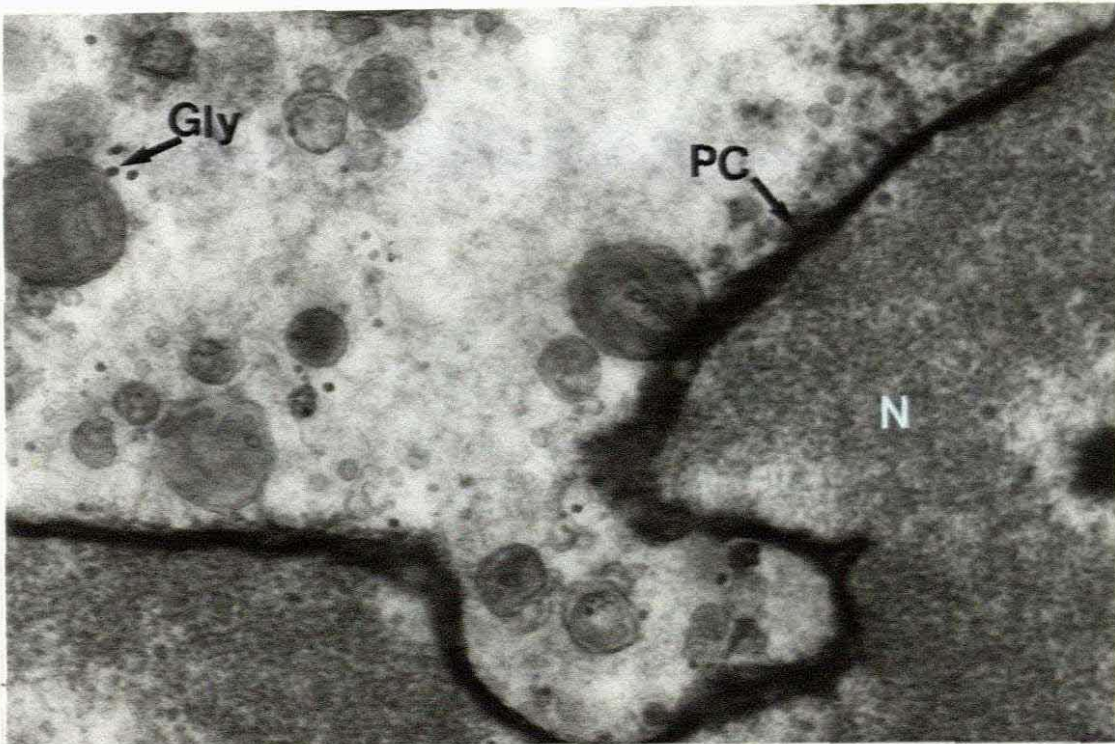


Plate 120

High magnification to show the reaction product in the perinuclear cisternae. (Lead, no uranyl X45000)



### 4.2.3 USE OF MPO IN THE DIAGNOSIS OF GRANULOCYTIC SARCOMA

At Tygerberg Hospital several patients had been seen that presented with maculo-papillary or nodular skin lesions. See plate 121 and 122 for the classic light microscopic appearance of this condition.

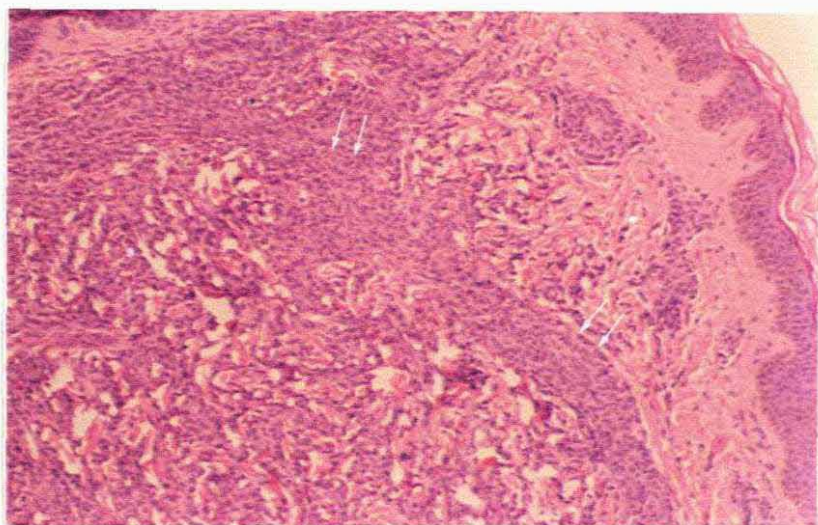


Plate 121

Paraffin wax section of a skin biopsy showing a diffuse, highly cellular malignant infiltrate of poorly differentiated cells (arrows). (H & E X115)

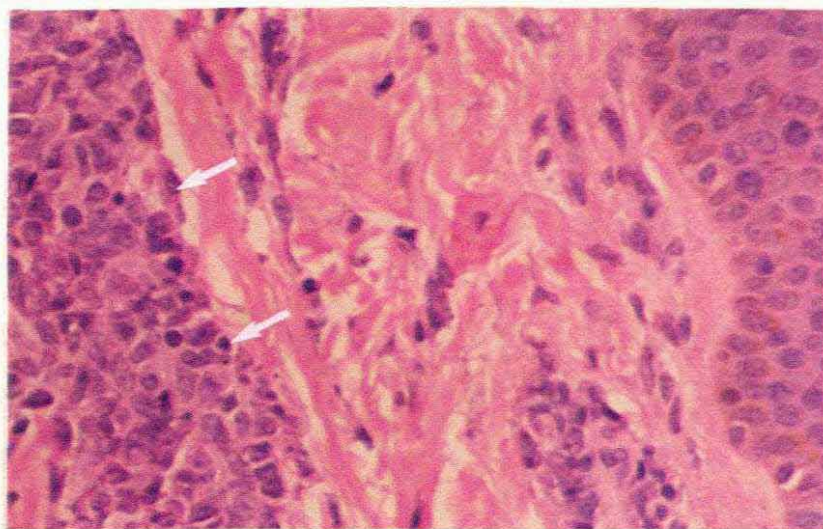


Plate 122

At higher magnification it can be seen that the malignant cells have nuclei with irregular outlines (arrows). (H & E X450)

Some of the patients had myeloid leukaemia, but others had no overt myeloid disease. Tissue from one of the cases was processed for electron microscopy and sections were cut and stained. In the sections stained with Toluidine blue, large myeloid-looking cells could be seen. (See plate 123 and 124.)

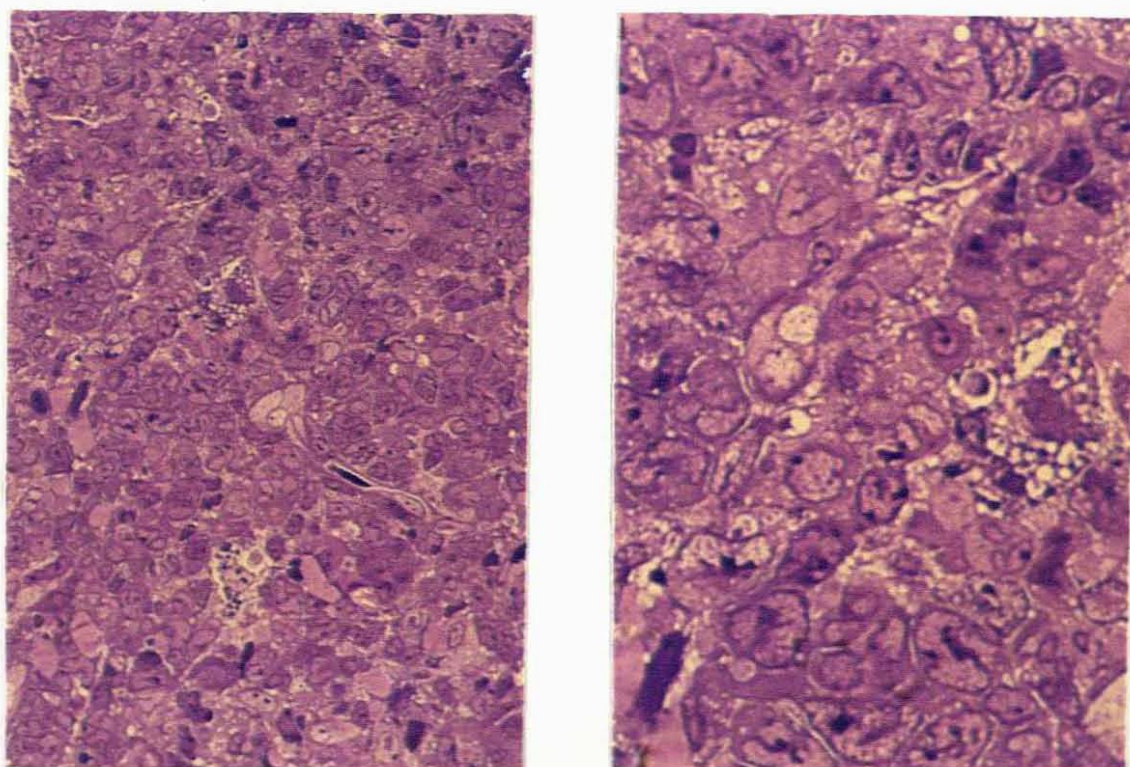


Plate 123 & 124

1 $\mu$ m resin section showing the cells of the skin biopsy in more detail. Many of the cells have prominent nucleoli. (Tol blue X450 & X1125)

Thin sections of the tissue viewed with the electron microscope, revealed large cells containing pleomorphic nuclei with irregular borders. The cells appeared immature and had little nuclear and cytoplasmic differentiation. Nucleoli were prominent and the cell cytoplasm contained a few granules and lipid droplets. (See plate 125.)



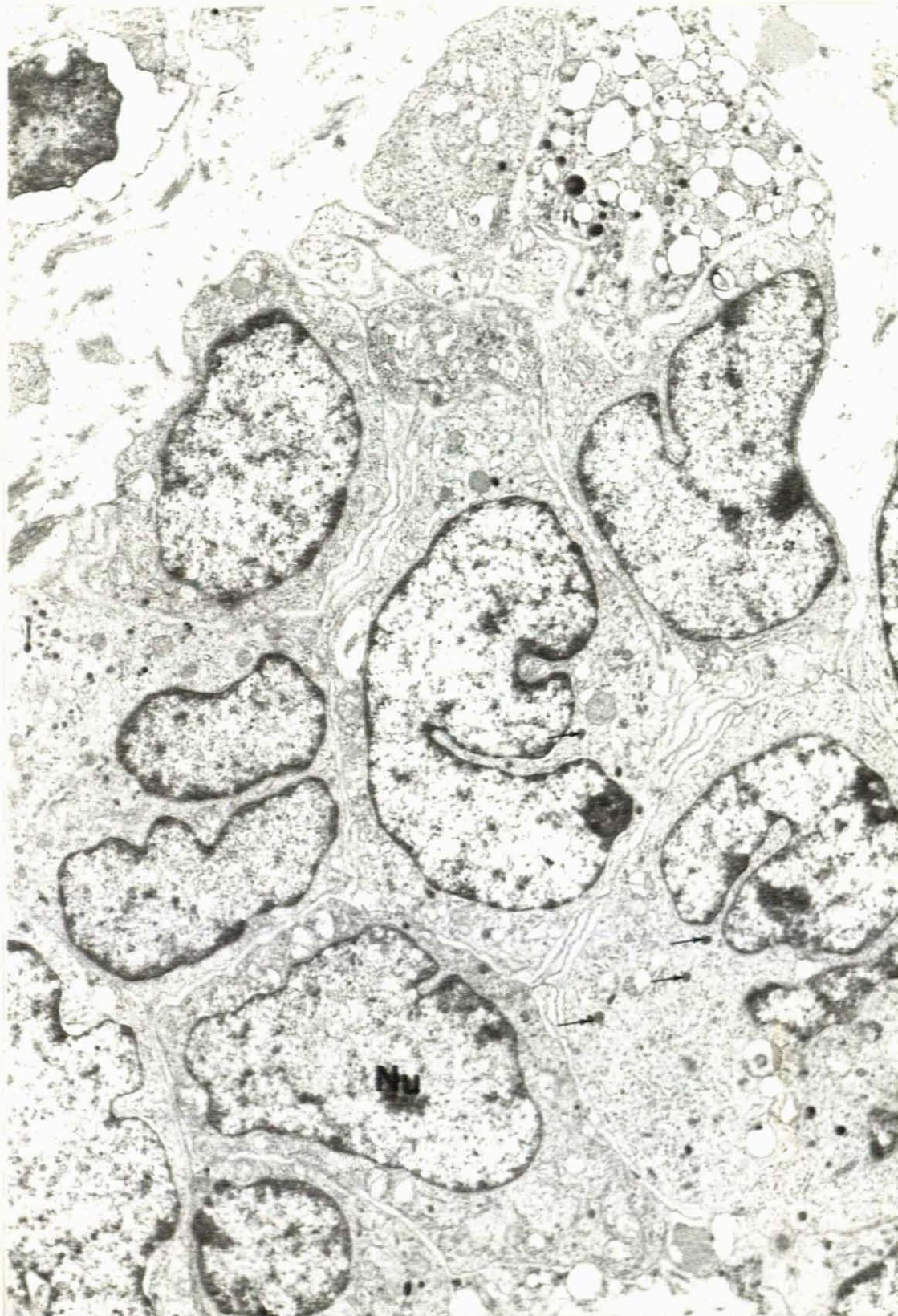


Plate 125

At low magnification, a section of the skin biopsy processed with the standard method shows poorly differentiated cells with irregular nuclei. The cytoplasm of the cells contain some granules (arrows) and many of the cells appear immature with little nuclear and cytoplasmic differentiation. (Lead and uranyl X7500)



At higher magnification, the detail of the nucleus with its irregular borders was seen. A few granules and one or two lipid droplets were also visible. (See plate 126.)



Plate 126

The irregular nuclear outline, cytoplasmic granules and lipid droplets are clearly seen at this magnification. (Lead and uranyl X15000)

High magnification of the cytoplasm showed the membrane bound granules in detail. Golgi apparatus is visible at the right of plate 127.

Before the advent of routine diagnostic electron microscopy, diagnosis of lymphoma had often been made on these cases, however when certain immunocytochemical tests were done, and the MPO method was carried out on the biopsies, these large cells with their prominent nucleoli were seen to contain positive DAB reaction product in their cytoplasm.



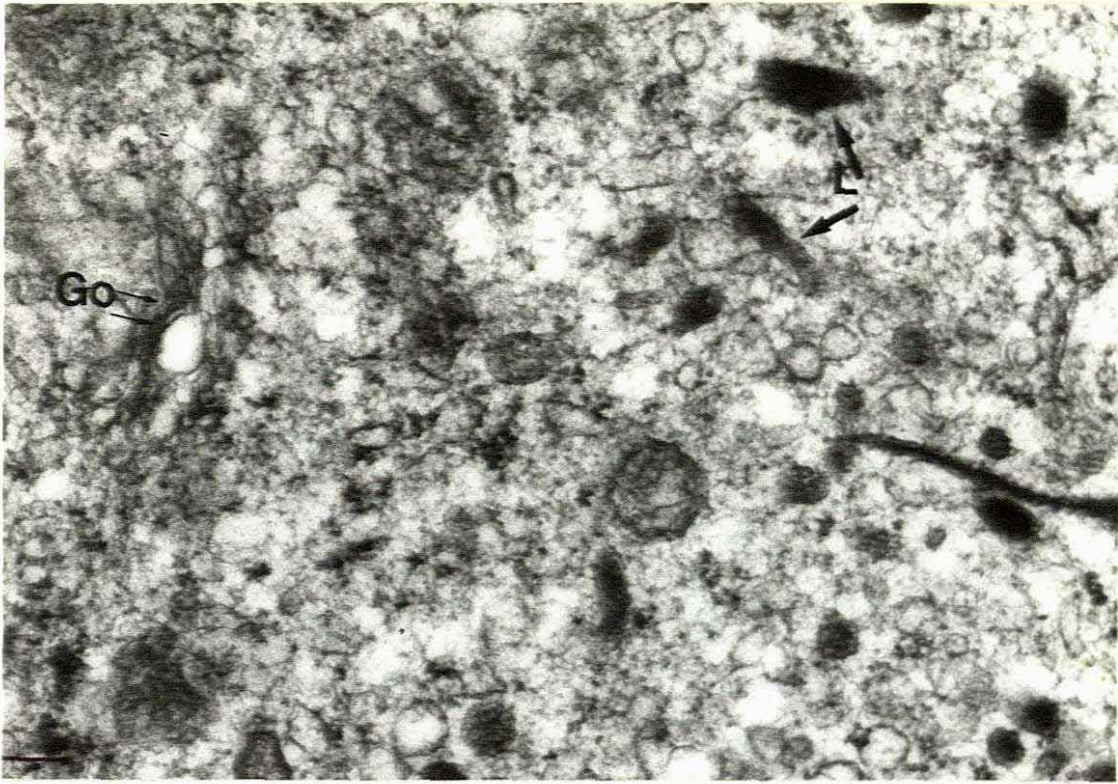


Plate 127

A high magnification of the Golgi region of the cell showing primary lysosomes. (Lead and uranyl X45000)

1  $\mu$ m resin sections of the tissue processed with the MPO method and stained with Toluidine blue stain showed DAB reaction product in the cytoplasm of the cells quite clearly. (See plate 128 and 129.)

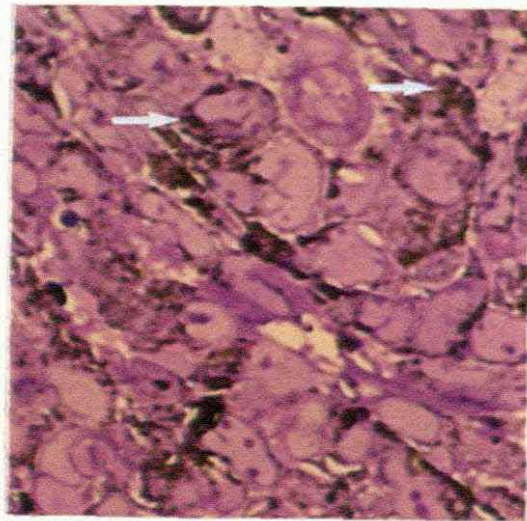
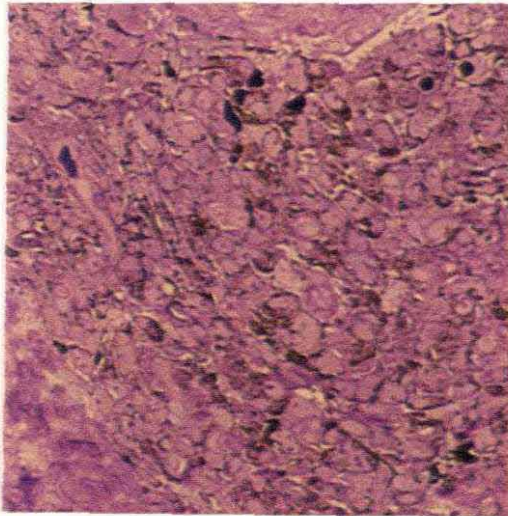


Plate 128 & 129

Tissue from the skin biopsy processed with the MPO/DAB method. Note the reaction product in the cytoplasm of the cells in plate 117 (arrows). (Tol blue X450 & X1125)



When thin sections of the tissue processed with the modified DAB method were viewed with the electron microscope, the cells are seen to have peroxidase-positive granules in the cytoplasm. (See plate 130.)

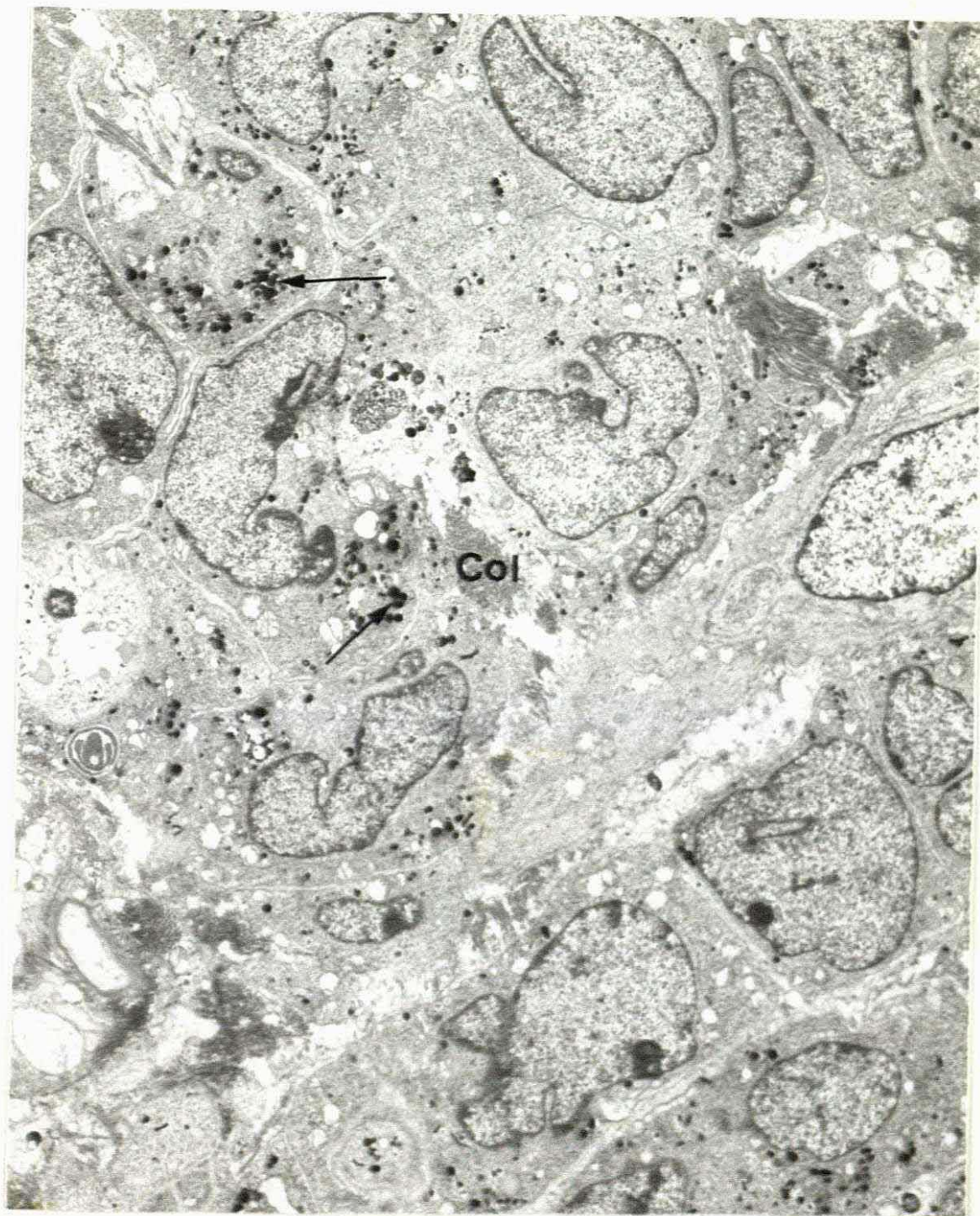


Plate 130

Enzyme histochemistry at ultrastructural level confirmed the presence of myelo-peroxidase in the granules (arrows). (Lead, no uranyl X4500)



At higher magnification, the myelo-peroxidase positivity in the granules was clearly seen. The lipid droplet in the bottom right of the photograph is negative. (See plate 131.)

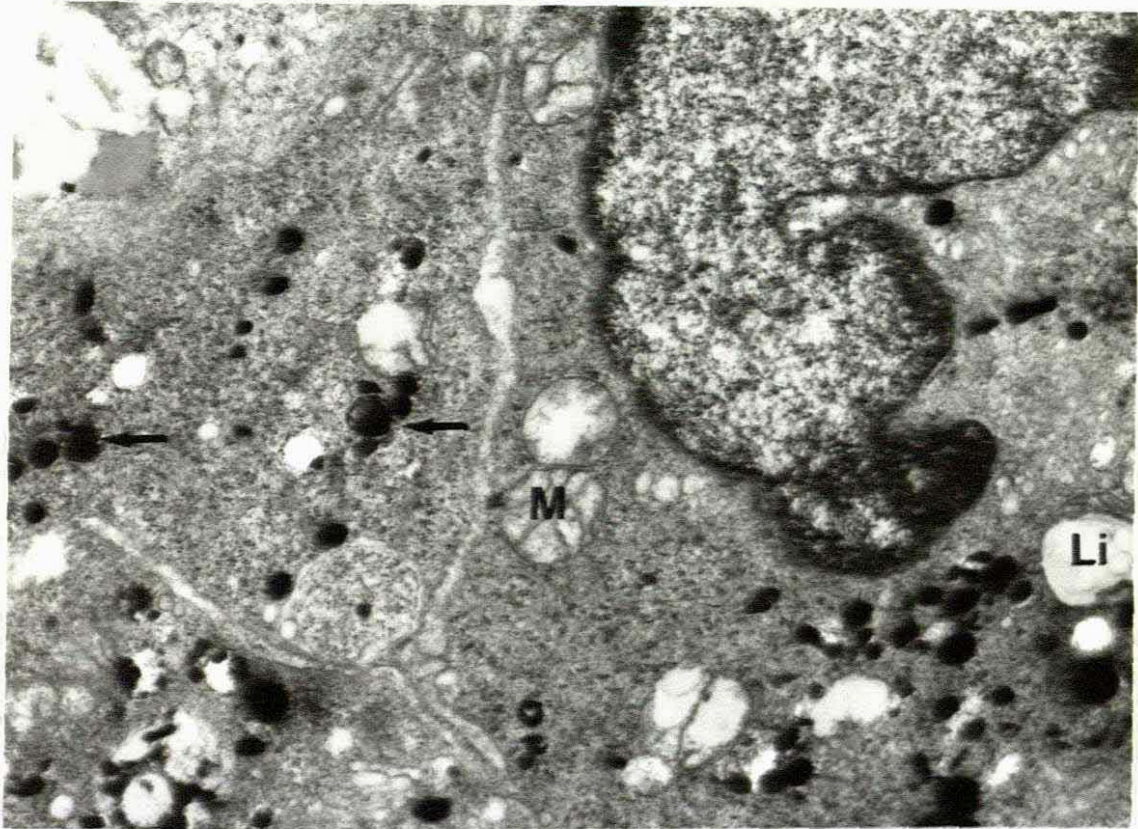


Plate 131

The positive reaction product of the MPO method can be seen clearly in the lysosomes (arrows). Note that the lipid is negative in the bottom right of the photo. (MPO, lead and uranyl X15000)

As with the blood and bone marrow, red cells were included in the field of view when photographs were taken as an internal positive control. In plate 132 & 133 the red cell in the field of view shows a positive reaction as well as the lysosomes in the tumour cells. A diagnosis of granulocytic sarcoma could therefore be made.

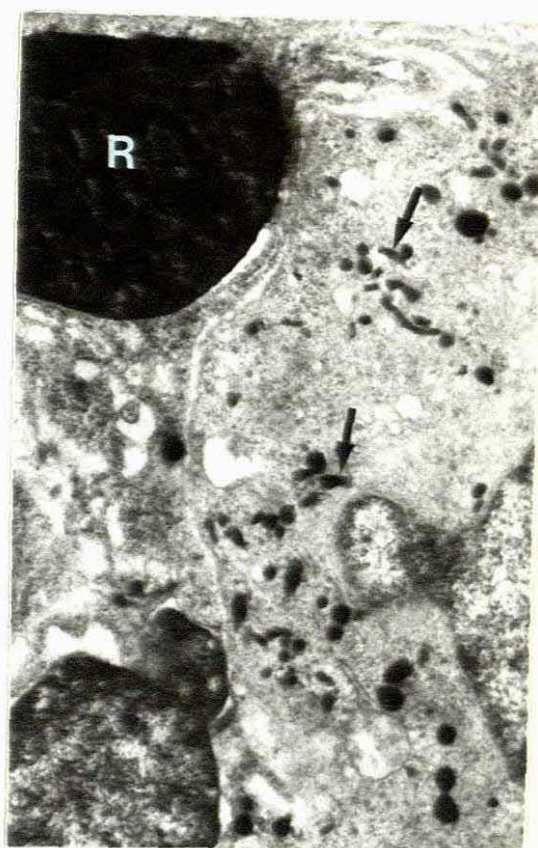
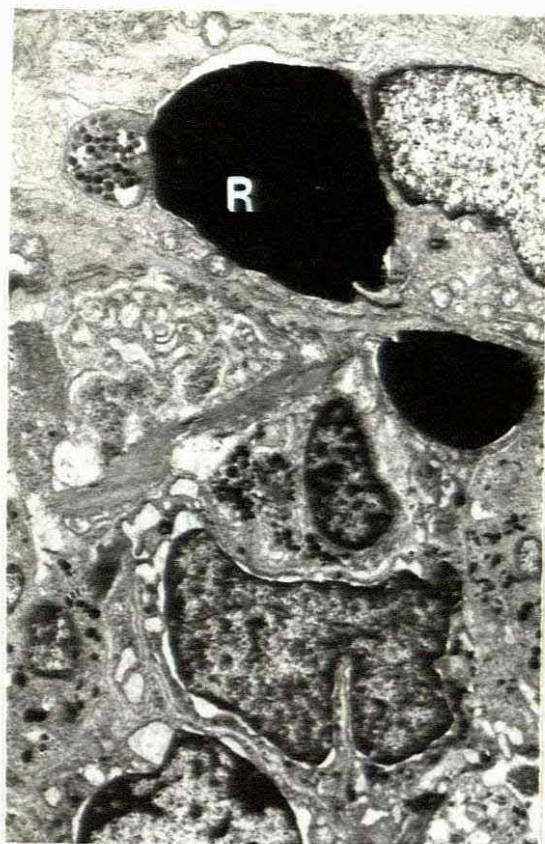


Plate 132 & 133

Red cells are used as an internal control for this method. The reaction product can be seen clearly in the red cell as well as the lysosomes (arrows). (MPO, lead and uranyl X4500 & X12000)

—ooOoo—



#### 4.2.4 COMPARATIVE SUMMARY OF PROCEDURES BLOOD, BONE MARROW AND TISSUE

	<u>TISSUE</u>	<u>BLOOD &amp; BONE MARROW</u>	
		<u>MPO</u>	<u>PPO</u>
ANTICOAGULANT	N/A	HEPARIN	HEPARIN
PELLETING	N/A	CENTRIFUGE	CENTRIFUGE
FIXATION	2.5% BUFFERED GLUTARALDEHYDE	DITTO OR TAFG	TAFG
POST-FIXATION	1.5% BUFFERED OSMIUM TETROXIDE	OPF	OPF
en bloc STAINING	ALCOHOLIC URANYL ACETATE SOLUTION	NONE	NONE
DEHYDRATION	GRADED ETHANOLS	DITTO	DITTO
IMPREGNATION	50:50 RESIN ALCOHOL	DITTO	DITTO
EMBEDDING	RESIN	DITTO	DITTO
POLYMERIZATION	18 HOURS AT 60°C	DITTO	DITTO
SECTIONING	60-90 nm SECTIONS	DITTO	DITTO
STAINING	LEAD & URANYL SALT SOLUTIONS	LEAD ONLY	LEAD ONLY
PHOTOGRAPHY	ELECTRON MICROSCOPE	DITTO	DITTO

#### 4.2.5 SUMMARY OF RESULTS FOR MPO/PPO

<u>TISSUE OR TUMOUR</u>	<u>MPO</u>	<u>PPO</u>	<u>DISTRIBUTION</u>
CHRONIC/ACUTE LYMPHOID LEUKAEMIA	+	-	ONLY IN GRANULES OF PMN's PRESENT
CHRONIC/ACUTE MYELOID LEUKAEMIA	++++	-	PRIMARY GRANULES OF PMN PRECURSORS
GRANULOCYTIC LEUKAEMIA	++++	++++	MPO IN GRANULES, PPO ONLY IN ER & PC OF MEGA PRECURSORS
GRANULOCYTIC SARCOMA	++++	-	GRANULES OF PMN SARCOMA CELLS

## 4.3 RESULTS OF THE DNA IN SITU HYBRIDIZATION METHOD

The original methods for non-isotopic detection of DNA hybrids, called for the use of an alkaline phosphatase enzyme linked immuno-assay which, although adequate for light microscopy, was not suitable for electron microscopy as the reaction products were soluble in alcohol. An alternative electron donor had to be found, which on its own, or together with another substance, would yield an electron dense reaction product visible with the electron microscope.

Anti-digoxigenin peroxidase conjugate became available, so that subsequently the digoxigenin marker could be coupled to peroxidase. This product could be detected with DAB which yielded an amorphous brown precipitate, which was not only visible with the light microscope, but also visible on its own with the electron microscope.

Tissue, which on light microscopic examination showed koilocytosis, was hybridized with HPV 6, 11, 16, 18, 31 and 33 DNA probes. Tissue from sections with the distinctive brown precipitate in the nuclei, were used for the pre-embedding EM technique, and the specimens subsequently chosen were both positive with the HPV 16 probe.

The cervical biopsies that were chosen for DNA in situ hybridization, showed typical koilocytosis as in plate 134 & 135.



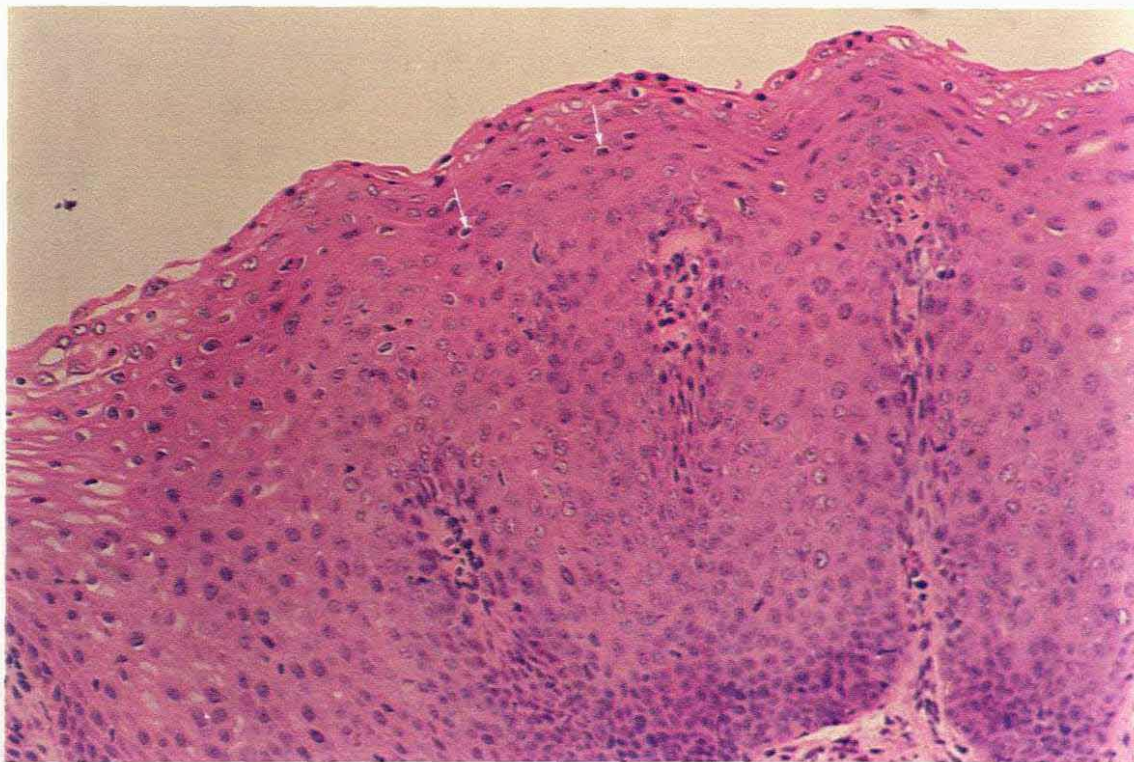


Plate. 134

Paraffin wax section of a cervical biopsy showing koilocytic changes in the cervical epithelium (arrows). (Haematoxylin & Eosin X115)

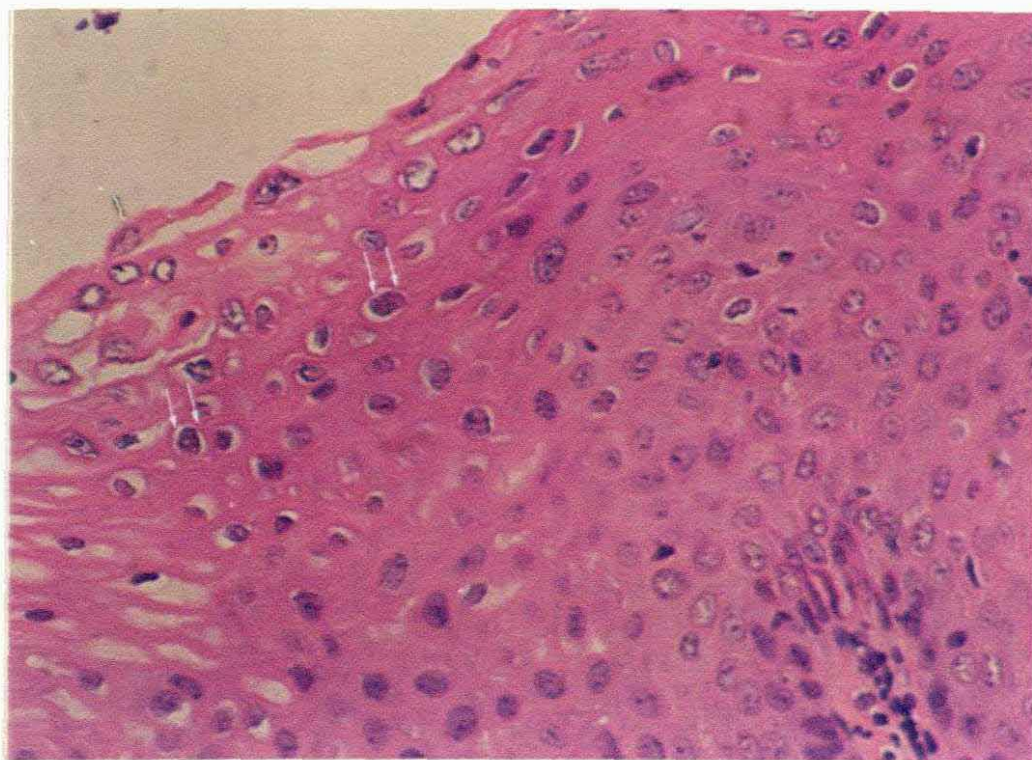


Plate. 135

Virus infected cervical epithelial cells showing the typical halos around the nuclei which is a characteristic of these cells (arrows). (Haematoxylin & Eosin X450)



Tissue from the cervical epithelium was processed for electron microscopy with the OPF method, to show the relative sizes of the glycogen and Human papilloma virus. See plate 136 through 139.



Plate 136

Low magnification of OCUB processed tissue for electron microscopy, showing a similar field of view as in the preceding LM photographs. The intercellular bridges, keratin filaments and empty looking cytoplasm (asterisk) of the koilocytes are easily seen. Virus particles are just discernible (arrows) in the nucleus in the of the plate. (Resin, Lead and Uranyl X7500)



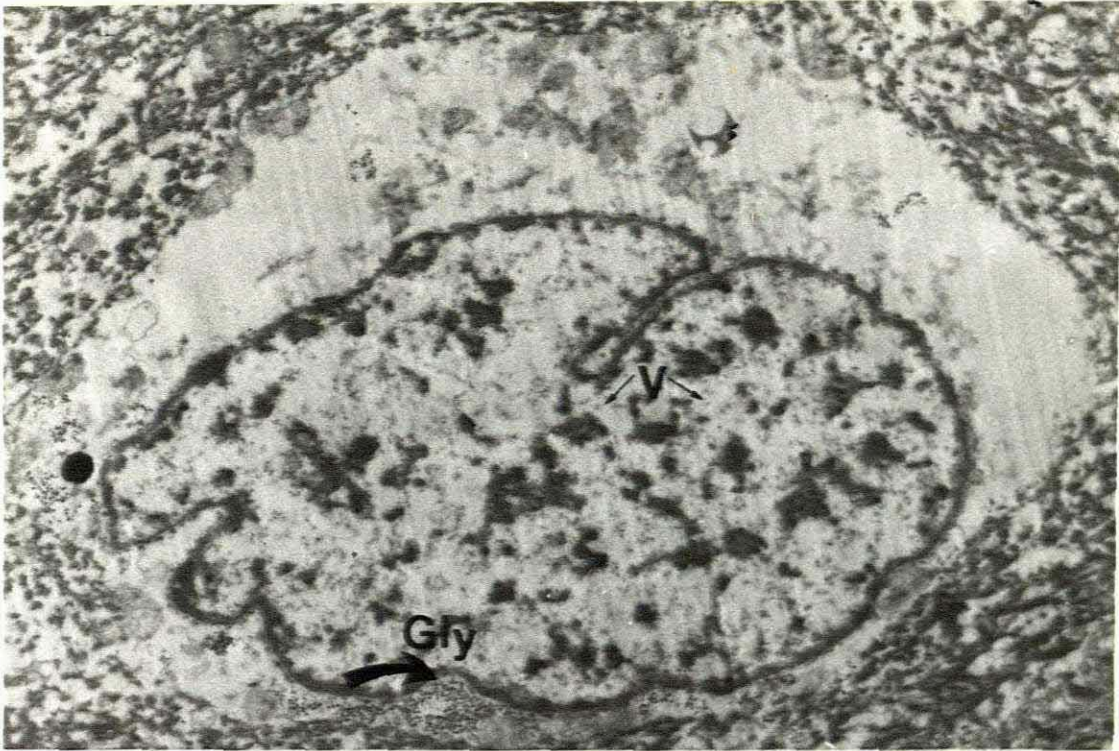


Plate 137

Koilocytic cell from OPF processed tissue showing glycogen (curved arrow) in the cytoplasm of the cell and virus particles in the nucleus (thin arrows).(Resin, Lead only X9000)

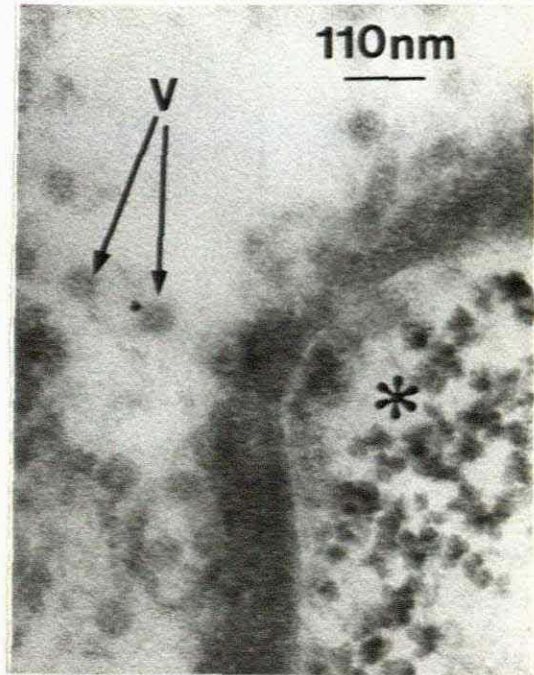
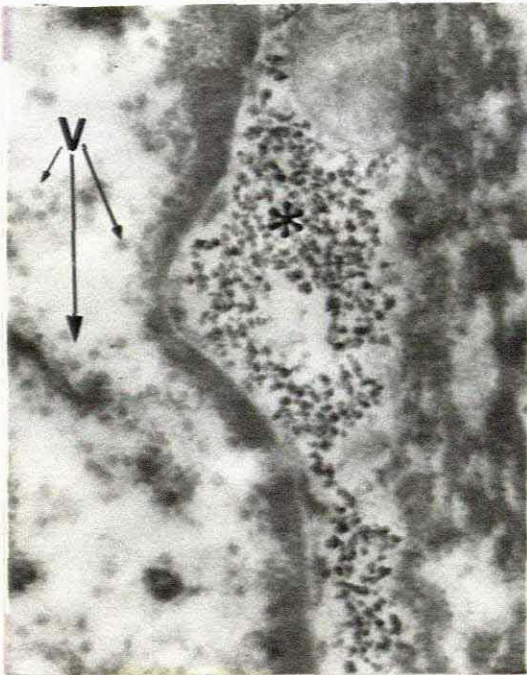


Plate 138 & 139

Higher magnification of the above specimen showing relative sizes of glycogen (~35nm) (asterisk) and viruses (~55nm) particles (arrows).(Resin, Lead only X30000 and X90000)



The appearance of a positive reaction with the <DIG> POD method is demonstrated in plates 140 through 142.

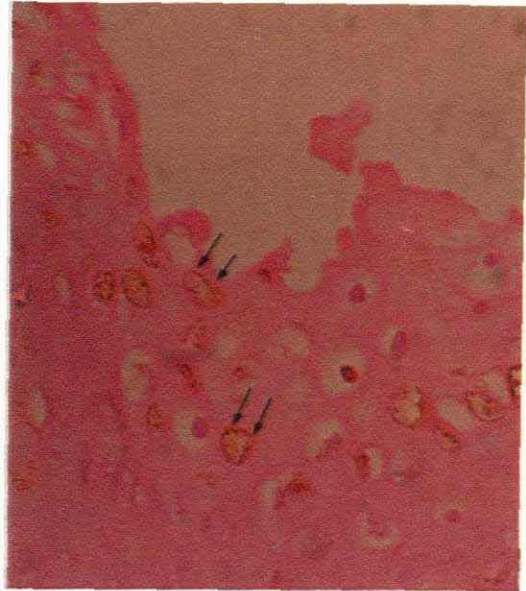


Plate 140 & 141

A low and intermediate magnification of tissue hybridized with Digoxigenin/DAB HPV 16 probes demonstrates that DAB positivity is seen in the koilocytes (arrows). (Light H & E counterstain X115 and X225)



Plate 142

At high magnification the typically granular DAB deposits can be seen in the nuclei of the cells (arrows). (Light H&E X1125)



When the tissue was prepared in the same way for electron microscopy, resin sections stained with toluidine showed a just discernible DAB positive reaction at the higher magnification. (See plate 143 and 144)

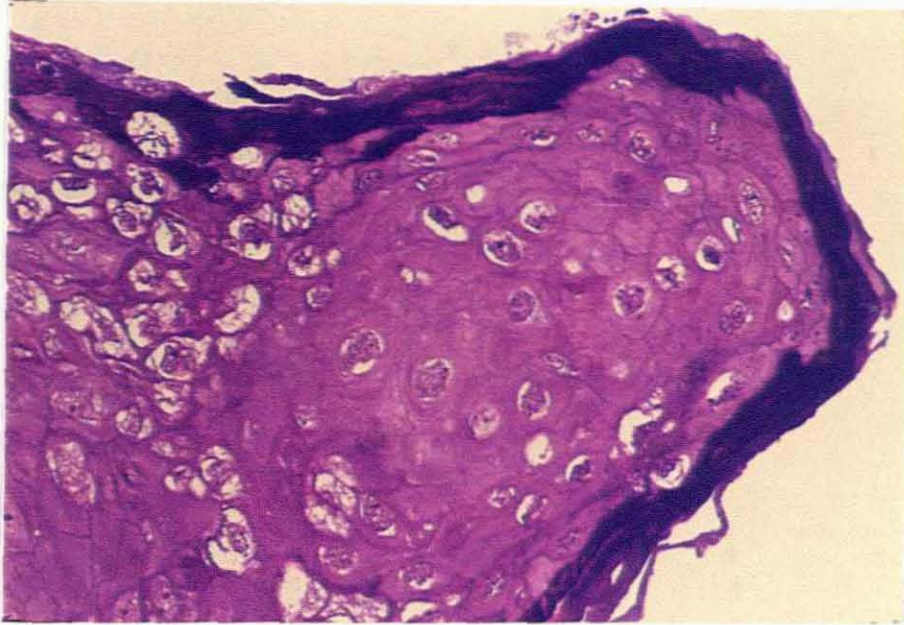


Plate 143

Low power magnification of 1 $\mu$  resin embedded tissue hybridized with Digoxigenin/DAB HPV 16 probes showing very slight positivity in the koilocytic cells. (Pre-embedding technique for EM in Spurr's resin Tol. blue X225)

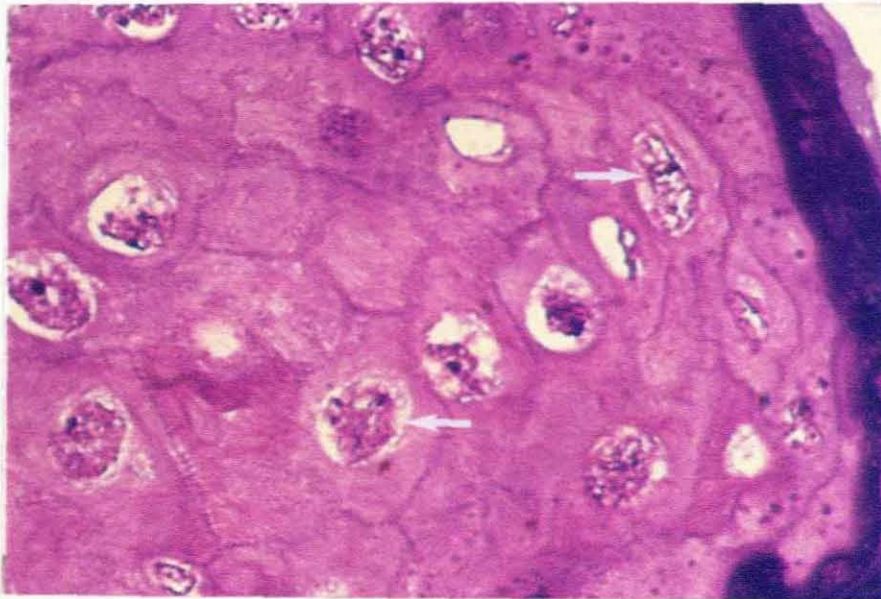


Plate 144

High magnification of the same tissue section showing finely granular precipitate in the koilocytic cells (arrows). (Resin, Tol. blue X1125)



As a negative control, the same tissue was also processed in this way, but with no probe added to the reagents. The results can be seen in the plates 145 through 147.

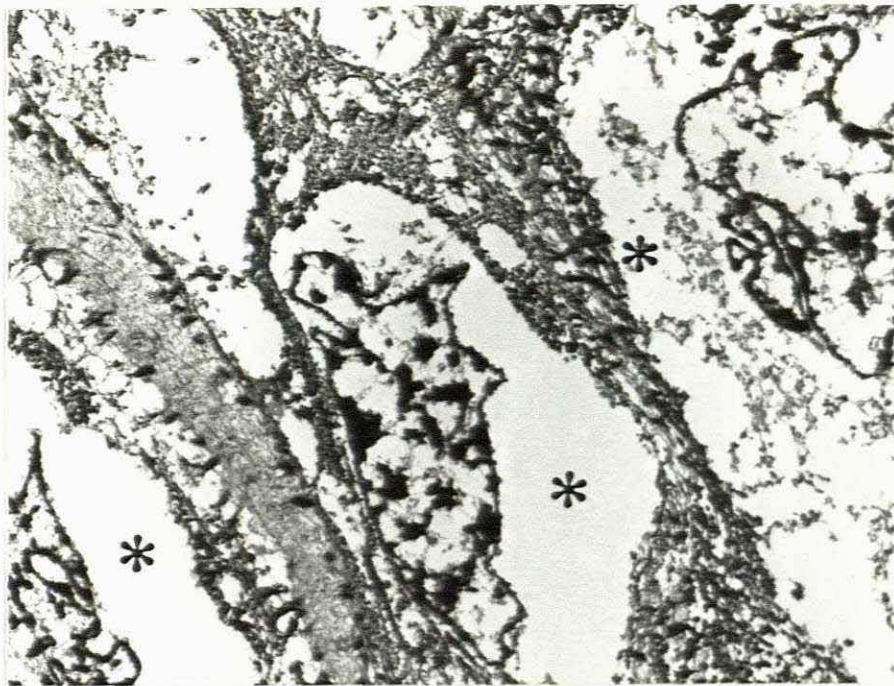


Plate 145

Low power magnification of koilocytic cells (asterisks) which have been incubated with the probe reagents without probe added are used as a negative control. (Resin, Lead and Uranyl X6000)

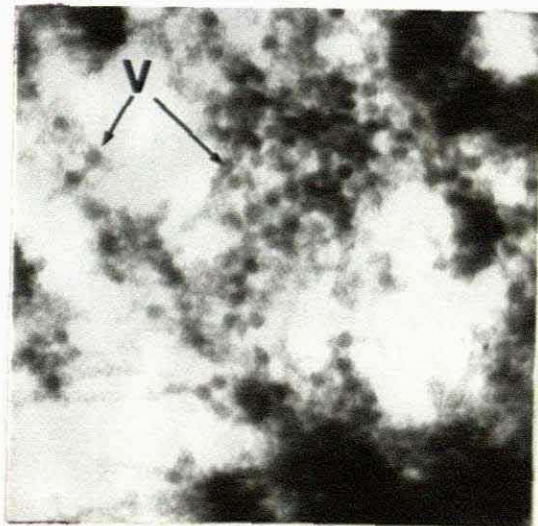
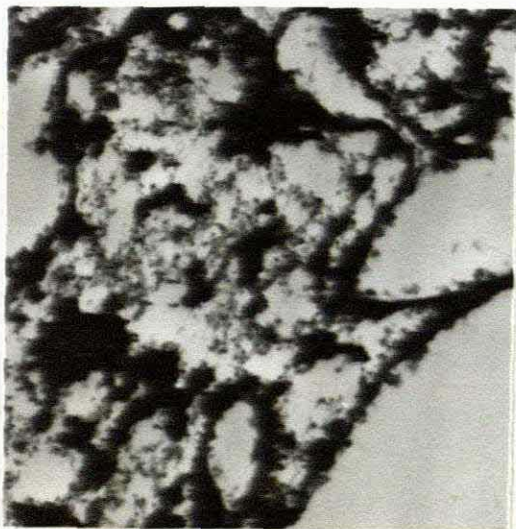


Plate 146 & 147

Intermediate and high magnifications to demonstrate the virus particles in the nucleus (arrows). Note that no DAB precipitate is visible. (Resin, Lead and Uranyl X15000 and X60000)



Unstained, (no lead and uranyl staining), control sections of the experimental tissue had precipitate in and around the nuclear chromatin although no virus particles were seen. See plates 148 through 150.

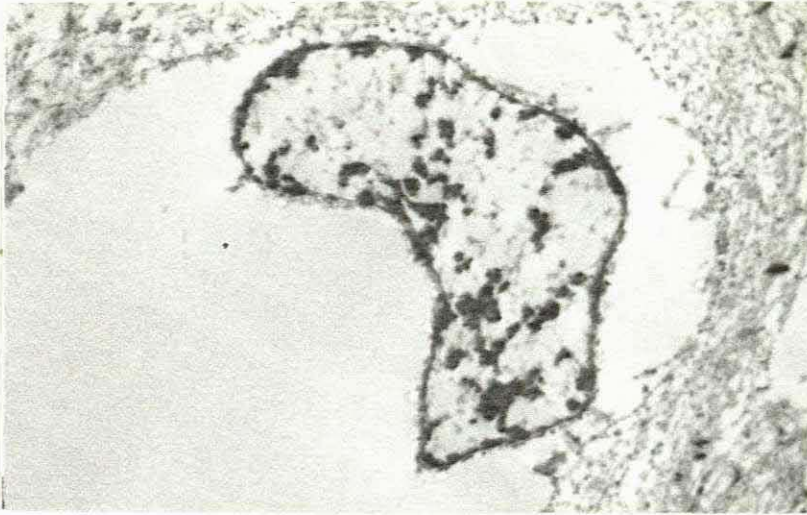


Plate 148

An unstained resin section to demonstrate DAB precipitate in the chromatin of the cells although no virus particles are apparent. (Resin, no staining X7500)

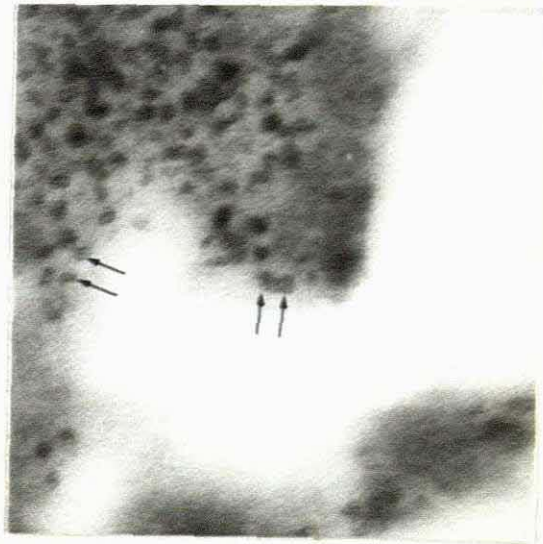
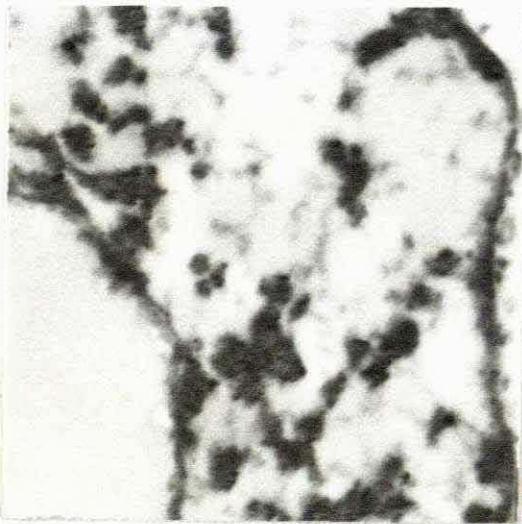


Plate 149 & 150

Two higher magnifications of the same section to demonstrate the DAB precipitate in the nuclei of the cells (arrows). (Resin, no staining X15000 and X90000)

Ultrastructurally, the experimental tissue showed reaction product in the koilocytes as well as in cells that did not have the typical appearance. The granular precipitate was found not only in the virus particles, but also in the nuclear chromatin even when there were no viruses visible. (Plate 151)



Plate 151

Low power magnification of tissue hybridized with Digoxigenin/DAB HPV 16 probes that demonstrates the strong positivity in the koilocytic nuclei (arrows). (Resin, Lead and Uranyl X4500)



At higher magnification, the positive DAB precipitate in the koilocytes is clearly seen. (See plate 152 through 154.)

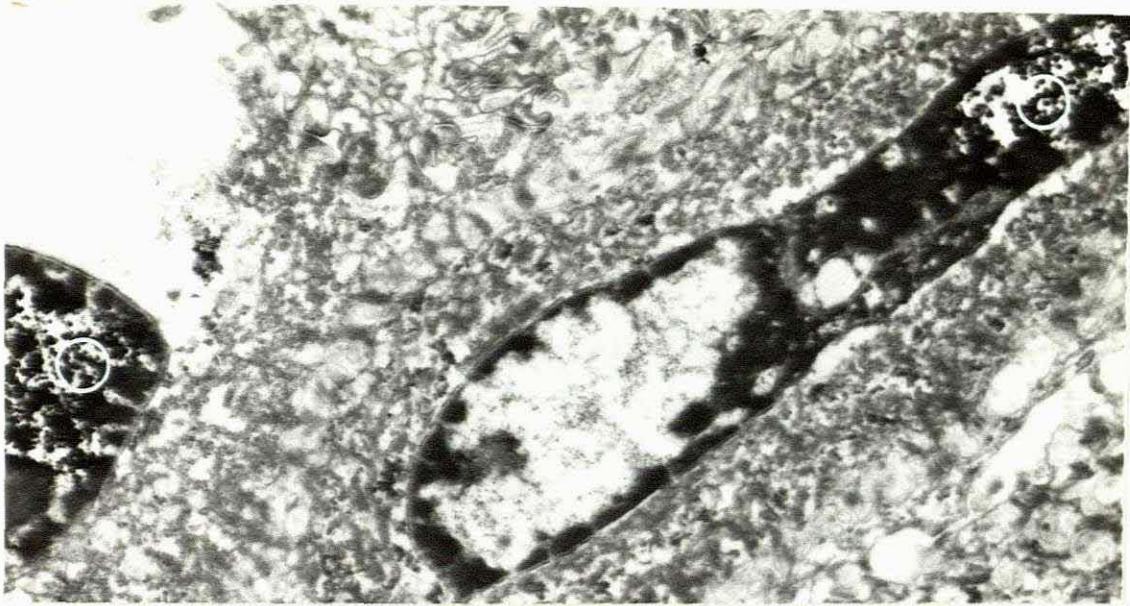


Plate 152

An intermediate magnification of two koilocytic nuclei showing a definite increase in density of the areas in and around the virus particles (circles). (Resin, Lead and Uranyl X10500)

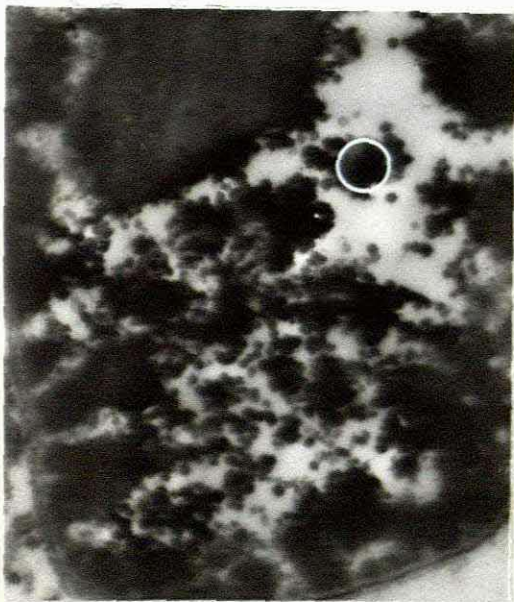


Plate 153 & 154

Higher magnifications of parts of the same two nuclei showing the dense DAB precipitate in and on the virus particles (circles). (Resin, Lead and Uranyl X24000)



High magnifications of two of the koilocytes shows the nature of the finely granular precipitate in the nuclear chromatin as well as in the viruses.(See plate 155 and 156.)

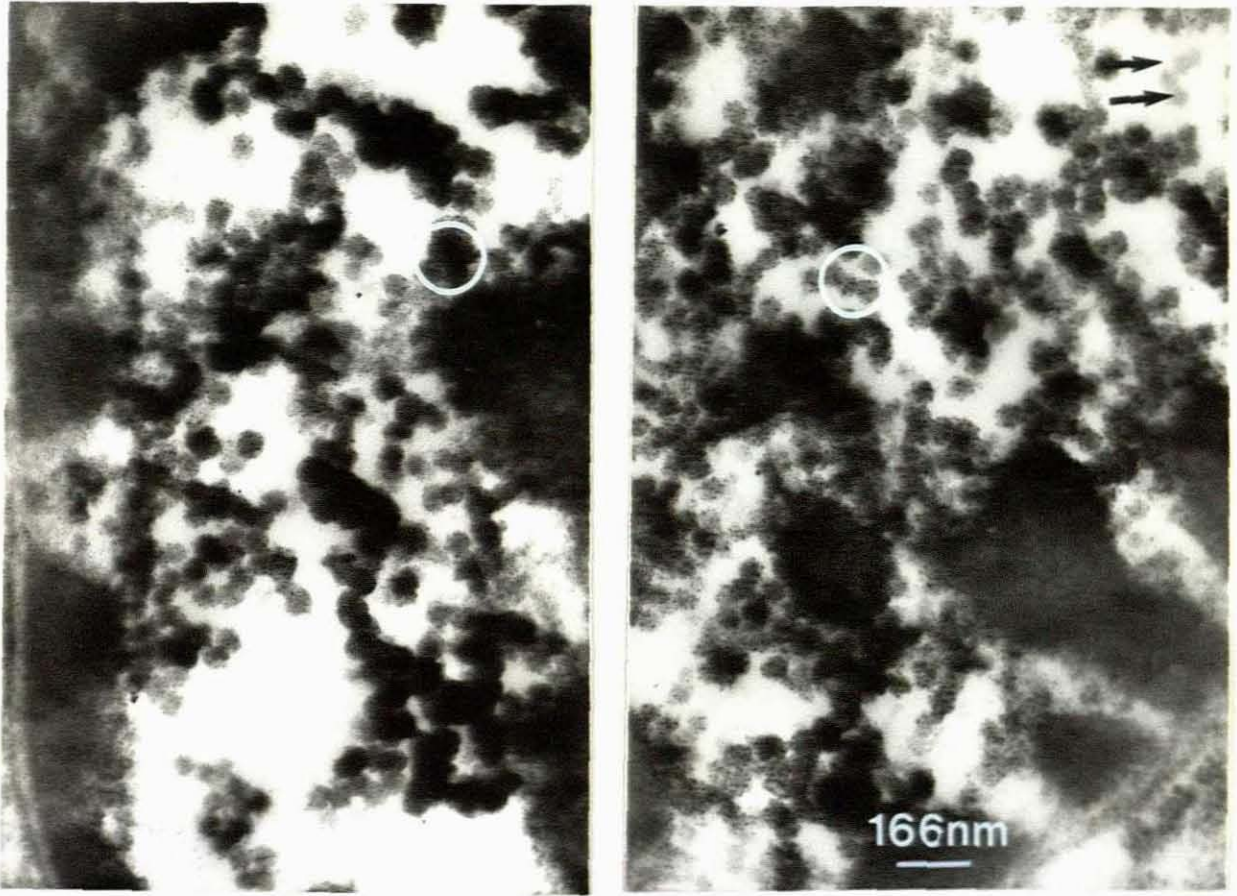


Plate 155 & 156

Two high power magnifications of the koilocytic cell nuclei to demonstrate the finely granular nature of the DAB precipitate (circles). Note that some of the viruses appear negative (arrow). (Resin, Lead and Uranyl X60000)

In previous comparative studies done at the light microscopic level with the alkaline phosphatase method and the DAB method, it was demonstrated that the peroxidase method was not as sensitive as the alkaline phosphatase method. The DAB method was however sensitive enough for it to be used successfully at the ultrastructural level.

# CHAPTER V

## DISCUSSION

## 5.0 DISCUSSION

### 5.1 THE OSMIUM TETROXIDE POTASSIUM FERROCYANIDE METHOD AS A GENERAL ULTRASTRUCTURAL GLYCOGEN STAIN.

The OPF method in its standard form, or in modified form was employed for the ultrastructural demonstration of glycogen, to answer the question whether this compound could be considered a general glycogen stain. From the foregoing results it became clear that this was indeed so.

The most striking difference between normally processed ( $\text{OsO}_4$ , uranyl acetate en bloc, resin) tissue and the modified OPF method was the increase in electron density of the particles characterised as glycogen, and the decrease in density of the ribosomal particles. Many parts of the cell cytoplasm, in tissue that had been processed with the standard method, had hitherto appeared devoid of any material. When tissue was processed with the OPF method however, these areas now had extremely dark electron dense particulate material. Due to the absence of ribosomal contrast, the modified OPF fixative was considered to selectively contrast glycogen, and hence the particles that were observed, were glycogen. The mechanism of this reaction is not fully understood; (de Bruijn and van Buitenen, 1973 and 1981) however in all the cases studied and especially in the control tissue, the contrasted particles not only mimicked the appearance of glycogen, but were found in those parts of the cell cytoplasm normally occupied by this substance. (de Bruijn and van Buitenen, 1973) It has



however been the experience of this laboratory and others, (de Groot et al, 1987) that not only did the OPF method enhance the ultrastructural appearance of glycogen, but more cellular detail was exhibited this way. A similar finding was published by Shepard et al (1989) who found that with this kind of fixation there was improved morphology in the tissues that they studied. With the careful fixation and processing procedure required by this technique a sensitive and reproducible method for the contrasting of glycogen in tissue was developed. The benefit derived from this was that glycogen was made visible ultrastructurally, and this aided the diagnosis of certain tumours that are rich in glycogen.

## 5.2 THE GLYCOGEN PARTICLE AS AN ULTRASTRUCTURAL DISTINGUISHING FEATURE IN TUMOURS RICH IN GLYCOGEN.

When glycogen-rich tumour tissue was processed with the OPF method the question was raised whether these tumours could be distinguished from each other by the ultrastructural appearance of the glycogen particle. For this reason normal liver and skeletal muscle were processed by the OPF method to obtain a standard for the appearance, distribution and approximate quantity of glycogen found in the cells of these organs.

Due to the OPF method being a qualitative technique, no absolute values could be attached to observations that were made. Large dense aggregates of glycogen, diffusely distributed in quantity, were generally found in normal liver.

Distribution of glycogen in normal muscle was in large, loose-lying aggregates in almost the same quantity as that found in liver. Single particles were also spread throughout the cell cytoplasm.

In most cases the tumour tissue did not approximate the normal healthy tissue as far as the appearance, quantity and distribution of the glycogen was concerned, and at low or high magnification (>X30000) the morphological appearance of the glycogen was similar in all the tumours as well as the control tissue studied.

### 5.3 SIGNIFICANCE OF THE OSMIUM TETROXIDE POTASSIUM FERROCYANIDE METHOD IN TUMOURS OF THE MESODERM AND ENDODERM.

#### 5.3.1 EWING'S SARCOMA

When tissue is processed with the standard method for electron microscopy, the cells in Ewing's sarcoma have large electron-lucent areas, that are quite prominent. One method of distinguishing this neoplasm from other tumours that are not rich in glycogen is by contrasting the glycogen with a special technique. Performing the OPF method on a sample of the tissue confirms the diagnosis when large and small aggregates of very electron-dense material is found in the cytoplasm of the tumour cells, thus emphasizing the usefulness of this technique.

### 5.3.2 LEIOMYOSARCOMA

Often, leiomyosarcomas have to be distinguished from other tumours with similar appearing cells, especially when these cells are primitive. With ordinary light and electron microscopic methods it is difficult to differentiate between these tumours. Frequently the salient features are very similar, except that in the suspected leiomyosarcoma cells large electron-lucent areas can be observed. When the OPF method is performed it becomes the confirmatory test when large and small aggregates of electron dense granules are seen, together with focal densities in the filamentous material of the suspected leiomyosarcoma.

### 5.3.3 RHABDOMYOSARCOMA

When the cells of rhabdomyosarcoma and Ewing's sarcoma are primitive and undifferentiated, they have a very similar appearance with the light microscope. When viewed with the electron microscope however, the cells have vastly different ultrastructural features. The rhabdomyosarcoma cells usually contain well developed striped muscle fibrils and, what appears to be large amounts of glycogen amongst these fibrils. When the OPF technique was performed on rhabdomyosarcoma cells, large aggregates of electron-dense glycogen were seen in these cells. This feature, plus the abundance of



fibrils in the cells confirmed the diagnosis of rhabdomyosarcoma.

#### 5.3.4 HEPATOCELLULAR CARCINOMA

The OPF method was performed not so much to distinguish hepatocellular carcinoma from other tumours but to illustrate the differences between glycogen, mucin and lipid.

When viewed with the electron microscope, large electron-lucent areas were seen in the cytoplasm of the cells which could not be completely resolved even at higher magnification. When the OPF technique was performed, most of these electron-lucent areas were seen to contain aggregates of electron-dense material. The OPF method was thus helpful in distinguishing glycogen from other material found in cells.

#### 5.3.5 THE EFFICACY OF THE OSMIUM TETROXIDE POTASSIUM FERROCYANIDE METHOD IN THE DIAGNOSIS OF TUMOURS.

Although the OPF method was found to be of great value for the demonstration of glycogen in various tumours and was indicative of the type of tumour being dealt with, it was not a conclusive marker for a specific tumour. A more intense study at molecular level of the glycogen in these tumours might reveal subtle features which could distinguish them from each other. Purely on ultrastructural level, all the other factors such as the

presence of intermediate filaments, junctional complexes, pinocytotic vesicles, lysosomes and intracellular lipid droplets etc, had to be taken into consideration to obtain an absolute diagnosis. Special stains as well as the immunocytochemical results and the ultrastructural morphology of the tumour with or without OPF staining had to be taken into consideration.

#### 5.4 USEFULNESS OF THE MYELOPEROXIDASE AND PLATELET SPECIFIC PEROXIDASE METHODS AND THE EFFECT OF THE OSMIUM TETROXIDE POTASSIUM FERROCYANIDE METHOD ON THESE TWO TECHNIQUES.

Modifications to a method for the demonstration of myeloperoxidase and a method for platelet specific peroxidase were described. After these modifications more consistent and reproducible results were obtained.

Taking the results into consideration, it was concluded that the tumours studied could not be distinguished by the ultrastructural appearance of the glycogen alone, but all the other above-mentioned factors had to be taken into consideration as well as the presence and appearance of glycogen demonstrated by the OPF method.

Various changes to the existing methods were effected, and can be set out in order below:

- a Modified fixation procedure as well as adherence to strict fixation times;
- b Use of heparin as anti-coagulant;

- c Increasing H<sub>2</sub>O<sub>2</sub> concentration to 0,02% in the DAB medium;
- d "Thin" tissue for processing, 0,5mm or thinner;
- e Incubation of the tissue in the substrate mixture in the dark;
- f Agitation during incubation;
- g Post-fixation in OPF mixture.

Taking these points in order, it was found that the correct fixative as well as a strict fixation protocol was required. Over-fixation and prolonged storage of the blood or bone marrow tended to inhibit the MPO partially and the PPO almost wholly, therefore blood for MPO was only fixed for a maximum of three hours before being placed in the storage buffer. Bone marrow or blood for determination of PPO was fixed in the modified fixative for one and a half hours before being placed in the storage buffer and was further processed within twenty four hours. When heparin was used as an anti-coagulant, sharper delineation of the membranes and a more precise location of the reaction product could be obtained. Increasing the concentration of the hydrogen peroxide resulted in a more electron-dense deposition of the reaction product. Cutting the pieces of tissue/blood/bone marrow thinly (< 0,5mm) as well as agitating the mixture aided penetration of reagents. The reaction product was further stabilised by incubation in the dark and post-fixation of the tissue in OPF mixture yielded an extremely electron dense reaction product. Not only did the OPF reaction enhance the MPO and PPO reaction product, but it served a two-fold



purpose in making intracellular glycogen visible in the cells of the blood and bone marrow.

In modified form the myelo-peroxidase method was employed as a differential marker between myeloblastic and lymphoblastic leukaemias and was found to be an extremely effective diagnostic marker for granulocytic sarcomas.

The carefully controlled PPO procedure was a very useful method for distinguishing between myeloblastic and megakaryocytic precursors and was found to be an excellent method for diagnosing granulocytic leukaemias.

## **5.5 TYPING OF HUMAN PAPILLOMA VIRUSES.**

DNA in situ hybridization (DISH) uses the principle that complementary DNA sequences pair under certain conditions. (Brigati et al, 1983) Under stringent conditions, DNA strands anneal only when over 85% of the DNA genome sequences are identical but under non-stringent conditions, complementary DNA strands pair when 67% of the genome sequences are identical. Using a homologous probe, 0,1-0,3 HPV DNA copies per cell could be detected by DNA hybridization and furthermore, DISH could detect immature virions as well as viral DNA integrated to host DNA.

In this study it was found that efficient unmasking of the viral DNA with as little loss of cellular detail as possible was essential. Efficient unmasking of the viral DNA by proteolysis of the histones was fixation-dependant. Hydrolysis of the phospho-diester linkages between the nucleotides and proteolysis of the histones, linked to the chromosomal DNA in

the nuclei of the infected cells, had to be carefully controlled so as not to damage the morphology. When buffered formalin was used, unmasking of the viral DNA proceeded more rapidly than when buffered glutaraldehyde was employed, possibly due to the better cross-linking properties of the dialdehyde. A buffered depolymerized paraformaldehyde/glutaraldehyde fixative (2%:0,5%) was eventually used. This yielded acceptable light microscopic Haematoxylin and Eosin sections as well as very good ultrastructural morphology.

Two other aspects of this study that came to light were the stringency of the washes and the freshness or potency of the anti<DIG>POD conjugate. Few problems were encountered with cross-reactivity, as hybridization was carried out at high stringency and the washes at medium stringency.

The anti<DIG>POD conjugate when stored dry at 4°C had an indefinite shelf life, but once diluted, lost potency after four months, although storage instructions were adhered to.

The present study demonstrated that viral particles were not present in the basal or intermediate squamous layer, but mostly in a number of koilocytic cells in the upper granular or horny layer in which ~55nm particles were distributed in the nuclei. DAB precipitate was however seen in other areas of the nuclei where no virions were identifiable. These findings suggested that these labelled probes could also hybridize pre-packaged viral DNA. (Wahl et al, 1987) This conclusion was in line with other workers (Yun et al, 1992) who suggested that the viral genome might not be fully matured to form complete virions until the infected cells reach the end of the superficial layer, and also that viral maturation might occur less

frequently than viral DNA replication. The results of this study supported the above suggestions. A spin-off of this study was that after the DAB reaction, even without standard osmium fixation or OPF fixation, the tissue fixed only in buffered glutaraldehyde, or the paraformaldehyde/glutaraldehyde fixatives, exhibited good, if not excellent ultrastructural cellular detail with enough contrast to obtain acceptable electron-micrographs.

## 5.6 ROLE AND USEFULNESS OF THE OSMIUM TETROXIDE/POTASSIUM FERROCYANIDE AND MYELOPEROXIDASE PROCEDURES IN THE TYPING OF HUMAN PAPILLOMA VIRUSES.

### 5.6.1 THE MYELOPEROXIDASE METHOD AND DETECTION OF VIRUSES IN TISSUE.

The original <DIG> method for HPV typing coupled the anti<DIG> molecule to alkaline phosphatase that was suitable only for light microscopy, and could not be used for ultrastructural purposes. Later, an anti<DIG>POD reagent was developed which could not only be used for light microscopy, but for electron microscopy as well. The modified MPO method was used following DNA in situ hybridization of target viral sequences and detecting peroxidase coupled to these sequences via the anti<DIG>POD reagent. Electron dense reaction product was successfully deposited on mature viruses as well as at the sites of virion production.



### 5.6.2 THE OSMIUM TETROXIDE/POTASSIUM FERROCYANIDE METHOD AS AN ENHANCER FOR GLYCOGEN IN HUMAN PAPILLOMA VIRUS TYPING.

Glycogen is a 35nm particle when it occurs in the  $\beta$  form, and to ensure that the particles seen after hybridization were viruses, the tissue was post-fixed in OPF mixture. Not only did the OPF mixture cause the reaction product to be more electron dense but it also stained the glycogen particles which could be distinguished from the papilloma viruses which are ~55nm in size. The value of this method was once again demonstrated, not only in its role as an ultra-structural glycogen marker, but also as a means of determining size relationships of other particles in tissue.

### 5.7 DEVELOPMENT OF FURTHER ELECTRON-HISTOCHEMICAL METHODS IN THE FUTURE

The DAB method in its modified form is an efficient technique for demonstrating peroxidase in polymorphonuclear granulocytes and their precursors. This will remain an excellent peroxidase-rich lysosomal marker until an efficient immunocytochemical marker is developed.

The OPF method has been proved to not only stain glycogen ultrastructurally, but was also useful in imparting more contrast to tissue even when no uranyl staining was used. It was also extremely useful as an ultrastructural size marker when DNA in situ hybridization was performed to differentiate between glycogen particles and the virus particles.

Peroxidase, when coupled to the <DIG> antibody is an efficient ultrastructural marker for viruses when used in the hybridization method, but the reaction product is a fraction too coarse and could possibly obscure finer detail of the interaction between the virus and the probe.

The technique relies on the reaction product being more electron-dense than the surrounding tissue, so it could be argued that not enough contrast might exist between the structures. There is however an anti<DIG> gold complex available currently, which has been used by Hamkalo et al (1989) with some success and this will be used in future to visualize finer detail in epoxy embedded tissue such as Spurr's resin. Some research has been done on the marking of glial fibres (Bettica and Johnson, 1990) from tissue embedded in EPON epoxy resin and Spurr's resin (Geiger, 1993) and the same protocol modified for virus studies could be used for this purpose.

—oooOooo—

# CHAPTER VI

## CONCLUSIONS



# **6.0 CONCLUSIONS**

## **6.1 GENERAL CONSIDERATIONS**

Modifications to existing electron histochemical techniques for detection of glycogen, myeloperoxidase and platelet specific peroxidase were described as well as an ultrastructural typing procedure for Human Papilloma Virus (HPV). With the advent of monoclonal antibodies and the development of simple immunocytochemical tests, procedures such as the OPF and the MPO/PPO technique lost prominence, but with some modifications are still extremely reliable diagnostic tools and yield specific and reproducible results.

This study was performed to lead progressively from a modified fixation technique for glycogen which was employed in an enzyme detection method later. Both of these methods were then combined and applied in a third technique for typing Human Papilloma Viruses.

The modified OPF method was used firstly to fix and detect glycogen in certain tumours. It was then applied in the MPO and PPO methods as a post-fixative. Both the MPO method and the OPF method were then combined in the DIG method for typing Human Papilloma Viruses. The MPO method was employed to detect peroxidase coupled to the digoxigenin antibody and the OPF to not only enhance the final reaction product, but also to be used as an ultrastructural size marker.

## 6.2 THE OPF METHOD

The OPF technique modified in this laboratory became a simple, reliable and quick method for contrasting glycogen in tissue and is a very good diagnostic marker for glycogen-rich tumours. Although no absolute distinction of the tumours could be made on the ultrastructural appearance of the contrasted glycogen particle at high magnification (>30000X), the amount, distribution and arrangement of the contrasted glycogen aggregates in all the cases studied, determined what kind of cell was present in the tumour and hence lead to a diagnosis of the disease state.

## 6.3 THE MPO AND PPO METHODS

The modified method for MPO and PPO raised a few additional questions as to the fixation and subsequent storage of the specimens were concerned. As previously stated the MPO was fixation dependant and disappeared from carefully stored specimens after a certain length of time which was conservatively judged to be three months. The catalase in the red cells could still be detected with the MPO method long after no reaction product was discernible in the granules of the white cells. The PPO was wholly fixation dependant and was inhibited by the concentration of the glutaraldehyde normally used in standard fixatives. A modified tannic acid/para-formaldehyde fixative and a careful fixation protocol, such as adhering to short fixation times, had therefore to be used. PPO also leached from fixed specimens at a rapid rate

even when stored at low temperature (~ 4°C) in fresh storage buffer and was undetectable by the modified PPO method within seven days of receipt. It was therefore imperative that the PPO method had to be performed on the tissue within that time. The tissue had to be post-fixed immediately and processed to the epoxy block stage so that as much enzyme as possible could be detected. Both the methods described, yielded extremely reliable and reproducible results and could be used as diagnostic tools on a routine basis.

#### 6.4 ULTRASTRUCTURAL HYBRIDIZATION OF HUMAN PAPILLOMA VIRUS

The development of non-isotopic methods for typing of viral diseases by in situ hybridization techniques simplified these procedures to a great extent and made them specific and sensitive as well. The digoxigenin method, which was as sensitive and even more reproducible than the radio-active isotopic methods developed earlier, made the ultrastructural detection of viruses that much quicker and easier.

The standard digoxigenin (DIG) light microscopic method was modified in this laboratory so that permanent preparations of the sections could be made. This entailed coupling the <DIG> to an anti<DIG> peroxidase FAB fragment and then subsequently detecting this product with the modified DAB method. The fixation procedure had to be modified so that not only acceptable light microscopic preparations could be made, but ultrastructural studies could also be performed. The method not only demonstrated mature virions, but also pre-packaged viral DNA, and this indicated that further study



in this direction should be considered. The enzyme detection method relies on deposition of an electron-dense precipitate at the site of enzyme activity. Because this electron-dense precipitate is usually diffusely spread, the method could possibly not be used when an in-depth study of the pre-packaged viral DNA was undertaken. An anti<DIG> colloidal gold marker in different particle sizes has been developed, and would be of greater use to give a more precise localization of the movement and replication of the viruses. The smaller particle size (3nm) could be used in the pre-embedding method, whereas the larger sizes (>3nm) could be used in a post-embedding method.

—ooOoo—

## APPENDIX

## 7.0 REAGENTS

### 1. Sørensen's Phosphate Buffer 0,1M pH 7,4

A	Di-sodium hydrogen orthophosphate (anhydrous)	28,39gm
	Distilled water	1000ml
B	Sodium di-hydrogen orthophosphate (anhydrous)	27,59gm
	Distilled water	1000ml

Working strength buffer is made by mixing:

A	210ml	
B	40ml	and diluting to 500ml with distilled water.

### 2. Sørensen's Phosphate Buffer 0,01M pH 6,0

A	87,7ml	
B	12,3ml	and diluting to 200ml with distilled water.

### 3. 2,5% Phosphate buffered glutaraldehyde fixative

0,1M Sørensen's phosphate buffer (1)	90ml
25% Glutaraldehyde (TAAB)	10ml

Glutaraldehyde is supplied in 10ml aliquots in sealed vials containing an inert gas and is very stable if kept at 4°C. (TAAB)

### 4. Standard phosphate buffered formalin

0,1M Sørensen's Phosphate buffer (1)	90ml
40% Formaldehyde (Merck)	10ml



5. 20% Paraformaldehyde

Paraformaldehyde (Merck)	20gm
Distilled water	100ml

The paraformaldehyde is added to the distilled water in a beaker. The mixture is heated over a Bunsen burner in a fume cupboard while 1M NaOH is slowly added drop by drop. On reaching approximately 60°C and neutrality, the paraformaldehyde will dissolve.

6. 2% Paraformaldehyde/Glutaraldehyde fixative.

20% Paraformaldehyde (5)	10ml
25% Glutaraldehyde	2ml
0,1M Sörensen's Phosphate buffer (1)	100ml

7. Tannic acid, Formaldehyde/Glutaraldehyde fixative.

Tannic acid (Sigma)	1gm
20% Paraformaldehyde (4)	10ml
25% Glutaraldehyde	2ml
0,1M Sörensen's Phosphate buffer (1) to make	100ml

The pH is restored to 7,4 by addition of either 1M HCl or 1M NaHCO<sub>3</sub>

8. Storage buffer

Sodium chloride (Merck)	3,715gm
0,1M Sörensen's Phosphate buffer (1)	500ml

9. 3% Aqueous osmium tetroxide

An ampoule containing 1gm of osmium tetroxide (Sigma), is scored with a diamond pen, washed in distilled water and broken inside an amber bottle containing 33ml distilled water. This must be done in a fume cupboard, as this chemical is extremely dangerous to the respiratory tract and the eyes. Osmium salts dissolve very slowly, so the solution should be made up at least a day before use.

10. Palade's buffer

Sodium veronal (barbital) (Merck)	14,4gm
Sodium acetate (anhydrous) (Merck)	5,75gm
Distilled water	500ml

11. 0,1M Hydrochloric acid

Hydrochloric acid (concentrated)	8,6ml
Distilled water	1000ml

Ampoules are available commercially to make 1 litre of 1M hydrochloric acid. 100ml of this solution made up to 1 litre with distilled water will give a 0,1M solution.

12. 1,5% Palade's buffered osmium tetroxide

Buffer solution (10)	5ml
0,1M hydrochloric acid (11)	5ml
Distilled water	2,5ml
3% Osmium tetroxide (9)	12,5ml

13. Buffered Osmium tetroxide/Potassium ferrocyanide

Sörensen's phosphate Buffer (2)	5ml
3% Osmium tetroxide (9)	5ml
Potassium ferrocyanide (Merck)	0,2gm

14. Karnovsky's Osmium tetroxide/Potassium ferrocyanide

3% Osmium tetroxide (9)	5ml
Potassium ferrocyanide	0,15gm
Distilled water	5ml

The potassium ferrocyanide is dissolved gradually with agitation.

15. Modified Osmium tetroxide/Potassium ferrocyanide

3% Osmium tetroxide (9)	5ml
Potassium ferrocyanide	0,2gm
Distilled water	5ml

16. Uranyl acetate "en bloc" stain

Uranyl acetate	2gm
70% Ethanol (Merck)	50ml

17. 1% Hydrogen peroxide

30% Hydrogen peroxide (Univar)	19ml
Distilled water	500ml



18. 0,1M Tris buffer

Tris (hydroxyaminomethyl)-methane (Merck)	1,211gm
Distilled water	100ml

19. 0,05M Working Tris buffer

0,1M Tris (18)	25ml
0,1M hydrochloric acid (9)	19ml
Distilled water to make	100ml

This mixture is at a pH of 7,6

20. Karnovsky's Diaminobenzidine medium (DAB)

3-3' Diaminobenzidine HCl (Sigma)	5mg
Buffer solution pH 7,6 (18)	0ml
1% H <sub>2</sub> O <sub>2</sub>	0,1ml (0,01%)

21. 1M Sodium bicarbonate

Sodium bicarbonate (Merck)	8,4gm
Distilled water	100ml

22. Breton-Gorius' DAB medium

3-3' Diaminobenzidine hydrochloride	20mg
Buffer (19)	10ml

The pH is restored to 7,6 by the addition of small amounts of solution (21).

Add 1% hydrogen peroxide	0,1ml (0,01%)
--------------------------	---------------

23. Diaminobenzidine medium (Tygerberg EM laboratory)

3-3' Diaminobenzidine HCl	10mg
Buffer (19)	10ml

The pH is restored to 7,6 by the addition of small amounts of solution (21). Add 0,15ml soln (17) to final concentration of 0,015% hydrogen peroxide.

24. 2% 3-amino propyl triethoxy silane (APES)

APES (Merck)	4ml
Acetone (Merck)	196ml

This solution degrades to form sulphuric acid so should be freshly made up before use.

25. Phosphate buffered saline (PBS)

Sodium chloride	8gm
Potassium chloride (Merck)	0,2gm
di-Sodium hydrogen orthophosphate	1,44gm
Potassium di-hydrogen orthophosphate	0,24gm
Distilled water	800ml

Adjust pH to 7,6 and make up to 1 litre with distilled water.

26. 0,02M Hydrochloric acid

1M Hydrochloric acid	20ml
Distilled water	1000ml

**27. 0,1% Triton X100**

Triton X100	1ml
Phosphate buffered saline (25)	1000ml

**28. 20% Acetic acid**

Glacial acetic acid (Merck)	200ml
Distilled water	1000ml

**29. 1% Hydrogen peroxide in 100% Methanol.**

30% hydrogen peroxide	8,3ml
100% Methanol	250ml

**30. Tris/ethylene diamine tetra-acetic acid buffer for digestion medium.**

0,05M Tris (18)	1000ml
EDTA (Sigma)	0,6gm

**31. Digestion medium**

Buffer 30	180ml
Protease (Type 24 Sigma)	36mg

The concentration of this solution is critical and should be standardized against parallel specimens to determine concentration and time of digestion.



32. 0,2% Glycine in PBS

Glycine (Merck)	2gm
PBS (25) to	1000ml

33. 4% Paraformaldehyde in PBS.

20% Paraformaldehyde (5)	200ml
PBS (25) to	1000ml

34. 20x Standard salt concentration (SSC).

Sodium chloride	175,3gm
Tri-sodium citrate (BDH)	88,2gm
Distilled water to	800ml

Adjust pH to 7.0 and then make up to 1L with dist H<sub>2</sub>O.

35. 50% Dextran sulphate.

Dextran sulphate (Merck)	50gm
Dist H <sub>2</sub> O to	100ml

Mix the dextran sulphate to a paste with some of the water, then add the rest of the water and place in a sealed container overnight in a water-bath at 60°C to dissolve completely.

36. Hybridization mixture. ( $T_m = -17^\circ\text{C}$ )

Probe fragments( $\pm$ 500ng)	50 $\mu$ l (500ng/ml)
20xSSC (34)	100 $\mu$ l (2xSSC)
50% Dextran sulphate (35)	200 $\mu$ l (10%)
10mg/ml Sheared herring sperm DNA	40 $\mu$ l (400 $\mu$ g/ml)
Formamide	100 $\mu$ l (10%)
100x Denhardt's solution	10 $\mu$ l
Dist H <sub>2</sub> O	500 $\mu$ l

37. Hybridization mixture. ( $T_m = -42^{\circ}\text{C}$ )

Probe fragments( $\pm$ 500ng)	50 $\mu\text{l}$ (500ng/ml)
20xSSC (34)	100 $\mu\text{l}$ (2xSSC)
50% Dextran sulphate (35)	200 $\mu\text{l}$ (10%)
10mg/ml Sheared herring sperm DNA	40 $\mu\text{l}$ (400 $\mu\text{g}/\text{ml}$ )
Formamide	500 $\mu\text{l}$ (50%)
100x Denhardt's	10 $\mu\text{l}$
Dist H <sub>2</sub> O	100 $\mu\text{l}$

These concentrations of Formamide and SSC give the stringency for HPV only!

38. 2x Standard salt concentration (2xSSC).

20xSSC (34)	100ml
Dist H <sub>2</sub> O to	1000ml

39. 0,2x Standard salt concentration (SSC).

2xSSC (38)	100ml
Dist H <sub>2</sub> O to	1000ml

40. Tris/Hydrochloric acid (Buffer 1).

Tris	12,1gm
Sodium chloride	8,77gm
Dist H <sub>2</sub> O to	800ml

Adjust pH to 7,5 with HCl then make up to 1L with distilled water.

41. Tris/Hydrochloric acid (Buffer 3).

Tris	12,1gm
Magnesium chloride (MgCl <sub>2</sub> .6H <sub>2</sub> O) (Merck)	10,17gm
Sodium chloride	5,84gm
Dirt H <sub>2</sub> O to	800ml

Adjust pH to 9.5 with HCl then make up to 1L with distilled water.

42. Tris/Hydrochloric acid (Buffer 4).

Tris	1,2gm
EDTA (Free acid) (Sigma)	0,3gm
Dist H <sub>2</sub> O to	800ml

Before adding the EDTA adjust the pH of the solution to 8 as this salt dissolves with difficulty; then make up to 1L with distilled water.

43. Anti digoxigenin alkaline phosphatase labelling solution.  
(Anti <DIG>AP)

Anti <DIG>AP-Conjugate	1 $\mu$ l
Buffer 41	5ml

This yields a 1:5000 dilution  
(From Boehringer Mannheim kit)

44. Hybridization colour reagent.

Nitro-blue Tetrazolium (NBT)	45 $\mu$ l
5-Bromo-4-chloro-3-indolyl phosphate	35 $\mu$ l
Buffer 40	10ml



45. Anti digoxigenin peroxidase labelling reagent. (Anti <DIG>POD)

Anti <DIG>POD FAB fragments	10 $\mu$ l
Dist H <sub>2</sub> O (Boehringer Mannheim)	1ml

46. Spurr's Resin (Bio-Rad)

Nonenyl Succinic Anhydride (hardener)	26gm
ERL 4206 (resin)	10gm
DER 736 (plasticizer)	6gm
S1 (dimethylaminoethanol accelerator)	0,4gm

This is a Bio-Rad product and has a stable shelf life.  
The mixture must be thoroughly mixed with a glass rod.

47. Sodium methoxide (Resin remover)

Metallic sodium (Merck)	5gm
Methanol (Merck)	100ml

After the sodium has dissolved 5ml benzene is added as a preservative.

48. 1% Sodium tetraborate

Sodium tetraborate (Merck)	10gm
Dist. H <sub>2</sub> O	1000ml

49. 1% Toluidine blue (semi-thin section stain)

Toluidine powder (Merck)	10gm
1% Sodium tetraborate (48)	1000ml

50. Uranyl acetate (thin section stain)

Uranyl acetate (Merck)	2gm
50% Ethanol (Merck)	50ml

This solution must be kept in the refrigerator and discarded if it shows any cloudiness.

51. 1M Sodium hydroxide

Sodium hydroxide (Merck)	4gm
Distilled water	100ml

52. Reynolds' lead citrate (thin section stain)

Lead nitrate (Merck)	1,33gm
Dist. H <sub>2</sub> O	15ml
Tri-sodium citrate	1,76gm
Dist. H <sub>2</sub> O	15ml

These two salts are dissolved separately in distilled water and then added together in a volumetric flask. A precipitate forms and the mixture is shaken vigorously for 30 sec, then intermittently for 30 minutes. 8ml of freshly prepared solution (51) is added. The precipitate should disappear, and the volume made up to 50ml with distilled water.

53. Diastase for digestion of glycogen.

Malt diastase	0,1gm
SÖrensens Phosphate buffer pH 6,9	10ml

This solution is made just prior to use.

—ooOoo—

## BIBLIOGRAPHY



## 8.0 BIBLIOGRAPHY

1. Alberts B, Bray D, and Lewis J, Raff M, Roberts K and Watson J D. *Molecular Biology of the Cell*. Garland N.Y. Second Edition. (1989)
2. Anderson D R. (1965) A method for preparing peripheral blood leucocytes for electron microscopy. *Ultrastructure Research*. 13, 263-268.
3. Beckmann A M, Myerson D, Daling J R, Kiviat N B, Fenoglio C M and McDougall J B. (1985) Detection and localization of Human Papillomavirus DNA in human genital condylomas by "in situ" hybridization with biotinylated probes. *Journal of Medical Virology*. 16, 265-273.
4. Bettica A, Johnson A B. (1990) Ultrastructural immunogold labelling of Glial filaments in osmicated and unosmicated Epoxy-embedded tissue. *Journal of Histochemistry and Cytochemistry*. 38, (5), 103-109.
5. Breton-Gorius J and Reyes F. (1976) Ultrastructure of human bone marrow cell maturation. *International review of cytology*. 46, 251-321.
6. Breton-Gorius J, Reyes F, Vernant J P, Tulliez M and Dreyfus B. (1978) The blast crisis of chronic Granulocytic Leukemia: Megakaryoblastic nature of cells as revealed by the presence of platelet peroxidase. A cytochemical ultrastructural study. *British Journal of Haematology*. 39, 295-303.
7. Brigati D J, Myerson D, Leavy J J, Spalholz B, Trais S Z, Fong C K Y, Hsiung G D and Ward D C. (1983) Detection of viral genomes in cultured cells and paraffin embedded tissue sections using biotin-labelled hybridization probes. *Virology*. 126, 32-50.

8. *Burstone M S. (1961) Histochemical demonstration of phosphatases in frozen sections with Naphthol-AS phosphates. Journal of Histochemistry and Cytochemistry. 9, 301-303.*
9. *Cavallo T. (1976) Cytochemical localization of endogenous peroxidase activity in renal medullary collecting tubules and papillary mucosa of the rat. Laboratory Investigations. 34, 223-228.*
10. *De Bruijn W C. (1973) Glycogen: Its chemistry and morphological appearance in the EM. Journal of Ultrastructural Research. 42, 29-50.*
11. *De Bruijn W C and Van Buitenen J M H. (1981) X-Ray microanalysis of non aldehyde fixed glycogen. Histochemical Journal. 13, 125-136.*
12. *De Groot J C, Veldman J E and Huizing R H. (1987) An improved fixation method for guinea pig cochlear tissues. Acta Otolaryngology. (Stockh) 104, (3-4), 234-242.*
13. *De Jong A S H, Van Kessel-Van Vark M and Raap A K. (1985) Sensitivity of various visualization methods for peroxidase and alkaline phosphatase activity in immunoenzyme histochemistry. Histochemical Journal. 17, 1119-1130.*
14. *Drochmans P. (1962) Morphology of glycogen. Electron microscopic study of the negative stains of particulate glycogen. Journal of Ultrastructural Research. 6, 141-163.*
15. *Dvorak A M, Hammond E M, Dvorak H F and Karnovsky M J. (1972) Loss of cell surface material from peritoneal exudate cells associated with lymphocyte mediated inhibition of macrophage migration from capillary tubes. Laboratory Investigation. 27, (6), 561-574.*
16. *Dvorak A M, Monahan R A and Dickersin G R. (1981) Diagnostic Electron Microscopy I. Haematology; Differential diagnosis of acute lymphoblastic and acute myeloblastic Leukemia. Use of*

ultrastructural peroxidase cytochemistry and routine electron microscopic technology. *Pathology Annual*. 16, (1), 101.

17. Escribano L M, Gabriel L C, Sainz T, Rocamora A, Arrazola J M and Navarro J L. (1984) Peroxidase activity in human cutaneous Mast cells: An ultrastructural demonstration. *Journal of Histo-chemistry and Cytochemistry*. 2, (6), 573-578.
18. Geiger D H. (1993) Immuno-electron microscopical characterisation of glial intermediate filaments in human gliomas. MSc thesis, University of Stellenbosch.
19. Gerrard J M, White J G, Rao G H R and Townsend D. (1976) Localization of platelet prostaglandin production in the platelet dense tubular system. *American Journal of Pathology*. 83, 283-298.
20. Graham R C and Karnovsky M J. (1966) The early stages of absorption of injected horseradish peroxidase in the proximal tubules of mouse kidney: Ultrastructural cytochemistry by a new technique. *Journal of Histochemistry and Cytochemistry*. 14, (4), 291-302.
21. Hamkalo B, Narayanswami S, and Lundgren K. (1989) Localization of nucleic acid sequences by EM "in situ" hybridization using colloidal gold labels. *American Journal of Anatomy*. 185, 197-204.
22. Hewson J W, Bradstock K F, Kern A and Rose R G. (1986) Characterization of "difficult" acute leukaemias. A combined electron microscope and immunological marker study. *Pathology*. 18, 99-110.
23. Heynen M J, Tricot G and Verwilghen R L. (1984) A reliable method with good cell preservation for the demonstration of peroxidase activity in human platelets and megakaryocytes. *Histochemistry*. 80, 79-84.



24. Howley P M, Israel M A, Law M F and Morton M A. (1979) A rapid method for detecting and mapping homology between heterologous DNAs. Evaluation of polyomavirus genomes. *Journal of Biological Chemistry*. 254, (11), 4876-4883.
25. Johnson A B, and Bettica A. (1989) On-Grid immunogold labelling of Glial intermediate filaments in epoxy-embedded tissue. *American Journal of Anatomy*. 185, 335-341.
26. Karnovsky M J. (1967) The ultrastructural basis of capillary permeability studied with peroxidase as a tracer. *Journal of Cell Biology*. 35, 213-236.
27. Karnovsky M J. (1971) Use of ferrocyanide reduced OsO<sub>4</sub> in electron microscopy. Abstracts: Proceedings of American Society of Cell Biology. 146, 11th Annual meeting; New Orleans.
28. Kiernan J A. *Histological and histochemical methods. Theory and practice*. Pergamon N.Y. 1st Edition.
29. Lewis F A, Griffiths S, Dunnicliff R, Wells M, Dudding N and Bird C C. (1987) Sensitive in-situ hybridization technique using biotin-streptavidin-polyalkaline phosphate complex. *Journal of Clinical Pathology*. 40, 163-166.
30. Long A A, Meuller J, Andre-Schwartz J, Barrett K J, Schwartz R and Wolfe H. (1992) High-specificity in-situ hybridization. *Methods and application. Diagnostic Molecular Pathology*. 1, 45-57.
31. McGilvery R W. *Biochemistry: A functional approach*. Saunders P.A. (1970)
32. Meis J M, Butler J J, Osborne B M and Manning J T. (1986) Granulocytic sarcoma in non-leukaemic patients. *Cancer*. 58, (12), 2697-2709.

33. Monahan R A and Dvorak A M. (1985) One micron plastic sections of human peripheral blood and bone marrow specimens and peroxidase cytochemistry: use in differential diagnosis of acute leukaemias. *Pathology Annual*. 20, (1), 383-401.
34. Multhaupt H A B, Rafferty P A and Warhol M J. (1992) Ultrastructural localization of Human Papilloma Virus by non-radioactive in situ hybridization on tissue of human cervical intra-epithelial neoplasia. *Laboratory Investigation*. 67, 512-518.
35. Myerson D, Hackman R C, Nelson J A, Ward D C and Mc Dougall J K. (1984) Widespread presence of histologically occult cytomegalovirus. *Human Pathology*. 15, (5), 430-439.
36. Nakahata T, Spicer S S, Cantey J R and Ogawa M. (1982) Clonal assay of mouse mast cell colonies in methylcellulose culture. *Blood*. 60, 352-361.
37. Nichols B A and Bainton D F. (1973) Differentiation of human monocytes in bone marrow and blood. Sequential formation of two granule populations. *Laboratory Investigation*. 29, (1), 27-40.
38. Novikoff A B and Goldfischer S. (1969) Visualization of peroxisomes and mitochondria with diaminobenzidine. *Journal of Histochemistry and Cytochemistry*. 17, 681-685.
39. O'Brien M, Catovsky D. and Costello C. (1980) Ultrastructural cytochemistry of leukemic cells: The characterization of the early small granules of monoblasts. *British Journal of Haematology*. 45, 201-208.
40. Padayachee A and Van Wyk C W. (1991) Human papillomavirus (HPV) DNA in focal epithelial hyperplasia by in-situ hybridization. *Journal of Oral Pathology Medicine*. 20, 210-214.
41. Reyes F, Gourdin M F, Farcet J P, Dreyfus B and Breton-Gorius J. (1978) Synthesis of peroxidase activity by cells of Hairy Cell

leukaemia: A study by ultrasrtuctural cytochemistry. *Blood*. 52, (3), 537-550.

42. Riemersma J C, Alsbach E J J and De Bruijn W C (1984) Clinical aspects of glycogen contrast staining by potassium osmate. *Histochemical Journal*. 16, 123-136.
43. Sato S, Okagaki T, Clark B A, Twiggs L B, Fukushima M, Ostrow R S and Faras A J. (1987) Sensitivity of koilocytosis, immunocytochemistry and electron microscopy as compared to DNA hybridization in detecting HPV in cervical and vaginal condyloma and intra-epithelial neoplasia. *International Journal of Gynaecological Pathology*. 5, 297-307.
44. Shepard N and Mitchell N. (Jan 1989) Improved chondrocyte morphology and glycogen retention in the secondary centre of ossification following osmium-potassium ferrocyanide fixation. *Journal of Electron Microscopic Technique*. 11, (1), 83-89.
45. Smith E L, Hill R L, Lehman I R, Lekowitz R J, Handler P and White A. *Principles of Biochemistry*. (1970).
46. Strauss W. (1962) Factors affecting the cytochemical reaction of peroxidase with benzidine and the stability of the blue reaction product. *Journal of Histochemistry and Cytochemistry*. 12, 462-469.
47. Strauss W. (1979) Peroxidase procedures. Technical problems encountered during their application. *Journal of Histochemistry and Cytochemistry*. 27, (10), 1349-1351.
48. Strauss W. (1982) Imidazole increases the sensitivity of the cytochemical reaction for peroxidase with diaminobenzidine at a neutral pH. *Journal of Histochemistry and Cytochemistry*. 30, 491-493.



49. Wahl G M, Berger S L and Kimmel A R. (1987) Molecular hybridization of immobilised nucleic acids: Theoretical concepts and practical considerations. *Methods in Enzymology*. 152, 399-407.
50. Watson J D, Hopkins N H, Roberts J W, Steutz J A and McWeiner A M. *Molecular Biology of the Gene*. Fourth Edition. (1987)
51. Wolber R A, Beals T F and Maassab H F. (1989) Ultrastructural localization of Herpes Simplex Virus RNA by in-situ hybridization. *Journal of Histochemistry and Cytochemistry*. 37, (1), 97-104.
52. Yun K and Sherwood M J. (1992) In situ hybridization at light and electron microscope levels: Identification of Human Papilloma Virus nucleic acids. *Pathology*. 24, 91-98.
53. Zucker-Franklin D. (1980) Ultrastructural evidence for the common origin of human mast cells and basophils. *Blood*. 56, 534.

—ooOoo—